The Role of Protein Tyrosine Phosphatases in Neuroblastoma

Owen Clark

University College London

Institute of Child Health

A thesis submitted for the degree of Doctor of Philosophy

October 2011

Declaration

I, Owen Clark, confirm that the work presented in this thesis is my own. Where information has been derived from other sources, I confirm that this has been indicated in the thesis.

London, December 2011

Table of contents

Abstract

Reversible phosphorylation of tyrosine residues on proteins is a cornerstone of cell to cell signalling, and is achieved through the concerted action of protein tyrosine kinases (PTKs) and protein tyrosine phosphatases (PTPs), which catalyse the addition and removal of phosphate moieties respectively. While the contribution of PTKs to oncogenesis and tumour maintenance has been well documented in a range of human cancers, knowledge of the specific role of PTPs has generally lagged behind. This thesis examines that role in neuroblastoma, a common and deadly sympathoadrenal tumour of infancy. We provide evidence that vanadium-based PTP inhibitors cause synergistic hyperactivation of Akt and Erk, which drives an irreversible differentiation and senescence program that is independent of p53, $p16^{INK4A}$ and PTEN. It is then shown that in another group of tumour cell lines, such compounds used alone can induce selective caspase-dependent, p53-independent apoptosis that is associated with activation of Akt and altered redox homeostasis. Lastly we examine the expression profile of the PTPome in a wide panel of neuroblastoma cell lines, providing preliminary evidence for candidate PTP oncogenes and tumour suppressors, as well as mediators of the effects of vanadium compounds.

Acknowledgements

This work would not have been possible without the contributions of others, for which I am extremely grateful. Of special mention are Jonathan Ham for generously agreeing to perform microinjection studies; Charlotte Cole for her expert construction of plasmid expression vectors; Mauritzio Mangolini for his efforts at resolving problems with troublesome antibodies; Simon Picker for lending his expertise in bioinformatics; Aris Tagalakis and Stephen Hart for their numerous donations of time and transfection reagents; Ayad Eddaoudi for his unending knowledge of flow cytometry; Fanny Schmidt for her generous efforts at conducting expression analyses; and Olesya Chayka for her uncanny ability to acquire things exactly when I need them…

Of course much help has come from the members of the ICH Neural Development Unit, of which I have had the great pleasure of working in for three years. First the group leaders; my supervisor Andy Stoker, the most patient man on earth, who has put up with more of my catastrophes than I can remember… (As well as providing constant intellectual insights of course); my secondary supervisor Alan Burns, always on hand for useful advice; The head of the unit Andy Copp, who would always lend an ear to my problems despite running an entire institute; And of course JP, who has and will always provide me with constant challenges to my arguments to the point that I end up forgetting what they were… The PhD students and postdocs are obviously the heart and soul of the unit, and no doubt each and every one will have lent their encouragement at some point; but special mention goes to Carles and Valentina, for their invaluable advice and support, and for putting the words 'and the Nobel prize goes to Owen Clark and Carles Gaston-Massuet' in the back of my mind; and Sandra and Sophie, for keeping me sane (almost).

Lastly, and for whom I owe the most gratitude, my family. My sister for probably believing in me more than I do myself, and for always validating my hard work; and my parents, for their unending support and commitment, especially my dad, whose enthusiasm for teaching me the wonders of science (including basement electroplating and home made explosives) helped spur me on to scientific research.

Abbreviations

NBL	Neuroblastoma
SNS	Sympathetic nervous system
EFS	Event-free survival
SA	Sympathoadrenal
NCC	Neural crest cells
ALK	Anaplastic lymphoma kinase
RA	Retinoic acid
NF1	Neurofibromin 1
Trks	Tropomyosin related kinases
NGF	Nerve growth factor
BDNF	Brain-derived neurotrophic factor
NT-3	Neurotrophin 3
MRD	Minimal residual disease
DM	Double minute bodies
HSRs	Homogenously staining regions
FAK	Focal adhesion kinase
Tsc2	Tuberous sclerosis 2
PTKs	Protein tyrosine kinases
PTPs	Protein tyrosine phosphatases
SH2	Src homology 2
PTB	Phosphotyrosine binding
RTKs	Receptor tyrosine kinases
EGFR	Epidermal growth factor receptor
ECM	Extracellular matrix
MAPK	Mitogen activated protein kinase
Erk	Extracellular signal-related kinase
PI3K	Phosphatidylinositol-3-kinase
PIP2	Phosphatidylinositol-4,-5-bisphosphate (Ptpins(4,5)P_2
PIP3	Phosphatidylinositol-4,-5-bisphosphate (Ptpins(3,4,5)P_3
PH	Plekstrin-homology

PDK1	Phosphoinositide-dependent kinase 1
PTEN	Phosphate and tensin homologue deleted on chromosome 10
CREB	Cyclic-AMP-response element binding protein
mTOR	Mammalian target of rapamycin
4EBPs	4E-binding proteins
ROS	Reactive oxygen species
CSC	Cancer stem cell
TIC	Tumour-initiating cell
IGF-1R	Insulin-like growth factor I receptor
ARF	ADP ribosylation factor
OIS	Oncogene-induced senescence
PIN	Prostrate intraepithelial neoplasia
SA-β-gal	Senescence-associated β-galactosidase
MEFs	Mouse embryonic fibroblasts
PICS	PTEN-loss-induced senescence
pTyr	Phosphotyrosine
RPTPs	Receptor-type PTPs
CAMs	Cell adhesion molecules
DSP	Dual specificity phosphatase
pSer	Phosphoserine
pThr	Phosphothreonine
Asp	Aspartic acid
Cys	Cysteine
Glu	Glutamine
PDGF-R	Platelet-derived growth factor
IR	Insulin receptor
LOH	Loss of heterozygosity
UTR	Untranslated region
V	Vanadium
BMOV	Bis(maltolato)oxovanadium(IV)
BEOV	Bis(ethylmaltolato)oxovanadium(IV)
VO-OH Pic	3-hydroxypicolinate vanadium(IV)

NAC	N-acetyl-L-cysteine
FDA	Food and drug administration
SOD	Superoxide dismutase
NADPH	Nicotinamide adenine dinucleotide phosphate
GSH	Reduced glutathione
GSSG	Oxidised glutathione
BSO	Buthionine sulfoximine
PKC	Protein kinase C
LB	Luria Bertani
RT	Room temperature
CIP	Calf intestinal phosphatase
TAE	Tris-acetate-EDTA
PCR	Polymerase chain reaction
dNTPs	Deoxynucleotide triphosphates
MW	Molecular weight
Tm	Melting temperature
Ct	Cross point values
CMV	Cytomegalovirus
SV40	Simian vacuolating virus 40
GFP	Green fluorescent protein
LC3	Microtubule-associated protein 1A/1B-light chain 3
CAβ	Chick beta-actin
PCD	Programmed cell death
DMEM	Dulbecco's modified Eagle's Medium
MEM	Eagle's Minimum Essential Medium
RPMI	Roswell Park Memorial Institute
HEPES	4-(2-hydroxyethyl)-1-piperazineethanesulfonic acid
FBS	Fetal bovine serum
P/S	Penicillin/streptomycin
PBS	Phosphate-buffered saline
HEK	human embryonic-kidney
dfp	Days post fertilisation

IgG	Immunoglobulin type G
BSA	Bovine serum albumin
DAPI	4',6-diamidino-2-phenylindole
PEI	Polyethyleneimine
DOTMA	N-[1-2(2,3-dioleyloxy)propyl]-n,n,n-trimethylammonium chloride
DOPE	Dioleoyl phophotidylethanolamine
RPM	Revolutions per minute
SDS-PAGE	Sodium dodecyl sulfate polyacrylamide electrophoresis
APS	Ammonium persulfate
TEMED	Tetramethylethylenediamine
PVDF	Polyvinyldiflouride
TBS	Tris-buffered saline
TBS-T	Tris-buffered saline-tween 20
ECL	Electrochemiluminescence
MTS	3-(4,5-dimethylthiazol-2-yl)-5-(3-carboxymethoxyphenyl)-2-(4-sulfophenyl)-2H-tetrazolium
DCFADA	2',7'-di-chlorodihydrofluorescein diacetate
DCF	2',7'-Di-chlorofluorescein
DMSO	Dimethyl sulfoxide
HBSS	Hank's balanced salt solution
LAR	Leukocyte common antigen related
FN	Fibronectin
IG	Immunoglobulin
IRES	Internal ribosome entry site
ICC	Immunocytochemistry
IB	Immunoblotting
WT	Wild type
NCAM	Neural cell adhesion molecule
STAT3	Signal transducer and activator of transcription 3
VA	Sodium orthovanadate
RET	Rearranged during transfection tyrosine kinase
SEM	Standard error of the mean

SD	Standard deviation
EHDH	Sodium etidronate
PAO	Phenylarsine oxide
pV(phen)	Sodium oxodiperoxo(1,10-phenanthroline)vanadate(V)
qPCR	Quantitative PCR
CML	Chronic myeloid leukaemia
NEM	N-ethylmaleomide
tTA	Tetracycline transactivator
TRE	Tetracycline response element
4-OHT	4-Hydroxytamoxifen
DHR	Dihydrorhodamine
PE	Phosphatidylenimine
GSK3β	Glycogen synthase kinase 3β
PP2A	Protein phosphatase 2A
S6K1	S6 kinase 1
TET	Tetracycline
TRAIL	Tumour necrosis factor (TNF)-related apoptosis-inducing ligand
MCB	Monochlorobimane
Myr	Myristoylated
DN	Dominant negative
RT-qPCR	Real-time qPCR
HKGs	House-keeping genes
CRC	Colorectal cancer
GBM	Glioblastoma multiforme
DNA	Deoxyribonucleic acid
RNA	Ribonucleic acid
RNAi	RNA interference
siRNA	Short-interfering RNA
TH	Tyrosine hydroxylase

List of figures and tables

Chapter 1.

Chapter 2.

Chapter 3.

Chapter 4.

Chapter 5.

Chapter 6.

Chapter 1. General introduction

1.1. Neuroblastoma: Clinical presentation and biological attributes

1.1.1. Incidence and outcome

Neuroblastoma (NBL) was first described independently over a century ago by the physicians Robert Hutchison, William Pepper and James Homer Wright (Rothenberg et al., 2009) and has been the subject of an intense amount of research culminating in fascinating key discoveries (See timeline accompanying (Maris, 2010)), expertly reviewed elsewhere (Brodeur, 2003; Janoueix-Lerosey et al., 2010; Maris, 2010; Maris et al., 2007).

NBL is the most common and deadly extracranial solid tumour of childhood, accounting for 7.8% of paediatric cancers diagnosed under the age of 15, with an incidence rate of 10.2 cases per million children in this age bracket (Goodman et al., 1999). NBL is also the most common cancer diagnosed within the first year of life, accounting for 28% of infant cancers with an incidence of 65 per million infants (**Figure 1.1.1**) (Smith et al., 1999)

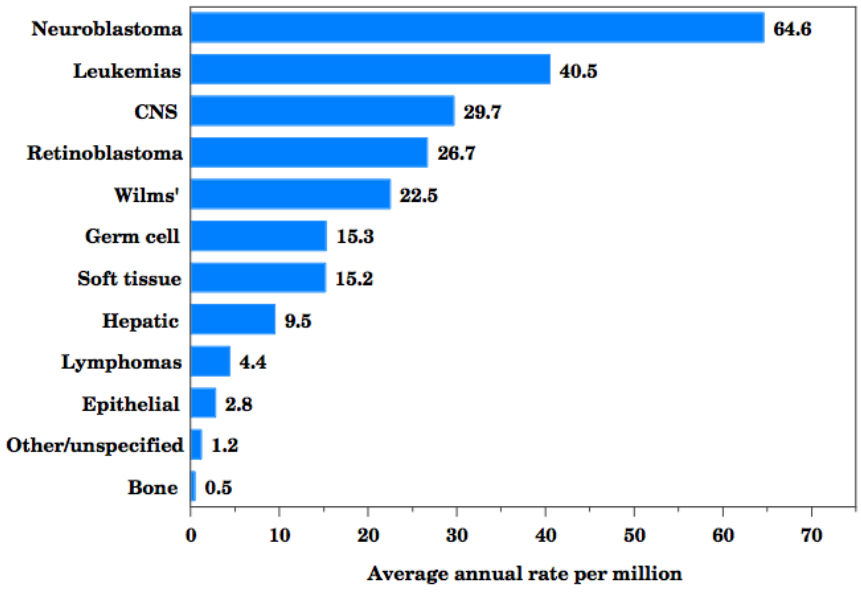

Figure 1.1.1. NBL is the most commonly occurring tumour of infancy. Graph shows annual incidence of tumours occurring within the 1st year of life in the US. Taken from (Gurney, Smith, Ross). (1999).

NBL is a malignancy of the sympathetic nervous system (SNS) (see below) and accounts for 97% of total SNS malignancies, representing 650 of 700 newly diagnosed children less than 20 years of age in the US each year (Goodman et al., 1999), with a prevalence of around 1 in 7000 live births (Brodeur, 2003). The median

age of diagnosis of NBL is 17 months (London et al., 2005), although the incidence rate of NBL more than doubles from 29/million to 64/million children diagnosed in the 2nd and 1st year of life respectively. Similarly, overall 16% of cases are diagnosed within the first month of life, and 41% within the first 3 months (Goodman et al., 1999).

NBL is also frequently deadly, accounting for 15% of fatalities resulting from paediatric malignancies (Brodeur, 2003). Event-free survival (EFS) rates have however improved from 52% between 1975-1977 to 74% between 1999-2005 (www.seer.cancer.gov). However, improvements in cure rates are most likely accounted for by the more benign forms of the disease, which present with favourable prognoses and require only surgical intervention and treatment of minimal residual disease. In fact, patient survival in those presenting with metastatic disease over the age of 1 is less than 40% (Matthay et al., 1999). Furthermore intensive multimodal therapy required in the case of treatment-resistant, aggressive disease frequently results in significant morbidities, including increased mortality rates and secondary neoplasms, infertility, as well as chronic health conditions and lowered rates of employment, marriage and socioeconomic status (Laverdiere et al., 2009).

1.1.2. Neural crest origin and clinical presentation

NBL has a sympathoadrenal (SA) lineage, where neural crest cells (NCC) are the putative cell of origin (Acosta et al., 2009; De Preter et al., 2006). The neural crest is a transitory population of cells that forms during development of the nervous system between the neural plate and the non-neural ectoderm. NCC are formed during the process of neurulation, when neural tissue folds inward to form the neural tube, generating regions at the borders of the neural plate referred to as the neural folds. A subset of cells at the dorsal region of the neural folds subsequently form a migratory cell population, the NCC, which migrates in particular routes to form a diverse lineage including craniofacial cartilage and bone, melanocytes, smooth muscle and the peripheral and enteric nervous system.

The fate of NCC is determined by a complex and dynamic interplay of intrinsic and extrinsic factors (reviewed by (Bronner Fraser, 1994). The trunk of the neural

tube gives rise to a subset of ventrally migrating NCCs that migrate through the anterior parts of the somites to form sensory and sympathetic neurons, chromaffin cells of the adrenal gland, peripheral glial cells and melanocytes (Loring and Erickson, 1987). Sympathetic neural cells and chromaffin cells develop from a putative fate-restricted SA progenitor that receives specification signals from bone-morphogenetic proteins in the dorsal aorta wall (Anderson and Axel, 1986). NCC that aggregate at the dorsal aorta undergo neuronal and catecholinergic differentiation resulting in the expression of tyrosine hydroxylase (TH) and dopamine β-hydroxylase, required for the synthesis of noradrenaline, and neuronal markers such as neurofilament and neuronal tubulin. SA cells are further specified by a host of transcription factors including the mammalian achaete-scute homolog 1, the paired homeodomain proteins Phox2a and Phox2b, Hand2 and GATA 2/3 (for reviews see (Cane and Anderson, 2009; Howard, 2005; Huber et al., 2009).

Thus the SA lineage is formed in a multistep process eventually resulting in paraspinal and extra-adrenal sympathetic ganglia, containing neurons characterized by the catecholaminergic neurotransmitter noradrenaline, of which NBL is believed to be an undifferentiated precursor. As a result, primary NBL tumours can present anywhere along the sympathetic chain (**Figure 1.1.2, A**). However the most common site of presentation is the abdomen (65%), normally centring on the adrenal medulla. Other sites include paraspinal sympathetic ganglia, at sites within the neck (5%), chest (20%) and pelvis (5%) (Janoueix-Lerosey et al., 2010).

The region of primary tumour formation often affects clinical presentation and side effects (Maris, 2010). For instance, paraspinal tumours frequently expand through the intraforaminal space resulting in compression of the spinal cord and paralysis (**Figure 1.1.2, B**). Tumours presenting in the neck or upper chest can cause damage to the SNS leading to Horner's syndrome, associated with ptosis (drooping of the eyelid), miosis (permanent-pupil contraction) and anhidrosis (decreased sweating on the affected side of the face). Furthermore, loco-regional invasion often results in tumours surrounding critical nerves and vessels such as the celiac-axis (a branch of the abdominal artery), preventing resection. Lastly, metastasis through the lymph nodes and hematopoietic system can result in colonization of secondary

tumours within the bone marrow and infiltration of bone cortex, as well as tumour formation in the liver (**Figure 1.1.2, C**).

1.1.3. Stratification and staging

Perhaps one of the most striking features of NBL is its extreme heterogeneity of presentation, with roughly an equal proportion of cases presenting with confined primary tumours easily treatable with surgical resection and minimal cycles of chemotherapy and cases presenting with advanced stage metastatic disease with unrelenting progression despite intense multimodal therapy. This clinical enigma has been recognized for 40 years, leading to the establishment of staging systems designed to stratify patients into risk group in order to base prognosis on clinical and biological factors (Evans et al., 1971).

Until recently, the most commonly used staging system was the International Neuroblastoma Staging System (INSS), which stratified patient prognosis based on clinical presentation and age, forming five subgroups of localised (stage 1 and 2), advanced locoregional (stage 3) and metastatic (stage 4 and 4S) (**Figure 1.1.3, A**) (Brodeur et al., 1993; Brodeur et al., 1988). Importantly stage 4S or 'the special stage' was recognized based on the bizarrely favourable prognosis (~75% 5 year EFS rate) of a subset (~5%) of advanced metastatic tumours, generally due to spontaneous remission (Evans et al., 1971). Notably patients under the age of 1 generally present with a favourable prognosis and low stage tumours, whereas those over one generally present with metastatic, treatment-resistant NBL (**Figure 1.1.3, B**).

Thus broadly speaking tumours commonly present as either locally manageable, low-risk with a favourable prognosis or highly malignant, high-risk with an unfavourable prognosis, aptly termed by the preeminent paediatric oncologist Audrey Evans as 'the goodies and the baddies' (Wellstein and Toretsky, 2011). Thus the basis of this clinical heterogeneity has focused on biological and genetic events stratifying these distinct subgroups.

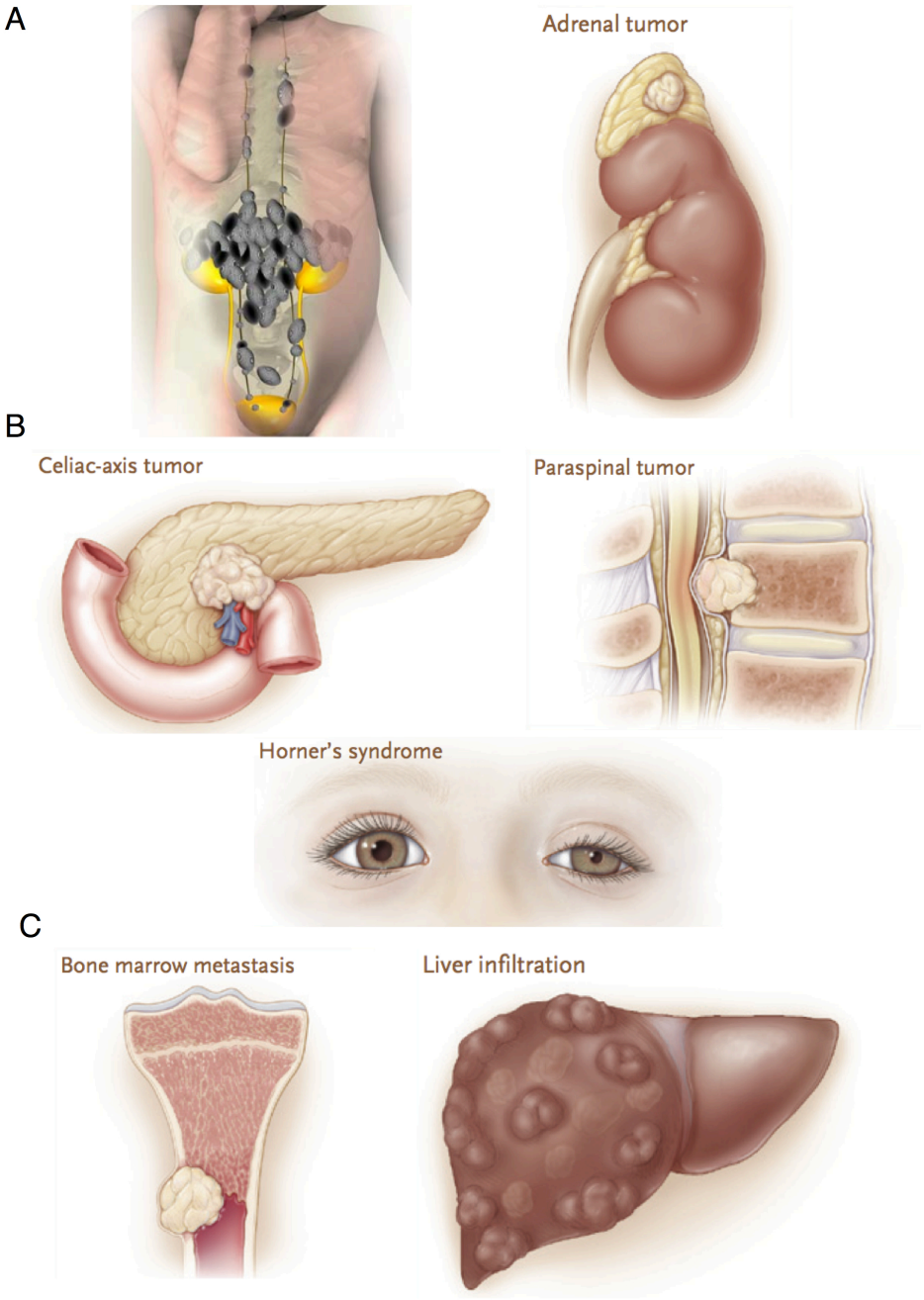

Figure 1.1.2. Clinical presentation of NBL. Primary NBL tumours occur anywhere within the sympathetic chain (e.g. adrenal medulla) **(A).** Primary tumours commonly result in secondary risk factors including surrounding vessels/nerves, spinal cord compression and degeneration of the SNS causing Horner's syndrome **(B)**. Tumour metastases infiltrate bone marrow/cortex via the hematopoietic system and liver especially in stage 4S (see below) **(C)**. Modified from (Johnsen et al., 2009; Maris, 2010).

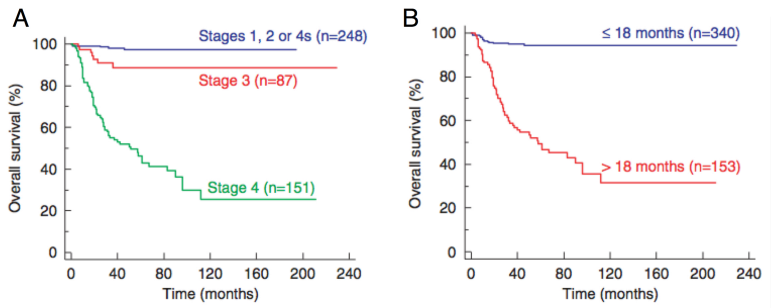

Figure 1.1.3. Prognostic stratification in NBL. Kaplan-Meier survival curve illustrating EFS of NBL tumours divided into stages (**A**). Prognosis also differs dramatically based on age at presentation (**B**). Taken from (Janoueix-Lerosey et al., 2010).

1.1.4. Genomic aberrations

The broad heterogeneity exhibited by NBL likely reflects underlying differences in tumour biology. For instance, cytogenetic abnormalities reflected in gross genomic patterns are highly predictive of patient outcome (Janoueix-Lerosey et al., 2009). Large-scale genomic application of the *MYCN* proto-oncogene at 2p24, observed in around 20% of NBL, is associated with treatment failure and unfavourable prognosis (Brodeur et al., 1984; Seeger et al., 1985), and is currently the only genetic-based prognostic marker allowing patient stratification (see below).

Numerical alterations resulting in whole-chromosome gains and losses (ploidy variations) are also an established means of stratification (**Figure 1.1.4**). Whole chromosomal gains resulting in a near-triploid or even pentaploid DNA index are associated with favourable tumours, whereas diploid DNA indices are associated with unfavourable tumours and treatment failure, with the former constituting >90% survival rates in patients below the age of 2 years (Look et al., 1991). Whole copy number variations occur exclusively without associated segmental alterations (see below) or genomic amplification (Janoueix-Lerosey et al., 2009; Kaneko et al., 1999). Triploidy has been suggested to result from endoreduplication or endomitosis, generating cells with one or two normal alleles of a tumour-suppressor gene homozygously deleted in diploid cells, exerting a suppressor effect resulting in low malignancy (Kaneko and Knudson, 2000).

One of the main features of unfavourable tumours is the presence of structural chromosomal aberrations (**Figure 1.1.4**) (Stallings et al., 2007) that are again correlated with amplification of Mycn, patient age and treatment failure

strongly predicting relapse (Janoueix-Lerosey et al., 2009). The best characterized of these are deletions of 1p36 and 11q23 (Schleiermacher et al., 1994) and gain of 17q23 (Bown et al., 1999), resulting from focal, acquired copy number variations associated with unbalanced translocation. Loss of 11q generally occurs in the absence of Mycn amplification, while 1p loss/17q gain is associated with this event.

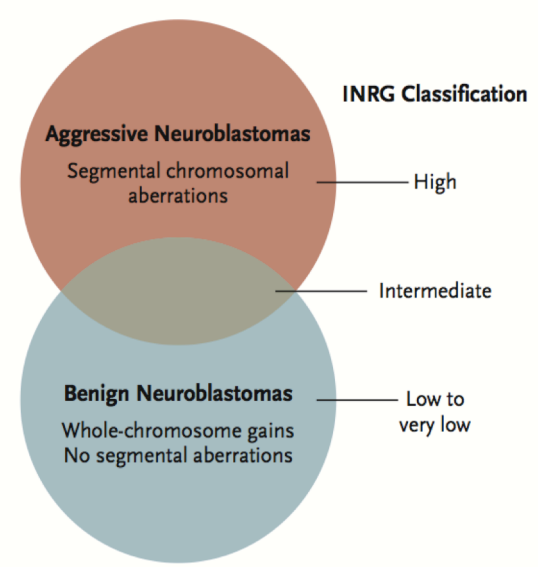

Figure 1.1.4. Genomic aberrations and prognosis. Good and poor prognosis are associated with whole chromosome gains and an absence of structural variations and diploidy with segmental alterations, respectively**.** Taken from (Maris, 2010).

1.1.5. Specific genetic lesions

Despite the evidence of chromosomal aberrations largely accounting for clinical behaviour of NBL, to date very few *bona fide* mutations in cancer genes have been identified. Thus the discovery by 4 independent groups of activating mutations in anaplastic lymphoma kinase (ALK) occuring in both familial and sporadic cases of NBL represents an exciting step in the understanding of NBL pathogenesis (Chen et al., 2008; George et al., 2008; Janoueix-Lerosey et al., 2008; Mossé et al., 2008).

These studies confirmed germline and somatically acquired mutations in the *ALK* gene, identifying 3 types of missense mutation, with the most frequent R1275Q, since shown to impair receptor trafficking (Mazot et al., 2011). Since then more than 50 mutations have been characterized in 680 sporadic cases, representing 8% of examined tumours (Janoueix-Lerosey et al., 2010), occurring at higher frequency in advanced stage disease and associated with Mycn amplification (De Brouwer et al.,

2010). ALK is upregulated in metastatic/highly malignant tumours (Passoni et al., 2009) and downregulated by retinoic acid (RA) treatment correlating with apoptosis (Futami and Sakai, 2010), making it an attractive target for selective therapy in NBL (Wellstein and Toretsky, 2011).

Another gene shown to be mutated in familial NBL is the paired like homoebox gene *PHOX2B* located at 4p12. Numerous missense and frameshift mutations have been identified as predisposing mutations in cases of familial NBL (Perri et al., 2005; Raabe et al., 2008). Although *PHOX2B* has been shown to contribute to a proliferative/undifferentiated phenotype in SA progenitors (Reiff et al., 2010), its contribution to NBL remains unclear due to the rare rate of somatic mutations. Lastly, the gene encoding neurofibromin 1 (NF1) represents an NBL tumour suppressor (Hölzel et al., 2010), where loss of NF1 predicts insensitivity to RA and poor outcome *in vivo* by repressing the activity of the transcriptional coactivator of RA receptors ZNF423 through activation of Ras-MEK signalling.

In sum only a handful of genes have been shown to functionally play a role in NBL pathogenesis, thus highlighting a need for increased identification of genetic contributing factors and treatment targets.

1.1.6. Trks and NBL prognosis

The tropomyosin related kinases (Trks) are a family of receptor tyrosine kinases consisting of TrkA, TrkB and TrkC. The Trks signal through their ligands nerve-growth factor (NGF), brain-derived neurotrophic factor (BDNF) and neurotrophin 3 (NT-3), respectively, controlling a diverse range of functions responsible for neuronal differentiation (Benitogutierrez et al., 2006). Trks are well-established mediators of biological response in NBL, whose expression pattern is significantly associated with outcome (Brodeur et al., 2009; Eggert et al., 2000; Schramm et al., 2005).

High expression of TrkA is strongly associated with favourable factors including young age and absence of Mycn amplification (Nakagawara et al., 1992; Nakagawara et al., 1993). Expression of TrkA is commonly seen in low stage tumours, and can inhibit growth (Lucarelli et al., 1997), decrease the expression of Mycn (Woo et al., 2004) and cause differentiation in the presence of NGF (Nakagawara and Brodeur, 1997). Here culturing explanted TrkA-expressing NBL cells in the absence of

NGF led to apoptosis after 7 days, suggestive of TrkA expression as a determinant of NBL spontaneous regression (Nakagawara, 1998). A truncated version of TrkA (TrkAIII), resulting from alternative mRNA splicing, actually promotes tumorigenesis, antagonizing TrkAI/NGF signalling (Tacconelli et al., 2004).

Conversely, expression of TrkB is strongly associated with unfavourable prognostic markers and poor response, where the addition of the TrkB ligand BDNF promotes the survival of undifferentiated neuroblasts (Nakagawara et al., 1994). High TrkB expression contributes to chemotherapy resistance (Ho et al., 2002) and promotes tumour angiogenesis (Eggert et al., 2002) and invasiveness (Hecht et al., 2005). Thus the expression pattern of Trks conforms to the notion of stratified biological markers underlying differences between unfavourable and favourable prognosis in NBL (**Figure 1.1.5**).

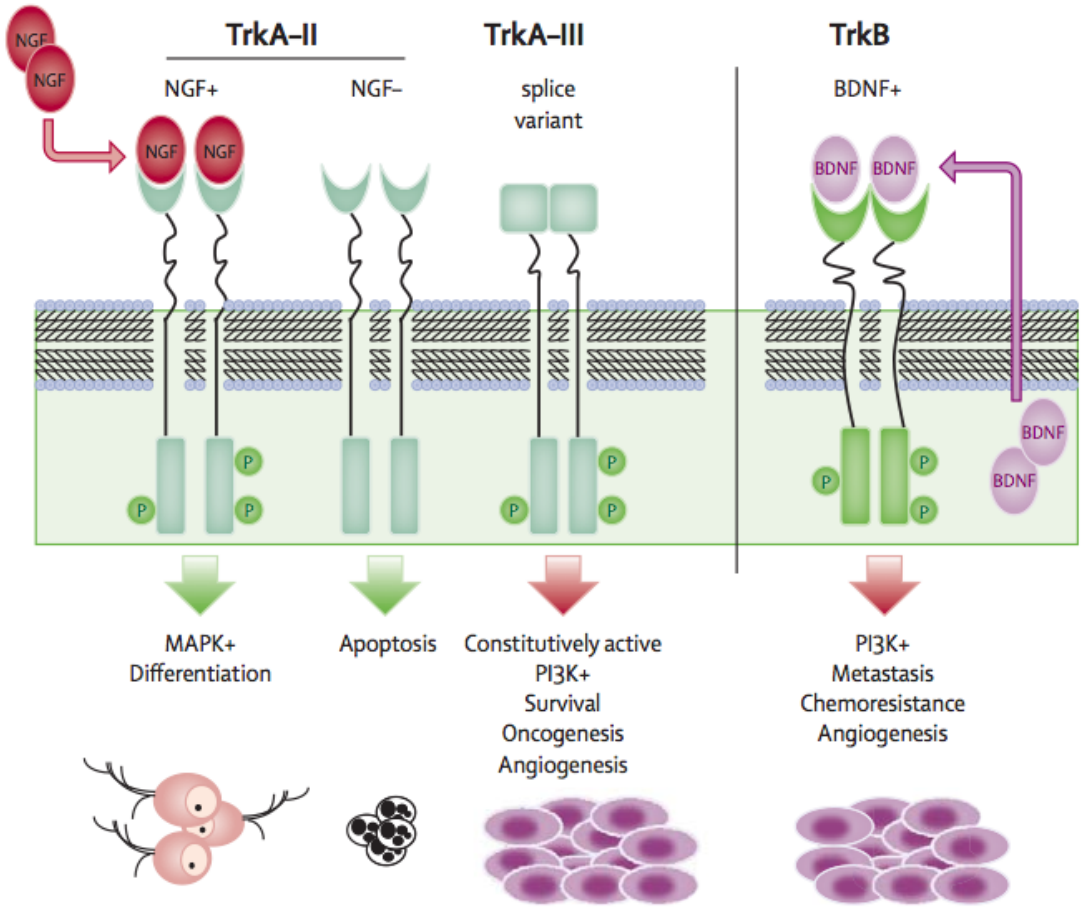

Figure 1.1.5. Trk expression stratifies with biological and clinical features of prognosis. Taken from (Maris et al., 2007).

TrkC likely functions in a similar manner to TrkA, and is expressed in a subset (25%) of TrkA expressing tumours and weakly associated with positive outcome (Brodeur et al., 1997). Thus Trk receptors represent an attractive therapeutic target given their ability to confer survival in the case of TrkB. As such multiple selective Trk inhibitors have been developed including AZ623 and CEP-751, with efficacy against NBL xenografts in preclinical testing, and are currently in phase 1 trials (Evans et al., 2001; Evans et al., 1999; Zage et al., 2010a). In sum the overall biology of NBL suggests a model whereby at least two subtypes of disease exist (**Figure 1.1.6**).

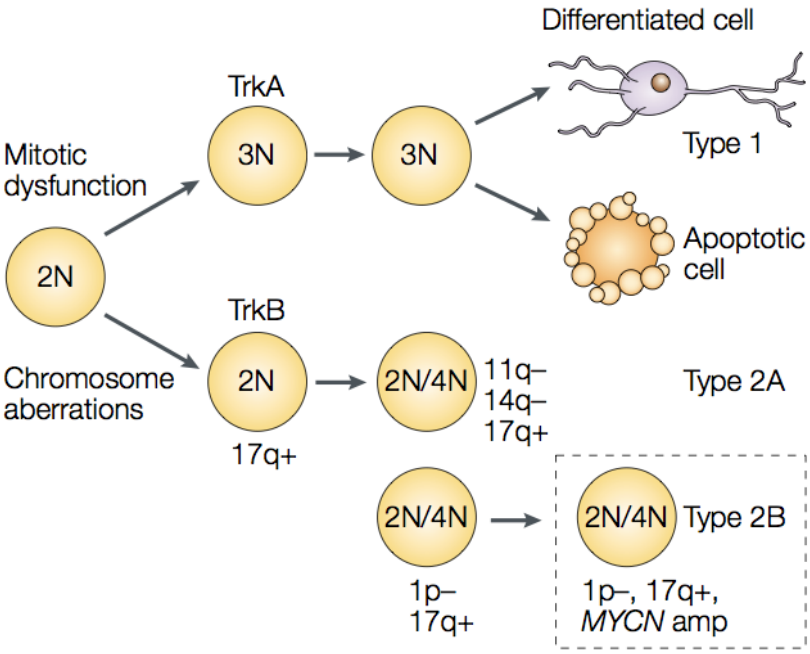

Figure 1.1.6. Unfavourable and favourable NBL tumours represent distinct biological subtypes. Tumours with favourable prognoses harbour few structural chromosomal abnormalities but do exhibit whole chromosome gains. These tumours often express TrkA making them prone to differentiation or apoptosis. Conversely tumours with unfavourable prognoses exhibit gross chromosomal abnormalities including loss of 1p, gain of 11q and 17q and amplification of Mycn, as well as expression of TrkB. Taken from (Brodeur, 2003).

1.1.7. The status of the p53 pathway

Mutation or functional inactivation of the tumour suppressor gene *TP53* encoding p53 are synonymous with human cancer, occurring in practically all known cancers at a very high frequency (Goh et al., 2010; Junttila and Evan, 2009). A surprising feature of NBL is that p53 mutations are very rare (<2%) at diagnosis (Tweddle, 2003), and p53 remains functional in both differentiated and undifferentiated NBL (Chen et al., 2007) as well as contributing to chemotherapy-induced apoptosis and

tumour regression *in vivo* (Chesler et al., 2008). However, NBL cells can circumvent the p53-driven tumour barrier by deregulation of the $p14^{ARF}$-MDM2-p53 axis, including upregulation of MDM2 and BMI1 and cytoplasmic sequestration of p53, all of which negatively regulate the activity of p53 (Van Maerken et al., 2009). Similarly, mutational inactivation of p53 occurs frequently following cytotoxic therapy (Tweddle et al., 2001) and represents a mechanism of patient relapse (Carr-Wilkinson et al., 2010), causing resistance to therapy (Keshelava et al., 2000).

Thus reactivating the p53 pathway is considered a therapeutic strategy in NBL. For example, positively increasing the activity of p53 with the small molecule MDM2 inhibitor nutlin-3 causes cytotoxicity and growth arrest (Van Maerken et al., 2006). However this approach may only be applicable to tumours with wild-type p53, and may require increased activity of $p14^{ARF}$ to achieve full effects (Van Maerken et al., 2011). Lastly, it should be pointed out that activation of p53 has also been suggested to be responsible for toxic side effects of chemotherapy where inhibiting its function may actually be desirable (Komarov et al., 1999; Morita et al., 2010).

1.1.8. Retinoic acid treatment

The carboxylic acid lipophillic small molecule RA is a derivative of the alcohol form of vitamin A (retinol), and is crucial for cellular differentiation during embryogenesis (Duester, 2008; Niederreither and Dollé, 2008). RA exerts its effects through binding to nuclear receptors of the retinoic acid (RARα, RARβ, RARγ) and retinoid X (RXRα, RXRβ, RXRγ) families of retinoic acid receptors. Here receptor-ligand binding initiates DNA binding, directly regulating the transcription of target genes.

Seminal studies by Neil Sidell in the 1980s revealed RA to be a highly effective differentiation agent in NBL cells, where treatment for as little as 48 hours can give rise to highly differentiated neuronal-like cells (Abemayor and Sidell, 1989; Sidell et al., 1983) and is considered a gold standard in NBL differentiation (Clagett-Dame et al., 2006). RA was later shown to mediate neuronal differentiation by inducing expression of TrkB and TrkA at nano and micromolar concentrations, respectively (Kaplan et al., 1993; Lucarelli et al., 1995), and sequential treatment with TrkB can enhance differentiation (Encinas et al., 2000b). RA also decreases the expression of

Mycn (Thiele et al., 1985), and effectively inhibits growth (Shea et al., 1985), causing decreased proliferation and mitotic arrest (Melino et al., 1997). In some circumstances RA has also been shown to cause apoptosis, for instance in SK-N-DZ NBL cells, due to constitutively high expression of RARα (Melino et al., 1997; Nagai et al., 2004).

Clinical trials conducted over the past ten years with RA on minimal residual disease (MRD), Showed that administration of RA following chemotherapy or bone marrow transplantation significantly improved EFS in children with progressive NBL (Matthay et al., 1999; Park et al., 2009; Villablanca et al., 1995). Thus RA has become a standard inclusion of the NBL therapeutic regimen, and retinoid derivatives have been developed to build on the success of RA (Reynolds et al., 2003; Villablanca et al., 2006).

However, there are still unresolved issues over RA dosage, toxicity and resistance (Maris, 2010), and its biological mediators are still unclear despite examinations of both transcriptional (Yuza et al., 2003) and signalling (Niles, 2004) changes following RA treatment. Among these studies, RA-induced differentiation has been shown to require PI3K/Akt (López-Carballo et al., 2002), PKC (Miloso et al., 2004), mTOR (Zeng and Zhou, 2008), JNK (Yu et al., 2003), presilin 1/Wnt (Uemura et al., 2003), GSK-3β (Castaño et al., 2010) and RET (Oppenheimer et al., 2007). RA also either upregulates or activates tissue transglutaminase/Rho GTPases (Joshi et al., 2006; Singh et al., 2003) and Erk (Singh et al., 2003), although the latter may be redundant (Miloso et al., 2004). Lastly, other transcriptional changes such as decreased expression of cyclin D1 and increased expression of cyclin-dependent kinase inhibitors such as $p27^{KIP1}$ are important for RA mediated growth arrest (Matsuo and Thiele, 1998; Niles, 2004). In sum, RA alters the expression/activation of multiple signalling pathways and genes involved in cell-cycle control (**Figure 1.1.7**).

Given that a number of transcriptional/transcriptional changes are crucial for RA-induced differentiation, genetic downregulation of such components may underlie therapeutic resistance to RA. For example, a recent RNAi screen found that the transcription factor ZNF423 is crucially required for RA differentiation by associating with RARα/RXRα (Huang et al., 2009), with low *ZNF423* expression

underlying treatment resistance in NBL patients with poor prognosis. The same group showed that loss of the tumour-suppressor *NF1* causes activation of Ras/MEK signalling suppressing ZNF423 (Huang et al., 2009). Combined loss leads to very poor prognosis, and responsiveness to RA can be improved with combined inhibition of MEK signalling. In addition to overcoming resistance to RA with targeted therapy, an alternative approach has been to augment the effects of RA with combination differentiation agent treatment. For instance phenylacetate (Sidell et al., 1995), vasoactive intestinal peptide (Chevrier et al., 2008), BDNF (Encinas et al., 2000a) and Notch-blocking gamma secretase inhibitors (Ferrari-Toninelli et al., 2010) all synergise with RA.

Effect of retinoic acid on signaling pathways in various tumor types

Tumor type	AP-1	Erk1/2	JNK	P38	PI-3K/Akt
Breast	↓	↓	↑	↑	↓
Squamous	↓	–	–	–	–
Lung	↓	–	↓	–	–
Neuroblastoma	↑	↑	↑	–	↑
Teratocarcinoma	↑	–	↑	–	–
Melanoma	↑	–	–	↓	–

Figure 1.1.7. Alteration of signalling pathways by RA in human cancers. The activation or inhibition (upwards and downwards arrows respectively) of major signalling pathways is cell type dependent.

In sum, though RA is a highly effective differentiation agent *in vitro* as well as a significant component of NBL therapy in the treatment of MRD, a number of issues such as failure to fully eradicate undifferentiated NBL cells, toxicity and treatment resistance have initiated efforts to improve its action, such as targeting of 'resistance-genes' and augmentation of differentiation.

1.2. Amplification of Mycn is the major negative prognostic marker in neuroblastoma

Among the genetic markers available for stratification of NBL prognosis, amplification of Mycn is by far the most robust (**Figure 2.1.1**) (Cohn and Tweddle, 2004). Mycn amplification was originally identified as correlative with advanced stage disease and tumour aggressiveness (Brodeur et al., 1984; Seeger et al., 1985), and extensive research has demonstrated mechanisms of amplification, biological consequences, and oncoprotein targets.

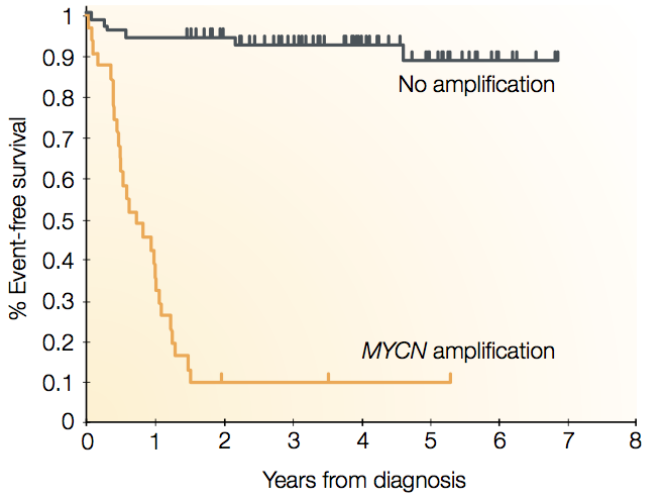

Figure 1.2.1. Amplification of Mycn and prognosis. Kaplan-Meier survival curve showing patients under the age of 1 with metastatic NBL. Taken from (Brodeur, 2003).

1.2.1. Mechanisms and adverse consequences of Mycn amplification

Genomic amplification of chromosomal DNA harbouring the *MYCN* gene on the distal short arm of chromosome 2 (2p) generates amplicons up to 1mb, and results in dramatically increased gene and protein expression. Amplification manifests as extrachromosomal double minute (DM) bodies or chromosomally integrated homogenously staining regions (HSRs) (**Figure 1.2.1**) (Brodeur and Seeger, 1986; Tanaka and Yao, 2009).

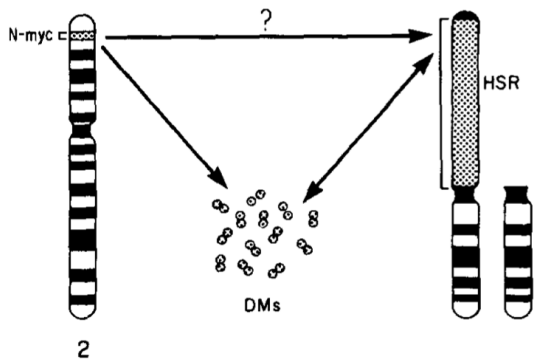

Figure 1.2.2. Manifestation of Mycn amplification. Increases in gene copy number result in homogenously staining regions and extrachromosomal double-minute bodies when visualized with fluorescence *in situ* hybridization).

MYCN encodes a 60-63kDa protein that functions as a basic helix-loop-helix transcription factor, forming heterodimeric complexes with MAX family proteins to regulate transcription of numerous target genes (Adhikary and Eilers, 2005). The adverse effects of Mycn amplification are well documented (Schwab, 2004). Mycn directly promotes tumorigenesis, causing oncogenic transformation of mammalian cells (Schwab et al., 1985) and stimulating autocrine survival loops by upregulating growth-factor receptors. This induces proliferation (Schweigerer et al., 1990), inhibition of cell-cycle arrest (Bell et al., 2006), genomic instability (Sugihara et al., 2004), cellular motility and invasiveness (Goodman et al., 1997), promotion of tumour angiogenesis (Fotsis et al., 1999), circumvention of immune response (Song et al., 2007), and therapeutic resistance (de Tudela et al., 2010). Furthermore, Mycn can directly drive NBL tumour formation, where transgenic mice conditionally expressing Mycn under the control of the TH promoter form tumours of the sympathetic nervous system that highly recapitulate human NBL in terms of both histology and pathology (Weiss et al., 1997). Here tumours form at a high penetrance (~33% hemizygous; 100% homozygous on a 129SvJ background) albeit exhibiting strain-dependent variable penetrance (Teitz et al., 2011). TH-Mycn-driven tumours arise in sympathoadrenal paraspinal ganglia, however surprisingly primary tumours are never observed in the adrenal medulla, in contrast to human tumours, a caveat that remains to be explained (Teitz et al., 2011). The TH-Mycn mouse is used as an important tool in the validation of novel therapies, in that tumours are reminiscent of aggressive NBL and retain many of the associated genetic aberrations of high-stage disease (Chesler and Weiss, 2011). Lastly the TH-Mycn mouse exhibits neuroblast hyperplasia one week after birth, which in contrast to mice with a normal background fails to regress, forming tumours by 6 weeks and showing a strong resistance to neurotrophin withdrawal, suggesting a lack of normal neural crest deletion underlying tumour formation (Hansford et al., 2004).

1.2.2. Survival and death: The paradox of Mycn

It is well accepted that Mycn can induce apoptosis both in embryonic development and in cancer, likely depending on signal intensity and cellular context (Murphy et al., 2008; Soucek and Evan, 2010). In NBL, overexpression of Mycn in non-Mycn

amplified cells enhances sensitivity to chemotherapeutic induced-cytotoxicity (Fulda et al., 2000; Fulda et al., 1999). Thus concomitant inactivation of apoptotic signalling is a prerequisite for tumour cell survival in the presence of increased Mycn expression (Hogarty, 2003). Mycn-induced apoptosis occurs through a putative DNA damage response, where Mycn stabilizes the p53 kinase HIPK2, causing phosphorylation of p53 (Petroni et al., 2011), implying that reactivating p53 could engage this response. Conversely, Mycn expression in non Mycn-amplified NBL cells results from reactivation of p53 signalling by MDM2 inhibition using nutlin-3, resulting in cytotoxicity induced by doxorubicin (Peirce, 2009). p53 itself is a direct transcriptional target of Mycn (Chen et al., 2010a), although the negative regulator of p53 MDM2 is also positively upregulated by Mycn (Slack et al., 2005).

1.2.3. Targets of Mycn and the search for negative regulators

The Mycn transcription factor is clearly an obvious therapeutic target, but it has historically been regarded as undruggable given the difficulty of disrupting protein-protein or protein-DNA interactions. Instead efforts have focused on the identification of Mycn targets themselves (Bell et al., 2010), as well as enzymatic regulators of Mycn stability and expression (Gustafson and Weiss, 2010). This approach is particularly appealing due to the plethora of kinase inhibitors developed in recent years.

Mycn controls the expression of numerous genes related to clinical behaviour in NBL. Among these Mycn increases the expression of the cellular retinoic acid-binding protein II (CRABP-II), thus promoting motility (Gupta et al., 2006), downregulates Dickkopf-1, thereby inhibiting proliferation (Koppen et al., 2007), upregulates microRNAs capable of repressing oestrogen receptor (alpha) expression and suppressing differentiation (Lovén et al., 2010), and increases the expression of the oncogenic survival factor focal adhesion kinase (FAK) (Beierle et al., 2007). However, while inhibiting Mycn targets may in some circumstances abrogate the effects of Mycn overexpression, there is likely to be a high level of redundancy given the very high number of potential Myc/Max dimer target genes (possibly ~25% of known promoters). Thus reducing Mycn protein levels is perhaps a more effective strategy.

The stability of Mycn depends on reversible phosphorylation by multiple enzymes (**Figure 1.2.3**) (Gustafson and Weiss, 2010). Mycn is stabilized by phosphorylation at S62, controlled by the cyclin-dependent kinase 1 (CDK1) (Sjostrom, 05). Phosphorylation at S62 promotes interactions with a complex containing Axin1, Pim1, PP2A and GSK3β (Arnold et al., 2009). Phosphorylation of Mycn at T58 is achieved by GSK3β, downstream of PI3K/Akt/mTOR. Protein-phosphatase 2A (PP2A) dephosphorylates Mycn at S62, where monophosphorylated T58 targets Mycn for ubiquitination and degradation (Arnold et al., 2009). The PI3K/Akt/mTOR pathway has several roles in contributing to the stabilization of Mycn. Firstly Akt, which is activated by PI3K, phosphorylates and inactivates GSK3β and stabilizes Mycn through blockage of T58 phosphorylation. Akt also phosphorylates and inhibits tuberous sclerosis 2 (Tsc2) that binds to Tsc1 allowing the GTPase Rheb to stimulate mTOR as part of the mTORC1 complex, resulting in downregulation of PP2A and further stabilizing Mycn. Inhibitors of PI3K result in Mycn degradation, a process dependent on phosphorylation (Chesler et al., 2006).

The cell cycle and spindle assembly regulator Aurora A kinase also stabilizes Mycn through both direct and ubiquitin ligase-mediated interactions (Otto et al., 2009), although this function is independent of Aurora A kinase activity and thus not directly affected by Aurora A inhibitors (Maris, 2009). Significantly, RA downregulates Mycn (Thiele et al., 1985), however clearly Mycn amplified tumours can circumvent RA induced-growth arrest as this drug fails to achieve tumour remission and prevention of relapse in all cases. Thus while targeting of Mycn is undoubtedly an important strategy in NBL therapy, it may prove disappointing, especially if addiction to Mycn does not underlie Mycn amplification in NBL (Weinstein, 2002; Weinstein and Joe, 2008).

1.3. Aberrant regulation of protein phosphorylation in human cancer and neuroblastoma

1.3.1. Constitutive activation of kinases as a hallmark of cancer

Deregulated cell growth resulting from aberrant intracellular signal transduction is a hallmark of all neoplasms (Hanahan and Weinberg, 2000). Constitutive activation of

protein tyrosine-kinases (PTKs) represents an overwhelming majority of such perturbations (Blume-Jensen and Hunter, 2001). Over-activation of PTKs can occur by gene amplification, overexpression or genetic mutations, but generally results in constitutive enzyme activity and loss of autoinhibitory mechanisms that normally safeguard cells from neoplastic transformation. Among deregulated PTKs, receptor-tyrosine kinases (RTKs) form a major contributor, becoming activated often in the presence of increased amounts of their cognate ligand to generate autocrine growth- factor loops.

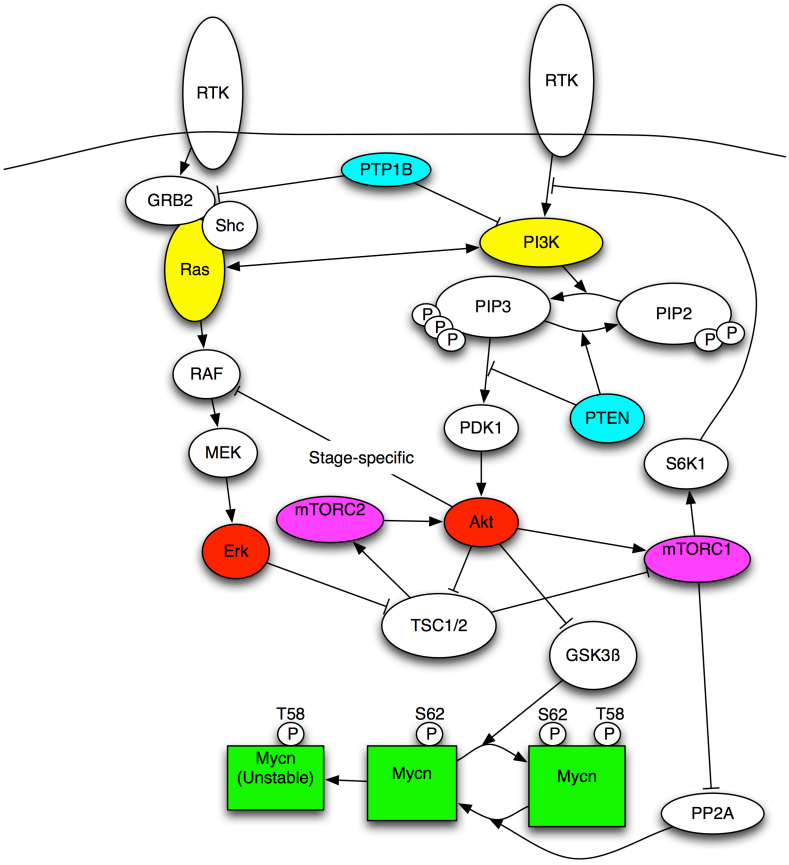

Figure 1.2.3. Signal transduction cascades regulating Mycn stability. Signalling downstream of receptor tyrosine kinases (RTKs) results in a number of changes altering Mycn phosphorylation. For instance Akt/mTOR-mediated inhibition of PP2A results in prevention of monophosphorylation at T58, an event that primes Mycn for degradation. Similarly Akt-mediated inhibition of GSK3β prevents phosphorylation at T58, also stabilizing Mycn.

RTKs recruit adaptor proteins containing SRC homology 2 (SH2) and phosphotyrosine binding (PTB) domains, and also activate downstream PTKs, triggering signal transduction cascades (Zwick et al., 2001). As a result a wealth of research has been

conducted on the role of aberrant PTK signalling, identifying key enzymes suitable for therapeutic intervention (Gschwind et al., 2004; Tibes et al., 2005; Traxler, 2003).

1.3.2. FAK and SRC as regulators of cell survival

Both the FAK family and c-SRC (SRC) non-receptor tyrosine kinases have been heavily implicated in human cancer, controlling vital processes such as cell motility and invasiveness, proliferation and survival (Brunton and Frame, 2008; Mitra and Schlaepfer, 2006) (**Figure 1.3.1**). c-SRC is the cellular orthologue of viral-(v)-SRC, the first viral oncogene to be identified (Moore and Chang, 2010), and has been implicated in numerous processes contributing to tumour maintenance and progression (Yeatman, 2004). It is commonly overexpressed and activated in cancers, most notably breast and colorectal tumours (Irby and Yeatman, 2000). SRC cooperates with growth factor receptors such as epidermal growth factor receptor (EGFR) to increase proliferation and invasiveness (Brunton et al., 1997), and stimulates cell spreading and motility by influencing integrin attachment (Jones et al., 2002). Recently SRC activation was observed to occur as a compensatory mechanism of resistance to chemotherapeutic inhibition of alternative oncogenic survival pathways after prolonged treatment with the commonly used ERBB2 inhibitor trastuzumab (Zhang et al., 2011). Here one of the causes of SRC activation was by mutational inactivation of PTEN, a common feature in cancer (see below), suggesting that this tumour-suppressive phosphatase is capable of negatively regulating SRC activity.

SRC is regulated by multiple protein tyrosine-phosphatases (PTPs). The receptor type PTPα dephosphorylates SRC at its terminal tyrosine, positively regulating its activity (Zheng et al., 1992). SRC is also activated by the cytoplasmic PTPs Shp1 (Frank et al., 2004), Shp2 (Zhang et al., 2004) and PTP1B (Bjorge et al., 2000). In fact PTP1B was recently demonstrated to be crucial for ErbB2-mediated transformation due to its ability to activate SRC in breast epithelial cells (Arias-Romero et al., 2009). PTP-PEST has also been shown to negatively regulate events downstream of SRC activation by dephosphorylating Y416 preventing the phosphorylation of villin 1 (Mathew et al., 2008).

FAK is expressed at sites of integrin clustering or focal adhesions where it carries out protein-protein adaptor functions regulating scaffolding to the extracellular matrix (ECM). FAK regulates integrin adhesions, control of the actin-cytoskeleton and stimulation of cell migration by assembly/disassembly of focal adhesion complexes at cell leading and trailing edges, as well as growth factor signalling and proliferation/survival (Mclean et al., 2005). In line with this FAK is commonly upregulated and activated in human cancers (Weiner et al., 1993), correlating with metastasis and malignancy as well as patient prognosis. The roles of FAK are closely intertwined with that of SRC. Autophosphorylation of FAK at Y397 leads to recruitment and binding of SH2 domain containing proteins, most notably SRC itself causing SRC kinase activity (Schaller et al., 1994). Binding of SRC causes phosphorylation of FAK at Y576/77 further increasing its activity, as well as phosphorylating other tyrosine residues including Y925 allowing the binding of Grb2 and concomitant activation of the Ras/MAPK pathway (Schlaepfer and Hunter, 1996).

The best-documented consequence of FAK stimulation is the turnover of focal adhesions and cell-cell cadherin junctions, and control of dynamic actin structures, all contributing to enhanced cell motility and invasiveness. However, upregulation of FAK also prevents apoptosis following detachment from the ECM (anoikis) in kidney epithelial cells. This provides indirect evidence for a role of FAK in promoting the survival of cancer cells following epithelial to mesenchymal transitions (EMT), which occurs prior to metastatic spread (Frisch et al., 1996).

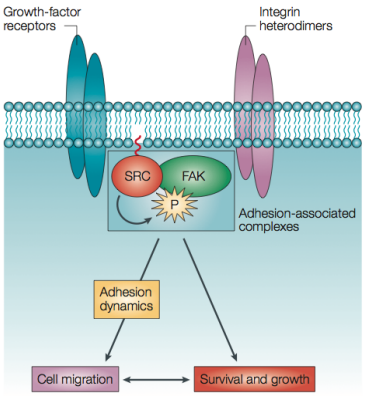

Figure 1.3.1. **Generalized role of FAK and SRC in human cancer.** Co-activation of FAK/SRC, both positively contributes to cell survival and motility by controlling adhesion dynamics. Taken from (Mclean et al., 2005).

Multiple lines of evidence have linked FAK/SRC to survival signalling in NBL. Dual inhibition of FAK and SRC increases NBL cell death by stimulating anoikis (Beierle et al., 2010). The same group demonstrated that FAK was a direct target of Mycn, which acted as a transcriptional activator causing upregulation of FAK after conditional expression of Mycn (Beierle et al., 2007; Madonna, 2010). As such, FAK is considered a promising target in NBL therapy (Gillory and Beierle, 2010). FAK also activates SRC/p130Cas to engage α5β1 and α4β1 integrin-mediated motility/invasion in NBL (Wu et al., 2008). SRC is involved in the differentiation of NBL cells (Bjelfman et al., 1990; den Hertog et al., 1993). Indeed, ligand independent activation of Trk receptors is blocked by SRC inhibition (Lee and Chao, 2001), and constitutively active SRC can enhance activation of TrkA by NGF and the resulting Erk-dependent differentiation (Tsuruda et al., 2004). However SRC dependent adhesion has been suggested to be facilitated by caspase 8-expression (Finlay and Vuori, 2007), which positively contributes to migration and metastasis in NBL (Barbero et al., 2009).

1.3.3. The Ras/RAF/MEK/Erk and PI3K/Akt pathways

Among the many intracellular signalling cascades aberrantly regulated in human cancer, both the Ras/RAF/MEK/Erk (McCubrey et al., 2007) and the PI3K/Akt (Hennessy et al., 2005) pathways have perhaps the most crucial and broad involvement in neoplastic transformation and tumour maintenance. Indeed activating mutations in Ras, the first proto-oncogene to be identified (Tabin et al., 1982), occur in 20-30% of tumours (Downward, 2003). Similarly, mutations in the negative regulator of PI3K/Akt signalling PTEN occur in 50-80% of sporadic tumours (Salmena et al., 2008). Mutations in the downstream effectors of Ras, RAF and mitogen-activated protein kinases (MAPK)/Extracellular signal-related kinases (Erk) kinase (MEK), are frequently observed in a range of cancers, and the gene encoding PI3K *PIK3CA* is similarly subject to activating mutations as well as amplification, making multiple components of both pathways a dominant feature in cancer biology.

Activation of Ras GTPases by upstream activation of growth factor receptors such as EGFR can stimulate multiple effectors, including PI3K and the RAF family of

serine/threonine kinases, which in turn activate MEK 1/2 dual-specificity kinases, resulting in Erk stimulation (**Figure 1.3.2**). Phosphorylation and activation of Erk results in both cytoplasmic enzymatic interactions and nuclear-translocation/transcription factor binding. Erk has at least 160 substrates, with its activation resulting in diverse consequences of proliferation, survival, apoptosis and differentiation depending on cellular context (von Kriegsheim et al., 2009).

The phosphatidylinositol-3-kinase (PI3K) family of lipid and serine/threonine kinases have similarly diverse functions. Class IA PI3K enzymes form heterodimers with an inhibitory adaptor/regulator p85 and catalytic p110 subunit. The former is capable of binding and integrating signals from upstream RTKs as well as intracellular enzymes such as PKC, SHP1, Ras and SRC. PI3K phosphorylates phosphatidylinositol-4,-5-bisphosphate (Ptpins(4,5)P_2; PIP2),, generating the second messenger Ptpins(3,4,5)P_3 (PIP3), which binds plekstrin-homology (PH) domain-containing proteins, most notably Akt. Akt is then recruited to the membrane, undergoes conformational change and phosphorylation of T308 by phosphoinositide-dependent kinase 1 (PDK1) and phosphorylation at S473 by PDK2, causing full activation (**Figure 1.3.2**). Phosphate and tensin homologue deleted on chromosome 10 (PTEN) dephosphorylates the 3'OH group of PIP3, representing the negative regulator of Akt activity. Class IA PI3K has 4 isoforms (p110α, β, γ and δ), of which only α is mutated in cancer, although all are capable of sustaining proliferation (Foukas et al., 2010).

Akt1, Akt2, Akt3 are each activated by PI3K signalling with similar substrate preferences. However, each may serve different functions contributing to motility/invasion (Akt2), hormone independence (Akt3) and general cell growth (Arboleda et al., 2003). Akt can regulate cell survival by inactivating proapoptotic factors including the mitochondrial apoptotic enzyme BAD, Forkhead transcription factors and caspase 9, as well as upregulating antiapoptotic genes such as cyclic-AMP-response element binding protein (CREB) (Paez and Sellers, 2003). Akt can also stimulate mammalian target of rapamycin (mTOR) (**Figure 1.3.2**) to engage proliferation (Wendel et al., 2004). mTOR activates protein-synthesis machinery including ribosomal protein S6 kinases ($p70^{S6K}$) and 4E-binding proteins (4EBPs),

resulting in the release of the translation initiation factor eIF4E itself capable of antiapoptotic/transforming functions (Schmelzle and Hall, 2000).

Unlike many cancers of adulthood, mutations in *RAS* and hyperactivity of Erk have not been described in NBL (Maris et al., 2007). In fact H-Ras is generally regarded as a favourable marker in NBL, and has been suggested to cause autophagic cell death (see below) and thus spontaneous regression (Kitanaka et al., 2002). Similarly, Ras-mediated activation of Erk is responsible for p53-independent cell death occurring after treatment with the platinum based chemotherapeutic cisplatin (Woessmann et al., 2002), and in hydrogen peroxide-induced cell death (Ruffels et al., 2004). However, the fatty acid based-protein tyrosine phosphatase (PTP) inhibitor docasahexaenoic acid causes neuritogenesis of NBL cells via Erk activation mediated by reactive oxygen species (ROS) (Wu et al., 2009).

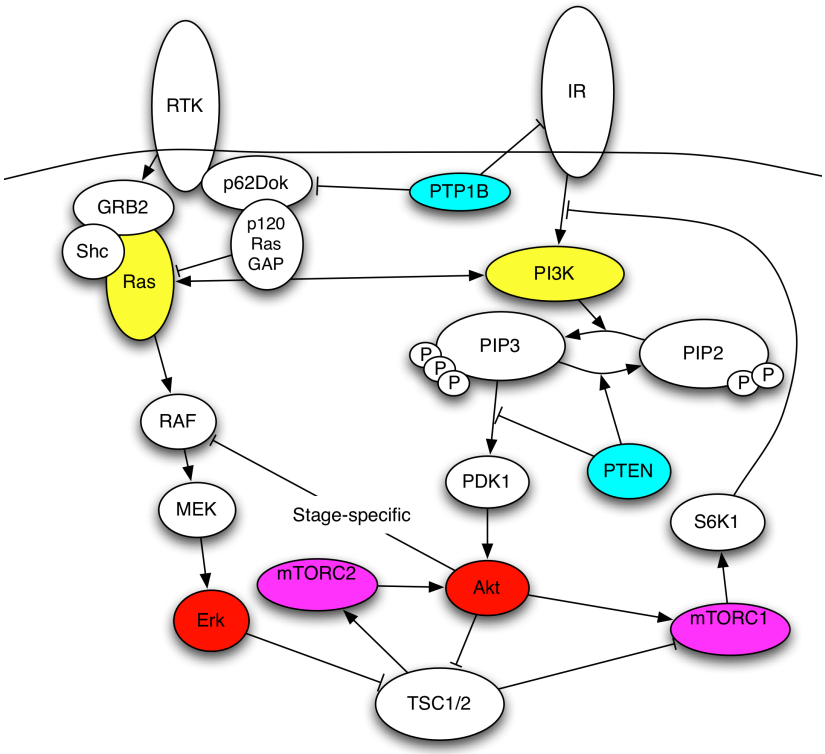

Figure 1.3.2. The Ras/RAF/MEK/Erk and PI3K/Akt/mTOR pathways. Growth factor mediated activation of RTKs leads to activation of Ras, in turn giving rise to Erk phosphorylation downstream of RAF/MEK. Similarly, activation of PI3K downstream of RTKs causes phosphorylation of PIP_2, leading to recruitment and activation of Akt via PDK1. Downstream activation of the mTOR complex 1 mediates negative feedback regulation of PI3K activity via phosphorylation of S6K1. PTPs exert both negative and positive regulation. For instance PTP1B dephosphorylates the insulin receptor (IR) RTK, attenuating PI3K activation, and also the Ras-inhibiting scaffold complex of p62Dok/p120RasGAP, promoting Ras activation. There is considerable cross talk between pathways.

Activation of ERK also occurs during RA-induced differentiation (Singh et al., 2003), although this is not crucial (Miloso et al., 2004). Lastly, Erk activation is involved in differentiation induced by Trks (Brodeur et al., 2009). Thus in line with its generally diverse functions, activation of Erk can either have positive or negative consequences on NBL cell survival/differentiation.

Although PI3K/Akt is required for RA-induced differentiation (López-Carballo et al., 2002), it generally contributes to NBL cell survival. This may also be true of differentiated cells, accounting for their survival following differentiation as in the case of Trk induced-differentiation (Brodeur et al., 2009). Activation of Akt is a negative prognostic marker in NBL (Opel et al., 2007), making it a firm target for therapeutic intervention (Brodeur, 2010; Li and Thiele, 2007).

The small molecule Akt inhibitor perifosine reduces NBL tumour growth *in vitro* and *in vivo* by p53-independent apoptosis (Li et al., 2010). Similarly inhibition of PI3K synergistically augments low dose chemotherapy *in vitro* by altering the ratio of antiapoptotic (Bcl-2, Bcl-X_L, Mcl-1) and pro-apoptotic (Bax, Bak and BH3) Bcl-2 family proteins, again reliant on p53 (Bender et al., 2011). Inhibition of PI3K with the selective PI3Kγ inhibitor AS605240 causes *in vivo* growth suppression in tumours characterized by high PI3Kγ expression (Spitzenberg et al., 2010). Indeed, targeting Akt is likely to be broadly effective given that multiple RTKs signal upstream of this node, thus preventing circumvention of therapy by compensation in alternative pathways (Brodeur, 2010). Activation of the downstream PI3K/Akt effector mTOR occurs with Akt activation in NBL, where the mTOR inhibitor rapamycin causes apoptosis, decreased proliferation and inhibition of angiogenesis *in vivo*, particularly in MYCN-driven tumours (Johnsen et al., 2008). NBL tumour-initiating cells (TICs), believed to represent a cancer stem cell (CSC) responsible for initiating tumour formation, metastasis and relapse (Hansford et al., 2007), are selectively and acutely sensitive to rapamycin (Smith et al., 2010).

1.3.4. PI3K/Akt/mTor inhibition: A double edged sword

Thus far it has been suggested that inhibition of the PI3K/Akt/mTor pathway is likely to form an effective treatment strategy in a range of cancers including NBL, given the

frequency of activation and its negative consequences on proliferation, survival and inhibition of apoptosis. However, a fundamental tenet of cancer biology is a dichotomy of consequences based either on cell context or adaptive strategies/natural selection in cancer cell populations (Greaves, 2010). As such targeting of survival pathways such as PI3K/Akt may have adverse consequences portending to treatment failure.

O'Reilly *et al.* were the first to demonstrate that inhibition of the PI3K/Akt effector mTOR induces the expression of insulin receptor substrate-I, abrogating negative feedback inhibition and resulting in paradoxical activation of Akt (O'Reilly et al., 2006), antagonizing the effects of rapamycin (Zoncu et al., 2011). It has been suggested that concomitant inhibition of PI3K and mTOR by dual inhibitors such as PI-103 (Fan et al., 2006) is a prerequisite for more effective targeting of this pathway (**Figure 1.3.3**).

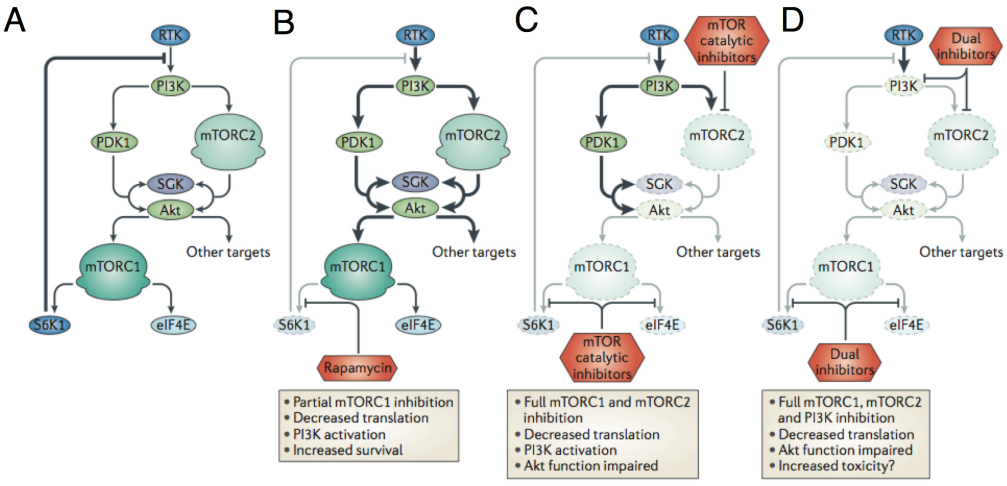

Figure 1.3.3. Consequences of mTOR inhibition due to relief of negative feedback. Signalling downstream of PI3K activates Akt followed by mTORC1, causing S6K1 activation exerting negative feedback on further PI3K stimulation (**A**). Inhibition of mTORC1 with rapamycin prevents activation of S6K1 relieving negative feedback of PI3K (**B**). Catalytic inhibitors of mTOR prevent Akt activation through mTORC2, but leave PI3K activation intact (**C**). Dual inhibitors of PI3K/mTOR prevent activation downstream of PI3K, however this may exert toxicity by shutting down an entire pathway crucial to cell survival (**D**).

However, inhibition of Akt itself may lead to similar effects. For instance, Chandarlapaty *et al.* recently demonstrated attenuation of negative feedback regulation due to Akt inhibition (Chandarlapaty et al., 2011). Specific Akt inhibitors caused both the induction and activation of multiple RTKs including HER3, Insulin-

like growth factor I receptor (IGF-1R) and the insulin receptor, primarily due to mTORC1 inhibition and FoxO activation dependent receptor expression in breast cancer cells driven by amplification of HER2, with combined HER3/Akt inhibition more effective than either treatment alone. PI3K inhibition can also relieve negative feedback inhibition of HER causing activation and stimulation of alternative signalling effectors such as Erk (Serra et al., 2011). Here Erk dependency ensued, allowing concomitant HER2 or MEK inhibition to drastically improve the efficacy of PI3K inhibition.

Another way in which cancer cells may circumvent PI3K/Akt targeted therapy is by the induction of survival mechanisms such as autophagy. For instance the inhibitors of mTOR and PI3K rapamycin and PI-103 were shown to potently induce macroautophagy (autophagy). Autophagy is a method of cell survival in the absence of adequate nutrition, or under other stress conditions (Mizushima et al., 2010). Inhibition of autophagy using chloroquine synergistically enhanced apoptosis (Fan et al., 2010).

Lastly, Akt activation itself may actually be beneficial in certain circumstances. For instance, Nogueira *et al.* showed that activation of Akt causes ROS dependent apoptosis by increasing oxygen consumption and inhibiting ROS scavengers downstream of FoxO (Nogueira et al., 2008). Boosting Akt activation using rapamycin actually enhanced cell death in etoposide resistant cancer cells via ROS production and ensuing apoptosis, suggesting that relieving Akt inhibition can actually be beneficial in some instances. This study also showed that Akt caused premature senescence in normal fibroblasts (See below).

1.3.5. Oncogene-induced senescence

2011 marks the anniversary of Hayflick and Moorhead's seminal description of cellular replicative senescence (Hayflick and Moorhead, 1961), whereby untransformed cells in contrast to cancer cells exhibit a finite replicative potential *in vitro*, undergoing irreversible growth arrest in the presence of mitogenic signals and sustained metabolic activity characterized by β-galactosidase activity at acidic pH (Dimri et al., 1995). Senescent cells also undergo telomere shortening, upregulation

of the *CDKN2A* locus encoding $p16^{INK4A}$/ADP ribosylation factor (ARF), DNA damage and cytoplasmic enlargement/vacuolation (Collado et al., 2007).

However, less than 15 years ago a distinct phenomenon termed "premature senescence" was observed following overexpression of proto-oncogenes in normal cells (Serrano et al., 1997). Thus the concept of oncogene-induced senescence (OIS) was born (Braig and Schmitt, 2006; Collado and Serrano, 2010), describing premature senescence attributed to overexpression of Ras and concomitant accumulation of p53 and $p16^{INK4A}$. Ras overexpression results in constitutive activation of MEK, which relies on p53/$p16^{INK4A}$ to cause growth arrest as a fail-safe barrier to sustained proliferation in the presence of mitogenic signals (Lin et al., 1998). Thus OIS represents a tumour-suppressive mechanism independent of the telomere clock (Jones et al., 2000). Since then OIS has been demonstrated as a *bona fide* barrier to tumorigenesis. For instance, Michaloglou *et al.* showed that despite activating mutations in the Ras effector BRAF ($BRAF^{V600E}$), human nevi (benign tumours of cutaneous melanocytes) lack proliferative activity for up to several years until, in a minority of cases, further lesions cause malignancy. Similarly mutations in $Kras^{G12D}$ drive premalignant lesions in the pancreas, lungs and skin, which are positive for senescence markers (Collado and Serrano, 2010). Indeed loss of the gene encoding NF1, a Ras GTPase activator, occurs in a number of human cancers including NBL, but underlies the familial cancer syndrome neurofibromatosis type 1, where increased activity of Ras leads to neurofibromas and senescence (Courtois-Cox et al., 2006).

The PI3K/Akt pathway can trigger a similar OIS. For instance, targeted expression of Akt1 to the prostate in mice results in prostrate intraepithelial neoplasia (PIN) with senescent markers (Majumder et al., 2008). In one of the defining studies of OIS, Chen *et al.* showed that conditional deletion of both alleles of PTEN, the negative regulator of Akt, resulted in p53-mediated senescence, greatly delaying the onset of invasive prostate cancer (Chen et al., 2005). However inactivation of both PTEN and p53 resulted in highly invasive prostate cancer with short latency, again underlying the notion that OIS exists as a fail-safe mechanism.

The exact logistics of OIS have often seemed unclear. For instance, expression of $p16^{INK4A}$ is observed in lymphomas in which senescence was bypassed,

and its expression is distinct to that of senescence-associated β-galactosidase (SA-β-gal) in human nevi (Braig and Schmitt, 2006). However transgenic disruption of $p16^{INK4A}$ in mice mediates escape from Ras driven senescence and accelerates tumour formation (Rane et al., 2002). Thus it has been suggested that $p16^{INK4A}$ may facilitate OIS whereas p53 is required to maintain it (Beauséjour et al., 2003). However oncogene dosage may also be crucial, as expression of Ras at normal levels fails to effectively stimulate downstream targets, and only high expression can surpass negative feedback inhibition and initiate OIS (Sarkisian et al., 2007).

A number of studies have now confirmed that OIS can be exploited as a treatment modality. Wu *et al.* demonstrated that by genetically inactivating the MYC oncogene following tumour onset, senescence and tumour regression occurs, a feat that was blocked by inactivation of p53 and $p16^{INK4A}$. This demonstrated that senescence programs can remain latent even after tumour onset and could be reactivated to induce regression. A similarly elegant transgenic mouse model developed by Xue *et al.* demonstrated that tumours induced by loss of p53 could be driven into senescence by its restoration (Xue et al., 2007). Indeed stabilization of p53 was originally suggested as a means by which senescence could be engaged in pre-existing tumours (Chen et al., 2005), and has effectively been demonstrated in NBL wild-type for p53 using an inhibitor of the negative regulator of p53 MDM2 nutlin-3 (Van Maerken et al., 2006). Similarly, DNA damage induced by chemotherapy has been shown to cause senescence *in vivo*, though this relies on correct functioning of p53 (Schmitt et al., 2002). Thus OIS represents both an interesting phenomenon and a means of cancer cell eradication.

1.3.4. PTEN-loss-induced senescence

PTEN was originally identified as the elusive tumour suppressor frequently deleted at 10q23 (Li et al., 1997), representing one of the most frequently lost tumour suppressors in many cancers (Salmena et al., 2008). Its tumour suppressive function is commonly related to its status as a negative regulator of Akt signalling. PTEN-deficient mice form tumours in multiple organs (Di Cristofano et al., 1998). However, acute loss of PTEN also activates a fail-safe senescence program dependent on p53 (Chen et al., 2005), explaining why complete loss of PTEN is rarely observed at

presentation. Perhaps the key to understanding this is the notion that specific PTEN levels are crucial to its cell biological effects (Carracedo et al., 2011). The classical model of a tumour suppressor involves genetic loss of one allele and subsequent loss of the remaining allele, comprising a 'second hit' (Knudson, 1971). However, haploinsufficiency can occur whereby loss of one allele is sufficient to abrogate wild type protein function (Berger and Pandolfi, 2010). Indeed, monoallelic loss of PTEN is sufficient to trigger tumour formation (Di Cristofano et al., 1998). PTEN is however often downregulated simply by epigenetic silencing and post-transcriptional regulation (Salmena et al., 2008). Thus PTEN protein dosage does not always correspond to 0, 50 or 100% of wild type levels, a factor that is crucial to the effects of PTEN loss.

The group of P.P Pandolfi elegantly demonstrated this by generating a 'hypomorphic PTEN allelic series' using conditional transgenic mice (Carracedo et al., 2011). Here PTEN heterozygous mutants, expressing 50% that of wild type levels, develop prostate intraepithelial neoplasia or prostate cancer *in situ* at incomplete penetrance, while PTEN 'hypo' mice, expressing 20-30% that of wild type animals develop prostate cancer lesions at full penetrance (Trotman et al., 2003). This suggests that subtle decreases in PTEN levels drastically affect tumour biology, confirmed by the formation of mammary or lung tumours even when PTEN was only reduced by 20% (Alimonti et al., 2010a). Thus PTEN is defined as 'quasi-insufficient', meaning that subtle reductions in gene dosage can cause tumorigenesis. Importantly, similar 20% reductions in PTEN expression were also observed in human tumours (Alimonti et al., 2010a). This has led to a model in which PTEN dose, altered by numerous causes, can exert a continuum of effects on cancer cells (**Figure 1.3.4**).

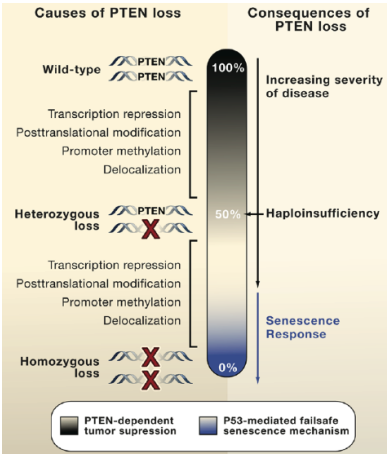

Figure 1.3.4. Causes and consequences of PTEN loss in cancer. Transcriptional repression, and posttranslational/epigenetic modification cause downregulation of PTEN expression. Although downregulation represents a continuum of severity of the consequences on tumour growth/survival, homozygous loss triggers a fail-safe senescence response. Taken from (Salmena et al., 2008).

These findings of PTEN-dose determining response led to the notion that the senescence response induced by PTEN loss might be manipulated in tumours depending on PTEN status. For instance Alimonti *et al.* showed that pharmacological inhibition of PTEN using the PTEN inhibitor VO-OH pictryhydrate (Mak et al., 2010) induced senescence in mouse embryonic fibroblasts (MEFs) in which one allele of PTEN was genetically deleted (Alimonti et al., 2010b). Importantly this response, termed PTEN-loss-induced senescence (PICS) depended on initial PTEN loss, as it was exhibited by prostate cancer cells with PTEN mutations but not wild type MEFs. Intriguingly PICS was suggested to be independent of OIS, as it failed to result in hyper proliferation or a DNA damage response, but was potentiated by stabilization of p53. Indeed PTEN status also determines the response to ionizing radiation, where PTEN-deficient cells undergo ROS dependent senescence and PTEN-proficient cells undergo apoptosis (Lee et al., 2011).

These results are complicated by the possibility that tumour suppression by PTEN is due in part to its nuclear localisation, where it regulates genomic stability, cell cycle progression, differentiation and gene expression. These are independent of its action on PIP_3 (Salmena et al., 2008). PTEN can interact with the tumour suppressor APC/C, promoting its interaction with CDH1 and enhancing APC/C-CDH1 tumour suppressive activity (Song et al., 2011). Here nuclear exclusion, but not abrogation of phosphatase activity, inhibited tumour suppression. Interestingly senescence was suggested to result from loss of CDH1, which otherwise prevents increases in $p16^{INK4A}$. Furthermore loss of PTEN hyper-sensitized cells to inhibition of APC/C-CDH1 targets such as Aurora A, the activity of which were increased as a compensatory mechanism. Thus taken together, levels of PTEN are likely to determine aspects of tumour biology, suggesting tumours with reduced levels of PTEN could paradoxically be targeted by PTEN inhibition. However it is unclear whether inhibition of phosphatase or nuclear activities should be targeted.

1.4. Reversible phosphorylation and the protein tyrosine-phosphatase gene family

1.4.1. Reversible phosphorylation and the PTP family

Reversible phosphorylation of tyrosine residues on proteins is arguably the single most important regulatory process of intracellular signal transduction, and is achieved by the concerted action of PTPs, which remove phosphate moieties, and protein tyrosine kinases PTKs that catalyse their addition (**Figure 1.4.1**) (See chapter 1.3 for information on PTKs) (Sun and Tonks, 1994). Rather than functioning as generic scavengers of intracellular phosphate, PTPs exert remarkably tight control of signal transduction in a positive and negative manner, often controlling the rate and duration of response where PTKs control its amplitude (Tonks, 2006). Thus although our knowledge of PTPs has generally lagged behind that of PTKs, recent years have seen much research on their diverse functions culminating in a number of apt reviews discussing their roles in signal transduction (Stoker, 2005), structure (Tabernero et al., 2008), regulation (Hertog et al., 2008; Majeti and Weiss, 2001), substrates (Tiganis and Bennett, 2007), function in neural development (Ensslen-Craig and Brady-Kalnay, 2004; Johnson and Van Vactor, 2003), cell adhesion (Beltran and Bixby, 2003; Sallee et al., 2006), and disease (Hendriks et al., 2008), as well as more general aspects of their function (Alonso et al., 2004; Hendriks and Stoker, 2008; Tonks, 2006; Tremblay, 2009).

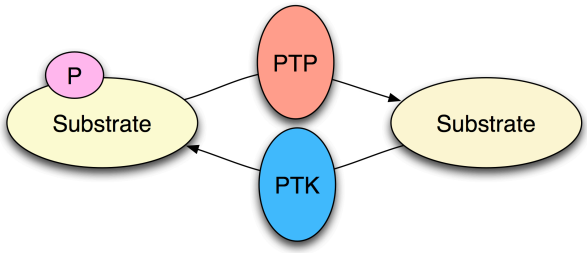

Figure 1.4.1. Reversible phosphorylation of proteins. Regulation of substrate function by the addition and removal of phosphate moieties (P) on tyrosine residues is catalysed by PTKs and PTPs respectively.

In total 107 genes encoding PTPs have been identified in the human genome, of which 38 show specificity for phosphotyrosine (pTyr), further divided into 17 subgroups based on their structural and functional diversity (Tonks, 2006) (**Figure 1.4.2**). Further diversity is generated through alternative promoters/splicing and posttranslational modifications. Although identification of substrates has proven

difficult due to poor specificity *in vitro*, some PTPs can show specificity for targets *in vivo* (Veeriah et al., 2009; Zhang et al., 2007). Of the 38 classical PTPs, 21 comprise receptor type PTPs (RPTPs) while the remaining 17 are distributed within the cytoplasm. RPTPs, capable of achieving ligand-controlled dephosphorylation, are generally characterized by the presence of immunoglobulin-like/fibronectin type III-like domains making up their extracellular domain, allowing them to function in some cases as cell adhesion molecules (CAMs) (Beltran and Bixby, 2003). Their catalytic activity generally resides in the D1 membrane-proximal intracellular phosphatase domain, linked to the extracellular domain via a transmembrane domain. However 12 RPTPs are characterized by a tandem repeat PTP domain arrangement, with a membrane distal D2 pseudophosphatase domain, which with the exception of PTPα (Buist et al., 1999) lacks catalytic activity. The remaining PTPs make up the dual specificity phosphatase (DSP) sub-family, capable of recognizing phosphorylated serine (pSer) and threonine (pThr) as well as pTyr residues (Pulido and van Huijsduijnen, 2008b). DSPs are less conserved in sequence to one another and have smaller catalytic domains than PTPs, but have recently emerged as having a similar diverse range of functions.

The PTP active site spans roughly 280 amino acid residues, characterized by the presence of a highly conserved HCX_5R motif on a cysteine residue. Catalysis is carried out by this nucleophilic cysteine, forming a cysteinyl phosphatase intermediate while undergoing a concomitant nucleophilic attack by the sulphur atom of the thiolate ion. Following this the substrate tyrosyl leaving group is protonated by a conserved aspartic acid (Asp) residue, and hydrolysis of the phosphoenzyme intermediate is mediated by the same Asp and a glutamine residue, causing release of a phosphate along with one molecule of water (**Figure 1.4.3**). Recently a secondary substrate binding pocket, separated from the catalytic site by a gateway region was proposed as a feature dictating substrate specificity (Tremblay, 2009). This second site may be crucial in generating specific inhibitors as has been demonstrated for PTP1B (Zhang and Zhang, 2007).

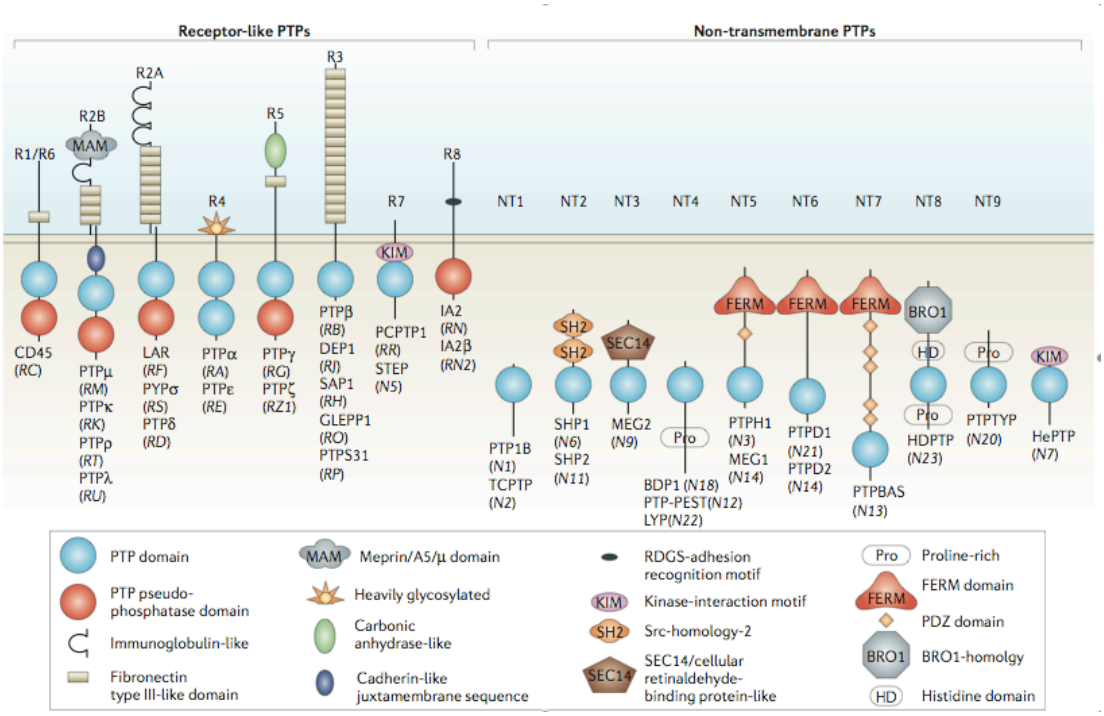

Figure 1.4.2. The classical PTP family. Tyrosine-specific PTPs are subdivided into receptor-like and cytoplasmic groups. Although all PTPs harbour a D1 phosphatase domain, diversity manifests in the presence of various other extracellular domains and adaptor domains. Taken from (Tonks, 2006).

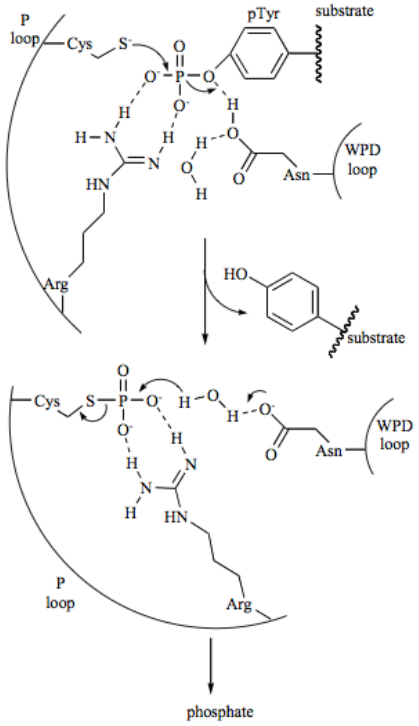

Figure 1.4.3. Mechanism of PTP catalysis. A conserved active site cysteine (Cys) binds substrate phosphotyrosyl forming a phosphoenzyme intermediate subsequently hydrolyzed involving a conserved aspartic acid (Asp) and glutamine (Glu) releasing a molecule of inorganic phosphate and water.

One of the major mechanisms of PTP regulation is reversible oxidation of the cysteine within the active site (den Hertog et al., 2005; Tonks, 2005; Xu et al., 2002). Oxidation by ROS such as hydrogen peroxide (H_2O_2) cause conformational changes

and stabilize an inactive catalytic site (Groen, 2005). The active site cysteine can be converted to either sulphenic (SOH), sulphinic (SO_2H) or sulphonic (SO_3H) acid, depending on the extent of oxidation. Higher oxidation represents an irreversible modification (Tonks, 2006), and is prevented in the case of the DSP PTEN by the presence of a second cysteine residue forming a disulphide bridge with the active site cysteine. Oxidation likely represents a major method of physiological PTP regulation, given that antigen receptor engagement and growth factors can generate ROS, which can inhibit PTPs normally attenuating downstream stimulation (den Hertog et al., 2005). Inactivation by oxidation is also likely to be transient due to the presence of natural reducing agents such as thioredoxin, catalase and glutathione within the cell (Eruslanov and Kusmartsev, 2010). It is unclear how oxidation exerts specificity, given the promiscuous nature of ROS, however it has been shown that PTPs are subject to differential oxidation related to pH changes in the active site microenvironment and also orientation of the PTP loop arginine (Groen et al., 2005). In addition, it is possible that RTK-generated ROS remain spatially fairly localised.

Another well-characterized method of PTP inactivation, at least in the case of RPTPs is ligand-independent dimerization (Van Der Wijk et al., 2005). In the case of RPTPα, the presence of a PTP 'wedge' on the transmembrane domain allows an interaction with the D1 pocket of a partner molecule, causing steric hindrance of the active site (Bilwes et al., 1996). The role of the PTP wedge domain in PTP inhibition by dimerization is best demonstrated by the finding that mutations in the wedge domain of CD95 attenuate dimerization (Majeti et al., 1998). However an alternative mechanism of dimerization was recently proposed whereby the presence of a flexible linker region in the transmembrane domain allows a head-to-toe D1 to D2 interaction of neighbouring RPTPs (Barr et al., 2009). Furthermore in the case of RPTPs that function as CAMS such as PTPσ, dimerization may actually facilitate substrate binding with heterophilic ligands in the extracellular domain (Lee et al., 2007).

One of the ways PTPs can modulate intracellular signal transduction is by directly regulating the activity of RTKs (Ostman and Böhmer, 2001). For example, ligand-independent activation of RTKs occurs following PTP inhibition (Jallal et al., 1992). In contrast, dephosphorylation of ligand-activated RTKs occurs immediately

following their inhibition, indicating that PTPs are constantly on hand to shut down RTK signalling (Sorby and Ostman, 1996). Many PTPs also negatively regulate RTK signalling. Deletion of PTP1B in mice results in prolonged insulin-stimulated phosphorylation of the insulin receptor (Elchebly et al., 1999), whereas inhibition of PTP-LAR results in increased stimulation of multiple RTKs including the receptors for platelet-derived growth factor (PDGF-R), epidermal growth factor (EGFR) and insulin (IR) resulting in downstream MAPK/PI3K activation (Kulas et al., 1995; Suarez Pestana et al., 1999). This also fits in with the inactivation of PTPs by oxidation, since the H_2O_2 produced after RTK stimulation (Rhee et al., 2001) is likely to prolong RTK signals. Some PTPs also facilitate RTK signal, including SHP-2, which mediates mitogen activated protein kinase (MAPK) signalling in a positive manner (Araki et al., 2003). PTPs such as PTPα also directly activate cytoplasmic PTKs of the SRC family (Zheng et al., 1992) (See section 1.3.2).

1.4.2. The tyrosine phosphatome in human cancer: Tumour suppressors

Given their ability to negatively regulate growth factor receptors, the PTP family are intuitive candidates for tumour suppressor genes. However, based on their diverse roles in a number of processes including differentiation, apoptosis, cell adhesion and motility, as well as their positive contribution to RTK signalling in some instances, it has become increasingly clear that this view is simplistic and instead PTPs may function both as oncogenes and tumour suppressors (Julien et al., 2011; Ostman et al., 2006). Unbiased RNAi screens of a phosphatase/kinase library in HeLa cells identified 32% of total phosphatases as positively regulating cell survival compared with only 11% of kinases (MacKeigan et al., 2005). Remarkably, only 5% of the phosphatome were survival limiting.

Gene silencing through methylation of CpG sites at the 5' end of genes has been observed to occur in *PTPRG* (van Doorn et al., 2005), *PTPRD* (Veeriah et al., 2009), *PTPRO* (Motiwala et al., 2004) and *PTPN13* (Yeh et al., 2006), in a range of cancers including adenocarcinoma, glioblastoma and squamous cell carcinoma, demonstrating a putative tumour suppressive role for these PTPs. However the most comprehensive demonstration of PTP tumour suppressors came from Wang *et al.*, in which a mutational analysis of the entire gene family discovered 83 tissue-specific

somatic mutations in *PTPRF, PTPRG, PTPRT, PTPN3, PTPN13* and *PTPN14*, occurring in 26% of colorectal cancers (Wang et al., 2004). Mutations in *PTPRT* occurred most frequently, affecting 17% of lung and gastric cancers, and 26% of colorectal cancers. Functional analysis of *PTPRT* mutations demonstrated downregulation of phosphatase activity and loss of growth-suppression and it has since been demonstrated that *ptprt* knockout mice are highly susceptible to tumours (Zhao et al., 2010). Tumour-derived mutations in *PTPRT* also cause defective cell adhesion, possibly hinting at a role in migration/metastasis (Yu et al., 2008). Korff *et al.* detected frequent frameshift mutations in *PTPRA, PTPRS, PTPN15, PTPN13, PTPN21* and *PTPN23* also in colorectal tumours (Korff et al., 2008). Focal deletions of *PTPN2*, encoding TC-PTP, also occur at high frequency in T cell acute lymphoblastic leukaemia, contributing to enhanced proliferation and cytokine sensitivity (Kleppe et al., 2010).

One of the most broadly mutated PTP genes is *PTPRD,* encoding PTPδ, mutated at relatively high frequency in head and neck squamous cell carcinoma (13%), melanoma (12%), lung cancer (9-11%) and glioblastoma (6%) (Kohno et al., 2010; Solomon et al., 2008; Veeriah et al., 2009). A number of mutations have been detected in both the extracellular and phosphatase domains of *PTPRD*, both of which generate non-functional protein products (Navis et al., 2010; Veeriah et al., 2009). Mutations in *PTPRD* in glioblastoma were also found to occur at higher frequency than mutations in PTEN (14% versus 9%), despite the firm status of the latter as a highly significant tumour suppressor in this cancer (Solomon et al., 2008).

Another hallmark of a tumour suppressor is loss of heterozygosity (LOH). This occurs in *PTPRJ* in cancer of the colon (49%), lung (50%) and breast (78%) cancer (Ruivenkamp et al., 2002), and association of LOH with disease progression was demonstrated in colorectal cancer (Ruivenkamp et al., 2003). Similarly missense mutations in the non-catalytic domain of DEP1 are enriched in brain metastases from primary breast tumours, suggesting a role in tumour progression (Ding et al., 2010). K1016A mutations in DEP1 affect its interaction with Erk1/2, positively affecting Ras/Erk signalling, providing an appealing explanation for its apparent tumour suppressive role (Sacco et al., 2009), although homozygous deletion of *Ptprj* in mice does not result in tumours (Trapasso et al., 2006).

The ability of PTPs to regulate signalling downstream of RTKS may underpin their tumour suppressive properties. For instance, DEP1 inhibits Ras/MAPK signalling and limits EGFR endocytosis (Tarcic et al., 2009). DEP1 also directly targets downstream effectors such as Erk1/2, further inhibiting activation of this pathway (Sacco et al., 2009). PTPRT dephosphorylates STAT3 at Y705 causing its inactivation following cytokine stimulation by soluble factors such as interleukin-6 (Zhang et al., 2007). Here STAT3 activation results in nuclear translocation and transcription of target genes such as the antiapoptotic proteins BCL_{XL}. A similar function has been noted for PTPRD, which also dephosphorylates STAT3 at Y705, a process that is abrogated by mutations in both the extracellular and phosphatase domains (Veeriah et al., 2009). PTPN13 negatively regulates SRC activity *in vitro* by dephosphorylation at Y416, and PTPN13 inhibition results in increased proliferation (Yeh et al., 2006). Lastly, *PTPN12* (encoding PTP-PEST) was recently identified as a potent negative regulator of multiple RTKs including EGFR and HER2 in triple negative breast cancer, being subject to posttranscriptional silencing leading to loss of expression in up to 60% of analysed tumour samples, leading to malignant transformation (Sun et al., 2011).

1.4.3. The tyrosine phosphatome in human cancer: Oncogenes

As well as deletions, mutations and LOH, genomic amplification of genes encoding PTPs (4/107) have also been documented, suggesting putative PTP oncogenes. For instance, Saha *et al.* found that *PTP4A3* is amplified in colorectal cancer resulting in encoded PRL3 overexpression specifically in metastatic cancer (Saha et al., 2001). Overexpression of PRL-3 occurs primarily in metastases, correlating with poor prognosis in liver cancer (Peng et al., 2004). Upregulation of PRL-3 promotes cell motility and invasion by mechanisms including regulation of Rho-family GTPases (Fiordalisi et al., 2006; Zeng et al., 2003), where monoclonal antibody targeting inhibits metastatic spread (Guo et al., 2008). *PTPN1* is also subject to genomic amplification in epithelial cancers as well as *DUSP26* (thyroid) and *PTPN7* (leukaemia) (Julien et al., 2011; Yu et al., 2007).

Aside form the large number of potential survival-promoting PTPs found in recent screens (MacKeigan et al., 2005), the only *bona fide* oncogene currently

identified is *PTPN11*, which encodes SHP2, a common target of somatic activating mutations in cancers (Chan et al., 2008; Matozaki et al., 2009). Tartaglia *et al*. identified autosomal dominant germline mutations in *PTPN11* as a cause of Noonan syndrome, a complex disorder that increases susceptibility to juvenile myelomonocytic leukaemia (Tartaglia et al., 2003). Activating mutations in *PTPN11* also occur in acute lymphoblastic leukaemia and acute myeloid leukaemia (6% and 5% respectively), as well as at low frequency in solid tumours (Bentires-Alj et al., 2004; Tartaglia et al., 2004), although the contribution of SHP2 to a wide range of tumours has been disputed (Martinelli et al., 2006). SHP2 is also involved in the growth and migration of anaplastic lymphoma cells (Voena et al., 2007). A recent finding has complicated the status of SHP2 as an oncogene, though, in demonstrating that deletion of SHP2 in hepatocytes caused tumours, and ablation enhanced tumour progression, attenuated by concomitant ablation of STAT3 (Bard-Chapeau et al., 2011).

SHP2 dephosphorylates sites on multiple RTKs that negatively regulate Ras/MAPK signalling, providing a functional basis for SHP2 mutations (Araki et al., 2003; Easton et al., 2006; Klinghoffer and Kazlauskas, 1995). SHP2 also positively regulates SRC activity by dephosphorylating the inhibitory, c-terminal tyrosine residue, again promoting downstream Ras/Erk activation (Zhang et al., 2004). Indeed inhibitors of SHP2 have recently been developed as potential therapeutic agents (Hellmuth et al., 2008; Zhang et al., 2010).

SRC is also activated by PTPα, leading to transformation of fibroblasts (Zheng et al., 2000). Given the PTPRA overexpression in colorectal cancer, it represents another potential PTP oncogene (Ardini et al., 2000). In addition to SHP2, other PTPs have been shown to act cooperatively with transforming lesions. Loss of *PTPN1* (encoding PTP1B) either through genetic deletion or inhibition in mice with constitutively active Erbb2 significantly increases tumour latency and progression to metastatic cancer, while overexpression induces tumour formation (Bentires-Alj and Neel, 2007; Julien et al., 2007). This is consistent with the role of PTP1B as a positive regulator of MAPK/Akt signalling (Haj et al., 2002; Tonks and Muthuswamy, 2007). More recently PTP1B was shown to drive Erbb2-dependent breast cancer by activation of SRC (Arias-Romero et al., 2009). Similarly loss of *PTPRH* (encoding SAP-

1) inhibits the formation of colon tumours initiated by loss of the tumour suppressor APC, explaining its overexpression in cancers including gastric, pancreatic and colon (Sadakata et al., 2009). The most recent demonstration on oncogenic cooperation was by Zhi *et al.*, who showed that PTPH1, which is overexpressed in breast cancer, stimulated cell growth by phosphatase-independent stabilization of the vitamin D receptor (Zhi et al., 2010).

1.4.4. The tyrosine phosphatome in neuroblastoma

Although research into the contribution of PTPs to cancer is still in its early stages, a handful of studies have already described roles for PTPs in the development and maintenance of NBL. One aberrantly expressed PTP is PTPδ, encoded by *PTPRD* (see above). De Preter *et al.* found that *PTPRD* mRNA is expressed at lower levels in NBL tumours compared with normal fetal adrenal neuroblasts (De Preter et al., 2006). Expression is lowest in high-stage metastatic tumours, suggesting a driving role in tumour progression. Mapping large-scale chromosomal imbalances in NBL, Stallings *et al.* also observed frequent microdeletions at the 5' untranslated region (5'UTR) of the *PTPRD* gene (Stallings et al., 2006). Homozygous deletions were also observed in two NBL cell lines, SK-N-AS and Kelly/N206, suggesting a fundamental role in tumour progression. The same group further characterized loss of *PTPRD*, showing that aberrant splicing causes loss of 5'UTR exons in over 50% of primary tumours and cell lines, mimicking microdeletions observed at this locus (Nair et al., 2008). Again lower expression of mRNA was confirmed in metastatic Mycn amplified tumours, suggesting impairment of mRNA stability as a mechanism for downregulation of PTPRD.

It has been suggested that rather than functioning to suppress tumour onset, the PTPδ protein may instead function as a suppressor of metastasis (De Preter et al., 2006; Stallings et al., 2006). Indeed evidence for this comes from the fact that PTPδ can interact with MIM-B, a putative metastasis suppressor protein capable of regulating actin cytoskeletal changes downstream of RTKs (Woodings et al., 2003). It is tempting to speculate that an ability of PTPδ to suppress metastatic growth may derive from its negative regulation of STAT3 (Veeriah et al., 2009), given that interleukin-6, which activates downstream STAT signalling is specifically secreted in

bone marrow metastases where it triggers growth and survival of NBL cells (Ara et al., 2009). However functional evidence for this hypothesis is lacking.

A second RPTP detected to be expressed at low levels in NBL by De Preter *et al.* was PTPRK, encoding PTPκ (De Preter et al., 2006). Although the relevance of this reduced expression in NBL is unclear, a tumour-suppressive role for PTPκ has been demonstrated in melanoma due to its ability to negatively regulate the transcriptional activity of β-catenin and promote the formation of E-cadherin/β-catenin complexes at adherens junctions (Novellino et al., 2008). Re-expression of *PTPRK* in cells harbouring mutations reduced proliferative and migrational capacity. Indeed β-catenin has been hypothesized to promote advanced NBL disease through induction of *MYC* and other target genes crucial to survival, as well as contributing to the maintenance of putative NBL stem cells (Maris et al., 2007).

In line with its general status as a PTP proto-oncogene, activating mutations in *PTPN11* have also been detected at low frequency (3%) in NBL primary tumours (Bentires-Alj et al., 2004), although others have failed to detect *PTPN11* mutations in NBL (Martinelli et al., 2006). SHP2 facilitates Ras/MAPK signalling by BDNF (Easton et al., 2006), which may contribute to survival signalling in NBL (See section 1.1.6).

Perhaps the best candidate PTP oncogene is the DSP DUSP26. Shang *et al.* elegantly demonstrated this by over-expressing DUSP26 in NBL cells, which inhibited p53 activation by the chemotherapeutic doxorubicin. In contrast, inhibiting DUSP26 expression activated p53 and augmented doxorubicin-induced apoptosis (Shang et al., 2010). Importantly DUSP26 was shown to directly dephosphorylate p53 at S20/37 *in vitro*, explaining its overexpression in NBL. This study is particularly useful given the recent development of the novel SHP1/2 inhibitor NSC-87877 showing specificity for DUSP6 (Song et al., 2009). It is also in line with previous reports of growth promotion in thyroid cancer by amplification of the gene encoding DUSP26 p38 MAPK inhibition (Yu et al., 2007). Indeed other DSPs have been identified as contributing to NBL pathogenesis in genome wide association studies (J.Maris, personal communication), making them interesting targets for further research (Patterson et al., 2009).

Thus despite some exciting recent developments concerning PTPs in the search for NBL cancer genes, a more extensive investigation into their contribution to this disease is warranted.

1.5. The development of phosphatase inhibitors and their use in cancer treatment

1.5.1. Phosphatase inhibitors: General mechanisms and problems

Due to their ability to regulate intracellular signal transduction in a number of diseases including cancer, targeting PTPs using small molecule inhibitors has been a topic of considerable interest (Bialy and Waldmann, 2005; Dewang et al., 2005; Ferreira et al., 2006; Heneberg, 2009; Jiang and Zhang, 2008; Umezawa et al., 2003; Vintonyak et al., 2009). Much of this work has centred on the cytoplasmic phosphatase PTP1B, a potent negative regulator of insulin signalling (Elchebly et al., 1999; Seely et al., 1996). Driven by the ever-increasing prevalence of type 2 diabetes, this research triggered a race to generate a specific inhibitor of PTP1B, expertly reviewed elsewhere (Taylor, 2003; Zhang and Zhang, 2007; Zhang and Lee, 2003). Current issues and promising developments in the generation of PTP inhibitors will now be discussed.

Strategies in developing PTP inhibitors have been based on the unusual active site of PTPs, which contains a deep pocket to accommodate substrate pTyr (9Å for classical PTPs versus 6Å for DSPs). Substrate binding induces a conformational change bringing the WPD loop over the binding pocket eliciting further stabilizing interactions crucial for substrate specificity and catalytic activity. Most active site catalytic PTP inhibitors are based around nonhydrolyzable pTyr mimetics directed towards the P loop at the active site base. However, the high charge density of pTyr mimetics has drastically limited the bioavailability of these inhibitors, as well as problems of degradation by proteases. The most notorious issue with all pTyr mimetic PTP inhibitors is also their lack of selectivity due to the highly conserved PTP active site. However, some key developments show promise in the circumvention of this problem. (Montalibet et al., 2006; Wiesmann et al., 2004).

Although PTP-specific inhibitors have remained a major technical challenge, a number of more general inhibitors, including those derived from natural products,

have shown specificity for PTPs and have been widely used in research (Heneberg, 2009). Indeed a number of PTP inhibitors including sodium stibogluconate, phenylarsine oxide, alendroate, etidronate, vanadate, gallium nitrate, suramin and aplidin have been approved for clinical testing (Heneberg, 2009). Sodium stibogluconate for example is currently undergoing phase I-II trials as a possible combinatorial therapeutic with interferon for the treatment of melanoma, lymphoma and myeloma (Julien et al., 2011). Furthermore inhibitors have recently been characterized that show some specificity towards PTPs implicated in carcinogenesis including Shp2 and DUSP26 (NSC-87877), Cdc25 (NSC-95397) and PRLs (thienopyridone) (Daouti et al., 2008; Lazo et al., 2002; Song et al., 2009). While the development of PTP inhibitors for cancer treatment clearly needs to go hand in hand with an increased understanding of the role PTPs play in oncogenesis, it is tempting to speculate that the degree of PTP inhibitors available could be highly beneficial for the development of novel treatments.

1.5.2. Vanadium compounds represent a major class of PTP inhibitors

Vanadium-based compounds are generally considered the gold standard of metal-containing phosphate mimetic PTP inhibitors and a number of derived compounds have already been developed for the potential treatment of diabetes (Smith et al., 2008; Srivastava and Mehdi, 2005; Thompson et al., 2009). The mechanism of PTP inhibition, chemical configuration and pre/clinical efficacy of such compounds will now be discussed.

Vanadium is a group V trace metal from the first transition series, and represents the 21st most common metal in the earth's crust. It is exists in four valency states, thus its chemistry is complex. The vanadyl (VO^{2+}) species occurs at a pH lower than 3.5, however the predominant form of vanadium is orthovanadate (VO_4^{3-}), chemically similar to the structure of phosphates (PO_4^{3-}) (**Figure 1.5.1**). Metavanadate (VO_3^-) in the +5 oxidation state commonly occurs in bodily fluids such as plasma, where it enters cells via anion transport systems and is normally reduced by endogenous glutathione to vanadyl (VO^{2+}) in the +4 oxidation state. Vanadium (V) compounds are more potent PTP inhibitors compared with vanadium (III)/(IV) compounds suggesting oxidation state is crucial (Thompson et al., 2009). Notably

vanadyl was actually shown to oppose the action of vanadate by inhibiting PTK activation, suggesting reversible oxidation as a physiological homeostatic mechanism that could be exploited for instance by conversion using hydrogen peroxide (Elberg et al., 1994). The total pool of vanadium in humans has been estimated at 100-200mg, with estimates of 0.014 to 7.2 µmols in mammalian cells (Srivastava and Mehdi, 2005).

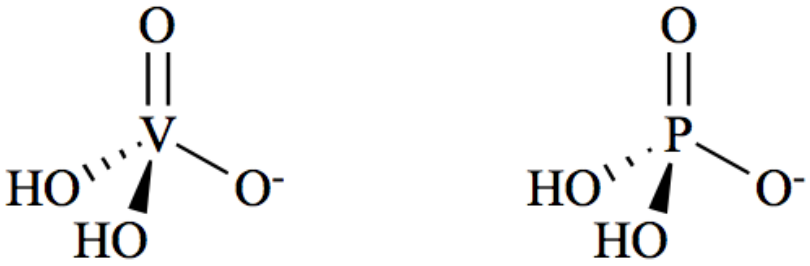

Figure 1.5.1. PTP inhibition by pTyr mimetics. Vanadate (V) (left) and phosphatase (right) exhibit remarkable structural similarity, thus vanadate can competitively inhibit all PTPs by mimicking the enzyme-phosphate transition state during catalysis. Taken from (Heneberg, 2009).

Vanadate exerts competitive, non-selective inhibition of PTPs due to its structural similarity to the transition state of phosphotyrosyl in the PTP active site. The mechanism of inhibition has been demonstrated by crystallographic analysis (Denu et al., 1996; Pannifer et al., 1998). Specifically binding occurs with a 2.5Å space between the conserved active site Cys and a vanadium atom, indicative of a covalent bond. The pentavalent, trigonal bipyramidal geometry of vanadate when bound highly resembles that of transition state thiol-phosphate. Furthermore a conserved aspartate residue undergoes hydrogen bonding of 2.8Å to the oxygen of vanadium, occupying the position of phenolic oxygen of phosphotyrosyl and water during hydrolysis. Vanadate can be complexed with H_2O_2 to form pervanadate, which achieves more potent inhibition by irreversibly oxidizing the catalytic Cys of PTPs. This contrasts with vanadate, which can be reversed with chelating agents such as EDTA (Huyer et al., 1997). Pervanadate more effectively increases cellular phosphotyrosine when compared with vanadate (Huyer et al., 1997), suggesting that

in situ H_2O_2 may increase the potency of vanadate. Peroxovanadium compounds are however much more toxic to the cell and can cause severe oxidative stress.

Vanadium compounds have proven efficacy as insulin mimetics, and have been used in preclinical and clinical testing for both type 1 and type 2 diabetes (Smith et al., 2008; Srivastava and Mehdi, 2005). These include inorganic vanadium salts such as sodium orthovanadate (Na_3VO_4), vanadyl-sulfate ($VOSO_4$ $3H_2O/4H_2O$), sodium metavanadate ($NaVO_3$, NaMV), and vanadyl pentaoxide (V_2O_5). In fact Lyonnet *et al.* tested sodium metavandate on human diabetes patients in 1899, 22 years before the discovery of insulin, where it was observed to improve symptoms in 2/3 patients (Srivastava and Mehdi, 2005). Vanadyl sulfate has been clinically tested in a number of studies, but encountered problems due to toxicity, limiting the suitable dosage (Goldfine et al., 2000). A number of gastrointestinal disturbances have been reported in response to daily treatment with vanadium compounds, commonly diarrhoea, decreased fluid intake and weight loss (Domingo, 2002), although these may be corrected by adding taking with NaCl, adjusting to pH neutral and gradually increasing dosage (Srivastava and Mehdi, 2005). Vanadium may also accumulate in bone after chronic treatment, causing latent toxicity issues (Domingo et al., 1995).

During the early 1990s, a strategy was devised to complex vanadium with organic ligands for improved bioavailability. A number of such organovanadium compounds have since been tested as potential treatments for diabetes such as bis(maltolato)oxovanadium(IV) (BMOV), vanadyl acetylacetone and bis(6-methylpicolinato)oxovanadium. Crucially these drugs completely lack the toxic effects of their inorganic counterparts (Thompson et al., 2009). Developed in 1992, BMOV, a complex of the orally available maltol ligand with vanadium, is now considered the benchmark of such compounds, however its ethylmaltol analogue bis(ethylmaltolato)oxovanadium(IV) (BEOV) has been shown to be similarly potent/orally available (**Figure 1.5.2**). These compounds are potent activators of insulin signalling and enhance phosphorylation of Akt, GSK3β and FOXO1 (Mehdi and Srivastava, 2005; Mehdi et al., 2006; Srivastava, 2009). Both compounds are 2-3 times as bioavailable as vanadyl sulfate, but act in a similar manner, probably achieving PTP inhibition by delivering unliganded-vanadium to the PTP active site

(Peters et al., 2003). Thus the superior effects of organovanadium compounds on glucose metabolism and greater tolerability reported are likely a consequence of more potent stimulation of insulin signalling (Reul et al., 1999), although greater absorption has also been suggested (Thompson et al., 2009). In July of 2008, a phase-IIa trial was released demonstrating efficacy and tolerability of BEOV in type II diabetic patients, when administered daily for 28 days at a 20mg dosage (5.8µmol V). This represents an important step in the transition of vanadium compounds from the bench to the bedside, as well as facilitating their use in drug redeployment for cancer treatment (see below).

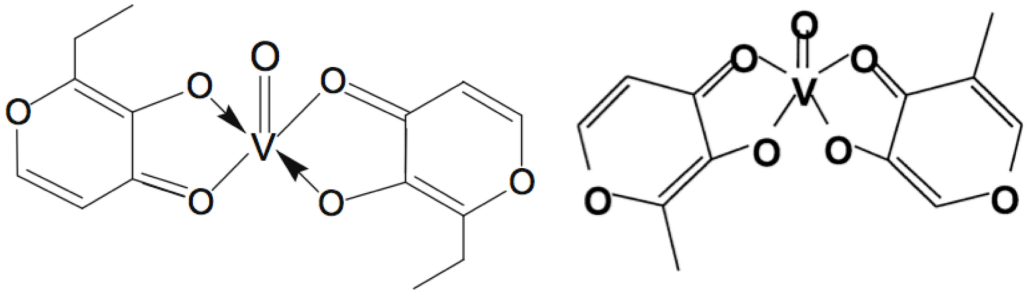

Figure 1.5.2. Chemical structure of BEOV/BMOV. BEOV (left) and BMOV (right) exhibit structural differences to vanadate (Figure 1.5.1.) due to the organic ligand ethyl maltol/maltol scaffolds respectively, although their putative mechanism of inhibition is identical. Taken from (Thompson et al., 2009; Willsky et al., 2001).

Of further note is the recent development of a specific inhibitor of PTEN, 3-hydroxypicolinate vanadium(IV) (VO-OH Pic), by complexing vanadyl with the organic moiety hydroxypicolinic acid (Rosivatz et al., 2006). VO-OH Pic achieves selectivity towards PTEN due to its wide active site pocket (8Å deep) and elliptical opening (5Å x 11Å) distinguishing it from other PTPs, inhibiting PTEN with an IC50 of 35nM. VO-OH Pic increased levels of cellular Ptpins(3,4,5)p_3 and caused increased membrane recruitment/phosphorylation of Akt as well as glucose uptake in adipocytes (Rosivatz et al., 2006). Although VO-OH Pic binds PTEN at the active site, its inhibitory action is suggested to be distinct from vanadate delivery to the active site (Mak et al., 2010). VO-OH Pic is thus potentially of great interest, as it represents arguably the first selective vanadium based inhibitor of a PTP, based on enzyme structure, and is selective towards PTEN, a protein with known roles in diabetes and cancer.

1.5.3. Vanadium compounds in the treatment of cancer

The ability of vanadium compounds to exert numerous effects on regulatory enzymes in cells has made them an interesting subject for anti-carcinogenic research. In fact a number of studies have already documented anti-cancerous properties of vanadium compounds and a clear ability to both inhibit tumorigenesis and enhance tumour regression in preclinical models of a number of cancers including breast, liver, lung and colon (reviewed in (Bishayee et al., 2010; Evangelou, 2002). Evidence for a role of vanadium compounds as therapeutic agents in cancer treatment will now be discussed.

Cytotoxic effects of vanadium compounds are well documented. For instance, the metallocene dichloride compound vanodecene causes p53-dependent acute apoptosis of testicular cancer cells *in vitro* (Ghosh et al., 2000). Huang *et al.* demonstrated transactivation of p53 as a result of ROS production induced by vanadate (50-400μM) in epidermal cells (Huang et al., 2000a). Here mitochondrial damage and apoptosis that ensued was blocked by the antioxidant reducing agent n-acetyl-L-cysteine (NAC) and the H_2O_2 inhibitor catalase and augmented by superoxide dismutase/NADPH due to their ability to increase intracellular ROS. This effect did not occur in $p53^{-/-}$ cells, which is of relevance to NBL given the low rate of p53 mutations in this cancer. Vanadate also causes S-phase arrest via Erk/p38 MAPK-induced increases in p21 only in $p53^{+/+}$ cells (Zhang et al., 2002). Paradoxically, vanadate was recently shown to inhibit p53-induced apoptosis via transcription-dependent and independent pathways at an even greater efficacy than the established pifithrin transcriptional inhibitors (Morita et al., 2010). Here it was argued that this function could dramatically limit gastrointestinal/haematopoietic problems resulting from radiation treatment.

A number of studies have focused on ROS as a mediator of the antiproliferative effects of vanadium. Indeed the increased sensitivity of insulin resistant adipocytes to vanadate treatment has been suggested to be the result of oxidative stress preventing the reduction of +5 vanadate to +4 vanadyl (Lu et al., 2001), of interest considering the high levels of oxidative stress attributed to cancer cells (See section 1.6). Gamero *et al.* demonstrated ROS-dependent apoptosis induced by a combination low-dose vanadate (5μM) and interferon-α treatment in

multiple cancer cells *in vitro* (Gamero and Larner, 2001). Interestingly neither treatment alone induced apoptosis, nor was p53 necessary for this response. In lung cancer cells vanadate-induced ROS are responsible for Erk/p38 MAPK phosphorylation that results in increased p21 expression and arrest at G2/M (Zhang et al., 2003). However this is again complicated by the recent illustration of ROS independent G1/S arrest resulting from vanadium compounds in hepatoma cells (Wang et al., 2010). Here it was suggested that increased ROS is responsible for cytotoxicity of normal cells induced by high concentrations of vanadium compounds (400μM), a negative side effect that could be limited by concomitant treatment with NAC.

Chin *et al.* have shown that vanadate can actually inhibit apoptosis in glioma cells (Chin et al., 1999). Here it was argued that dual activation of Erk/p38 MAPK and PI3K/Akt resulted in both survival and apoptotic signalling, where inhibiting the latter caused cell death. Indeed this highlights the cell type dependency and role of contextual signals in determining the fate of tumour cells treated with vanadium compounds, for instance activation of downstream effectors such as Erk/Akt and NF-kappaB may result in either survival or apoptosis. Klarund *et al.* showed that vanadate can even cause oncogenic transformation *in vitro* by increasing intracellular pTyr (Klarlund, 1985). While this highlights the paradoxical opposing effects of vanadium and demonstrates a need for caution in promoting its use in cancer therapy, the US food and drug administration (FDA) has not listed vanadium as a known carcinogen.

Apart from directly affecting proliferation and apoptosis, vanadium may exert other potentially anti-cancerous effects, such as the modulation of motility or invasiveness. For example vanadate can inhibit cell adhesion and cell spreading in both normal and transformed cells *in vitro* (Edwards et al., 1991). More recently vanadate was found to exert inhibition of matrix metalloproteinases (MMPs), enzymes with putative roles in metastasis (Chintala et al., 1999). Here vanadate treatment reduced actin polymerization, and cell spreading and migration/invasion in glioma cells, providing indirect evidence that vanadate may limit invasiveness and thus metastatic spread.

A role of vanadium in stimulating neuronal differentiation has also been documented. Following ischemic injury, treatment with the organovanadium compound bis(1-oxy-3-pyridimethiolato)oxovanadium(IV) results in enhanced hippocampal neurogenesis via increasing PI3K/Akt and Erk signalling (Shioda et al., 2008; Shioda et al., 2007). Similarly, vanadate can activate TrkA signalling via Akt/Erk stimulation and mediate neurotrophin-independent survival in hippocampal neurons (Gerling et al., 2004). This apparent ability of vanadium compounds to behave as neurotrophic factor mimetics suggests a role in differentiation of neural cells, a key determinant of NBL regression (Brodeur et al., 2009; Nakagawara, 1998). In fact Rogers *et al.* showed that vanadate could stimulate neurite extension, a cell-structural parameter of neuritogenesis, in human NBL cells (Rogers et al., 1994), although the mechanisms behind this effect are unclear. Similarly an oxovanadium compound causes decreased proliferation and reversible G2/M phase cell cycle arrest in both NBL and glioma cells (Faure et al., 1995). This suggests that distinct to apoptosis, vanadium may promote differentiation in neuronal cancer cells.

Clearly, definitive proof of the anti-cancerous effects of vanadium compounds requires *in vivo* demonstrations of efficacy against tumours. Indeed numerous such demonstrations exist currently; dating back to 1965 when anticancer effects of vanadium salts were first published (Bishayee et al., 2010). The first controlled animal study into the chemopreventive effects of vanadyl sulfate was published by Thompson *et al.*, documenting a decrease in both the incidence of cancer and number of cancers per rat in a model of induced mammary carcinogenesis (Thompson et al., 1984). Bishayee *et al.* similarly showed that ammonium monovanadate given either throughout or prior to initiation of liver tumour formation in rats, gave significant protection from carcinogenesis and increased animal survival (Bishayee et al., 1997). Demonstrating efficacy as a single agent chemotherapeutic against existing murine lymphoma tumours, Sardar *et al.* found that ammonium mononium monovanadate caused significant tumour regression and increased survival when supplemented daily (Sardar et al., 1993). Although numerous other studies have shown similar such benefits in liver, breast, lung and colon cancer as well as tumours of both the haematological system and connective tissue (Bishayee et al., 2010), only one documented study has examined

its effects on a nervous system tumour. Here it was shown that the organovanadium(IV) compound bis(4,7-dimethyl-1,10-phenanthroline) sulfatooxovanadium(IV) (metvan) displayed highly significant antitumor activity in mice, delaying tumour progression and prolonging survival time in both glioblastoma and breast cancer (Narla et al., 2001). Remarkably, metvan induced apoptosis in a range of different tumour types *in vitro* including treatment resistant tumour-derived cells, at greater efficacy than standard chemotherapeutics, as well as inhibiting migration/invasion.

In sum, multiple vanadium compounds exert various effects on a range of processes that could be detrimental for tumour maintenance and progression (**Figure 1.5.3**). Thus in light of this mounting evidence, we are in an exciting position to pursue such therapies given the extensive synthesis of numerous derivatives and toxicity testing in both mice and men, as well as the accompanying evidence that PTPs form a novel group of enzymes worth targeting in numerous human cancers. However, the non-PTP dependent effects of vanadium compounds are also worthy of consideration, as processes such as DNA damage and ROS are likely to significant contribute to cytotoxicity. The impact of ROS production of cancer cells will be discussed below.

1.6. Reactive oxygen species as mediators of cellular processes and tumour cell survival

1.6.1. Intracellular redox regulation and the generation of reactive oxygen species

Cellular aerobic respiration constantly generates ROS including the superoxide anion (O_2^-), singlet oxygen ($^1O_2$), hydroxyl radicals ($OH^{\cdot}$), peroxides (ROOR'), hydroperoxides (ROOH), and hydrogen peroxide (H_2O_2) (Eruslanov and Kusmartsev, 2010). It is estimated that 1-2% of electrons in the mitochondrial electron transport chain leak, forming the superoxide ion O_2^-. The enzyme superoxide dismutase (SOD) then catalyses the formation of H_2O_2 from O_2^-, which can react with Fe^{2+} to generate damaging hydroxyl radicals via Fenton reactions. Nicotinamide adenine dinucleotide phosphate (NADPH) oxidase in the plasma membrane, xanthine oxidase in the cytosol and cytochrome p450 in the endoplasmic reticulum are also sources of free

radicals. Increases in the production of ROS can result directly from mitochondrial respiratorial chain leakage or indirectly from attenuation of the antioxidant defence system. In both cases alteration of redox homeostasis results in oxidative stress, causing DNA damage resulting in mutations, modifying/damaging macromolecules such as proteins and lipids, and deregulating enzymatic-signalling cascades (Trachootham et al., 2008). Importantly, however, cellular ROS also have a role in maintaining homeostasis, functioning as second messengers in intracellular signal transduction (Finkel, 2000; Gulati et al., 2001; Herrlich and Bohmer, 2000).

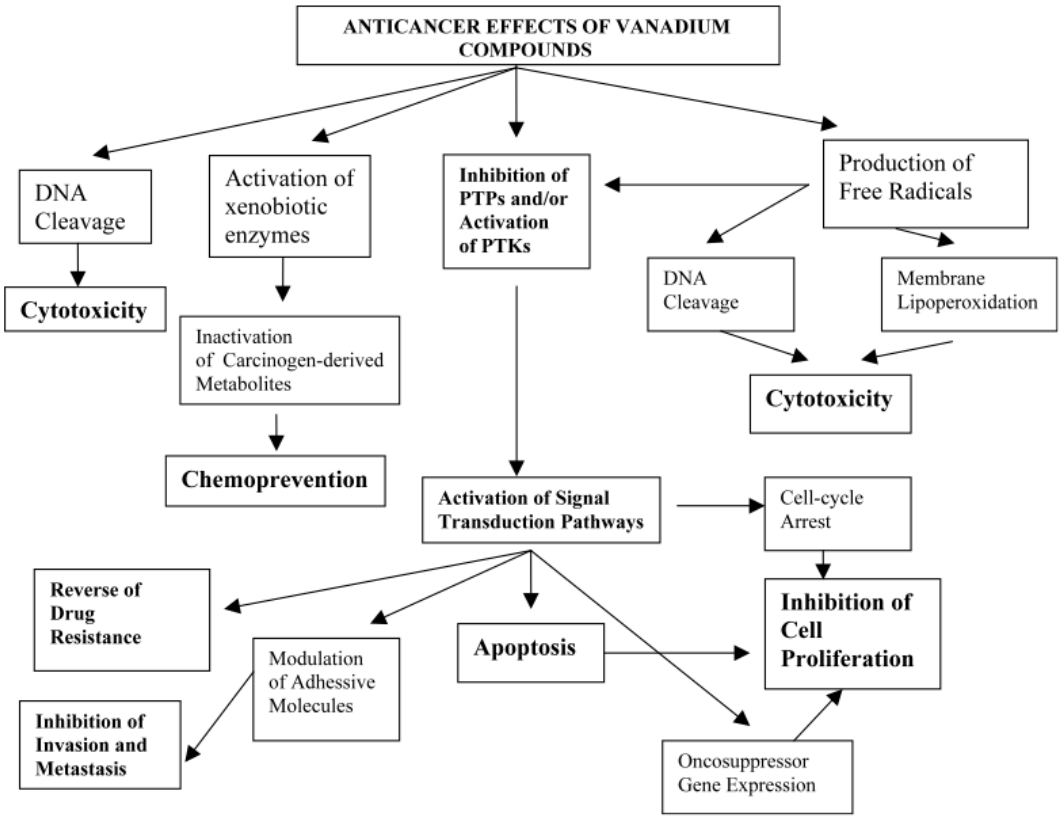

Figure 1.5.3. Vanadium compounds as anticancer agents. Summary of the effects of vanadium compounds detrimental to cancer cells. These include inhibition of invasion via modulation of adhesion, apoptosis via DNA damage/ROS production and reduced proliferation/cell cycle arrest through enzymatic regulation. Taken from (Evangelou, 2002).

Due to the ability of oxidative stress to cause damage to biological macromolecules, cells have evolved extensive antioxidant defences to intercept and thus abrogate ROS (Eruslanov and Kusmartsev, 2010). The enzymes SOD, glutathione peroxidase, catalase and thioredoxin reductase can all interfere with ROS production and

function as reducing agents. For instance catalase catalyses the reduction of H_2O_2 into a molecule of water and oxygen. One of the most important defence mechanisms against H_2O_2, as well as an intrinsic regulator of redox homeostasis, is the enzyme glutathione peroxidase, which functions through the glutathione (GSH) redox cycle within the mitochondria and cytoplasm (Filomeni et al., 2002). The tripeptide GSH (γ-Glu-Cys-Gly) behaves as a ROS scavenger, reducing free radicals via electron donation. Glutathione peroxidase catalyses the reduction of H_2O_2, and other peroxidases. GSH is itself regulated by glutathione peroxidase, converting it to an oxidised disulphide form (GSSG) and glutathione reductase, reducing it back to GSH. This process is important both in the synthesis of GSH and its role in acutely managing oxidative stress, increasing GSH through reduction of GSSG. The rate-limiting step in GSH synthesis is catalysed by the enzyme L-γ-glutamyl-cysteine synthetase, which can be inhibited by the compound buthionine sulfoximine (BSO). In sum physiological levels of ROS are affected by numerous stimuli and thus are kept tightly regulated through multiple antioxidant defence mechanisms (**Figure 1.6.1**).

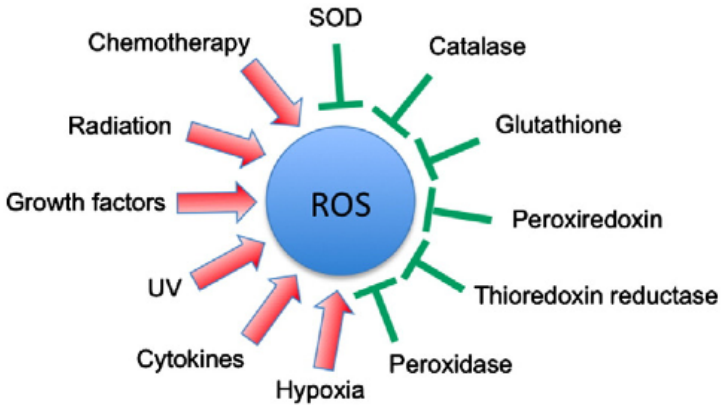

Figure 1.6.1. Stimuli/defence mechanisms regulating ROS. Numerous stimuli contribute to the generation of ROS especially in human cancer such as radiation, chemotherapy and hypoxia, however these are countered by antioxidant defence systems including glutathione, catalase and SOD (Reuter et al., 2010).

1.6.2. The role of ROS in cancer: A double edged sword

Due their ability to cause DNA damage and increase mutations, ROS are considered an important player in the development of cancer (Halliwell, 2007). However, they function as a 'double-edged sword' in cancer, as they clearly have the converse ability to reduce cell survival/proliferation and enhance cytotoxicity in tumour cells

(Engel and Evens, 2006). The reasons for these diametrically opposing functions in cancer biology will now briefly be discussed.

Perhaps the most obvious role of ROS in triggering cancer is via DNA damage-induced mutations, activating oncogenes and inactivating tumour suppressors. In fact the increased incidences in cancer in the elderly have been attributed to a lifetime of ROS attack, causing accumulating mutations (Halliwell, 2007; Wellen and Thompson, 2010). In established tumours, altered cellular metabolism can cause 'nutrient stress' both from oncogene driven increases in nutrient metabolism and nutrient deprivation driven by hypoxia/inadequate vascularisation, driving ROS production in the tumour micro-environment (Wellen and Thompson, 2010). The tumour suppressor p53 has been hypothesized to play a role in invoking antioxidant defence systems and p53 is transactivated by ROS (Sablina et al., 2005). As such, mutations in p53, which could be generated by ROS themselves, may potentiate the ability of ROS to promote tumorigenesis.

ROS can also inactivate/activate enzymes crucial to survival and apoptosis respectively. For example, increases in O_2^- can increase cytoplasmic pH and decrease the activation of caspases, allowing cell survival (Akram et al., 2005). Similarly H_2O_2 inactivates the tumour suppressor PTEN via oxidation of its active site cysteine, leading to increases in levels of PIP_3 and activation of Akt as a survival mechanism (Lee, 2002). PTEN is however regulated by the GSH antioxidant defence system. This reduces oxidized PTEN and may limit its inactivation by H_2O_2 generated from growth factor signalling (Kim et al., 2010). Stimulation of Akt itself generates ROS due to increased oxygen consumption and decreased ROS scavenger expression downstream of FoxO inhibition (Nogueira et al., 2008).

Perhaps the most emphatic evidence for the role of ROS in tumorigenesis is the finding that transgenic mice harbouring deletions in genes encoding for components of the antioxidant defence system are more prone to cancer (Neumann et al., 2003). However, ROS also promotes growth of existing tumours, for instance mediating anchorage independent growth in tumours driven by mutations in the K-Ras oncogene (Weinberg et al., 2010). In sum, ROS can promote tumorigenesis through multiple mechanisms, although larger increases in ROS may contribute to cell death (see below) (**Figure 1.6.2**).

As previously stated ROS exhibit a double-edged action in promoting tumorigenesis/expansion while also stimulating tumour regression depending on contextual factors such as dynamic interactions and spatial localisation (Halliwell, 2007). For instance transactivation of p53 by ROS due to DNA damage can trigger a senescence response, with p53 activity generating further ROS, representing a positive feedback loop (Bensaad and Vousden, 2005). H_2O_2 can decrease cytoplasmic pH and cause caspase activation, thus inducing apoptosis, in contrast to its opposite effect promoting survival (Hampton and Orrenius, 1997). Inactivation of cytochrome oxidases may also decrease ATP formation and thus tumour growth, and deactivation of numerous survival signalling enzymes such as mTOR may also engage apoptosis (Chen et al., 2009; Chen et al., 2010b). As well as the aforementioned findings that genetic inactivation of antioxidant defence systems promotes tumorigenesis, the most important antioxidant GSH is actually elevated in therapy-resistant tumour cells and decreased in cells sensitive to anticancer drugs (de Tudela et al., 2010). Lastly ROS can mediate apoptosis by directly activating both the extrinsic and intrinsic mitochondrial death pathways (Engel and Evens, 2006).

One commonly noted caveat is the suggestion that *in vitro* studies may be somewhat unreliable given the supraphysiological levels of ROS in cells cultured in hyperoxic conditions (5% CO_2), as well as in medium lacking antioxidants (Halliwell, 2007). Thus cancer cell lines may adapt to hyperoxia and thus increased ROS through increased production and subsequent reliance on antioxidant defences. Although this is certainly worth noting, numerous *in vivo* studies have also documented increased ROS levels in tumours. This has led to a recurrent strategy to target tumour cells by increasing already high levels of ROS, effectively 'tipping cells over the edge' (Huang et al., 2000b). One potential benefit of this strategy is that normal non-neoplastic cells should be preferentially spared given their lower endogenous levels of ROS, provided levels are not pushed too high. The aforementioned study by Nogueira *et al.* elegantly demonstrated that increases in the activity of Akt, while promoting survival, actually render cells highly sensitive to oxidative apoptosis due to enhanced oxygen consumption, producing ROS and sensitizing tumour cells to death through inhibition of the GSH antioxidant system (Nogueira et al., 2008). Similarly low ROS levels may mediate resistance to therapy. Putative TICs or CSCs

where shown to have lower ROS levels *in vivo* than their non-tumorigenic counterparts, rendering them insensitive to radiation therapy (Diehn et al., 2009). Again pharmacological depletion of antioxidants decreased the clonogenicity of CSCs and dramatically increased sensitivity to radiation-induced cytotoxicity, representing an effective way to combat cells that often circumvent standard therapies due to their relative quiescence (Gupta et al., 2009).

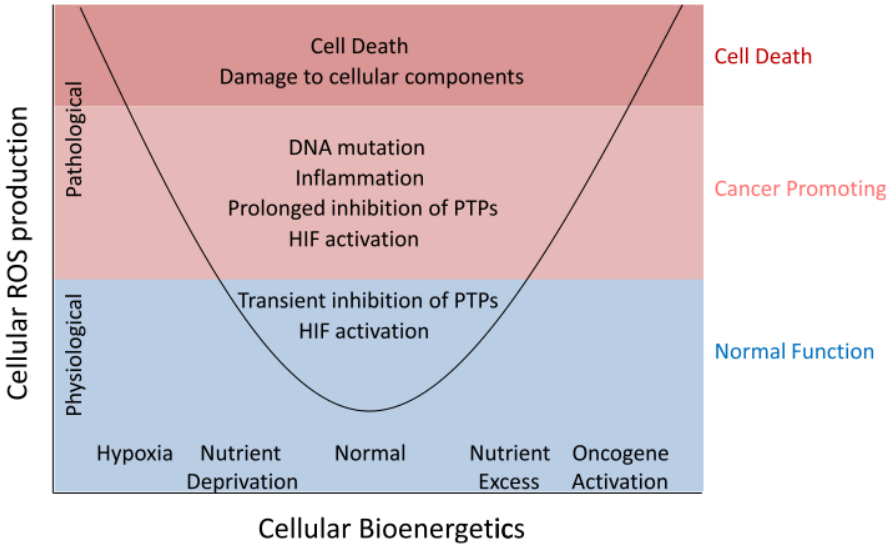

Figure 1.6.2. The effects of ROS on cancer. Increases in ROS production may promote tumorigenesis, which could be further augmented by tumour formation e.g. through excess nutrient consumption of oncogene activation. Pathological levels of ROS may however have the converse effect, stimulating cell death (See below). Taken from (Wellen and Thompson, 2010).

The notion that ROS are crucial to cytotoxicity of chemotherapy has been around since the 1960s, and demonstrated for standard front-line chemotherapeutics such as cisplatin and etoposide (Kurosu et al., 2003). Many studies have thus tested the ability of inhibitors of antioxidants to augment chemotherapy (Engel and Evens, 2006). As previously mentioned, the GSH synthesis inhibitor BSO has formed a crucial part of these studies. Twenty years ago BSO was shown to cause macrophage-mediated cytolysis of tumour cells *in vitro* (Nathan et al., 1981). Furthermore cytotoxicity induced by arsenic trioxide, itself capable of producing ROS, is potentiated by BSO in treatment-resistant multiple myeloma cells (Gartenhaus et al., 2002). BSO alone can activate caspase 8, where pre-treatment of

tumour cells sensitized to arsenic trioxide induced cell death (Kitamura et al., 2000). Importantly BSO was well tolerated in two phase I clinical trials in humans (Engel and Evens, 2006), suggesting promise as a broadly applicable anti-cancer therapy. However in addition to BSO, numerous antioxidants exist such as ascorbic acid, imexon and motexafin gadolinium, with similar efficacy (Engel and Evens, 2006).

1.6.3. BSO-mediated sensitization to chemotherapy in NBL

The numerous demonstrations of BSO-induced sensitisation to chemotherapy also extend to NBL, where ROS have been shown to play a causative role in response outcome (Marengo et al., 2005). Anderson *et al.* were the first to document cytotoxicity induced by BSO in NBL lines, demonstrating IC_{90} ranges of 2.1-1000μM in 17 of 18 cell lines, suggested to be lower than steady state plasma levels of BSO reported in adult human trials (Anderson et al., 1999). Yang *et al.* demonstrated that BSO treatment alone-induced apoptosis in NBL cells cultured in normoxic conditions (20% O_2) but not in hypoxic conditions (2% O_2) (Yang et al., 2003). Importantly this may reflect differences in ROS production depending on the tumour microenvironment, e.g. in hypoxic conditions found in bone marrow, which underlie treatment resistance. Tirapazamine, a bioreductive agent capable of generating ROS in hypoxic conditions, reversed hypoxic inhibition of BSO activity, causing increased ROS and apoptosis.

The protein kinase C (PKC) family of enzymes has been highlighted as a crucial determinant of NBL cells to ROS (Marengo et al., 2005). Domenicotti *et al.* demonstrated that decreased GSH levels caused by BSO treatment differentially regulated PKC isoforms, causing inactivation of classical PKCs but activation of the proapoptotic PKCδ isoform (Domenicotti et al., 2000). The same group extended this work to NBL cells *in vitro*, showing that high dose BSO treatment of a Mycn amplified NBL cell line caused ~50% increase in ROS as well as a shift in the ratio of GSH/GSSG accompanied by increased and decreased activity in PKCδ and PKCα respectively (Domenicotti et al., 2003a; Domenicotti et al., 2003b). Importantly these effects triggered apoptosis that was blocked by the PKC inhibitor rottlerin and the antioxidant vitamin C. Recently a causative function in ROS-induced apoptosis was demonstrated for PKCδ has (Marengo et al., 2011). Here overexpression of PKCδ

sensitized BSO-resistance NBL cells to apoptosis by increasing DNA oxidation and ROS production, as well as potentiating the effect of BSO on cells already sensitive to this treatment. Furthermore PKCδ overexpression also increased the effectiveness of the standard chemotherapeutic etoposide, confirming the role of ROS in cytotoxicity induced by front line agents and highlighting PKCδ as a novel target to augment it.

Mycn amplification status plays a crucial role in determining the response of NBL cells to BSO treatment, where Mycn amplified cells exhibit increased sensitivity to BSO treatment (Anderson et al., 1999). Marengo *et al.* found that Mycn-amplified NBL cell lines have higher basal levels of ROS production and exhibit more dramatic increases following BSO treatment (Marengo et al., 2008). This was suggested to result from higher levels of SOD-1 in Mycn amplified cells, which was stimulated by BSO. A recent finding elegantly demonstrated that Mycn amplification can confer resistance to ROS-induced apoptosis (de Tudela et al., 2010). Here Mycn increased the expression of the catalytic subunit of L-γ-glutamate-cysteine ligase (GCL(cat)), a rate limiting step in GSH synthesis, possibly explaining the heightened sensitivity of Mycn amplified cells to BSO treatment.

In sum ROS have a well defined role in cytotoxicity induced by chemotherapy and intracellular ROS levels may underlie therapeutic resistance for example in CSCs or Mycn amplified NBL cells. Furthermore ROS are crucial mediators of enzymatic signalling cascades, capable of acting as second messengers as well as inactivating enzymes such as PTPs. Thus redox dependent apoptosis represents a very interesting and largely unexplored area of NBL tumour biology.

1.7. Project aims

Thus given the increasing evidence that PTPs are involved in fundamental aspects of tumour biology, we wish to characterise the contribution played by this enzyme group in NBL. Thus the specific aims of this project are to document the effects of broad PTP inhibition achieved through vanadium-based phosphotyrosine mimetics. We hypothesise that by controlling proliferative ability and cell survival, the PTP family might harbour members that suppress differentiation (Chapter 3) and apoptosis (Chapter 4) in NBL. Thus PTP-inhibition could potentially enhance the effects of the differentiation agent RA, while also acting alone in a cytotoxic manner,

providing a possible targeted therapy for a tumour still lacking in targets. Given that broad PTP inhibition is likely to increase the activity of intracellular signalling cascades such as Ras/RAF/MEK/Erk and PI3K/Akt, we hope to reveal undocumented roles for their activation in NBL cell death and differentiation. Furthermore as vanadium compounds are known to cause ROS production, we aim to analyse the interaction between oxidative stress and activation of said pathways. Lastly candidate PTPs specifically involved in these processes will be identified based on expression profiling and clustering analysis (Chapter 5), with the aim of stimulating future molecular genetic approaches required to delineate the function of individual members of the PTP family in NBL cell survival/differentiation. The applicability of these findings to NBL biology and treatment will be discussed (Chapter 6).

Chapter 2: Materials and methods

2.1. Nucleic acid methods

2.1.1. DNA purification using QUIAGEN Plasmid midi kit

Purification of plasmid DNA was performed by the alkaline lysis method as described (Birnboim and Doly, 1979; Ish-Horowicz and Burke, 1981) using a QUIAGEN plasmid midi kit (Quiagen Inc, Valencia, CA, USA). Single bacterial colonies were picked from ampicillin-resistant Luria Bertani (LB) agar plates and grown for 12 hours at 37°C with rigorous shaking in 2ml LB broth starter-cultures containing 50µg/ml ampicillin. Starter cultures were then transferred to 100ml of LB broth containing 50µg/ml ampicillin and grown for 12-16 hours in the same conditions.

Bacterial cells were harvested by centrifugation at 4400 RPM for 15 minutes at 4°C, then resuspended in 4ml of resuspension buffer P1 (50mM Tris-HCl, pH 8.0; 10mM EDTA; 100µg/ml RNase A). 4ml of lysis buffer P2 (200mM NaOH; 1% SDS w/v) was then added and gently mixed followed by 5 minutes of incubation at room temperature (RT). 4ml of neutralization buffer P3 (3.0M Potassium acetate, pH 5.5), pre-chilled on wet ice, was then added, mixed and incubated for 15 minutes on ice. Lysates were centrifuged at 12,000 RPM in 30ml polypropylene tubes at 4°C to remove precipitate.

A QUIAGEN-tip 100 purification column was equilibrated with 4ml of equilibration buffer QBT (750mM NaCl, 50mM MOPS, pH 7.0; 15% isopropanol (v/v); 0.15% Triton® X-100 (v/v)), and the supernatant from the bacterial lysate was allowed to flow through the column by gravity flow. The column was then washed twice with 10ml of wash buffer QC (1.0M NaCl; 50mM MOPS, pH 7.0; 15% isopropanol (v/v)) to remove contaminants, and eluted into a 30ml polypropylene tube with 5ml of elution buffer QF (1.25M NaCl; 50mM Tris-HCl, pH 8.5; 15% isopropanol (v/v)). Eluted DNA was then precipitated by the addition of 3.5ml isopropanol and centrifuged for at 12,000 RPM for 30 minutes at 4°C. DNA was then rinsed with 70% ethanol and centrifuged at 12,000 RPM for 10 minutes at 4°C. DNA was air dried and resuspended in 100µl of buffer TE (10mM Tris-HCl, pH 8.0; 1mM EDTA).

General plasmid DNA precipitations were carried out by mixing DNA solutions with 0.7 volumes of isopropanol and centrifuging at 12,000 RPM for 30 minutes at

4°C. Precipitated DNA was washed with 1ml of 70% ethanol and centrifuged at 12,000 RPM for 10 minutes at 4°C. After air-drying at RT for 5 minutes, DNA was resuspended in 100µl of elution buffer TE (10mM Tris-Cl, pH 8.0; 1mM EDTA). In cases where the presence of EDTA could inhibit further reactions, the elution buffer EB (10mM Tris-Cl, pH 8.5) was used.

2.1.2. Restriction digestion and DNA electrophoresis

During the construction of recombinant DNA plasmids, restriction enzymes were used to cut double stranded DNA molecules at restriction sites. Plasmid DNA was combined with restriction enzymes at ~4 units/µg (enzyme: DNA) along with an appropriate 10x buffer and diluted in 75% water and incubated at 37°C for several hours. Following digestion enzyme products were combined with 5x bromophenol blue loading buffer (Bioline Ltd, London, UK) allowing visualisation of migration distance and separated by agarose gel electrophoresis using 0.7-1% agarose gels in tris-acetate-EDTA (TAE) buffer containing 0.0003% of the fluorescent DNA intercalating agent ethidium bromide. DNA size was visualised by concurrent electrophoresis with DNA HyperLadder 1 (Bioline Ltd, London, UK) and DNA bands recorded using a fluorescent transilluminator.

2.1.3. Elution of DNA from agarose gels

Gel elution was performed using a QIAquick gel extraction kit (Quiagen Inc, Valencia, CA, USA). Differentially sized DNA bands were separated by electrophoresis, and excised using a scalpel under a fluorescent transilluminator. Excised agarose was then incubated with 3x w/v of the solubilisation buffer QG (Quiagen Inc, Valencia, CA, USA) at 50°C for 10 minutes. DNA fragments between 500bp and 400kb were precipitated by adding an equal volume of isopropanol (isopropanol: agarose) then bound to a QIAquick spin column by centrifugation at 12,000 RPM for 1 minute. Trace agarose was removed by centrifugation at 12,000 RPM for one minute with 0.5ml of buffer QG, and any remaining contaminants were removed by an additional one minute, 12,000 RPM centrifugation step with 0.75 ml of the PE wash buffer. The QIAquick spin columns were transferred to clean 1.6 ml microcentrifuge tubes and

DNA was eluted by adding 30µl of the elution buffer EB (10mM tris-Cl, pH 8.5) for one minute followed by centrifugation at 12,000 RPM for one minute.

2.1.4. DNA ligation

DNA ligations were performed as described (Weiss and Richardson, 1967). Specifically circular plasmid DNA vectors and DNA fragment inserts were digested with restriction enzymes to yield linear DNA molecules with cohesive ends capable of annealing to one another forming a covalent bond. Digested vector DNA was then treated with calf intestinal phosphatase (CIP) (Roche Applied Science, Mannheim, Germany) in the presence of 10x phosphorylation buffer (0.5M Tris-HCl; 1mM EDTA; pH 8.5) for two hours at 37°C in order to prevent self-ligation. Re-purified vector DNA was then ligated to DNA inserts using an equal ratio of DNA using T4 DNA ligase (Roche Applied Science, Mannheim, Germany) with 10x ligase buffer (660mM Tris-HCl; 50mM $MgCl_2$; 50mM DTT; 10mM ATP; pH 7.5) overnight at 14°C. Vector-insert ligations were judged by the presence of increased molecular weight DNA as revealed by agarose electrophoresis.

2.1.5. Transformation of DNA

Incorporation of exogenous DNA into competent bacterial cells was performed as described (Chen and Dubnau, 2004). Briefly ~1ng DNA dissolved in 3µl of MilliQ water was incubated in the presence of 40µl of either the Library Efficiency® DH5α™ (Invitrogen, Carlsbad, CA, USA) or the JM109 (Promega, Fitchburg, WI, USA) clone of the bacterial cell *Escherichia coli* for 45 minutes on wet ice. Bacteria/DNA solutions were then heat-shocked by incubation at 42°C for one minute followed by incubation on wet ice for 1 minute. 1ml of LB broth growth medium was then added under a sterile environment and further incubated for 45 minutes at 37°C. 100-200µl of solution was then transferred under sterile conditions to a 10cm Petri dish containing LB agar with 50µg/ml of the antibiotic ampicillin and spread using a glass Pasteur pipette. Petri dishes were then incubated overnight at 37°C.

2.1.6. Detection of recombinant clones in bacterial colonies

Following transformation of ligated DNA, bacterial colonies were screened for the presence of supercoiled plasmids using the MICROPREP method (Sekar et al., 1987). Agarose gel electrophoresis (See 2.1.2) was performed using 0.8% agarose dissolved in Tris-acetate-EDTA (TAE) buffer (40mM Tris-acetate; 1mM EDTA) containing 0.05% SDS.

Bacterial colonies were picked from agar plates using a sterile p20 pipette-tip and gently vortexed into 6µl of protoplaster buffer (30mM Tris.Cl, pH 8; 5mM Na_2EDTA; 50mM NaCl; 20% sucrose) containing 50µg/ml RNase A (Sigma-Aldrich, St. Louis, MO, USA) and 50µg/ml lysozyme (Sigma-Aldrich, St. Louis, MO, USA) After 10 minutes of incubation, 5µl of each cell/protoplaster buffer suspension was added directly to agarose gel wells containing 3µls of lysis solution (TAE buffer; 2% SDS; 5% sucrose; 20% bromophenol blue). Circular/supercoiled vector DNA prepared in the same manner was used as a negative control.

Samples were electrophoresed in TAE buffer at 40v for 15 minutes followed by 100v for 2 hours, stained with ethidium bromide, and then photographed. Recombinant clones were judged on the basis of an increased size of supercoiled DNA when compared with vector alone.

2.1.7. Polymerase chain reaction (PCR)

Polymerase chain reaction (PCR) was used to generate DNA fragments for plasmid insertion as previously described (Saiki et al., 1988). Briefly 37.75µl of distilled water (Sigma-Aldrich, St. Louis, MO, USA) was combined with 5µl of 10x *PfuUltra* II reaction buffer (Stratagene, La Jolla, CA, USA), 25mM deoxynucleotide triphosphates (dNTPs), 0.025nmol of two oligonucleotide primers and 2ng of plasmid DNA. Oligonucleotide primers were diluted in distilled water (Sigma-Aldrich, St. Louis, MO, USA) at a stock concentration of 1nmol/µl. Specific primer information can be found in table 2.1. PCR was run using a PTC-200 Peltier thermal cycler machine (MJ Research, Waltham, MA, USA) with the following cycle: a) 95°C for 5 minutes, b) 85°C hold, c) 1U of PfuUltra II Fusion HS DNA polymerase (Stratagene, La Jolla, CA, USA) was added along with 1 drop of mineral oil (Sigma-Aldrich, St. Louis, MO, USA), d) 95°C for 1

minute, e) 55°C for 1 minute, f) 72°C for one to four minutes; repeat d-f for 28 cycles.

No	Oligo name	Sequence (5'→3')	Tm (°C)	GC content	MW (g/mol)
1	Ptprdfl1	AACTGGTCTACAAAGATGGGGAGCATGGAC	68.1	50%	9369
2	Ptprdfl1	TCAAGTTGTCATTTGCTTTCAATCCTCTTTCAATGTG	63.4	32.4%	10378
3	Ptprdfl3	GGTTTGTTTACTTCCAAGTTGAATGTTCCCAAG	65.9	38.2%	10428
4	FLbg1-1	GCCGTGTCCCACCAAGATTGTGTATCC	86	55.6%	8131
5	FLbg1-2	AATGGTCGTATTAAGCAGTTACGATCAGAATCTATTGG	67.3	36.8%	11755
6	HatagF	CTAGGTATCCCTACGATGTACCCGAGTAGCCTGACTCGAGT	>75	54.8%	12890
7	HatagR	CTAGACTCGAGTCAGCGAGTCGGGTACATCGTAGGGATAC	>75	54.8%	13099

Table 2.1. Summary of oligonucleotide primers used as templates for PCR reactions. MW = molecular weight; Tm = Melting temperature

2.1.8. Extraction of RNA using RNeasy mini kit

Genomic RNA was purified from cultured cells using an RNeasy mini kit (Quiagen Inc, Valencia, CA, USA). One to three million cells were trypsinised using trypsin-EDTA, and rinsed in PBS on ice. Cells were centrifuged at 1000 RPM for 5 minutes at RT, resuspended in 350µl of buffer RLT containing freshly added 1% β-mercaptoethanol, then homogenized by passing through a 22-gauge needle fitted to an RNase-free syringe 5-10 times.

Following homogenization, 1 volume of 70% ethanol was added and mixed by pipetting, transferred to an RNeasy spin column placed in a 2ml collection tube, and centrifuged for 15 seconds at 12,000 RPM. After discarding the flow-through, 700µl of buffer RW1 was added to the column and re-centrifuged, followed by 500µl of buffer RPE and further centrifugation for 2 minutes at 12,000 RPM. The spin column was placed in a 1.5ml collection tube, and 30µl of RNase-free water was added to the centre of the membrane. RNA was then eluted by centrifugation at 12,000 RPM for 1 minute.

The concentration of RNA was then determined by reading absorbance at 260nm using a NanoDrop® ND-1000 spectrophotometer (NanoDrop, Wilmington,

DE, USA) where quality was judged by the 260nm: 280nm and 260nm: 230nm ratios. Additional quality control measures were undertaken by the bioanalysis service provided by UCL genomics (UCL, London, UK).

2.1.9. Generation of cDNA and real time quantitative PCR analysis

All reactions were carried out by Dr. Fanny Schmidt (Merck Serono, Geneva, Switzerland), according to the following method. 1µg of RNA was used as a template for reverse transcription using the qscript cDNA synthesis kit (Quanta Biosciences Inc, Gaithersburg, MD, USA), containing a master-mixture of oligo(dT)20, reverse transcriptase Superscript III and random primers (Invitrogen, Carlsbad, CA, USA). RNA was then cycled for 1) 5 minutes at 25°C, 2) 30-minutes at 42°C, 3) 5 minutes at 85°C and 5) 10°C *ad infinitum*.

2.5µl of cDNA diluted 100 fold was then added to a mixture of 2.5µl of pre-mixed primer pairs and 5µl of SYBR Green PCR master mix (Quantifast, Quiagen Inc, Valencia, CA, USA) in 384-well plate. Each reaction was run in triplicate in a 7900HT Fast real-time PCR system (Applied Biosystems, Carlsbad, CA, USA) with the cycling protocol 1) 2 minutes at 50°C, 2) 10 minutes at 95°C, 3) 1 minute at 60°C. Dissociation curves were prepared following each qPCR run to determine primer specificity. Relative mRNA levels were determined by expressing as a percentage expression versus four housekeeping genes (HKGs). Briefly cross point values (Ct) obtained for each sample were normalized to the average of four reference genes Actin, Canx, Psmb3 and Hbms using the equation $2^{-\Delta Ct}$, where ΔCt = Ct (sample) – Mean Ct (reference genes).

2.1.10. DNA Sequencing

During plasmid construction gene inserts were verified using Sanger sequencing. Briefly high quality DNA was purified (see 2.1.1) and resuspended in distilled H_20 at a concentration of 100ng/µl. Primers (see table 2.1) were diluted at 2-5pmoles/µl. Sequencing was carried out through the DNA sequencing service provided by the Wolfson Institute for Biomedical Research (University College London, London, UK). Sequences were visualized using 4Peaks software (MEKentosj, Amsterdam, The Netherlands).

2.1.11. Plasmid expression vectors

For construction of plasmids expressing the *ptprd* gene, a pCH vector backbone was used containing the compound CAG promoter, a combination of the cytomelagovirus (CMV) early enhancer element and the chick beta-actin promoter that drives high gene expression levels (Niwa et al., 1991).

For overexpression of Src, the pSLX vector backbone containing a CMV promoter was used expressing either a wild type murine *c-Src* gene, or a mutant version in which the inhibitory tyrosine at site 529 has been replaced by phenylalanine (Y529F) causing the enzyme to be constitutively active (den Hertog et al., 1994). Both plasmids were a kind gift of Prof. Jeroen Den Hertog (Hubrecht Institute, Utrecht, The Netherlands).

For overexpression of Akt, two plasmids were used. Firstly a pCMV5 vector backbone expressing a HA-tagged mutant version of the murine *Akt1* gene under the control of the CMV promoter, in which the lysine of the ATP-binding site at position 179 is replaced by a methionine (K179M) causing loss of kinase activity was used as a dominant negative to attenuate the function of wild-type Akt (Franke et al., 1995). For expression of a constitutively active form of the Akt protein, a pECE vector backbone expressing containing the Simian vacuolating virus 40 (SV40) promoter was used to express the murine *Akt1* gene containing a 14 amino acid src myristoylation signal sequence (Cross et al., 1984) fused to the N terminus of Akt Δ4-129, which lacks a pH domain, causing constitutive activation of Akt via its targeting to the membrane (Kohn et al., 1996).

For detection of autophagy, a plasmid encoding enhanced green fluorescent protein (GFP) fused to microtubule-associated protein 1A/1B-light chain 3 (LC3-I) was transfected into cells prior to drug treatment. LC3-I is a cytoplasmic protein expressed in a diffuse manner in healthy cells that is cleaved and processed to form LC3-II, which is recruited to autophagosomal membranes during autophagy forming a punctate distribution of GFP that specifically marks autophagosomes (Mizushima et al., 2010). For monitoring of transfection efficiency, a plasmid was used that expresses enhanced-GFP under the control of the chick beta-actin promoter (CAβ-GFP) (Niwa et al., 1991).

2.2. Cell and protein methods

2.2.1. Propidium iodide staining for DNA content

DNA content was used to assess both cell-cycle distribution and DNA fragmentation indicative of programmed cell death (PCD) as described (Ormerod, 2002). $5x10^4$ Cells were plated onto 35mm multiwell plates. Following 6 days of treatment, cells were trypsinised and fixed in 1ml ice-cold 70% ethanol for 30 minutes on ice. Cells were rinsed twice in phosphate-citrate buffer (0.2M Na_2HPO_4/0.1M citric acid) by centrifugation at 2000 rpm, and resuspended in 200µl propidium iodide solution (50µg/ml in PBS; Sigma-Aldrich, St. Louis, MO, USA) and 50 µl RNaseA (Sigma-Aldrich, St. Louis, MO, USA) solution (100µg/ml in water). Cells were then transferred to polypropylene FACS tubes and subjected to flow cytometry using a BD™ LSRII flow cytometer system (Beckman-Dickson Biosciences, San Diego, CA, USA). A maximum of 10,000 events were collected per sample at a speed of between 100-1000 events/second depending on the total number of cells. Light scatter was used to determine the cell population for collection/exclude cell debris based on size (forward-scatter) and complexity/shape (side scatter) (**figure 2.1**).

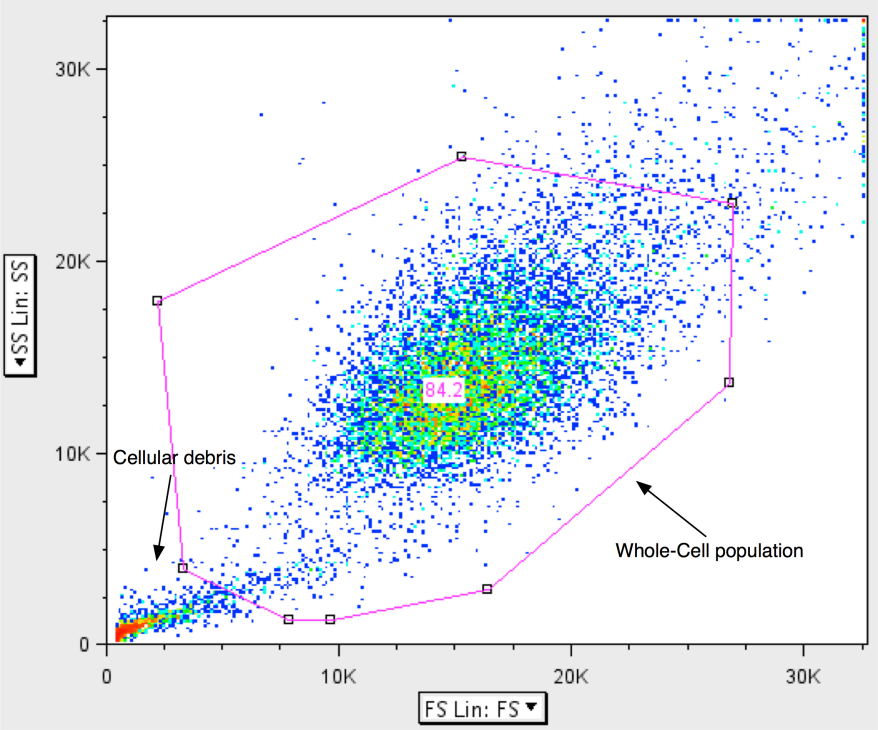

Figure 2.1. **Gating of whole cells during flow cytometry.** Histogram based on forward and side light scatter.

Data was analysed using Flo-jo V8 software (Tree Star Inc, Ashland, OR, USA). Single cells (singlets) were judged based on a histogram plotting area against height, and gated manually, excluding cell debris (**figure 2.2**). Sub-G1, G1, S and G2/M phase gates were applied to a histogram of DNA content and distribution peaks determining the percentage of cells in each phase of the cell cycle were judged manually (**figure 2.3**). Sub-G1 peaks were removed from the analysis when examining cell cycle distribution, but included when examining cell viability as a marker of DNA fragmentation that follows PCD. Independent samples, two-tailed student's t-tests were computed on the means of at least 3 independent experiments.

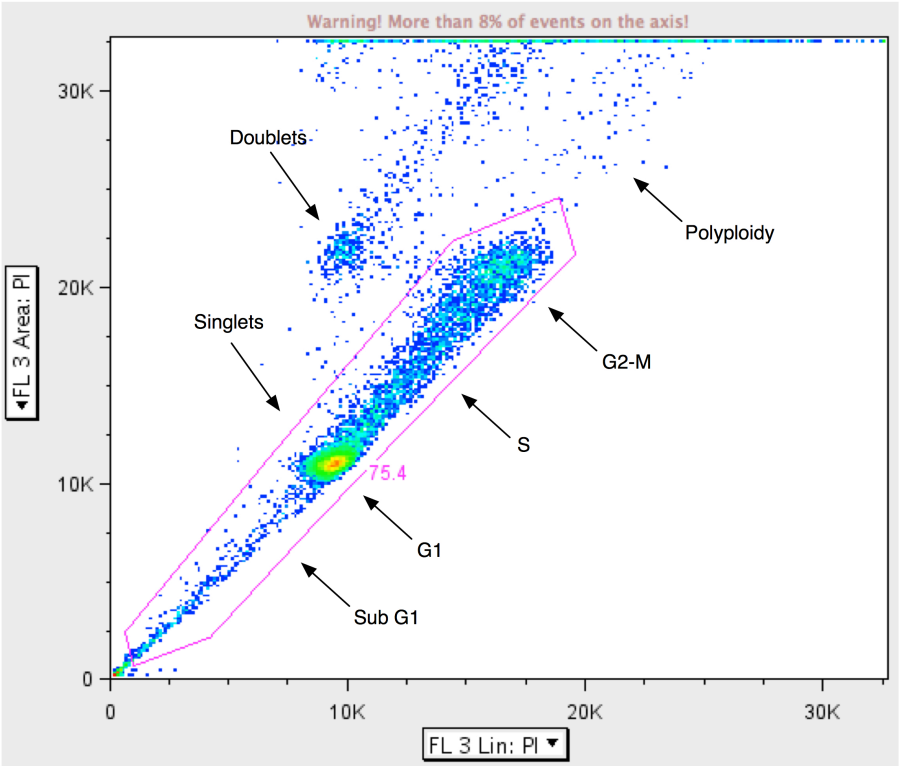

Figure 2.2. **Gating of single cells during flow cytometry**. Histogram based on area (y) and height (x) of signal.

2.2.2. Propagation of cells

Cells were maintained in a humidified incubator with 5% CO_2. Cells were cultured in different formulations of growth medium, depending on recommendations from the cell line supplier. All formulations of medium were supplemented with 10% (v/v)

heat-inactivated fetal-bovine serum (FBS) (PAA, Pasching, Austria) and 100 U/ml penicillin and 100 µg/ml streptomycin (1% (v/v) P/S) (Invitrogen, Carlsbad, CA, USA).

A

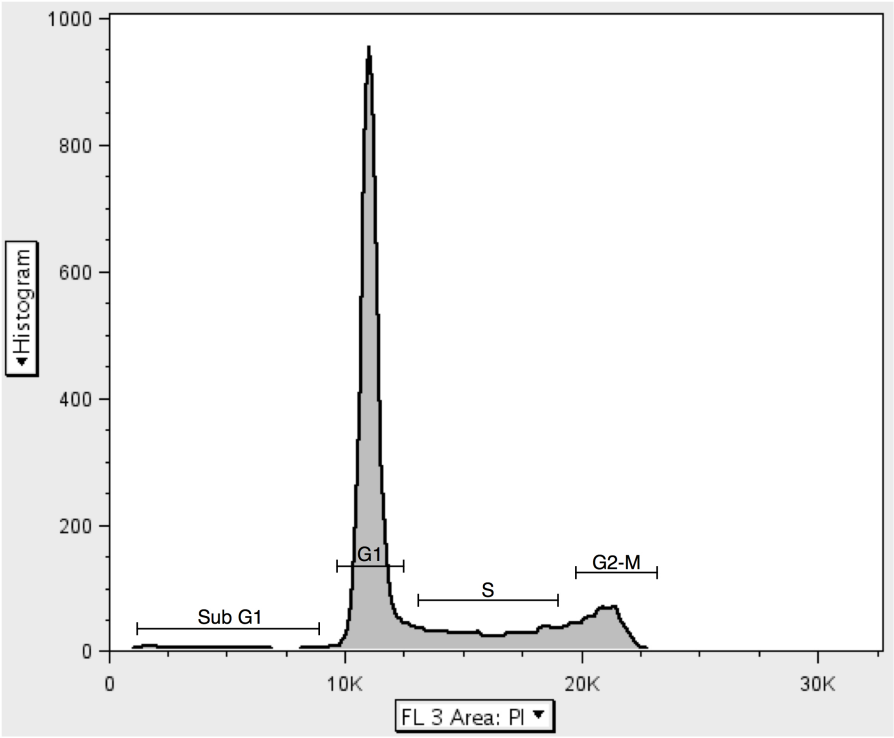

B

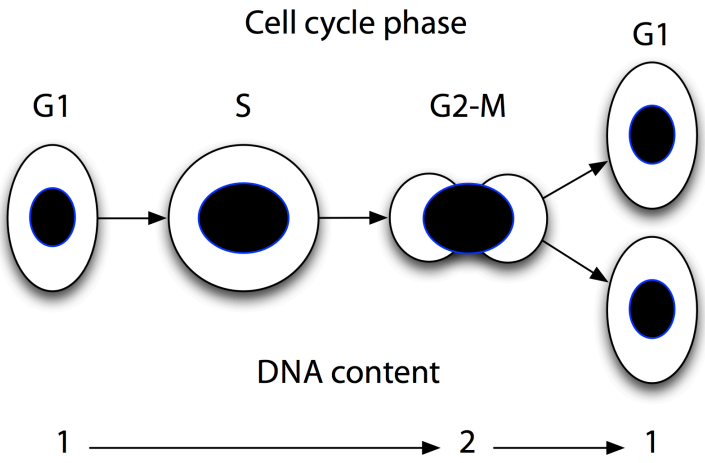

Figure 2.3. **Cell cycle distribution.** (**A**) Gating of cell cycle distribution peaks based on histogram of PI signal area, an analogue of cell cycle phase based on DNA content (**B**).

Dulbecco's modified Eagle's Medium (DMEM) (Gibco, Grand Island, NY, USA) was used for the culture of HEK-293T, U118, Res259 and T98G cells. Eagle's Minimum Essential Medium (MEM) (Gibco, Grand Island, NY, USA) was supplemented with the essential amino acid 2mM L-glutamine (Invitrogen, Carlsbad, CA, USA) dissolved in MilliQ distilled H_20 (Millipore, Billerica, MA, USA), and used for the culture of SK-N-SH, SH-SY5Y and PC63 cells. Roswell Park Memorial Institute (RPMI) 1640 (Gibco, Grand Island, NY, USA) was supplemented with the buffering agent 4-(2-hydroxyethyl)-1-piperazineethanesulfonic acid (HEPES) (Sigma-Aldrich, St. Louis, MO, USA)) at a concentration of 25mM and used for the culture of SK-N-AS, LAN-5, SK-N-DZ, SMS-KCN, SMS-KCNR, IMR-32 and Kelly cells. An additional formulation of RPMI 1640 was supplemented with 20% (v/v) FBS, 0.000007% (v/v) β mercaptoethanol (Sigma-Aldrich, St. Louis, MO, USA). 1% non-essential amino acids (Sigma-Aldrich, St. Louis, MO, USA) and the buffering agent sodium-pyruvate (Sigma-Aldrich, St. Louis, MO, USA) at a concentration of 10mM and used for the culture of IPhNB1 cells. All medium was replaced every 3-5 days.

All cell lines were grown as adherent monolayers, and passaged at sub-confluency. Prior to Passaging, cells were briefly rinsed with 37^{o}C phosphate-buffered saline (PBS) to remove all traces of medium. Cells were then trypsinised using 37^{o}C trypsin-EDTA solution (Sigma-Aldrich, St. Louis, MO, USA) for five to ten minutes in a humidified incubator at 37^{o}C. Cells were then resuspended in 37^{o}C medium and centrifuged at 1000 RPM for 5 minutes. Medium containing trypsin solution was aspirated and cells were resuspended in fresh medium then seeded at low density on vented tissue culture flasks (TPP, Trasadingen, Switzerland).

2.2.3. Control cell line information

The following non-NBL cell lines were used for the purpose of either optimisation, or as positive/negative controls, when compared to NBL cell lines. For details of NBL cell line properties see below.

HEK 293-T

The human embryonic-kidney 293T (HEK 293T) line was used as a positive control for the transfection of foreign DNA into cells. The HEK-293 cell line was generated

through the exposure of human embryonic-kidney cells to sheared fragments of the human adenovirus type 5, causing transformation and immortalization (Graham et al., 1977). The HEK-293T variant was generated through the addition of the SV40 large T antigen, allowing episomal replication of foreign plasmids containing the SV40 origin of replication and thus amplification of gene expression (Mellon et al., 1981). HEK-293T cells were also used to test for cytotoxic specificity of chemical compounds given their similarity with immature neuronal cells (Shaw et al., 2002).

PC63

The PC63 cell line (provided by Dr John Ham, ICH, London, UK) is a sub-clone of the PC12 cell line, which was originally derived from a pheochromocytoma of the rat adrenal medulla. These cells differentiate into post-mitotic neurons following treatment with nerve-growth factor (NGF), and subsequently become dependent on NGF for their survival (Obermeier et al., 1994). Thus these cells were used to test neuronal differentiation markers. PC63 cells were also used to test for cytotoxic specificity.

T98G

The T98G cell line was derived from a human malignant glioblastoma-multiforme and was used as a positive control for the suppression of colony formation by *PTPRD* (Veeriah et al., 2009). T98G cells were also used to test for cytotoxic specificity. Obtained from Human Protection Agency, UK.

COS7

COS7 is a form of the COS cell line, which was generated through immortalization of the CV-1 cell line derived from kidney cells of the monkey with the SV40 Large T antigen (Gluzman, 1981) and were used to test for cytotoxic specificity. Cells were originally obtained from the Oxford cell line repository.

U118 MG

The U118 MG (U118) cell line (provided by Dr Stephen Hart, ICH, London, UK) was derived from a malignant glioma of a human adult and was used to test for cytotoxic specificity.

U251 MG

The U251 MG (U251) cell line (provided by Dr. Jenni Jayalapan, Queen Mary University of London, London, UK) was derived from a malignant glioma of a human adult and was used as a positive control for the suppression of colony formation by *PTPRD* (Veeriah et al., 2009).

Mouse embryonic fibroblasts (MEFs)

Mouse embryonic fibroblasts were obtained from wild-type CD-1 mouse embryos, (provided by Dr. Sandra Castro, ICH, London, UK) at 16 days post fertilisation (dpf). Briefly embryos were dissected in PBS to remove organs and skin tissue was homogenised using a sterile razor blade. Cells were then dissociated in trypsin-EDTA for 20 minutes at 37°C and centrifuged at 1000 RPM for 5 minutes. Dissociated cells were then resuspended in culture medium. MEFs were used to test for cytotoxic specificity.

2.2.4. Chemical treatment of cells

The following chemicals were prepared and applied to cell culture medium as follows.

1. Retinoic acid ($C_{20}H_{22}0_2$) (Sigma-Aldrich, St. Louis, MO, USA) was diluted to 10mM in ethanol and added directly to cell culture medium at a final concentration of 5µM.
2. Sodium orthovanadate (Na_2VO_4) (Sigma-Aldrich, St. Louis, MO, USA) was added directly to cell culture medium from 100mM stock solution at a final concentration of 5µM.

3. Bis(maltolato)oxovanadium(IV) (BMOV) ($C_{12}H_{10}O_7V$) (Sigma-Aldrich, St. Louis, MO, USA) was diluted to 10mM in distilled H_20 and added to cell culture medium at a final concentration of 10µM to 20µM.
4. VO-OH Pic trihydrate ($C_{12}H_8N_2O_7V_3H_2O$) (Sigma-Aldrich, St. Louis, MO, USA) was diluted to 10mM in DMSO and added to cell culture medium at a final concentration of 0.5-5µM.
5. Nerve growth factor (NGF) (Promega, Fitchburg, WI, USA) was diluted to 1mg/ml in distilled H_20 and added directly to cell culture medium at a final concentration of 1µg/ml.
6. Propidium iodide ($C_{27}H_{34}I_2N_4$)(Sigma-Aldrich, St. Louis, MO, USA) was diluted to 50mg/ml in PBS, and added directly to cell culture medium at a final concentration of 5µg/ml.
7. NSC-87877 ($C_{19}H_{13}N_3O_7S_2$) (Santa Cruz Biotechnology, Santa Cruz, CA, USA) was diluted to 10mM in distilled H_20 and added directly to cell culture medium at a final concentration range of 50-100µM.
8. Sodium etidronate ($C_2H_6Na_2O_7P_2$) (Sigma-Aldrich, St. Louis, MO, USA) was diluted to 100mM in distilled H_2O and added directly to cell culture medium at a final concentration of 100µM.
9. Phenylarsine oxide (PAO) (C_6H_5AsO) (Sigma-Aldrich, St. Louis, MO, USA) was diluted to 10mM in DMSO and added to cell culture medium at a final concentration range of 0.1-0.3µM.
10. 3-4 Dephostatin ($C_7H_8N_2O_3$) (Sigma-Aldrich, St.Louis, MO, USA) was diluted to 10mM in DMSO and added to cell culture medium at a final concentration of 5µM.
11. U0126 ($C_{18}H_{16}N_6S_2$) (Cell Signalling Technologies Inc, Danvers, MA, USA) was diluted to 10mM in DMSO and added to cell culture medium at a final concentration range of 1-20µM.
12. LY294002 ($C_{19}H_{17}NO_3$) (Cell Signalling Technologies Inc, Danvers, MA, USA) was diluted to 10mM in DMSO and added to cell culture medium at a final concentration range of 1-20µM.

13. Rapamycin ($C_{51}H_{79}NO_{13}$) (a kind gift of Dr. Thomas Jacques, ICH, London, UK) was diluted to 200µM in DMSO and added to cell culture medium at a final concentration range of 100-200nM.
14. PI-103 ($C_{19}H_{16}N_4O_3$) (Cayman Chemical, Ann Arbor, MI, USA) was diluted to 1mM in DMSO and added to cell culture medium at a final concentration range of 0.5-1µM.
15. PP2 ($C_{15}H_{16}ClN_5$) (Calbiochem, La Jolla, CA, USA) was diluted to 10mM in DMSO and added to cell culture medium at a final concentration of 10µM.
16. PP3 ($C_{11}H_9N_5$) (Calbiochem, La Jolla, CA, USA) was diluted to 10mM in DMSO and added to cell culture medium at a final concentration of 10µM.
17. N-Acetyl-L-cysteine (NAC) ($C_5H_9NO_3S$) (Sigma-Aldrich, St. Louis, MO, USA) was diluted to 1M in distilled H_2O and pH adjusted to pH7.4 using sodium hydroxide then added to cell culture medium at a final concentration range of 0.1-2.5mM.
18. Buthionine sulfoximine (BSO) ($C_8H_{18}N_2O_3S$) (Sigma-Aldrich, St. Louis, MO, USA) was diluted to 10mM in distilled H_2O and added to cell culture medium at a final concentration of 10µM.
19. Hygromycin B ($C_{20}H_{37}N_3O_{13}$) (PAA, Pasching, Austria) was diluted to 200mg/ml in distilled H_2O and added to cell culture medium at a final concentration of 200µg/ml.
20. G418 ($C_{20}H_{40}N_4O_{10}$) (Sigma-Aldrich, St. Louis, MO, USA) was diluted to 500mg/ml in distilled H_20 and added to cell culture medium at a final concentration of 500µg/ml.

2.2.5. Antibodies

A number of antibodies were used for the detection of antigens during immunocytochemistry and immunoblotting. Table 1 contains a summary of primary antibodies and table 2 contains a summary of secondary antibodies. All antibodies used were immunoglobulin type G (IgG).

Antigen/size	Host Species	Clone	Clonality	Supplier
HA-Peroxidase conjugated	Rat	BMG-3F10	Monoclonal	Roche Applied Science
B-Actin	Mouse	AC-74	Monoclonal	Sigma-Aldrich
βIII-Tubulin	Mouse	TU-20	Monoclonal	Chemicon
PTPδ	Goat	C-18	Polyclonal	Santa Cruz Biotechnology
HA	Rabbit	-	Polyclonal	Abcam
Trk	Rabbit	C-14	Polyclonal	Santa Cruz Biotechnology
Ki67	Rabbit	NCL	Polyclonal	Novo Castra
Stat3	Mouse	124H6	Monoclonal	Cell Signalling Technologies
Phospho-Stat3(Tyr705)	Mouse	M9C6	Monoclonal	Cell Signalling Technologies
P44/42 MAPK (Erk1/2)	Rabbit	-	Polyclonal	Cell Signalling Technologies
p38 MAPK	Rabbit	-	Polyclonal	Cell Signalling Technologies
Mycn	Mouse	B8.4.B	Polyclonal	Santa Cruz Biotechnology
Cleaved caspase-3 (Asp175)	Rabbit	-	Polyclonal	Cell Signalling Technologies
Akt	Rabbit	-	Polyclonal	Cell Signalling Technologies
Phospho-Src Family (Tyr416)	Rabbit	-	Polyclonal	Cell Signalling Technologies
c-Src	Rabbit	N-16	Polyclonal	Santa Cruz Biotechnology
Phospho-4E-BPI (Thr37/46)	Rabbit	236B4	Monoclonal	Cell Signalling Technologies
Phospho-Akt (Ser473)	Rabbit	D9E	Monoclonal	Cell Signalling Technologies
Phospho-p44/42 MAPK (Erk1/2) (Thr202/Tyr204)	Mouse	E10	Monoclonal	Cell Signalling Technologies
FAK	Mouse	77/FAK	Monoclonal	BD biosciences

Phospho-FAK (Tyr379	Mouse	14/FAK(Y397)	Monoclonal	BD biosciences
PTEN	Rabbit	-	Polyclonal	Millipore
p53	Rabbit	Sc-6243	Polyclonal	Santa Cruz Biotechnology
Phosphotyrosine	Mouse	4G10	Polyclonal	Millipore

Table 2.2. List of primary antibodies. Antibody clone is stated where given.
Santa Cruz Biotechnology (Santa Cruz, CA, USA); Millipore (Bedford, MA, USA); Beckman-Dickson (BD) Biosciences (San Diego, CA, USA); Cell Signalling Technologies Inc (Danvers, MA, USA); Roche Applied Science (Mannheim, Germany); Sigma-Aldrich (St.Louis, MO, USA); Chemicon (Millipore, Bedford, MA, USA); Abcam (Cambridge, UK); Novo Castra (Newcastle, UK).

Antigen	Host Species	Supplier
Rabbit immunoglobulins/HRP	Mouse	Dako
Mouse immunoglobulins/HRP	Rabbit	Dako
Goat immunoglobulins/HRP	Rabbit	Dako
Rabbit immunoglobulins/biotinylated	Mouse	Dako
Mouse immunoglobulins/biotinylated	Rabbit	Dako
Goat immunoglobulins/biotinylated	Rabbit	Dako
Rabbit Alexa-fluor® 588	Goat	Invitrogen
Mouse Alexa-fluor® 477	Rabbit	Invitrogen

Table 2.3. List of secondary antibodies. Used for the detection of bound primary antibodies. Dako (Carpinteria, CA, USA); Invitrogen (Carlsbad, CA, USA).

2.2.6. Preparation of coverslips for cell seeding

For experiments involving immunocytochemistry and high magnification (63x objective) microscopy, cells were seeded onto pretreated/coated glass coverslips. 13mm, no.1 thickness, glass coverslips (VWR international, West Chester, PA, USA) were cleaned by rinsing for 30 minutes in concentrated nitric acid (BDH laboratory Supplies, Poole, UK) at RT, followed by distilled water for 30 minutes, and finally absolute methanol (Fisher Scientific, Loughborough, UK) for 30 minutes. Following this, coverslips were autoclaved and dried over night in a conventional oven at 75°C.

To facilitate adherence of cell monolayers, sterile coverslips were coated with poly-L-lysine then the extracellular matrix protein fibronectin. 100µl of 0.01% (w/v) poly-L-lysine (Sigma-Aldrich, St. Louis, MO, USA) diluted in water was added to each 13mm coverslip under a tissue culture hood and left to coat for 30 minutes at RT.

The remaining solution was then aspirated and coverslips were air dried for a further 30 minutes, then coated for 30 minutes with 1µg fibronectin diluted in MilliQ water from a stock solution of 1mg/ml fibronectin diluted in 0.5M NaCl, 0.05M Tris, pH 7.5 (Sigma-Aldrich, St. Louis, MO, USA). Cells were plated directly onto coverslips following coating.

2.2.7. Immunocytochemistry

Following completion of the experimental time course, medium was removed and cells were fixed either directly on coverslips or tissue culture dishes using a 4% solution of the protein cross-linking agent paraformaldehyde (Fisher Scientific, Loughborough, UK) in PBS for 30 minutes at RT. In order to prevent non-specific binding of antibodies, fixed cells were rinsed with PBS and pre-blocked for 45 minutes in a blocking solution of PBS containing 1% bovine serum albumin (BSA) (Sigma-Aldrich, St. Louis, MO, USA) which contains immunoglobulins capable of binding to epitopes on proteins, and permeabilised with 0.05% triton-X (Sigma-Aldrich, St. Louis, MO, USA). Blocking solution was removed and replaced with primary antibody diluted in incubation buffer (PBS; 3% BSA; 0.05% triton) for one hour. Primary antibody was removed by gentle shaking for 3x 10 minutes with wash buffer (PBS; 0.01% BSA; 0.05% triton). Next, secondary antibody was applied, diluted in incubation buffer (PBS; 3% BSA; 0.05% triton-X) for one hour, followed by 3 washes with wash buffer. When signal strength of the primary antibody was considered strong, a secondary antibody with a directly conjugated fluorophore was applied. However when signal strength was considered weak, a biotin-conjugated secondary antibody was used, followed by incubation with the fluorophore Cy-5 conjugated to strepdavidin (GE Healthcare, Little Chalfont, UK), diluted at 250x in incubation buffer (PBS; 1% BSA; 0.05% triton-X) for one hour. Dishes were wrapped in aluminium foil to avoid bleaching from light during stages involving fluorophores.

Following the final incubation, remaining solutions were removed by 3 washes with wash buffer, then coverslips (13mm) were either mounted on Superfrost® Plus glass slides (VWR international, West Chester, PA, USA), or if cells were fixed directly on 35mm plates, the base of the plate was covered with a coverslip (32mm) following the addition of 25µl of hard-set Vector shield mounting

solution (Vector Laboratories, Burlingame, CA, USA) containing 4',6-diamidino-2-phenylindole (DAPI), and left to harden overnight at 4°C.

2.2.8. Transfection of DNA

Incorporation of plasmid DNA into cells was achieved using various methods of transfection. For the first method, transfection was carried out using the cationic polymer polyethyleneimine (PEI) (Sigma-Aldrich, St. Louis, MO, USA). PEI confers a positive charge to condensed DNA molecules allowing them to bind to anionic cell-surface residues and pass through the cell membrane by endocytosis. Protonation of amine groups present on branched PEI molecules then causes an influx of anions and thus a reduction in osmotic potential resulting in osmotic swelling and vesicle bursting, thus releasing DNA polyplexes into the cell (Boussif et al., 1995).

PEI was prepared by dilution of the usual 25 kDa, branched form, made as a 1 mg/ml stock in water (Sigma-Aldrich, St. Louis, MO, USA). For transfection of one 35 mm dish, 2µg total DNA was diluted in 250µl, reduced serum OPTI-MEM with GlutaMAX^{TM} media (OPTI-MEM) (Invitrogen, Carlsbad, CA, USA). Where necessary a reporter construct expressing GFP was added at 10% of the total volume of DNA for co-transfection. 8µg PEI was then diluted in 250µl OPTI-MEM and combined with DNA for 25 minutes at RT. This was then added drop wise to wells containing 2ml of serum-containing medium and incubated for at least 4 hours at 37°C, before replacing with normal medium.

In the second method, lipopolyplex formulations were prepared as described (Hart et al., 1998). Here the liposome-based transfection reagent Lipofectin (Invitrogen, Carlsbad, CA, USA) composed of a 1:1 (w/w) formulation of the cationic lipids N-[1-2(2,3-dioleyloxy)propyl]-n,n,n-trimethylammonium chloride (DOTMA) and dioleoyl phophotidylethanolamine (DOPE) (Felgner et al., 1987), and the peptide (K) 16 GACYGLPHKFCG (peptide Y) (Irvine et al., 2008), a kind gift of Dr. Stephen Hart (ICH, London, UK) were combined to generate lipopolyplexes.

For transfection of one 35mm dish, 2µg total DNA was diluted in 200µl OPTI-MEM. Where necessary a reporter construct expressing enhanced-GFP was added at 10% of the total volume of DNA for co-transfection. 2µg of 1mg/ml Lipofectin was then combined with 8µg of peptide Y (0.1mg/ml in endotoxin-free water) and

diluted in 118µl OPTI-MEM, giving an equal volume of DNA: Lipid/peptide solution. The DNA solution was then added to the lipid: peptide complex and this was incubated at RT for 60 minutes. The DNA: lipid: peptide complex was then combined with 1.6ml of OPTI-MEM to create a total volume of 2ml, which was added drop-wise to the well and incubated at 37°C for 4 hours then replaced with serum-containing medium. Transfection efficiency was monitored by expression of co-transfected CAβ-GFP 24 and 48 hours post transfection.

2.2.9. Optical microscopy

For image capture of live cells, photographs were taken using a Zeiss Axiovert 135 microscope (Zeiss, Obercochen, Germany) fitted with an Exfo X-Cite series 120 UV lamp (Exfo, Quebec City, Canada), and a Hamamatsu ORCA-ER digital camera (Hamamatsu, Hamamatsu, Japan). Volocity software (Improvision, Coventry, UK) was used for image capture. Both 10x and 32x objective lenses were used to obtain images at 100x and 320x resolution respectively.

For image capture of fixed cells, photographs were taken using a Zeiss Axiophot microscope (Zeiss, Obercochen, Germany) fitted with a Leica DC500 camera (Leica, Solms, Germany) and a Exfo X-Cite series 120 UV lamp (Exfo, Quebec City, Canada). Leica FireCam V1.7.1 (Leica, Solms, Germany) was used for image capture. Both microscopes were fitted with the UV filter cubes G 365, exciting at 365^{+}/- 10nm and emitting at >420nm; BP 450-490, exciting at 450-490nm and emitting at 515nm; and BP 546/12, exciting at 546^{+}/-12nm and emitting at >590. Both 20x and 63x objective lenses were used to obtain images at 200x and 630x resolution respectively.

2.2.10. Generation of whole-cell lysates and determination of protein concentration

Whole cell lysates were prepared by lysing cell monolayers with lysis buffer (50mM Tris-HCl, pH 7.4; 150mM NaCl; 1% Triton X-100). Degradation of proteins of interest was prevented by the addition of 50x EDTA-free proteinase-inhibitor cocktail (Roche Applied Sciences, Mannheim, Germany). Protein phosphorylation status was preserved by the addition of 1mM sodium orthovanadate, 10mM sodium

pyrophosphate, and 25mM sodium fluoride (Sigma-Aldrich, St. Louis, MO, USA). Cells were lysed for 30 minutes on wet ice in order to inhibit enzymatic activity and thus protein degradation. After 15 minutes of lysis monolayers were detached from plates using a 24-cm cell-scraper (TPP, Trasadingen, Switzerland). Lysates were then centrifuged at 14,000 RPM for 30 minutes at 4°C.

Lysate protein concentration was determined with the Bradford Ultra reagent (Bio-Rad, Hercules, CA, USA), a Coomassie-based protein quantitation reagent suitable for use with detergent-containing lysis buffers. Briefly 20µl of lysate was combined with 300µl of reagent in a 96 well tissue culture plate. An equal volume of BSA/lysis buffer solution was diluted at 0.5, 1, 1.5 and 2 µg/ml to generate a standard curve of protein concentrations. Absorbance was read at 590nm using a Model 680 automated microplate reader (Bio-Rad, Hercules, CA, USA).

Protein concentration was determined by plotting a line-of-best-fit from the BSA standard curve values, which generated the equation, y (OD value) = (gradient) x + y-intercept, where x = protein concentration. This equation was then rearranged such that x = (y – y-intercept)/gradient, to generate a protein concentration as determined by OD value. A sample containing lysis buffer only was used as a background measurement and subtracted from each sample value.

2.2.11. Immunoblotting

Depending on the avidity of the antibody and the abundance of the protein, between 10-20µg-lysate protein was separated by sodium dodecyl sulfate polyacrylamide electrophoresis (SDS-PAGE) as described (Burnette, 1981; Laemmli, 1970; Towbin et al., 1979). Whole cell lysates were solubilised by heating at 100°C for 5 minutes with loading buffer (25mM Tris-HCl, pH 6.8; 60% glycerol (v/v); 8% SDS (w/v); 0.1% bromophenol blue (w/v)) containing 10% (v/v) freshly added reducing agent β-mercaptoethanol (Sigma-Aldrich, St. Louis, MO, USA), required to cleave disulphide bridges, at a ratio of 3:1 lysate to buffer.

Depending on the size of the protein of interest either 7.5%, 10% or 12% polyacrylamide resolving gels were made by combining varying amounts of 30% acrylamide and distilled water. Osmolarity and pH were maintained by the addition of 25% total volume resolving gel buffer (1.5M tris-base, pH 8.8). Resolving gels

contained 1% (w/v) of the anionic detergent sodium dodecyl sulfate, required to disrupt non-covalent bonds and thus the secondary, tertiary and quaternary structure of proteins, causing them to denature and conferring them with a negative charge thus allowing them to separate by electrophoresis on the basis of size. The polymerization of acrylamide monomers was catalyzed by the addition of 0.0075% (v/v) final volume of 10% ammonium persulfate (APS) (Sigma-Aldrich, St. Louis, MO, USA) diluted in distilled water, and 0.0012% Tetramethylethylenediamine (TEMED) (Sigma-Aldrich, St. Louis, MO, USA). The mixture was poured between 1mm spacer plates and outer plates, using a Bio-Rad Mini-PROTEAN 3 kit (Bio-Rad, Hercules, CA, USA), and polymerised for twenty minutes at RT. 1ml of Isopropanol alcohol was added after pouring to prevent unevenness and avoid air contact at the gel surface. A 5% polyacrylamide stacking gel was made by combining water with 0.132% total volume of 30% acrylamide, in addition to 1% SDS, 25% stacking-gel buffer containing 0.5M tris-base (pH 6.8), 0.01% APS and 0.0012% TEMED. Stacking gel solution was added onto the polymerised resolving gel, and a 1mm comb was inserted.

Up to 25µl of sample was loaded in each well, along with Precision Plus Protein standards (Bio-Rad, Hercules, CA, USA) providing a protein ladder of known sizes. Proteins were then separated by electrophoresis in a mini-PROTEAN 3-cell electrophoresis tank (Bio-Rad, Hercules, CA, USA) filled with running buffer (water with 5mM tris-base; 40mM glycine; 1% SDS), at a constant current of 20 mA/gel, limited to 200 V.

Following electrophoresis, separated proteins were transferred to Immobilon-P 0.45µM polyvinyldifluoride (PVDF) membranes (Sigma-Aldrich, St. Louis, MO, USA) in a Trans-Blot SD semi-dry electrophoretic transfer cell (Bio-Rad, Hercules, CA, USA). Specifically, PVDF membranes were soaked in absolute methanol for 5 minutes followed by a transfer buffer (water with 44mM tris-base; 52mM glycine; 20% methanol) for a further 5 minutes. 6 sheets of 3mm chromatography paper (Whatman, Maidstone, USA) corresponding in size to PVDF membranes were also soaked in transfer buffer for 5 minutes. 3 sheets of paper were then placed on the semi-dry transfer apparatus, followed by the PVDF membrane, followed by the polyacrylamide gel, followed by a further 3 sheets of paper. Proteins were then transferred at a constant voltage of 18 V, limited to 500 mA, for 30-60 minutes

depending on the number of gels and the size of the protein of interest. Following transfer, PVDF membranes were re-soaked in absolute methanol, and then briefly washed with distilled water.

Membranes were blocked overnight either in 5% non-fat milk powder (Marvel) or 5% BSA diluted in tris-based saline (50mM tris-base, pH 7.4; 150mM NaCl) with 0.1% tween-20 (TBS-T). Membranes were then incubated with primary antibody diluted in blocking solution for 1-12 hours depending on the antibody, on a roller at RT, then washed 3 times in TBS-T. Secondary antibodies labelled with horseradish peroxidase (HRP) were diluted in TBS-T at 10,000x and incubated for 1 hour on a roller at RT, then washed 3 times in TBS-T. HRP was detected using the electrochemiluminescence (ECL) Plus kit (GE Healthcare, Little Chalfont, UK) Immediately before use, 2ml of solution A were combined with 50µl of solution B/blot then incubated for 5 minutes. Here the combination of HRP and peroxide catalyses the oxidation of the Lumigen PS-3 acridan susbstrate generating acrinidium ester intermediates that react with peroxide to produce a sustained emission of 430nm light (Akhavan-Tafti et al., 1994). Light was detected by autoradiography using X-ray film (Kodak, Rochester, NY, USA) that was developed using a Xograph Compact X4 X-ray developer (Xograph healthcare LTD, Tetbury, UK).

2.2.12. Coomassie staining of protein following SDS-PAGE

In cases where the number of lysed cells was judged to be too low for detection by the Bradford Ultra method, protein levels in whole-cell lysates were determined using Coomassie staining. Briefly a duplicate SDS-polyacrylamide gel was run alongside of the gel that was subjected to protein transfer, then stained with Coomassie stain (0.025% Brilliant Blue; 40% methanol; 10% acetic acid) for 30 minutes with gentle shaking and de-stained with Coomassie-de-stain (40% methanol; 10% acetic acid) overnight. Protein levels were judged by the intensity of stained protein bands.

2.2.13. Stripping of polyvinyl diflouride (PVDF) membranes

In all cases were more than two proteins were detected; antigens were stripped and membranes were re-probed with alternative antibodies. PVDF membranes were

washed in water twice for 10 minutes with gentle shaking, immersed in 0.2M NaOH at 37°C for 20 minutes, then shaken for 10 minutes at RT. NaOH was then removed with one wash of TBS-T for 10 minutes and membranes were re-blocked in blocking solution. In cases where high protein abundance/antibody avidity prevented the use of NaOH as a stripping buffer, an alternative β-mercaptoethanol containing buffer was used. Here PVDF membranes were incubated with stripping buffer (62.5mM tris-HCl, pH 6.8; 20% SDS; 0.008% β-mercaptoethanol) at 50°C for 45 minutes then washed once with water for 1 hour with gentle shaking followed by TBS-T for 10 minutes, then re-blocked in blocking solution.

2.2.14. Neurite outgrowth quantification

Cells were seeded at low density ($5x10^4$) one day prior to the addition of chemical compounds. The degree of neuritogenesis was determined after 3 and 6 days of treatment by calculating the average neurite length and the percentage of cells with neurites, using Openlab V5.5 software (Perkin Elmer, Waltham, MA, USA). Specifically around 50 frames were photographed using a 10x objective lens, and neurites were measured on single dispersed cells that were not contacted by neighbouring cells. For each condition at each time point around 200-300 neurites were measured from at least 10 separate photographs. A neurite was defined as any process equal to or greater than two times the length of the cell body, and was measured from the cell body to the tip of the process.

2.2.15. Cell viability staining using crystal violet

To analyse the degree of cell viability after chemical treatment, cells were fixed in 4% paraformaldehyde for 30 minutes then rinsed in PBS. Remaining cells were stained using the protein dye crystal violet (hexamethyl pararosaniline chloride) solution (0.1% crystal violet/10% EtOH in distilled water) for 30 minutes, then rinsed three times with water and air dried overnight. Where viability was quantified, the remaining dye was solubilised using 20% acetic acid solution (500µl/35mm) and further diluted 1:3 in water. 100µl of the solution was transferred to a 96 well plate and a colorimetric reading was obtained at 495 nm using a Model 680 automated microplate reader (Bio-Rad, Hercules, CA, USA).

2.2.16. CellTiter 96 aqueous non-radioactive cell proliferation assay

For determination of the number of viable cells following chemical treatment, the reduction of the tetrazolium compound 3-(4,5-dimethylthiazol-2-yl)-5-(3-carboxymethoxyphenyl)-2-(4-sulfophenyl)-2H-tetrazolium (MTS) (Promega, Fitchburg, WI, USA) was used to generate a soluble formazan product, accomplished by dehydrogenase enzymes present within cells and thus directly proportional to the number of viable cells (Goodwin et al., 1995).

0.002% MTS reagent (diluted in PBS, pH6.5) was combined with 0.092% phenazine methosulfate (Sigma-Aldrich, St. Louis, MO, USA) (diluted in PBS) at 20:1 immediately before use and diluted in cell culture medium at 10% of the total volume, then added to cell culture plates and incubated for 4 hours at 37°C. 100µl of the culture medium containing soluble formazan product was then removed and transferred to a 96 well plate. The absorbance of formazan was read at 495 nm using a Model 680 automated microplate reader (Bio-Rad, Hercules, CA, USA).

2.2.17. Detection of cell senescence

For detection of senescent cells the senescence-associated-β-galactosidase assay was used, which detects senescent cells at an acidic pH (Dimri et al., 1995). Cells were fixed in 4% paraformaldehyde for 30 minutes then rinsed with PBS. A staining solution was combined immediately before incubation containing 5mM potassium ferrocyanide; 5mM potassium ferricyanide; 2mM magnesium chloride; 150mM sodium chloride; 30mM citric acid/phosphate buffer (0.1M citric acid; 0.2M sodium phosphate dibasic; pH 6) and 1mg/ml Xgal solution (20mg/ml 5-bromo-4-chloro-3-indoly- β-D-galactopyranoside diluted in dimethyl formamide). Approximately 1ml of solution was added to each 35mm well and cells were incubated overnight at 37°C. Staining solution was then removed and wells were washed with water.

2.2.18. Detection of reactive oxygen species using 2',7'-di-chlorodihydrofluorescein diacetate

Cellular generated reactive oxygen species (ROS) were detected via an increase in fluorescence that occurs following the conversion of the cell-permeable, non-fluorescent dye 2',7'-di-chlorodihydrofluorescein diacetate (DCFDA) to 2',7'-Di-

chlorofluorescein (DCF) after esterase-mediated cleavage, cellular accumulation and oxidation by ROS, as described (Eruslanov and Kusmartsev, 2010). Briefly DCFDA (Invitrogen, Carlsbad, CA, USA) was dissolved in dimethyl sulfoxide (DMSO) (Sigma-Aldrich, St. Louis, MO, USA) at a concentration of 5mM and added to Hank's balanced salt solution (HBSS) (Gibco, Grand Island, NY, USA) pre-warmed to 37°C at a final concentration of 5µM. The solution was kept in a light-resistant tube. Cells were then washed in HBSS and DCFDA was added to each well (2ml/35mm) then in a humidified 37°C incubator for 10 minutes under aluminium foil. DCFDA was then aspirated and cells were rinsed once with HBSS. Fresh HBSS was then added to each well, with cells being kept in the dark as much as possible, and cells were photographed using a microscope and a fluorescence filter microscope excited at 485nm. Intensity of fluorescence was quantified using Volocity software (Improvision, Coventry, UK).

Chapter 3: The effects of vanadium-based tyrosine phosphatase inhibitors as combinatorial agents with retinoic acid on differentiation and senescence

3.1. Introduction

Conventional treatment of cancer involves the selective induction of cell death in tumour cells through single or combined cytotoxic agents that induce DNA-damage, thus targeting dividing cells. Although this largely forms the basis of modern cancer therapy, it is widely acknowledged that most cytotoxics exhibit considerable side effects related to targeting of normal organs such as the bone marrow or gastrointestinal tract that harbour large populations of dividing cells. However an alternative approach to chemotherapy involves the induction of differentiation, forcing proliferative, pluripotent tumour cells down their respective lineages into mature, mitotically arrested cells, preventing tumour progression and potentially circumventing toxic side effects involved in standard chemotherapy (Reynolds, 1991). Perhaps the best-characterised example of such differentiation therapy is the clinical use of all-trans retinoic acid (RA), which shows remarkable efficacy against acute-promyelocytic leukaemia, demonstrated by a cure rate of ~90% (Huang et al., 1988). Although this task may be more complicated in cancers of polygenic origins, the induction of differentiation still represents a powerful tool in cancer treatment.

NBL has one of the highest rates of spontaneous regression of any human cancer, whereby the tumour resolves with minimal therapy, occurring in 5-10% of clinical cases but probably occurring at even higher rates in cases of asymptomatic NBL. Spontaneous regression often results from differentiation whereby immature proliferative neuroblasts differentiate *in situ* into mature ganglion cells forming the benign tumour ganglioneuroma. Although the molecular basis of spontaneous regression is unclear, it likely involves influences from pathways normally governing neuronal development e.g. neurotrophic factors (Nakagawara, 1998). In fact, the original description of spontaneous regression of NBL by Cushing and Wolbach in 1927 hinted to this hypothesis prior to the discovery of neurotrophins, stating “one is forced to conclude that the cells of this tumour as a whole have responded to the influences or factors governing the normal differentiation of the nervous system” (Cushing and Wolbach, 1927). Thus the discovery that NBL could spontaneously differentiate into a benign tumour led to the idea that differentiation induction could represent a clinically effective tool in NBL treatment.

RA represents a gold standard differentiation-inducing agent. However, due to issues of resistance, toxicity and relapse, research has often centred around improving retinoid therapy through the use of additional differentiation agents, which potentially impinge on both common and distinct pathways (Chevrier et al., 2008; Encinas et al., 2000a; Lucarelli et al., 1995; Sidell et al., 1995). Of potential interest here is that the PTP inhibitor sodium orthovanadate (VA), was shown like RA, to induce morphological differentiation in NBL *in vitro* (Rogers et al., 1994). Although the molecular details of this effect are unclear, VA represents a potentially novel agent in combination differentiation therapy.

Pro-senescence therapy is a distinct but related concept centring on the activation of senescence programs that lay dormant in tumour cells to prevent cell replication and thus tumour progression (Nardella et al., 2011). It is likely that as well as inducing apoptosis, conventional cytotoxic therapy induces a significant amount of senescence that contributes to its efficacy, although this is difficult to prove in human patients. However, as well as a side effect of therapy, a senescence response could potentially be targeted pharmacologically. One such example of this is the inhibition of the dual-specificity PTP PTEN, whereby acute loss of PTEN through small molecule inhibition following its monoallelic loss results in a p53-dependent senescence response (Alimonti et al., 2010b). Thus targeting other PTPs may potentially have similar effects due to loss of negative feedback regulation of oncogenic pathways such as PI3K/Akt or Ras/RAF/MEK/Erk.

Indeed pro-senescence therapy has been considered in the treatment of NBL, due to the rareness of p53 mutations at presentation, and the fact that both oncogene-induced senescence and PTEN-loss-induced senescence generally require p53 induction. One such therapeutic strategy is the stabilization of p53 using nutlin-3, a small molecule that antagonizes the p53 inhibitor MDM2 (Van Maerken et al., 2011; Van Maerken et al., 2006). Nutlin-3 has been shown to be effective *in vitro* against NBL cells due to its potent ability to induce senescence, and is currently in phase 1 clinical trials in other cancers. Similarly RA has been shown to cause senescence in NBL cells of specific lineages based on their molecular profile (Wainwright et al., 2001), although it is currently unclear whether senescence represents a significant component of the clinical response to RA.

Thus based on this evidence we sought to examine whether PTP inhibition can cause differentiation and/or senescence in NBL cells, hypothesising that such effects may result from the activation of tyrosine-kinase driven pathways controlling such responses. We also tested whether PTP inhibition would augment the effects of RA, potentially through activation of similar pathways, leading to a more effective differentiation or senescence response.

3.2. Experimental procedures

3.2.1. Neuroblastoma cell lines

A large number of NBL cell lines have been isolated from explanted tumour tissue and propagated *in vitro* for the characterisation of cell behaviour and propensity to differentiate from immature neuroblasts to mature sympathetic neurons. Of the hundred or so NBL cell lines established to date, many have been characterised for biological characteristics such as Mycn status, chromosomal aberrations and the expression of enzymes involved in the synthesis of catecholamines (Thiele, 2006). Generally speaking all NBL cell lines are derived from aggressive high stage (3-4) tumours, however a number of distinctions have been made due to phenotypic variation between cell lines, reflecting tumour heterogeneity.

The most common factor in distinguishing NBL cell lines is the cell phenotype, where three variants have been described, namely neuroblastic or N-type, Schwannian/substrate-adherent or S-type and intermediate or I-type. These categories reflect phenotypic properties, where N-type cell lines are composed of small neuroblasts that harbour neuritic processes, capable of undergoing neuronal differentiation in response to chemicals such as retinoic acid. In contrast S-type cell lines are composed of flattened fibroblastic/epithelioid cells which lack processes and are precursors to the non-neuronal lineages of the neural crest i.e. Schwann cells/smooth muscle cells/melanocytes (Ross and Spengler, 2007). I type cells represent an intermediate between the two, although obviously a number of cell lines contain mixed populations of the three cell types. Perhaps one of the most interesting factors distinguishing NBL cell type is their relative differences in malignancy, whereby I type cells have a 3-4 fold higher ability to form tumours in

xenografts models in contrast to N type cells, which are less malignant, and S type cells which do not spontaneously form tumours at all (Ross et al., 2003; Ross and Spengler, 2007; Walton et al., 2004). As such I type cells have been deemed a putative NBL cancer stem cell.

We sought to test a number of phenotypically and molecularly distinct NBL cell lines, in order to reflect the heterogeneity of NBL tumours in terms of efficacy of therapeutics. These cell lines harboured differences in cytogenetics, origin and Mycn amplification status (**Table 3.1**). As described, NBL cell lines (**Figure 3.1**) were chosen to represent a range of phenotypic categories including N type (SH-SY5Y, SK-N-SH, LAN5 and SMS-KCNR), S type (SMS-KCN, SK-N-AS, Kelly), and I type (IMR32, SK-N-DZ, SK-N-BE(2). Note that these are not formal classifications and reflect the authors judgement based on morphology, as such these may vary depending on the study (See (Thiele, 2006) for further discussion). SH-SY5Y cells were also originally derived from SK-N-SH cells, representing a neuronal type subclone (Biedler et al., 1978). Lastly the present study made use of a recently generated cell line derived from a treatment-resistant tumour of a patient at Great Ormond Street Hospital, IPhNB1, generously provided by Izabella Piotrowska and Arturo Sala (UCL Institute of Child Health, London, UK) (**Figure 3.2**).

SH-SY5Y and SK-N-SH were maintained in minimum essential medium Eagle (MEME) supplemented with 10% FBS, 1% Pen Strep and 2mM L-glutamine. All other cell lines were maintained in Roswell Park Memorial Institute (RPMI 1640) supplemented with 10% FBS, 1% Pen Strep and 25mM Hepes (pH 7.4).

3.3. Results

3.3.1. Vanadate augments retinoic acid-induced neuritogenesis and upregulation of neuronal differentiation markers

Vanadate (VA) has been shown to induce neurite elongation in SH-SY5Y human NBL and neuritogenesis in PC-12 pheochromocytoma cells (Rogers et al., 1994). Thus we sought to extend these findings by testing the efficacy of VA on a range of NBL cell lines exhibiting varying phenotypic characteristics and genetic backgrounds.

Cell Line	Morphology	MYCN Amplification	1p36 Deletion	11q Deletion	17q Gain	Treatment
IMR32	I	Y	Y	Y	Y	None
SK-N-SH	N/S	N	N	Y	Y	CT/RT
SH-SY5Y	N/S	N	N	N	Y	CT/RT
LAN5	N	Y	Y	N	Y	Unk.
SK-N-DZ	I	Y	N	Y	Y	Unk.
SK-N-BE(2)	I	Y	Y	Y	Y	CT
SMS-KCN	S	Y	Y	N	Y	None
SMS-KCNR	N	Y	Y	Y	Y	CT
SK-N-AS	S	N	Y	Y	Y	CT/RT
Kelly(N206)	S	Y	Y	Y	Y	Unk.

Table 3.1. Neuroblastoma cell lines information. Table shows the status of common cytogenetic abnormalities (1p/11q deletion, 17q gain) as well as Mycn amplification status, phenotypic classification and known treatments of primary tumours from which cell lines were derived. N = Neuronal; S = Schwannian; I = Intermediate. CT = Chemotherapy; RT = Radiotherapy; Unk. = Unknown.

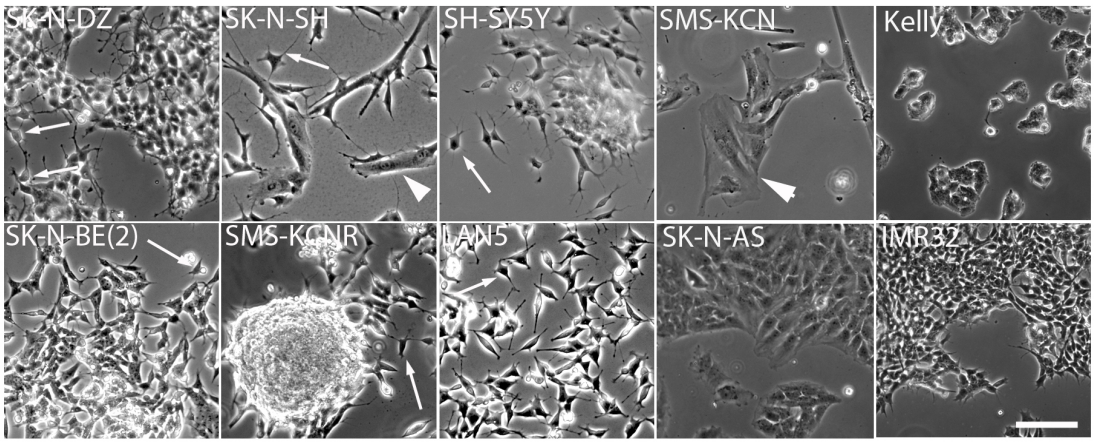

Figure 3.1. Neuroblastoma cell line phenotype. Examples of untreated NBL cell lines. Scale bar = 10 microns. Arrows refer to neuroblasts; arrowheads refer to S type cells. Note that some cell lines, e.g. SK-N-SH contain a mixed population of N and S type, whereas some cell lines contain I type cells with less obvious distinguishing features.

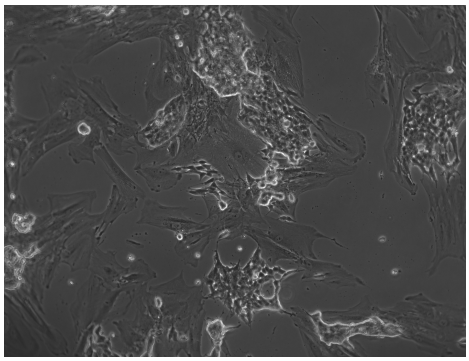

Figure 3.2. Primary tumour derived cell line. The cell line IPhNB1 was recently established by Izabella Piotrowska and Arturo Sala, from a primary tumour specimen taken from a treatment-resistant NBL. Note the presence of S and N type cells.

Furthermore we hypothesized that the VA-induced neurite extension documented by (Rogers et al., 1994) might cause additive gains in retinoic-acid induced neuritogenesis, given that other differentiation agents have been shown to augment the effects of retinoic acid, including vandetanib, an inhibitor of vascular endothelial growth factor receptor, epidermal growth factor receptor and rearranged during transfection tyrosine kinase (RET) (Zage et al., 2010b), phenylacetate (Sidell et al., 1995) and vasoactive-intestinal peptide (Chevrier et al., 2008).

Initial serial dosage testing suggested that VA had potentially non-specific toxic effects beyond 10-20µM, preventing phenotypic analysis (data not shown). Thus NBL cells were treated with 5µM VA over a 6-day period (see Chapter 2). VA induced significant neurite extension in LAN-5, SH-SY5Y and SK-N-SH cells (**Figure 3.3, D, E, F**). Notably these cells are primarily neuroblastic in morphology, and harbour small, neuritic processes endogenously, which were found to extend following VA treatment. We further tested the cell lines SMS-KCNR, SMS-KCN, SK-N-BE(2), SK-N-AS, Kelly, IMR-32 and SK-N-DZ and found that VA was unable to stimulate neurite extension (data not shown), although with the exception of SMS-KCN and SMS-KCN-R these cell lines do not undergo differentiation in response to RA, suggesting they may be from a less mature progeny.

As RA also stimulated neurite extension in LAN-5, SH-SY5Y and SK-N-SH (**Figure 3.3 G, H, I**), we sought to examine whether a combination of VA and RA treatment (VA/RA hereafter) induced greater phenotypic differentiation. VA/RA treatment led to a more highly differentiated phenotype in all cell lines (**Figure 3.3, J, K, I**). This was particularly evident in both LAN-5 cells, which exhibited longer and

denser axonal-like neurites, and SK-N-SH, which exhibited an almost entirely uniform population of differentiated neuronal-type cells rather than mixed clones of epithelioid/neuronal cells caused by RA treatment alone.

We quantified both the average length of neurite per cell across the population of cells and the percentage of cells with extended neurites (defined as any neuritic process twice the length of the cell body), revealing that six days of VA treatment was sufficient to induce significant gains in both average neurite length and the percentage of cells with neurites compared with untreated control cells (**Figure 3.4**, light grey bars), fully comparable to that induced by RA (**Figure 3.4**, dark grey bars). However combination VA/RA treatment significantly increased both of these parameters when compared to single-agent treatment (**Figure 3.4**, black bars). A noteworthy finding is that VA/RA treatment caused a near homogenous population (70-80%) of neurite-extended cells, compared to RA alone (50%).

We next sought to see whether these cell-structural effects of VA and VA/RA were mimicked by changes in expression levels of neuronal proteins. A number of proteins have been shown to be either involved in, or a consequence of, retinoic acid-induced neuronal differentiation. We chose to examine the neuron specific βIII tubulin, a cytoskeletal protein involved in microtubule structure, and the tropomyosin-related kinase (Trk) family, both of which increase in expression levels following neuronal differentiation (Eggert et al., 2000).

Both SH-SY5Y and LAN-5 cells responded to VA/RA treatment by increasing the expression of Trk significantly beyond that induced by RA alone (**Figure 3.5**). Similarly VA treatment caused an increase in the levels of βIII tubulin, which was further increased by VA/RA treatment in SH-SY5Y cells, although this protein was expressed at relatively high levels endogenously in both SK-N-SH and LAN-5, suggesting that it may mark immature cells of a neuronal lineage.

In sum, while both VA and RA are capable of effectively stimulating both cell structural and biochemical differentiation as single agents, both of these parameters are significantly enhanced with a combination of VA/RA treatment.

3.3.2. Vanadate has only modest effects on the distribution of cells within the cell cycle, and does not enhance retinoic acid-induced growth arrest

We next sought to examine whether the effects of VA on cell-structural and biochemical differentiation altered the proliferative capacity of NBL cells. Vanadium compounds have been shown to cause cell cycle arrest at both the G1 and G2/M phase in lung and kidney cancer cells, through stimulation of ROS and activation of Erk (Wang et al., 2010; Zhang et al., 2003). Similarly peroxovanadium-based inhibitors, which irreversibly inhibit PTPs through oxidation of the active site cysteine residue, have been shown to decrease proliferation resulting in accumulation in the G2/M phase of the cell cycle in NB-12 NBL cells (Faure et al., 1995). RA has been shown to decrease proliferation, resulting in cell-cycle arrest primarily at the G1 stage (For a review see (Melino et al., 1997)). Thus we predicted VA/RA treatment would enhance growth arrest induced by both compounds

We first conducted cell-cycle profile analysis using flow cytometry. RA was observed to increase the proportion of cells in G1 phase (SH-SY5Y, LAN-5) accompanied by decreases in the number of G2/M phase cells (SH-SY5Y, SK-N-SH) and S phase cells (LAN-5) (**Figure 3.6**). Although VA did significantly increase the proportion of cells in G2/M phase (SH-SY5Y, SK-N-SH), this increase was modest in comparison to that induced by RA and was unlikely to be the result of cell-cycle arrest. This apparent discrepancy between vanadate/peroxovanadium based PTP inhibitors inducing G1 or G2/M cell-cycle arrest (Faure et al., 1995; Wang et al., 2010; Zhang et al., 2003) probably reflects the low dosage of VA used in the present study and the fact that peroxovanadium compounds cause irreversible PTP inhibition.

Unlike the effects of VA/RA on neuritogenesis and biochemical differentiation, combination treatment did not enhance the effects of RA alone. Conversely we observed a significant reduction in the G1 increase (SH-SY5Y, LAN-5) G2/M decrease (SK-N-SH, SH-SY5Y) and S phase decrease (SH-SY5Y) that was induced by RA following combination VA/RA treatment (**Figure 3.6**, black bars versus dark grey bars). This suggests that both compounds exert their effects on cell-cycle progression through distinct targets, which when combined may result in competition, thus shifting the proportions of each cell cycle phase, i.e. VA induced G2/M increases partially attenuate RA induced G2/M decreases. However this would not necessarily result in increased proliferation if each compound caused stalling in

different cell-cycle phases, and may actually result in additive gains in cell-cycle blockade.

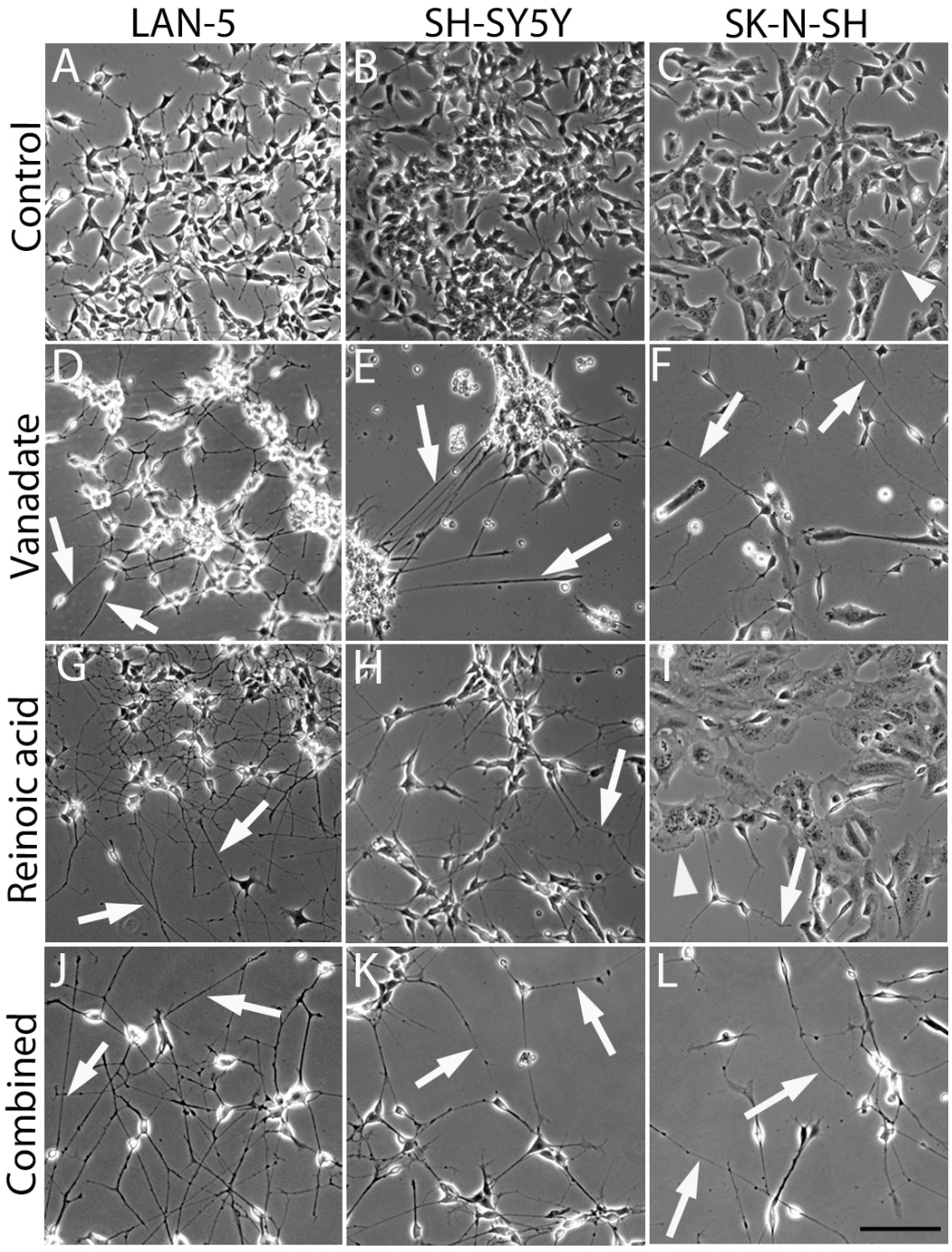

Figure 3.3. Vanadate treatment causes neurite outgrowth. Cells treated for 6 days with VA (5µM) and RA (5µM), alone or in combination. Both treatments induced neurite outgrowth (white arrows – D-F and G-I respectively), while VA enhanced phenotypic differentiation induced by retinoic acid (J-L). SK-N-SH cells also exhibted a flattened S-type morphology following RA treatment (arrowheads) Scale bar – 10 microns.

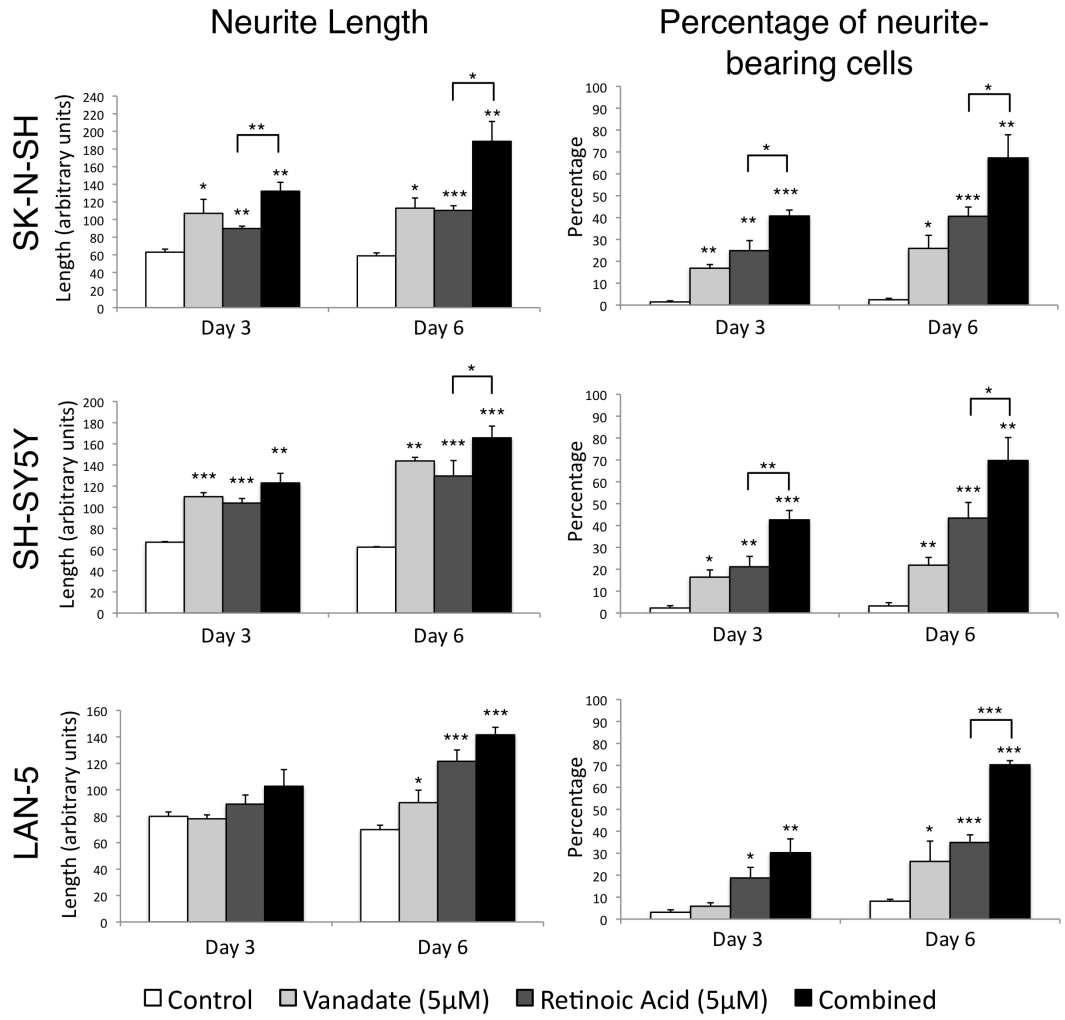

Figure 3.4. Quantification of neuritogenesis. Vanadate treatment significantly increases both neurite length and the percentage of neurite-bearing cells, and significantly enhances the effects of retinoic acid alone. Graphs show means and SEM. Statistical comparisons show two-tailed, independent samples student's t-tests, where * = P<0.05; ** = P<0.005, ***=P<0.001.

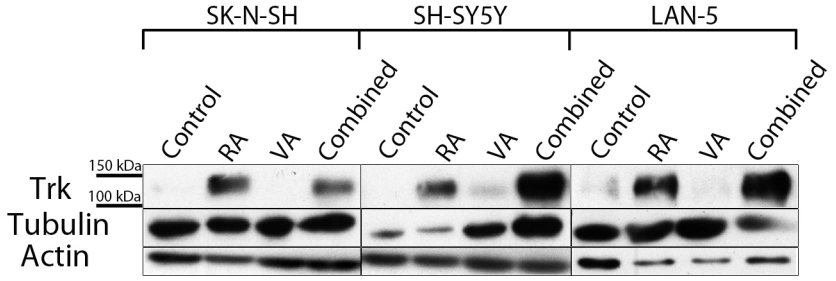

Figure 3.5. The effects of VA/RA on the expression of neural differentiation markers. Cells were treated for 6 days with VA (5µM) and RA (5µM) either separately or in combination. Total Trk levels (pan-Trk) and βIII tubulin levels are shown by immunoblotting.

Given that the influence of VA and RA on distinct phases of the cell cycle could still result in increases in growth arrest, we sought to see whether VA/RA led to terminal differentiation and cell cycle exit, by immunostaining for the proliferation marker Ki67, an antigen of unknown function that is expressed in all stages of the cell-cycle but absent in G0 cells (Endl and Gerdes, 2000).

As expected RA treatment induced significant decreases in the percentage of Ki67 positive cells, indicative of cell-cycle exit (**Figure 3.7**). However VA/RA treatment did not significantly decrease the number of Ki67 positive cells beyond RA treatment alone, although we did observe a small non-significant decrease in SK-N-SH cells (**Figure 3.7, B**). Similarly VA alone did not alter the number of Ki67 positive cells. Thus based on these data it is unlikely that VA exerts any major influence on the cell cycle and the proliferative capacity of NBL cells over 6 days of treatment, despite causing cell-structural differentiation. Viewed from a different perspective, if VA is exerting its effects primarily through inhibition of PTPs, one might expect an increase in cell proliferation, given that PTPs often counter the growth-stimulatory effects of PTKs in cancer cells (See Chapter 1), however VA did not stimulate proliferation when used as a single agent and did not counter RA.

In sum, 6 days VA treatment does not result in terminal differentiation, and thus cell-structural changes resulting in neurite extension are more likely the result of further neuronal specification that does not culminate in terminal differentiation and mitotic arrest. Similarly VA does not augment the growth-suppressing capabilities of RA, however it also does not attenuate RA-induced cell cycle exit.

3.3.3. Effects of an organometallic vanadium derivative bis(maltolato)-oxovanadium IV (BMOV) and non-vanadium based PTP inhibitors on neuritogenesis

Vanadium has been documented to influence several enzyme groups other than PTPs including ATPases, peroxidases, ribonucleases, PTKs and oxidoreductases, as well as stimulating changes in gene expression and altering cellular redox state (Evangelou, 2002; Mukherjee et al., 2004). Thus we sought to confirm that the effects of VA on neuritogenesis where primarily due to the inhibition of PTPs by

examining the effects of the established PTP inhibitors sodium etidronate (EHDH) and phenylarsine oxide (PAO) on the morphology of NBL cells.

In contrast to VA, neither PAO nor EHDH caused neurite extension in the tested NBL cell lines. Specifically PAO caused cytotoxicity at comparatively low doses (100-300nM), whereas cells were unresponsive to comparatively high doses (200μM) of EHDH (data not shown). We next sought to see whether the failure of PAO or EHDH to stimulate neurite extension was due to weak affinity for PTPs by examining changes in total cellular phosphotyrosine (pTyr) levels following short-term treatment. However we did not observe any consistent, gross changes in pTyr following treatment with any PTP inhibitor, including VA, at the doses used (**Figure 3.8).**

We next sought to examine whether the neuritogenesis stimulating ability of VA was specific to vanadium compounds rather than a general property of PTP inhibition. Thus we tested the organometallic vanadium derivative bis(maltolato)oxovanadium IV (BMOV), a reversible, competitive phosphatase inhibitor with a similar ability of VA to deliver uncomplexed vanadium (VO_4) to the active site of PTPs (Peters et al., 2003). BMOV was found to cause neurite-extension to a similar degree to VA (**Figure 3.9**). The neuritogenesis exhibited by BMOV-treated NBL cells was highly reminiscent of VA treated cells, with aggregating cell bodies extending elongated neurites rather than forming dispersed neuronal networks. Although a 10μM dose of BMOV was required to achieve a similar degree of neuritogenesis, we did not note non-specific cytotoxicity at this or a two-fold higher dosage (data not shown).

Figure 3.6. The effects of VA/RA on cell-cycle distribution. Cells were treated for 6 days with VA (5μM) and RA (5μM) both alone and in combination, then processed for flow cytometry using propidium iodide. The proportions of the cells in each stage of the cell cycle are shown in representative cell-cycle distribution histograms (**A**) and means of data taken from 6 experiments (**B**). Graphs show means and SEM. Statistical comparisons show two-tailed, independent samples student's t-tests, where * = $P<0.05$; ** = $P<0.005$, ***=$P<0.001$.

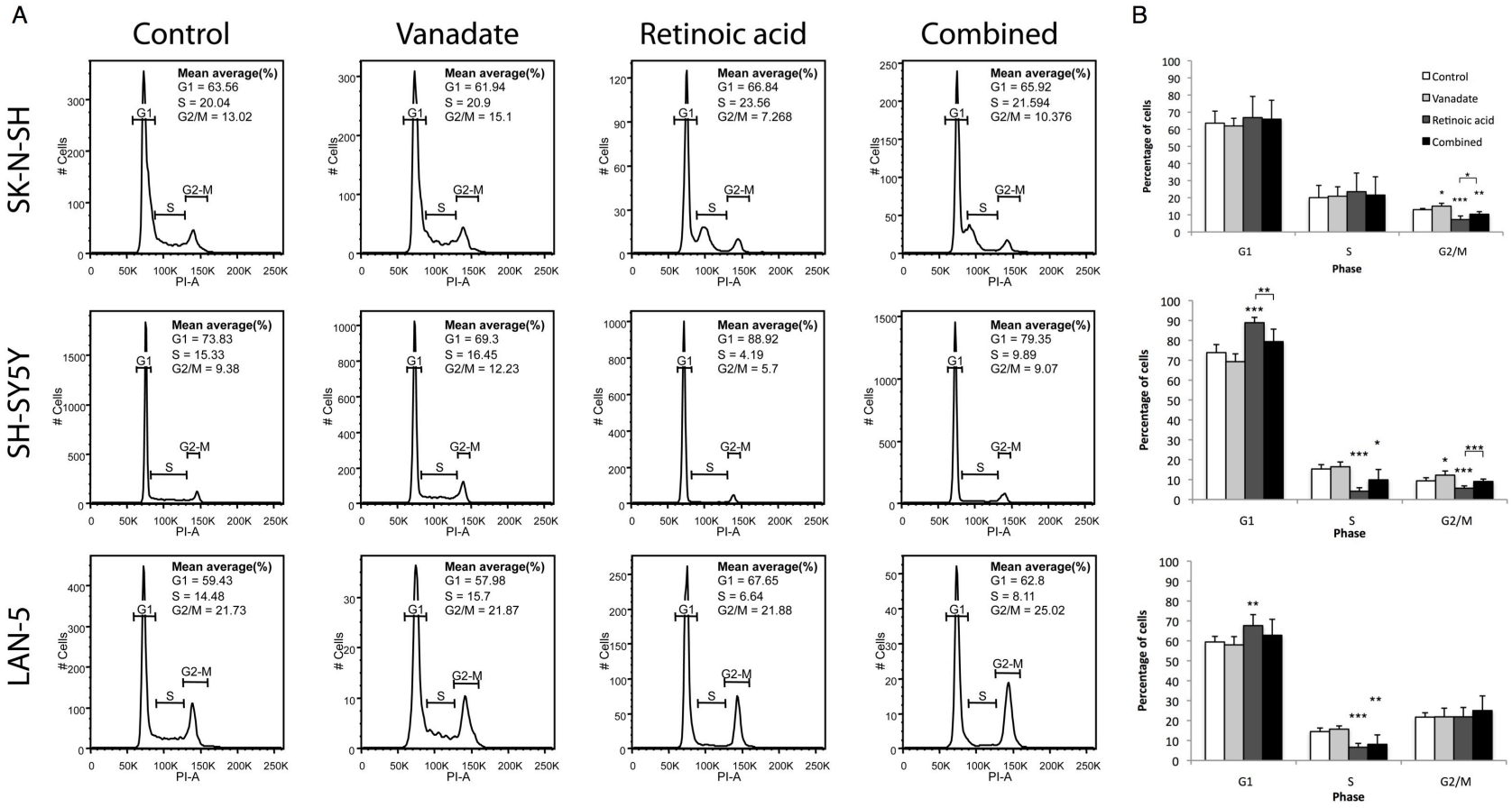
A
Control
Vanadate
Retinoic acid
Combined
SK-N-SH
SH-SY5Y
LAN-5
Mean average(%)
G1 = 63.56
S = 20.04
G2/M = 13.02
G1 = 61.94
S = 20.9
G2/M = 15.1
G1 = 66.84
S = 23.56
G2/M = 7.268
G1 = 65.92
S = 21.594
G2/M = 10.376
G1 = 73.83
S = 15.33
G2/M = 9.38
G1 = 69.3
S = 16.45
G2/M = 12.23
G1 = 88.92
S = 4.19
G2/M = 5.7
G1 = 79.35
S = 9.89
G2/M = 9.07
G1 = 59.43
S = 14.48
G2/M = 21.73
G1 = 57.98
S = 15.7
G2/M = 21.87
G1 = 67.65
S = 6.64
G2/M = 21.88
G1 = 62.8
S = 8.11
G2/M = 25.02
G1
S
G2-M
Cells
PI-A
B
Control
Vanadate
Retinoic acid
Combined
Percentage of cells
Phase
G1
S
G2/M

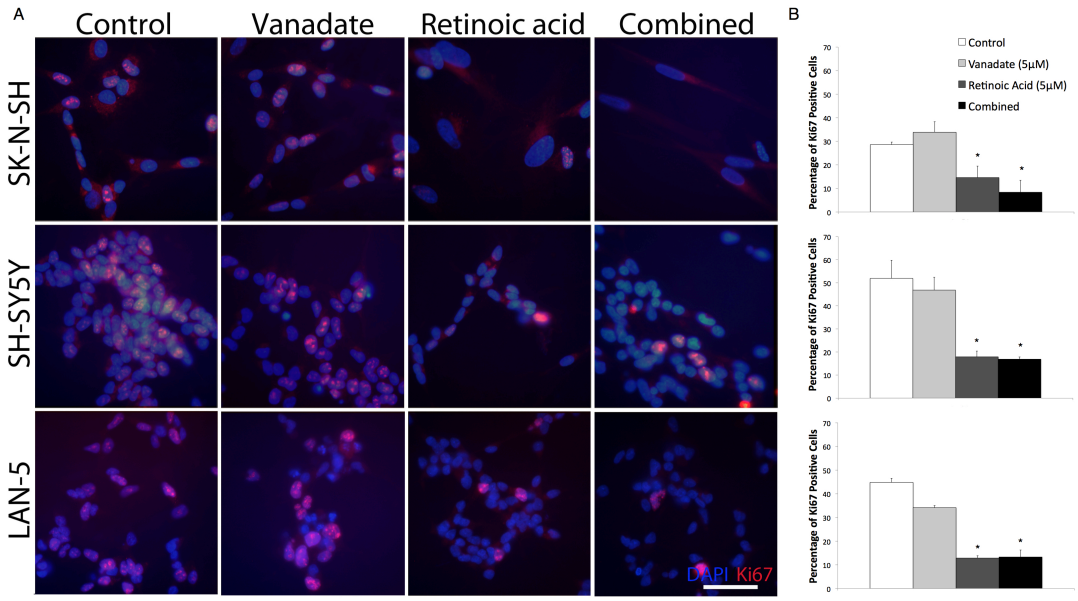

Figure 3.7. VA does not cause cell-cycle arrest. Cells were treated for 6 days with VA (5μM) and RA (5μM) both alone and in combination. Representative images (**A**) and histograms (**B**) showing the proportion of Ki67 positive cells, which is decreased by RA but not VA. Scale bar = 10 microns. Graphs show means and SEM. Statistical comparisons show two-tailed, independent samples student's t-tests, where * = P<0.05; ** = P<0.005, ***=P<0.001.

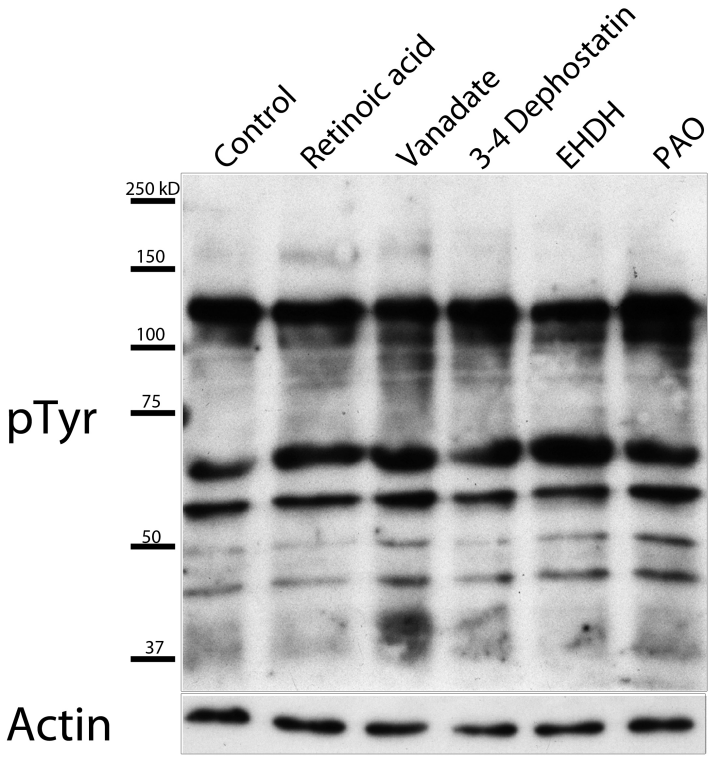

Figure 3.8. Phosphotyrosine levels after PTP inhibition. 2 hour treatment of LAN5 NBL cells with (5μM) VA or RA does not alter intracellular levels of pTyr, nor do the alternative phosphatase inhibitors 3-4 dephostatin (5μM), PAO (200nm) and EHDH (200μM).

We next tested whether low-dose BMOV treatment stimulated gross changes in cellular pTyr levels, indicative of widespread PTP inhibition. Immunoblotting for pTyr revealed a lack of gross changes in pTyr levels induced by BMOV treatment up to 100µM, similar to the effects of VA (**Figure 3.10**). This is in accordance with previous findings suggesting that neither VA nor BMOV stimulate pTyr accumulation compared to the peroxovanadium compound sodium oxodiperoxo(1,10-phenanthroline)vanadate(V) (pV(phen)), an irreversible inhibitor of PTPs (Krejsa et al., 1997). This suggests that rather than non-specifically inhibiting the entire PTP family with similar efficacy, both VA and BMOV may exert their actions through more selective inhibition of a smaller range of enzymes, thus leading to only minor changes in pTyr levels. Alternatively VA and BMOV induced neurite-extension could be achieved independently of PTPs, given that vanadium compounds exert effects on a number of enzyme groups, as well as stimulating the production of ROS (see section). In line with this Kresja *et al.* suggest that pV(phen) induced intracellular pTyr accumulation is primarily the result of ROS stimulation rather than PTP inhibition alone (Krejsa et al., 1997).

In sum, the effects of VA on neuritogenesis are not shared by non-vanadium based PTP inhibitors, but are mimicked by the vanadium derivative BMOV. Furthermore neither BMOV nor VA causes detectable changes in total pTyr levels, suggesting that their effects may be the result of either more selective PTP inhibition or non-PTP related consequences of vanadium treatment. However analysis of signal transduction following BMOV and VA treatment suggests that PTP inhibition is a likely candidate in mediating the phenotypic effects of vanadium compounds (see below).

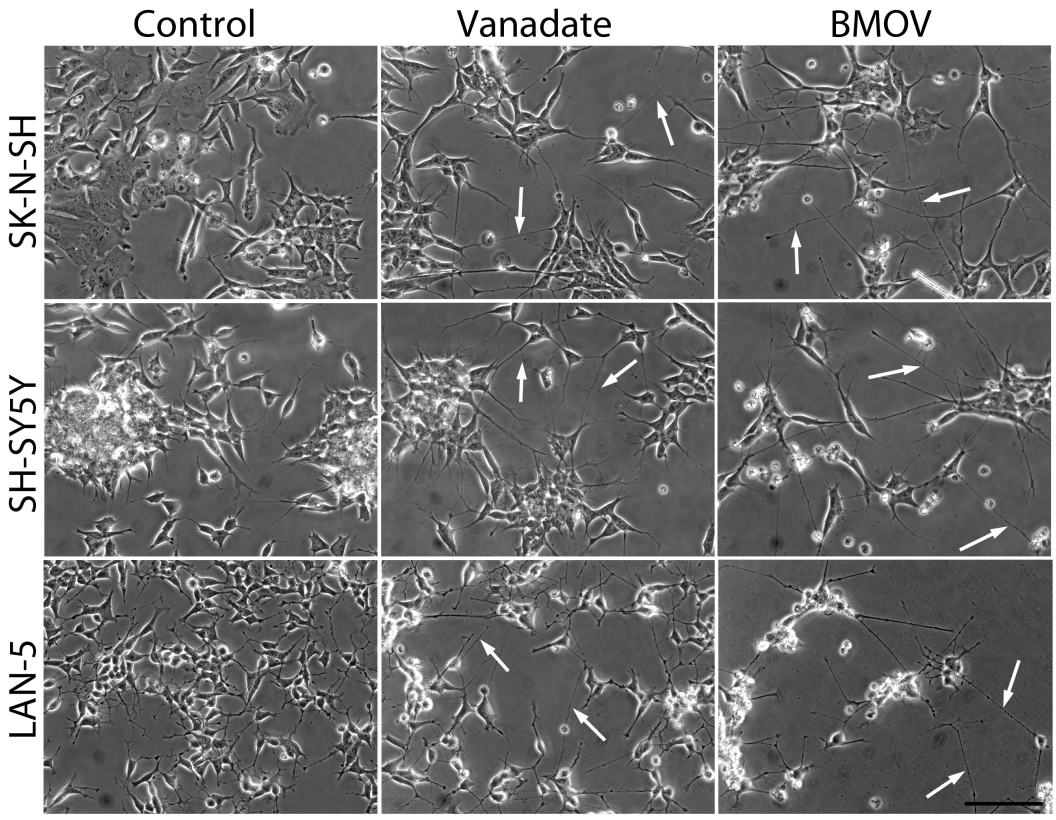

Figure 3.9. Bis(maltolato)oxovanadium IV (BMOV) induces neurite-extension. Cells treated for 6 days with VA (5µM) or BMOV (10µM) both exhibit neurite outgrowth (white arrows) to a similar degree. Scale bar = 10 microns.

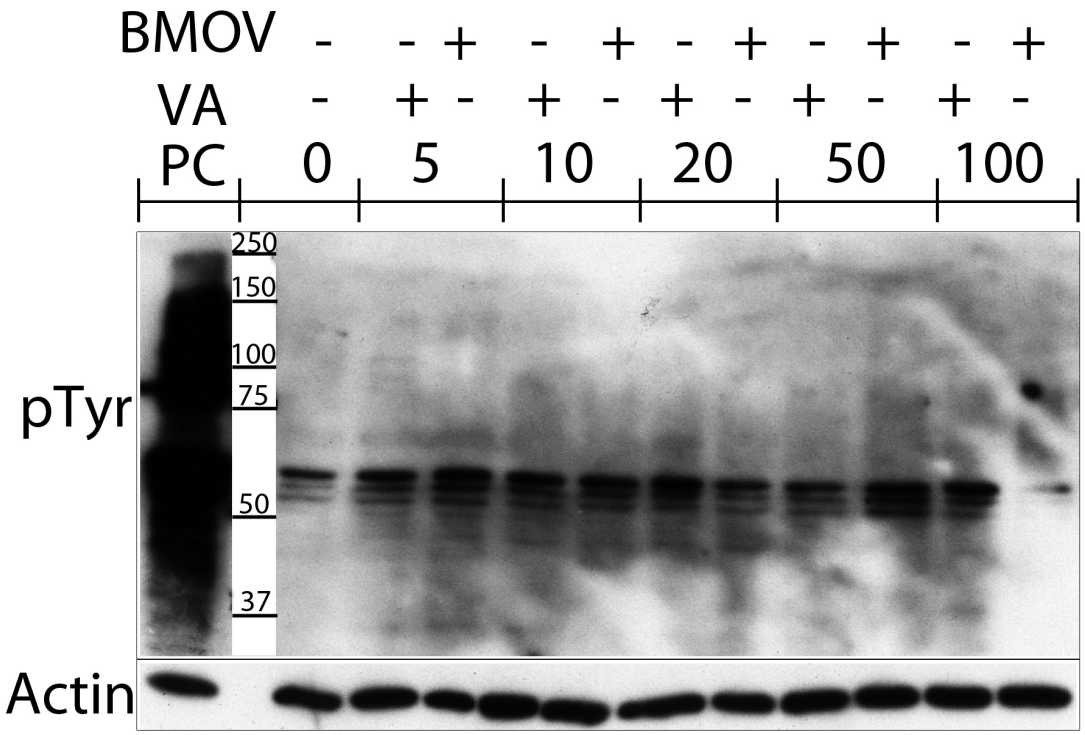

Figure 3.10. Phosphotyrosine levels following treatment with BMOV and VA. LAN5 cells treated for 2 hours with BMOV and VA at varying doses. Neither compound causes detectable alterations in cellular pTyr levels at dosages capable of stimulating phenotypic effects. PC = positive control of 5 minute treatment with 1mM pervanadate.

3.3.4. Vanadium compounds and retinoic acid synergistically activate both Erk1/2 and Akt, which is sustained throughout differentiation and is independent of ROS production

Although neither BMOV nor VA treatment led to an obvious accumulation of intracellular pTyr, we hypothesized that both compounds may be exerting more selective alterations in phosphotyrosine signalling within a limited set of intracellular signalling cascades. We also predicted that activation of signalling nodes might underlie the enhancement of RA-induced neuritogenesis with combination VA/RA treatment, given that a number of major signalling pathways have been implicated in RA-induced differentiation (Niles, 2004).

We initially focused on the Ras/RAF/MEK/Erk and the PI3K/Akt pathways, owing to their importance in a number of cellular processes including differentiation, proliferation and programmed-cell death (see Chapter 1). Immunoblotting revealed that both RA and VA activated Erk1/2 (Erk hereafter) and Akt, the effectors of both of these pathways respectively, to a similar degree in two NBL cell lines (SK-N-SH,

LAN-5) that respond to both treatments with neuritogenesis (**Figure 3.11, A**). However, more surprisingly combination VA/RA and BMOV/RA treatment induced a clearly synergistic augmentation of this response, causing hyperactivation of both pathways. Importantly this effect was not exhibited in two NBL cell lines (SK-N-AS, SK-N-DZ) that did not undergo neuritogenesis following treatment with either compound (**Figure 3.11, C**), but it did occur in two NBL cell lines that respond to vanadium compounds by undergoing cell death and to RA by undergoing growth-suppression (**Figure 3.11, B**) (See Chapter 5), suggesting that this was not a non-specific consequence of vanadium compound treatment.

We also examined the expression levels of the prognostic marker Mycn (see Chapter 1), which have been documented to decrease following RA treatment (Thiele et al., 1985) and increase following PI3K stimulation (Chesler et al., 2006). Although VA and BMOV alone caused a slight upregulation of Mycn (SK-N-DZ, LAN5), neither compound affected the ability of RA to decrease expression levels (**Figure 3.11**), despite hyperactivation of Akt suggestive of PI3K stimulation.

The functional consequences of intracellular signalling cascades are highly dependent on the duration of activation. For instance, Erk activation has been shown to exert contrasting effects of proliferation and differentiation following either transient or sustained stimulation respectively, in PC12 cells (Marshall, 1995). This has been suggested to be a consequence of differential interaction of effector proteins (von Kriegsheim et al., 2009). Thus we sought to characterize the time-course of Erk/Akt stimulation induced by vanadium compounds and retinoic acid in combination, primarily focusing on BMOV. Activation of both Erk and Akt failed to occur following short-term treatment with BMOV/RA (**Figure 3.12, A**). In fact stimulation only became apparent between 2.5-10 hours, sharply peaking at the latter, despite the effects of PTP inhibitors often occurring following as little as 5 minutes of treatment (Mak et al., 2010).

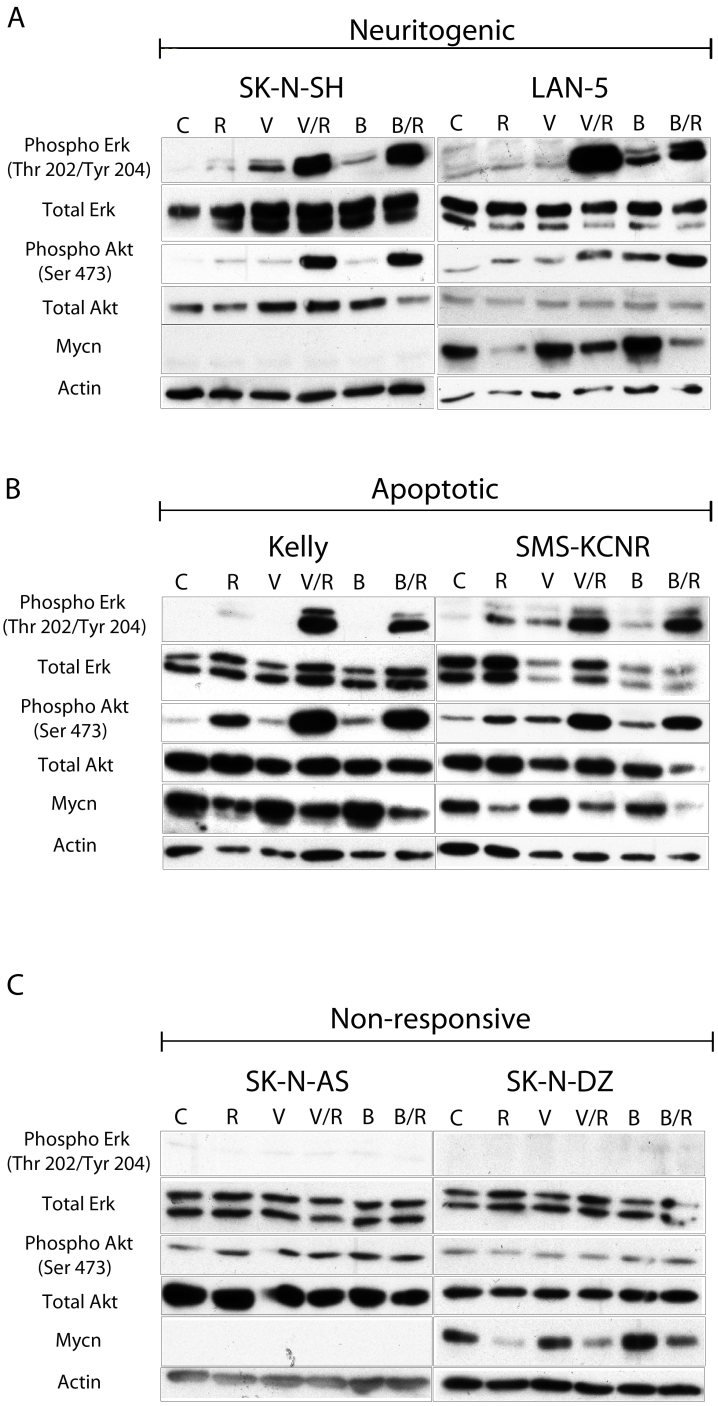

Figure 3.11. Hyperactivation of Akt and Erk following VA/RA and BMOV/RA treatment. Cells were treated for 24 hours with VA (5µM), BMOV (10µM) and RA (5µM). Both cell lines that respond to vanadium compounds and/or RA by undergoing neuritogenesis **(A)** and vanadium compounds alone by undergoing cell death **(B)** respond to combination VA/RA or BMOV/RA treatment by hyperactivation of Akt and Erk while cell lines which are phenotypically unresponsive to treatment **(C)** do not. Vanadium compounds do not reduce the expression of Mycn but do not interfere with its downregulation by RA in Mycn amplified cell lines (LAN-5, KCNR, Kelly, SK-N-DZ).

Given that long-term stimulation is associated with cellular differentiation, we next sought to examine whether the latent activation of Akt/Erk was sustained or whether this activation was a transient event. Following BMOV/RA treatment both Akt and Erk remained activated at a steady state for 72 hours following the initial activation at 10 hours (**Figure 3.12, B**). Again SK-N-SH cells exhibited maximal stimulation after 12 hours that remained constant, while LAN-5 cells were only partially activated after 12 hours requiring 48 hours to achieve full stimulation.

Given that the morphological effects of retinoic acid induced differentiation generally manifest after 48-72 hours treatment, we wished to examine whether activation of Akt/Erk by BMOV/RA treatment occurred prior to the onset of morphological differentiation before returning to basal levels following differentiation. However after 6 days of treatment NBL cells still exhibited hyperactivation of both Akt and Erk, remaining comparable to that seen after shorter treatment periods (**Figure 3.12, C**). As before SK-N-SH cells remained fully activated from 3-6 days with the intensity of signalling still rising between 3 and 6 days of treatment, while LAN-5 cells exhibited a similar profile but to a lesser degree of stimulation.

Activation of protein-kinases following PTK receptor stimulation is a likely consequence of PTP inhibition, given that the latter exert negative regulation of PTK driven signalling cascades (Ostman and Böhmer, 2001). However we obtained no formal proof that the effects of vanadium compounds are solely due to PTP inhibition (See section 4.3.3). Thus we sought to rule out the possibility that stimulation of Akt and Erk was the result of auxiliary consequences of BMOV treatment i.e. the production of ROS, which are frequently induced by vanadium compounds (Wang et al., 2010; Wu et al., 2009) leading to the activation of intracellular signalling cascades. Thus we examined Akt and Erk stimulation following treatment with the reducing agent NAC in order to reduce free radicals. NAC however caused no discernible reduction in the stimulation of either Akt or Erk in both SK-N-SH and LAN-5 cells (**Figure 3.12, D**).

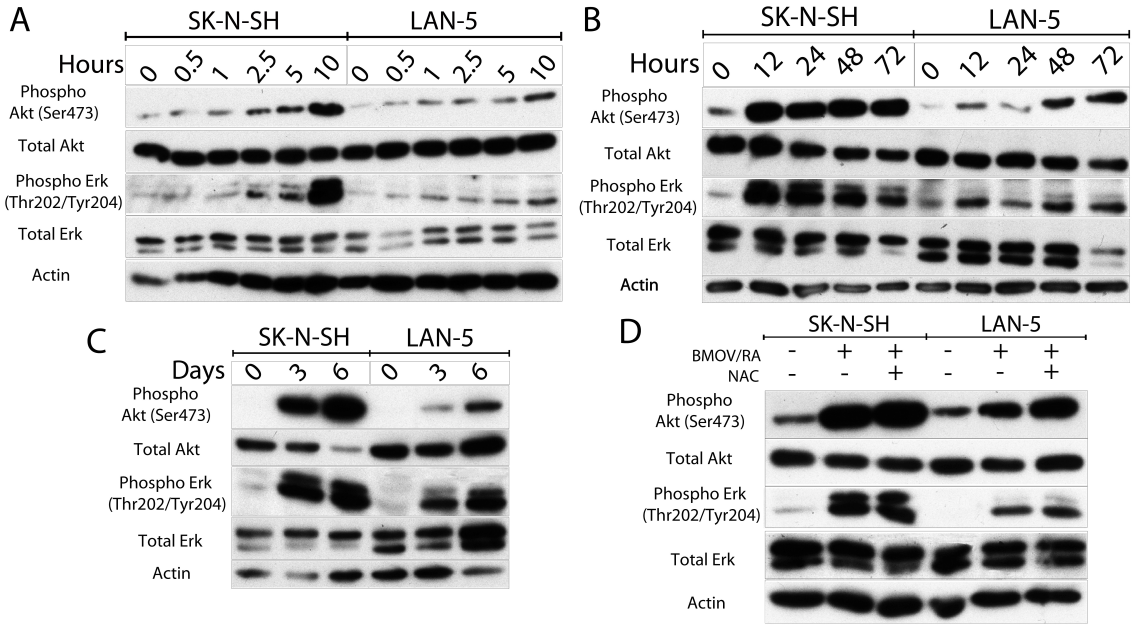

Figure 3.12. Timecourse and ROS-independence of Akt and Erk hyperactivation. (A) Activation of both Akt and Erk occurs following treatment of NBL cells with a combination of BMOV (10µM) and RA (5µM) after 2.5 hours but sharply peaks after 10 hours. **(B)** Akt and Erk remain highly activated following activation onset up to 72 hours after stimulation with BMOV/RA. **(C)** Activation of Akt and Erk is fully sustained throughout 6 days of BMOV/RA treatment. **(D)** Cells were pretreated with the reducing agent NAC (2mM) for 2 hours, followed by 24 hour treatment with BMOV/RA, revealing Akt and Erk activation is independent of ROS production.

In sum, it has been shown that while RA and both of the vanadium compounds BMOV and VA independently cause activation of both Akt and Erk, the level of activation seen following combination treatment is suggestive of synergistic hyperactivation, which occurs only in NBL lines that respond phenotypically to vanadium compounds. Furthermore, rather than being an acute, transient effect of treatment, the activation kinetics of these enzymes occur several hours following treatment and are sustained throughout 6 days of treatment, over which time morphological differentiation occurs. Finally activation of both of these enzymes is not a consequence of ROS production, suggestive of PTP inhibition being responsible instead.

3.3.5. The functional consequences of Akt and Erk activation by BMOV/RA treatment on cellular differentiation and cell survival

As previously discussed, activation of both Akt and Erk can result in diverse outcomes ranging from altered proliferative ability, enhanced cell survival,

differentiation or PCD, often depending on the time-course of stimulation (see Chapter 1). RA-induced differentiation of SH-SY5Y NBL cells has been suggested to be both independent of Erk (Miloso et al., 2004) and dependent on PI3K signalling (López-Carballo et al., 2002), although the role of different signalling pathways is clouded due to conflicting evidence of involvement of any one pathway (Clagett-Dame et al., 2006). Inhibition of PTPs using the omega-3 fatty acid docosahexaenoic acid has also been shown to rely on Erk activation for neurite extension in the same cell type (Wu et al., 2009). Thus we hypothesized that the hyperactivation of Erk and/or Akt exhibited by BMOV/RA-treated cells that precedes neuronal differentiation and remains following it, could be functionally responsible for augmentation of retinoic acid induced-morphological differentiation and upregulation of neuronal markers following combined vanadium compound treatment (See 4.3.1).

In order to test this possibility, we used inhibitors of both MEK and PI3K, enzymes upstream of Erk and Akt respectively and examined morphological differentiation following treatment with BMOV, RA and BMOV/RA for 6 days. Inhibition of MEK (and hence Erk) with U0126 effectively blocked BMOV-induced neurite extension in SK-N-SH, LAN-5 and SH-SY5Y cells (**Figure 3.13, A, B, C respectively**), which was unaffected by inhibition of PI3K/Akt with LY294002 except in the case of SH-SY5Y cells. In contrast, RA-induced neurite outgrowth was unaffected by MEK/Erk inhibition, but was abrogated in both SK-N-SH and SH-SY5Y, but not LAN-5 cells, by inhibition of PI3K/Akt with LY294002. BMOV/RA-mediated neurite outgrowth was only partially attenuated by PI3K/Akt inhibition (SK-N-SH) and both MEK/Erk and PI3K/Akt inhibition (SH-SY5Y) though this did not extend to LAN-5 cells.

These results are difficult to interpret given that the toxicity associated with the first generation MEK (U0126) and PI3K (LY294002) inhibitors respectively at doses that achieve effective enzyme inhibition precluded quantitative analysis of neurite length/percentage of neuritogenesis and immunoblotting to determine the expression of differentiation markers. However, taken together this again suggests that the abilities of both BMOV and RA to promote neurite extension are at least partly independent of each other, and mediated by Erk+Akt and Akt activation,

respectively. In the case of combined BMOV/RA treatment, which causes hyperactivation of both pathways, there may be a very strong neurite-extension signal, giving rise to redundancy between the two pathways manifesting in neurite-extension that is affected to a lesser degree by either MEK/Erk inhibition or PI3K/Akt inhibition alone. This again could support distinct but overlapping signalling networks affected by BMOV and RA. Alternatively both U0126/LY294002 may simply be achieving less effective inhibition of cells treated with BMOV/RA in combination compared with those treated separately due to higher activation levels. In either case these data argues against a functional role for hyperactivation of Akt and Erk in neurite-extension, given that the morphological difference observed between RA treated cells versus BMOV/RA treated cells is relatively minor compared to the difference in activation state.

Given that hyperactivation of Akt and Erk caused by BMOV/RA treatment does not seem to result in comparable increases in neuritogenesis, we instead hypothesized that it may enhance cell-survival of morphologically differentiated cells. Thus we analysed cell viability following 6 days of treatment with BMOV and RA both separately and in combination with inhibitors of MEK and PI3K. As expected we observed a decrease in cell numbers following treatment with BMOV, RA and BMOV/RA following 6 days treatment (**Figure 3.14**) presumably due to decreased proliferative rates (SK-N-SH) and decreased cell viability for BMOV (LAN-5). RA treatment was highly effective at reducing cell numbers, while BMOV/RA modestly but not significantly reduced this effect in SK-N-SH cells, suggesting that while morphological differentiation occurred in SK-N-SH following BMOV/RA treatment, cell division/survival was not suppressed to quite the same level as with RA alone. However both U0126 and LY294002 reduced this effect in SK-N-SH cells, suggesting that the hyperactivation of Akt/Erk seen in BMOV/RA treated cells compared with RA alone results in a small increase in cell-survival/proliferation, that is abrogated by inhibition of both of these enzymes.

Figure 3.13. Effects of MEK/PI3K inhibition on morphological differentiation induced by BMOV/RA. Cells were treated with BMOV (10μM) and RA (5μM) both alone and in combination, with and without the MEK inhibitor U0126 (20μM) and the PI3K inhibitor LY294002 (20μM) for 6 days. U0126 partially abrogated BMOV induced neurite outgrowth (white arrows) instead causing cells to exhibit small, neuroblastic processes (arrow heads), while a similar effect was observed with RA treatment by LY294002. Scale bar = 10 microns.

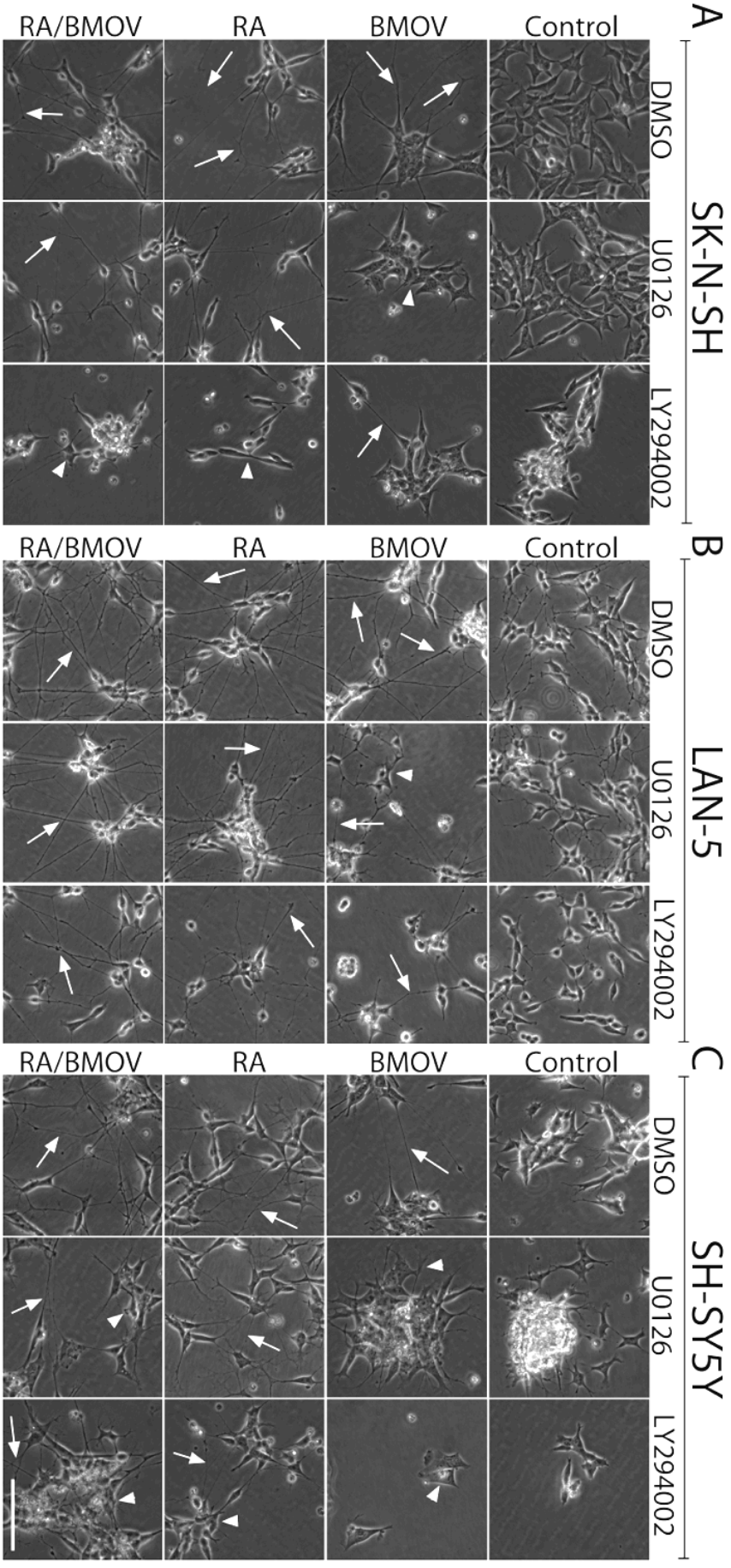
A
SK-N-SH
RA/BMOV
RA
BMOV
Control
DMSO
U0126
LY294002
B
LAN-5
RA/BMOV
RA
BMOV
Control
DMSO
U0126
LY294002
C
SH-SY5Y
RA/BMOV
RA
BMOV
Control
DMSO
U0126
LY294002

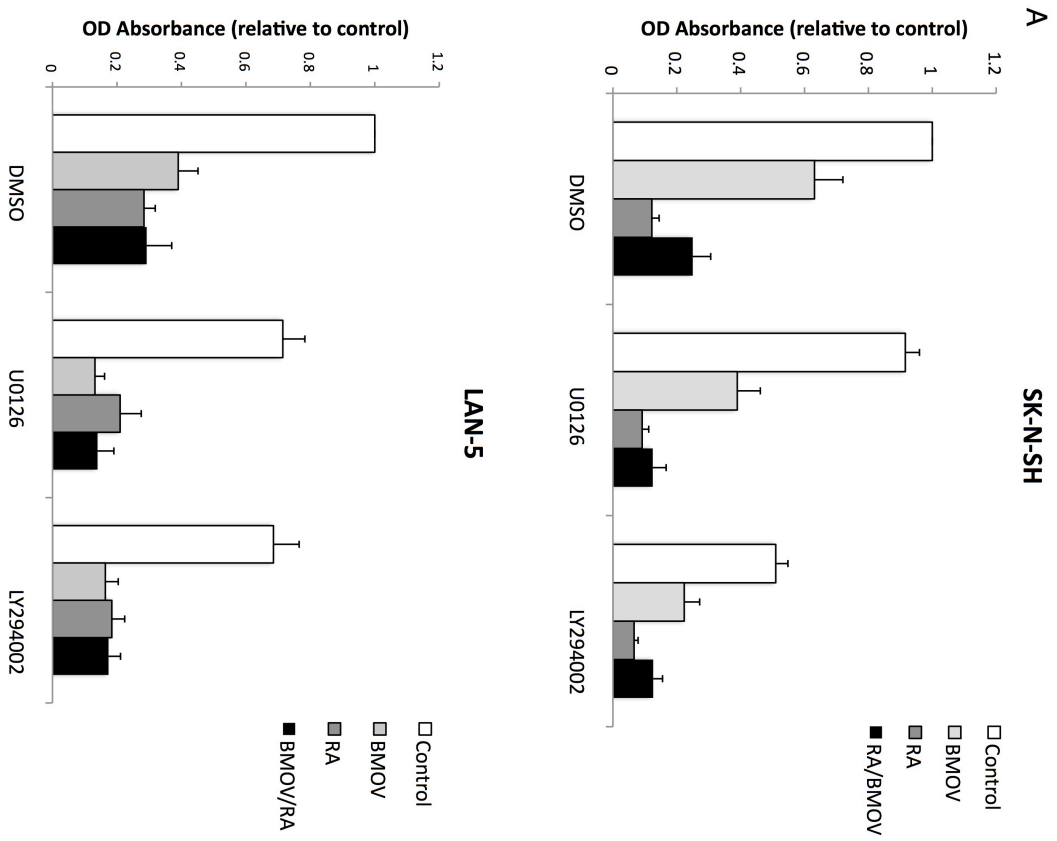

Figure 3.14. Effects of MEK/PI3K inhibition on growth arrest induced by BMOV/RA. Cells were treated with BMOV (10µM) and RA (5µM) alone and in combination as well as with and without the MEK inhibitor U0126 (20µM) and the PI3K inhibitor LY294002 (20µM) for 6 days. Neither U0126 nor LY294002 significantly abrogated RA/BMOV-induced decreases in the percentage of viable cells as assayed by crystal violet staining. Means and standard deviation from 3 independent experiments.

In sum, inhibiting BMOV-induced activation of Erk and to a lesser extent Akt, inhibited neurite extension while inhibiting RA induced activation of Akt not Erk had the same effect, suggesting that neurite-extension is mediated by distinct signalling pathways in the case of BMOV and RA, which cause additive effects. Inhibition of both Akt and Erk in the case of combined BMOV/RA treated cells was less effective at abrogating neurite extension, however this may suggest redundancy between these two pathways. BMOV/RA treatment also resulted in a modest increase in the number of viable cells in SKNSH compared with RA treatment alone, which was attenuated by inhibition of Akt and Erk, suggesting that hyperactivation could enhance cell-survival following differentiation although this effect was limited to SK-N-SH cells only.

3.3.6. BMOV sustains retinoic acid-induced differentiation in the absence of ongoing treatment, causing senescence

Oncogene-induced senescence (OIS) is a form of replicative senescence that occurs following the activation of proto-oncogenes as a fail-safe mechanism against tumour formation (Braig and Schmitt, 2006; Collado and Serrano, 2010). OIS has been shown to result from constitutive activation of both Ras/MAPK (Lin et al., 1998; Michaloglou et al., 2005; Serrano et al., 1997; Wajapeyee et al., 2008) and PI3K/Akt (Chen et al., 2005; Nogueira et al., 2008) signalling, and generally occurs via a DNA damage response invoking p53 and/or cell cycle inhibitors such as $p16^{4INK4A}$ (Beauséjour et al., 2003; Schmitt et al., 2002). The activation of OIS has been shown to directly result in tumour regression and thus could be viewed as a novel means of tumour targeting, especially due to the lack of obvious side effects (Wu et al., 2007; Xue et al., 2007).

Several lines of evidence link the novel NBL combination therapy of BMOV/RA treatment with OIS. First, hyperactivation of proto-oncogene signalling pathways has been demonstrated to be crucial for OIS induction (Sarkisian et al., 2007). This is applicable to the current study given the dramatic increases in both Akt and Erk activation following BMOV/RA treatment. Second, the effects of BMOV are thought to occur primarily via PTP inhibition, which could clearly either directly or indirectly activate targets of OIS via upstream RTK signalling. This has been demonstrated for instance by inhibition of the dual-specificity PTP PTEN, which increases the levels of activated Akt, resulting in senescence (Alimonti et al., 2010b). Furthermore RA has actually been demonstrated to activate replicative senescence in an schwannian-type subclone of the NBL line SK-N-SH (Wainwright et al., 2001). Last, the wild-type p53 status of a number of NBL cell lines has been suggested to prime them for the induction of senescence for instance by stabilization of p53 (Van Maerken et al., 2006).

Although we did not observe changes in the level of cell-cycle exit/proliferative index following short-term (6 day) treatment with BMOV/RA (See 4.3.3-4), we sought to examine whether longer-term treatment with these compounds enhanced growth arrest further than RA alone. Further more we obtained evidence that hyperactivation of Akt and Erk was still increasing following 6

days of treatment, which could drive cells into senescence. To test this, we reasoned that if BMOV/RA induced replicative senescence then this should ensue during treatment but crucially remain after treatment withdrawal. Thus cells were treated with both RA and RA/BMOV for a period of 12 days, followed by a 'rescue' period during which treatment was removed and replaced with normal culture medium. Remarkably in SK-N-SH and LAN-5 this resulted in cells that remained highly differentiated, as judged by elongated processes and condensed cell bodies, only in cells treated with BMOV/RA (**Figure 3.15**). While undergoing similar initial morphological differentiation, cells treated with RA (only) were observed to revert back to a proliferative neuroblastic phenotype resembling untreated cells. Notably BMOV/RA treatment often resulted in the formation of pseudo-ganglia, i.e. aggregates of differentiated cell bodies projecting processes outwards reminiscent of the phenotype of dorsal-root ganglia *in vitro*. Although this has previously been reported for RA treatment, these structures remained in the absence of any treatment in the BMOV/RA condition.

Given the apparent growth arrest of BMOV/RA rescued cells, we wished to examine whether these cells had undergone replicative senescence. To test this we assessed levels of senescence-associated β-galactosidase (SA-β-Gal), following the same treatment-rescue procedure. SA-β-Gal has been shown to specifically label senescent cells at an acidic pH (pH 6.0) due to the accumulation of lysosomal β-galactosidase in senescent cells (Dimri et al., 1995). Indeed treatment of two NBL cell lines (SK-N-SH, SH-SY5Y) with BMOV/RA (12 days followed by 20 days withdrawal) produced clear evidence of SA-β-Gal activity and at a much higher rate than RA treatment (**Figure 3.16**). Furthermore we observed intense SA-β-Gal staining in pseudo ganglia, the remnants of which remained in RA treated cultures, although this may be due to confluence-induced quiescence due to high cell density in these structures, which has been suggested to occur in fibroblasts resulting in increased SA-β-Gal activity (Yang and Hu, 2005). Staining of BMOV/RA-treated cells commonly occurred in cells with a highly flattened, enlarged and vacuolated cytoplasm, also a common morphological marker of senescence (Collado and Serrano, 2010). Interestingly although an apparent growth arrest also occurred in LAN5 cells, we failed to detect SA-β-Gal labelling even in LAN5 pseudo ganglia (data not shown).

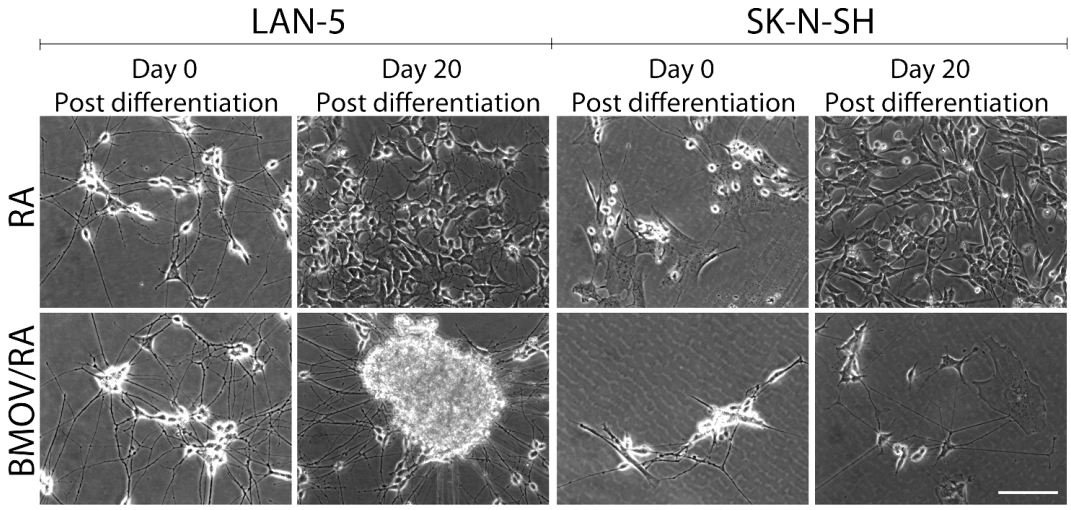

Figure 3.15. Prevention of relapse from morphological differentiation/growth arrest by BMOV/RA. Cells were treated for 12 days with either RA (5μM) or BMOV (10μM) with RA (Day 0 of removal), then cultured in the absence of treatment for a further twenty days (Day 20 of removal). Cells treated with RA alone reverted to rapidly dividing neuroblastic cells lacking elongated neurites, while cells treated with BMOV/RA remained highly differentiated, forming networks of processes and pseudo-ganglia. Scale bar = 10 microns.

Lastly we sought to characterise the timing of senescence induction in SH-SY5Y cells. OIS has been shown to result from acute activation of proto-oncogenes in a relatively fast manner (3-6 days), however we previously failed to detect enhanced growth arrest in BMOV/RA treated cells during this time period, suggestive of a lack of terminal differentiation. In concordance with this, SA-β-Gal activity was absent from both RA and RA/BMOV treated cells after 3 and 6-day constant treatment periods (**Figure 3.17**), despite morphological differentiation. However, following 9 days of treatment both RA and RA/BMOV caused a marked increase in SA-β-Gal labelled cells, which further increased after 14 days of treatment. It is noteworthy that the proportion of SA-β-Gal labelled cells following BMOV/RA treatment roughly corresponded with that following RA treatment alone, suggesting an initial response followed by reversion in the absence of treatment after RA treatment alone. This is perhaps in conflict with the notion of replicative senescence, which should be characterized by irreversible growth arrest. This raises the caveat that RA and perhaps BMOV/RA treatment might instead induce quiescence rather than *bona fide* senescence, although SA-β-Gal has been suggested to distinguish quiescent and pre-senescent cells from senescence (Dimri et al., 1995).

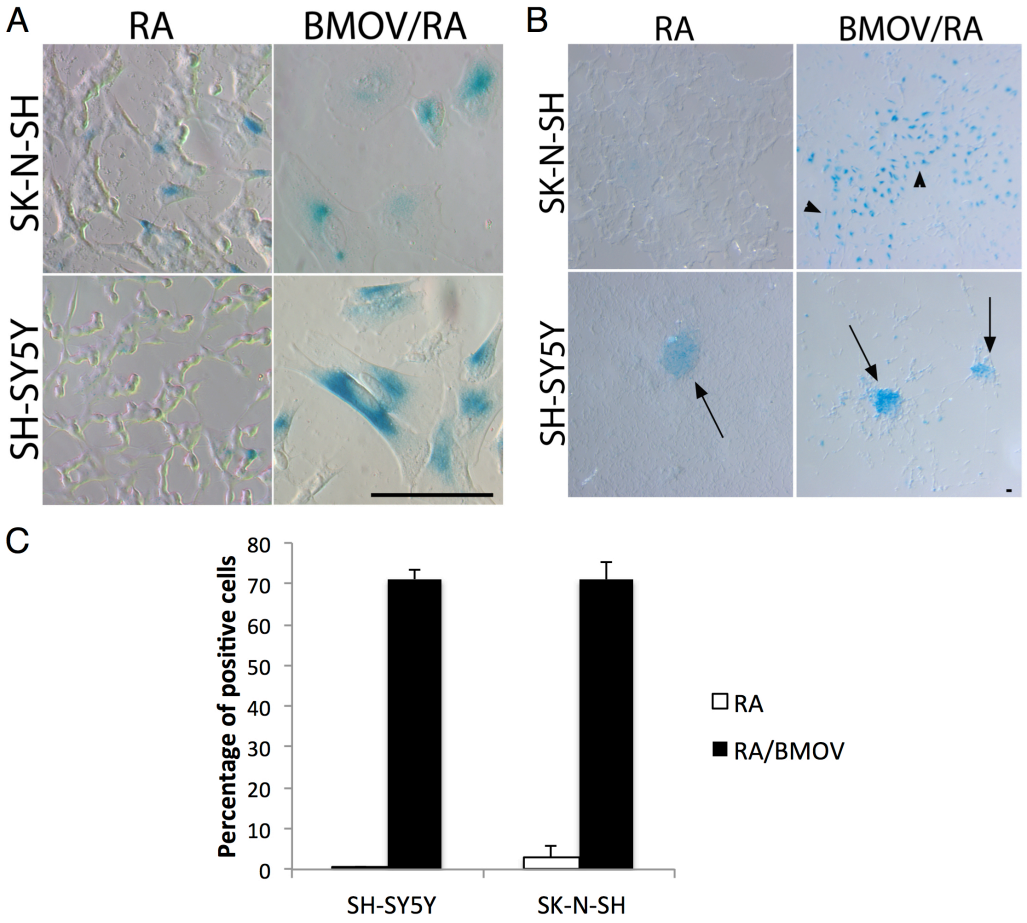

Figure 3.16. β-Gal staining for replicative senescence. Cells were treated for 12 days with either RA (5μM) or BMOV (10μM) with RA then cultured in the absence of treatment for a further 14 days. Cells were then fixed and stained for β-Gal activity. (**A**) RA/BMOV treated cells exhibited morphological evidence of senescence as well as increases in the number of β-Gal positive cells. (**B**) 5x objective magnification showing the presence of colonies of β-Galactosidase positive cells following treatment with BMOV/RA (arrowheads). RA alone did cause the formation of pseudo-ganglia that often stained positive (arrows). Scale bar = 10 microns. (**C**) Histogram revealing mean and SEM for the number of β-Gal positive cells (N=2).

Thus in sum, BMOV/RA treatment induces a latent differentiation/growth arrest which remains in the absence of on going treatment, which is not matched by RA treatment alone, the removal of which allows a reversion back to a proliferative neuroblastic state. Importantly, the presence of senescent cells was confirmed during refractory periods, suggesting that BMOV/RA activates a senescence response that once engaged, remains following treatment removal. This may have crucial benefits for RA-therapy, given the high levels of relapse due to minimal-residual disease.

3.3.7. The effects of BMOV/RA appear independent of PTEN

In contrast to the majority of human neoplasms, mutations in PTEN have been rarely documented in NBL, and have been suggested to occur in only a small fraction of tumours (Muñoz et al., 2004), although downregulation through mechanisms such as promoter hypermethylation may account for reduced expression independently of mutations (Lázcoz et al., 2007). Consequently little research has been done into the function of PTEN in NBL, despite recent advances in the characterisation of PI3K/Akt activation in a large proportion of NBL cases, accounting for cell survival/proliferation and tumour progression (Bender et al., 2011; Li et al., 2010; Opel et al., 2007). With Akt now considered a major drug target in NBL (Brodeur, 2010), it is surprising that so little is known about the status of the primary negative regulator of its activity.

We previously demonstrated that BMOV induces potent activation of Akt especially when combined with RA treatment, as well as causing cell senescence. This makes PTEN an interesting candidate as a determinant of the effects of BMOV. Thus we sought to examine whether PTEN inhibition mimics the effects of BMOV treatment in NBL cells. As previously mentioned, VO-OH Pic is a recently developed small-molecule compound that has been shown to achieve effective and selective inhibition due to its ability to specifically bind to the PTEN active site based on its wide cleft in comparison to other PTPs, inhibiting PTEN at nanomolar concentrations (IC50 = 35nM) (Rosivatz et al., 2006). VO-OH Pic has also been shown to act maximally on PTEN in live cells at 500nM (Mak et al., 2010).

We first sought to determine the effects of VO-OH Pic on Akt stimulation, in comparison with BMOV, to examine whether VO-OH PIC could achieve Akt activation at 500nM. This assay was done in KCNR and Kelly cells due to their intermediate levels of PTEN protein expression (see figure 3.20) and the high levels of Akt stimulation we observed with BMOV treatment (see figure 3.11). However neither compound was observed to activate Akt at doses below 5µM (**Figure 3.18, A**). At concentrations ≥ 5µM, VO-OH Pic did appear more effective at inducing Akt

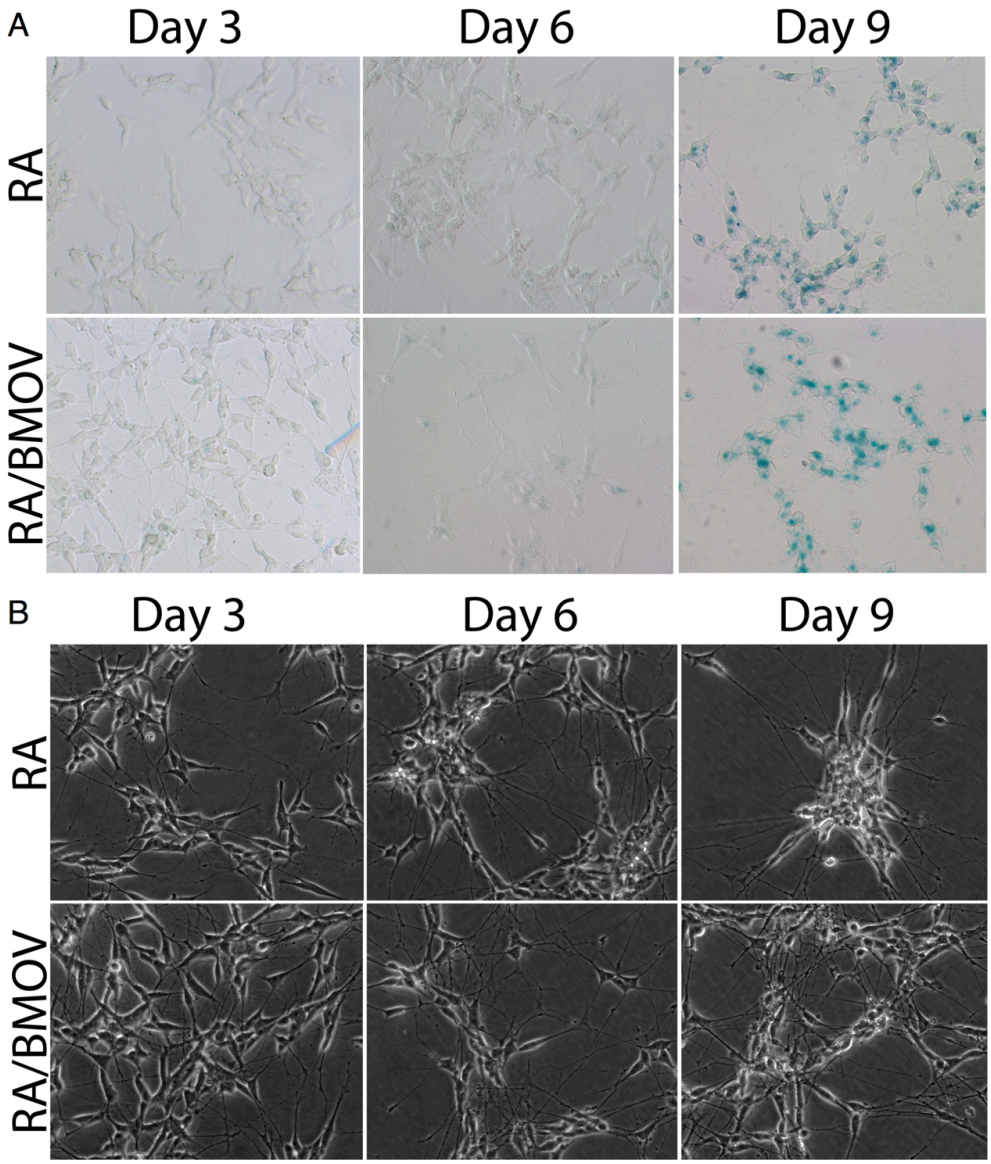

Figure 3.17. Timecourse of senescence. Cells were treated for 3, 6 or 9 days with RA (5µM) or BMOV (10µM)/RA and analysed for SA-β-Gal activity. Although all treatments induced morphological differentiation (**B**), SA-β-Gal activity was only observed after 9 days of treatment in both RA and RA/BMOV treated cells (**B**).

activation than BMOV, achieving similar levels at 5µM when compared with BMOV at 10µM (**Figure 3.18, A**). This is however difficult to interpret for a number of reasons. Firstly VO-OH Pic has been suggested to cause Akt phosphorylation at 40nM, achieving saturation at 75nM (Rosivatz et al., 2006), however both levels of activation induced in the present study by higher doses of BMOV and VO-OH Pic far exceeds the level of activation documented by Rosivatz *et al.*, which is barely detectable. Similarly it was suggested that VO-OH Pic failed to affect tyrosine-

phosphorylation at 10μM, and that IC50 ranges for other PTPs far exceeded that of PTEN, suggesting good specificity for PTEN. It is difficult to explain a lack of stimulation at doses below 5μM without invoking non-specific PTP stimulation. This is especially pertinent given that other PTPs have been shown to negatively control Akt that would be targeted by BMOV, and both inhibitors showed the same level of Akt stimulation (albeit at a 2 fold higher dose) (Omerovic et al., 2010). However these caveats aside, VO-OH Pic was used at a dosage shown to activate Akt signalling.

We next sought to determine whether VO-OH Pic mimicked the effects of VA and BMOV in synergistically activating both Akt and Erk when used in combination with RA. Remarkably VO-OH Pic at 5μM displayed the exact same profile as BMOV inducing activation of Akt and Erk when used alone, but also synergistically enhanced RA driven activation of both of these enzymes (**Figure 3.18, B**). Here activation was clearly synergistic, vastly exceeding that seen by either treatment alone in two cell lines (KCNR/Kelly). Interestingly Erk was activated to a similar extent as Akt, despite an overwhelming amount of evidence suggesting the latter to be the main target of PTEN. This perhaps suggests as previously noted that VO-OH Pic may be acting non-specifically at this dosage, although others have suggested Ras/MAPK may be affected by PTEN (Gu et al., 1998). Thus VO-OH Pic clearly causes similar consequences to BMOV with regards to signal transduction, activating Akt and Erk alone as well as synergising with RA, albeit at ten fold higher doses compared with those published previously.

Given the similarity between biochemical effects of VO-OH Pic and BMOV, we next sought to examine whether both of these compounds could induce neurite outgrowth, as has previously been shown for BMOV and VA. Indeed longer-term (6 day) treatment with VO-OH Pic caused neurite extension in both SH-SY5Y and SK-N-SH cells, to a similar degree as BMOV, at a 2 fold lower dosage (**Figure 3.19**). Again it should be stated that VO-OH Pic failed to induce neuritogenesis below micromolar dosages, raising the recurring issue of specificity. However this provides some evidence that PTEN may be one target of BMOV, responsible for both biochemical alterations in signal transduction, as well as cell-structural changes in differentiation. Interestingly this is not the first demonstration that PTEN inhibition can facilitate

neurite outgrowth (Christie et al., 2010), and the activation for Erk/Akt that may occur following this inhibition could be a primary determinant of this response.

The former studies with VO-OH Pic provide some evidence for the involvement of PTEN in the response of NBL cells to BMOV. However the fact that VO-OH Pic only resulted in phenotypic and biochemical effects at a ten fold higher dosage than that at which PTEN was said to be saturated (Rosivatz et al., 2006), raises serious concerns that these effects are instead the result of vanadium delivery to a wider range of PTPs. This discrepancy could potentially be answered by asking the question of whether PTEN status is the primary explanation for variability between the responses of individual NBL cell lines to BMOV treatment. For instance, it has been argued that PTEN status confers susceptibility to PTEN-loss induced senescence following PTEN inhibition using VO-OH Pic (Alimonti et al., 2010a; Alimonti et al., 2010b; Carracedo et al., 2011). This begs the question of whether low levels of endogenous PTEN account for BMOV-induced senescence, due to acute loss of PTEN and induction of a fail-safe senescence response. Importantly this hypothesis would predict high levels of PTEN in BMOV-unresponsive cells (SK-N-AS/SK-N-DZ) preventing the activation of PI3K/Akt signalling following BMOV/RA treatment. Conversely through previously unspecified mechanisms such as transcriptional downregulation, post-translational modification or epigenetic regulation, BMOV-responsive cells capable of undergoing senescence would have low endogenous levels of PTEN, and thus less subject to dampening of PI3K/Akt signalling following stimulation by BMOV/RA, allowing a putative threshold to be surpassed where senescence would ensue (**Figure 3.19**). This is a tempting explanation for the low levels of activated Akt in BMOV-unresponsive cells (See figure 3.11).

Thus we conducted qPCR analysis of NBL cell lines in comparison with each other as well as non-neoplastic nervous system control tissue to examine relative levels of *PTEN* mRNA. These qPCR data are extracted from a larger dataset discussed in chapter 6. First, PTEN expression was vastly reduced in all NBL lines in comparison with non-neoplastic neural tissue (**Figure 3.20, A**). This is significant given the previously reported evidence for a lack of tumour-suppressive function for PTEN in NBL (Muñoz et al., 2004), as PTEN expression was fairly similar to that observed in

the putatively PTEN-deficient glioma cell line U118. However, we failed to observe a correlation between the levels of PTEN and responsiveness to BMOV in NBL cells. PTEN expression was highest in BMOV-unresponsive SK-N-AS cells followed by IPhNB1, IMR32 and Kelly, all of which failed to undergo senescence, however other cell lines which had lower levels of PTEN were mixed in their responsiveness to BMOV/RA, with two undergoing senescence (SH-SY5Y, SK-N-SH), two responding with Akt activation and undergoing differentiation, but failing to undergo senescence (LAN-5, KCNR) and two failing to respond to BMOV at all (SK-N-BE(2), SK-N-DZ).

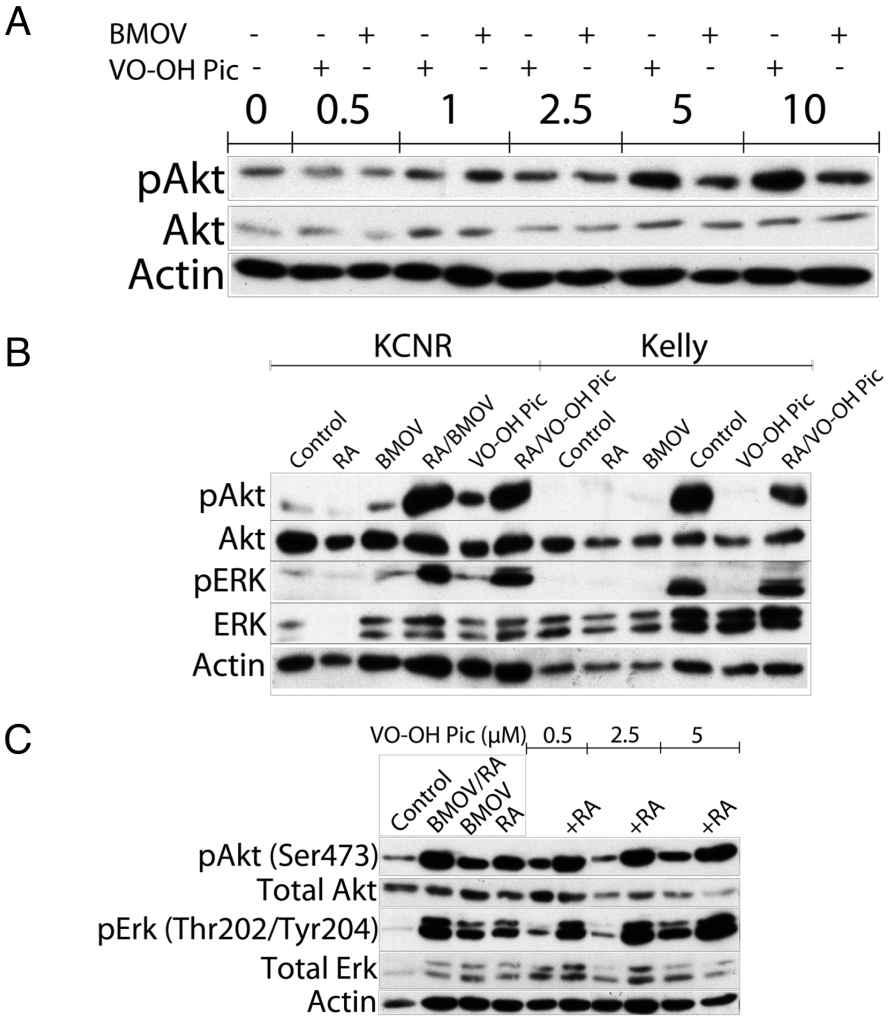

Figure 3.18. The biochemical effects of VO-OH Pic. Cells treated for 24 hours with increasing doses of BMOV and VO-OH Pic. The effects of the PTEN inhibitor VO-OH Pic are shown both alone on the PTEN effector Akt in KCNR cells and in combination with retinoic acid (RA) on both Akt and Erk. VO-OH Pic treatment caused Akt phosphorylation at Ser473 as expected to a similar degree as BMOV in KCNR cells, but only at 5μM and above (**A**). VO-OH Pic (5μM) synergistically activated both Erk and Akt in combination with RA (5μM) in a similar fashion to BMOV (10μM) in both KCNR and Kelly cells (**B**), however this hyperactivation was less apparent at 500nM in SK-N-SH cells (**C**).

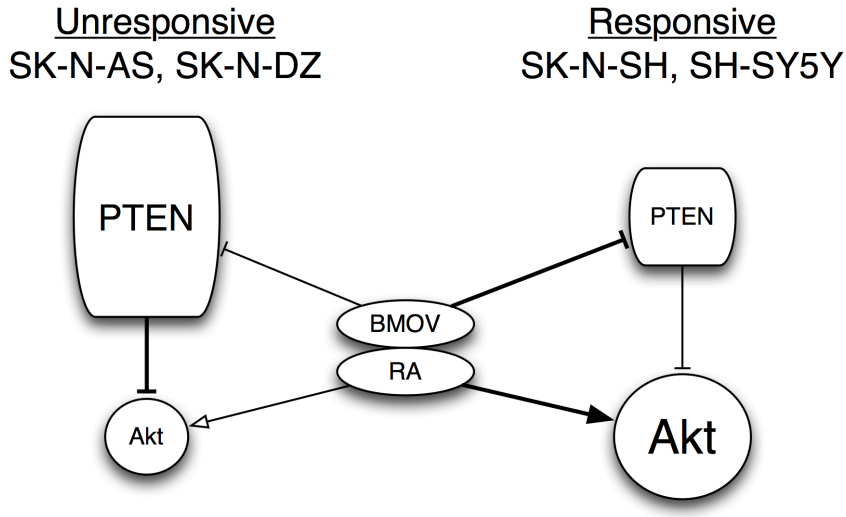

Figure. 3.19. A hypothesis concerning relative PTEN expression and functional consequences of BMOV/RA treatment. This model predicts that BMOV-unresponsive cell lines such as SK-N-AS/SK-N-DZ harbour relatively high levels of PTEN protein, causing ineffective inhibition by BMOV (thin line), effective Akt inhibition (thick line) and consequently ineffective stimulation of Akt by BMOV/RA (thin line). In contrast, BMOV responsive lines (SK-N-SH, SH-SY5Y) harbour relatively lower levels of PTEN, which is effectively inhibited by BMOV (thick line) preventing Akt inhibition (thin line) and achieving high overall stimulation of Akt from BMOV/RA (thick line).

However as previously stated, BMOV/RA-induced senescence is unlikely to result simply from activation of Akt alone, as this occurred in Kelly cells which failed to undergo senescence in response to RA (data not shown). Instead this response may require a particular transcriptional program induced by RA along with concomitant Akt hyperactivation caused by combined BMOV/RA. Furthermore these data reflect PTEN at the mRNA expression level only, which often fails to completely correlate with protein level. Indeed T98G and U118 glioma cells were shown to have similar levels of PTEN, despite being classified as PTEN deficient and PTEN proficient respectively. We therefore sought to confirm these data by examining protein level of PTEN via immunoblotting. Indeed PTEN protein expression did fail to correlate with mRNA expression (**Figure 3.20, B**). However we still failed to observe cell-line specific PTEN levels in fitting with the former prediction. Here SK-N-SH and KCNR cells had the highest levels of PTEN, despite both undergoing BMOV/RA-induced senescence/differentiation, respectively. Similarly SH-SY5Y cells that responded to BMOV/RA had much lower relative PTEN expression. Lastly SK-N-AS and SK-N-DZ

cells that failed to respond to either BMOV alone or BMOV/RA either phenotypically or by activating Akt had similarly low levels of PTEN protein. Thus PTEN protein expression failed to conform to the model of PTEN status as an indicator of BMOV/RA responsiveness. We next examined endogenous activation of Akt, to determine whether differences in PTEN protein expression manifested in alterations in basal signal strength. However again PTEN expression failed to correlate with Akt activation, the basal levels of which were broadly comparable across all tested NBL lines (**Figure 3.20, B**).

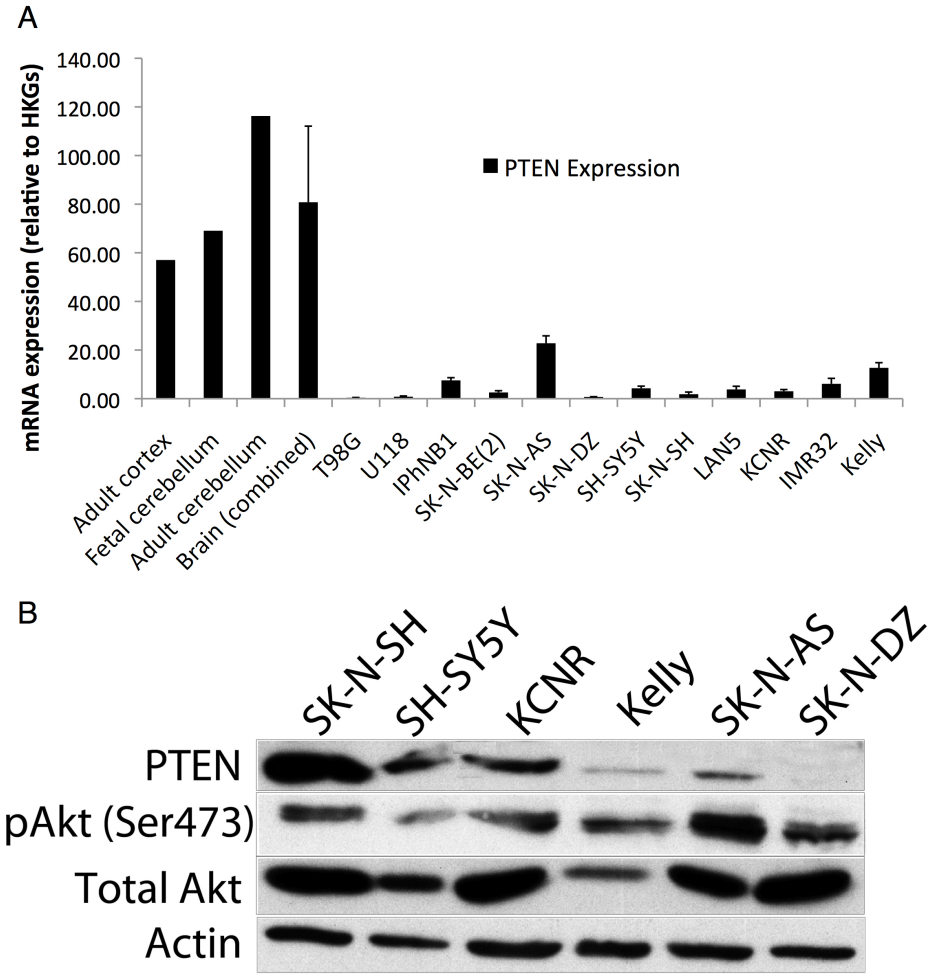

Figure. 3.20. Expression of PTEN in NBL cell lines. (**A**) qPCR showing expression of PTEN relative to 4 HKGs in both control non-neoplastic nervous system tissue, glioma and NBL. Although PTEN expression in NBL is lower than control tissue and comparable to that of PTEN-deficient glioma cells (U118) suggestive of a tumour suppressive function, levels do not correlate well with responsiveness to BMOV e.g. compare SK-N-DZ with SH-SY5Y. (**B**) Immunoblot showing endogenous protein expression of PTEN as well as phosphorylated Akt. Protein expression fails to correlate with mRNA expression (compare A versus B), but confirms a lack of correlation between BMOV responsiveness and PTEN expression (e.g. compare SK-N-SH with SK-N-DZ). Note that basal Akt phosphorylation also fails to correlate with PTEN expression.

Lastly we tested the efficacy of VO-OH Pic at inducing senescence in combination with RA treatment, using a 500nM dosage given that PICS occurs without RA at this dosage (Alimonti et al., 2010b). However cells treated for 14 days with VO-OH Pic/RA were phenotypically indistinguishable from cells treated with RA alone after a 14 day treatment removal period, exhibiting a similar low frequency of SA-β-Gal positive cells and a lack of morphological evidence of senescence (**Figure 3.21**).

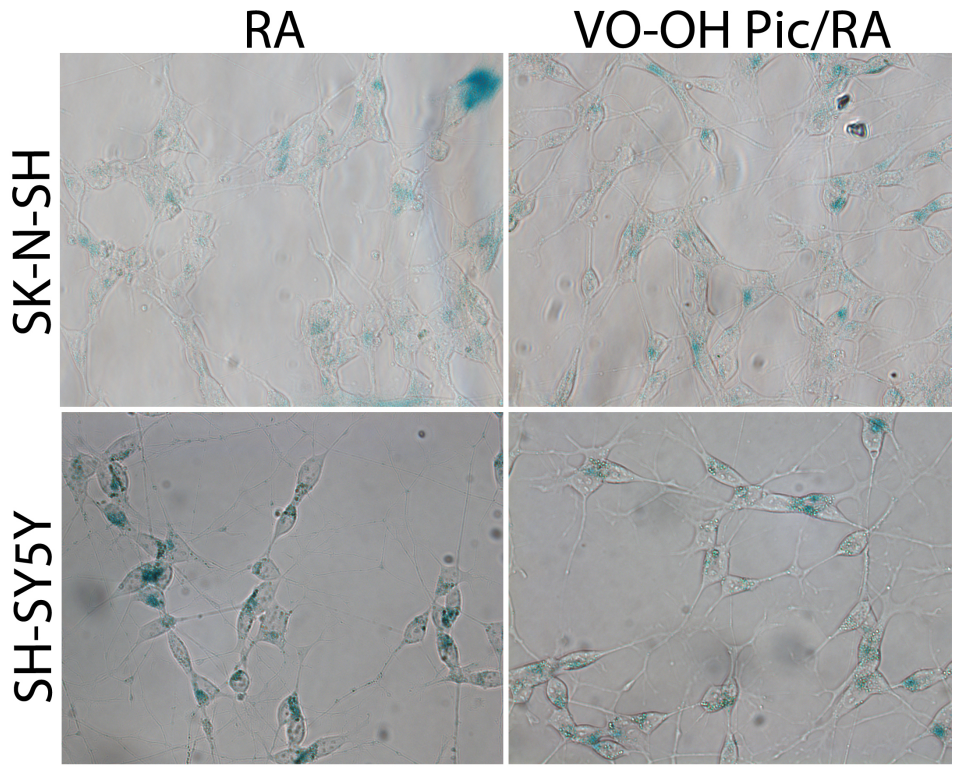

Figure 3.21. VO-OH Pic does not augment RA-induced senescence. Cells treated for 14 days with RA (5μM) with and without VO-OH Pic (500nM) followed by 14 days of culture in treatment-free medium and stained for β-gal activity indicative of senescence. Both cell types are indistinguishable both in morphology and frequency of SA-β-Gal staining.

In sum, the PTEN inhibitor VO-OH Pic induces similar effects to BMOV, including increases in Akt activation, synergistic hyperactivation of Akt/Erk in combination with RA, and phenotypic neurite outgrowth. However the substantial caveat arguing against these responses stemming solely from PTEN inhibition is that these effects required a ten fold higher dose of VO-OH Pic than commonly used, while VO-OH Pic used at a dosage sufficient to cause senescence in prostate cancer cells (Alimonti et al., 2010b) did not mimic BMOV/RA induced senescence in NBL cells. Although it has

been argued that VO-OH Pic should retain its specificity for PTEN at higher doses, it cannot be ruled out that this compound is simply delivering uncomplexed vanadium generically to multiple PTPs when used at higher doses. Its activation of Erk may argue for this. Furthermore although differences in the status of PTEN between cell lines is a convenient hypothesis to explain responsiveness to BMOV at the level of Akt/Erk activation, neurite outgrowth and BMOV/RA-induced senescence, both mRNA and protein levels failed to correlate with BMOV phenotypic behaviour across most NBL cell lines. Similarly while low levels of PTEN argue for a tumour suppressive function in NBL, PTEN protein expression failed to correlate with Akt activation, suggesting other mechanisms may predominate in driving PI3K/Akt signalling in this tumour type, although alternatively PTEN may be non-functional in some instances where high expression is accompanied with high Akt activation.

3.3.8. BMOV/RA-induced senescence is independent of p53/p16INK4A

Oncogene induced senescence (OIS) typically involves the initiation of a DNA damage response centring on the activation of the tumour suppressors p53 and $p16^{INK4A}$ (Lin et al., 1998; Schmitt et al., 2002; Serrano et al., 1997). Thus these genes are frequently mutated in numerous human cancers, however when functional the induction of OIS is accompanied by the accumulation of both p53/$p16^{INK4A}$, where loss of function of either gene abrogates this effect (Beauséjour et al., 2003). Similarly PTEN-loss-induced senescence (PICS) is accompanied by the accumulation of p53 expression, and functional p53 is a prerequisite for this response (Alimonti et al., 2010b; Chen et al., 2005).

Intriguingly, p53 mutations are rarely observed at presentation in NBL. However fail-safe barriers to tumorigenesis exerted by p53 are often circumvented by other means such as the p53 inhibitor MDM2 (Van Maerken et al., 2009). This has led to the approach of inhibition of MDM2 using the small-molecule nutlin-3 as a means of p53 stabilization, which has been shown to induce senescence (SK-N-SH cells) and differentiation (NGP, GLB-GA cells) *in vitro* (Van Maerken et al., 2006). However this is complicated by the finding that downstream effectors of p53 are generally intact in NBL, raising the question of whether senescence might be activated without the need for p53 reactivation (Van Maerken et al., 2011). This

point is further emphasised by the fact that mutations in the *CDKN2A* locus are rarely observed in both primary NBL and cell lines, suggesting that $p16^{INK4A}$ is potentially functional (Beltinger et al., 1995). It is also noteworthy that while *RAS* proto-oncogenes are frequently targeted by activating mutations in human cancer, at least the *HRAS* member of this family is actually expressed at high levels in favourable tumours, where it has been suggested to potentially contribute to regression (Kitanaka et al., 2002). The Possibility of an intact Ras, $p16^{INK4A}$ and p53 raises the question of whether senescence is a feature of NBL tumours at baseline or following chemotherapy, and if not how might NBL tumours attenuate OIS.

It has been shown that accumulation of $p16^{INK4A}$ contributes to replicative senescence caused by RA in a schwannian type sub-clone of the NBL line SK-N-SH (Wainwright et al., 2001), where it was suggested that neuronal-type SK-N-SH cells preferentially undergo differentiation in contrast to senescence due to an absence of $p16^{INK4A}$. The finding that SH-SY5Y/SK-N-SH/KCNR cells are capable of undergoing senescence as shown by positive staining for SA-β-Gal and evidence of growth arrest begs the question of whether BMOV/RA treatment causes the accumulation of p53 and/or $p16^{INK4A}$, and whether these proteins are required for a senescence response. Thus we sought to examine p53/$p16^{INK4A}$ levels following BMOV/RA treatment.

We conducted immunoblotting for both p53 and $p16^{INK4A}$ following 14 days of continuous treatment with BMOV/RA in two cell lines that are SA-β-Gal positive following such a treatment course (SH-SY5Y and SK-N-SH). However neither cell line exhibited evidence of p53 or $p16^{INK4A}$ induction/accumulation in either treatment condition (BMOV/RA separately and in combination) (**Figure 3.22**). This finding is difficult to explain, given that both cell lines have a wild-type p53 gene, and that $p16^{INK4A}$ induction has been shown to occur following RA treatment (Wainwright et al., 2001). It is entirely possible that detection of both proteins was not possible owing to limitations of the used antibodies, given that both p53 and $p16^{INK4A}$ are often expressed at very low levels, and that the chosen positive controls were not thoroughly matched. However this also raises the possibility that BMOV/RA treatment induces cell senescence that is independent of either protein. This may be potentially useful given that at there is evidence at least for p53, that mutations may occur following chemotherapy, leading to therapeutic resistance (Carr-Wilkinson et

al., 2010). This also suggests that BMOV/RA-induced senescence is distinct from PICS, which requires the induction of p53 (Alimonti et al., 2010b).

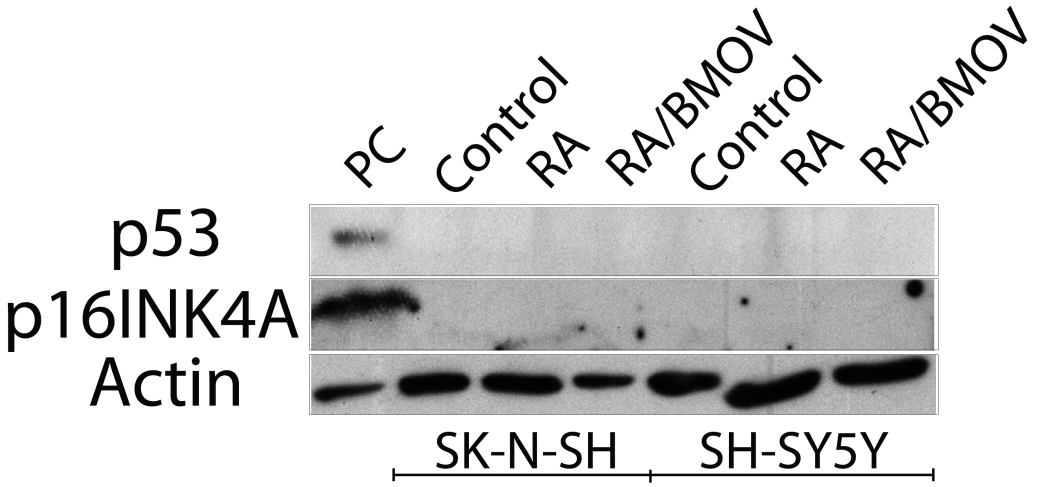

Figure 3.22. Absence of p53/p16^{INK4A} accumulation following long-term BMOV/RA treatment. Immunoblotting for p53/p16^{INK4A} reveals an absence of protein expression following treatment for 14 days with RA (5μM) and BMOV (10μM) both separately and in combination. PC represents positive control of Kelly cells (p53) and murine brain tissue (p16^{INK4A}). However it should be noted that detection of p16^{INK4A} might be more difficult in human tissue compared with mouse, thus making human brain a more suitable positive control.

3.3.9. BMOV/RA-induced senescence is dependent on Akt and Erk

We hypothesized that the hyperactivation of both Erk and Akt caused by BMOV/RA treatment might be responsible for senescence, given that OIS frequently occurs in a dose dependent manner (Sarkisian et al., 2007), following stimulation of both of these oncogenic signalling nodes. Thus we treated cells with BMOV/RA for 14 days followed by a 14-21 day treatment-removal period in the presence of absence of the PI3K inhibitor PI103 or the MEK inhibitor U0126. In both SK-N-SH and SH-SY5Y, inhibition of both Akt and Erk caused a substantial reduction in BMOV/RA-induced SA-β-Gal staining following treatment removal (**Figure 3.23**), (although there was little evidence of morphological differences between treatment conditions (**Figure 3.24**), suggesting a causal role for enzymes in this senescence response. Although SA-β-Gal activity was noted following treatment with 10μM BMOV, we observed more variability in this response during these experiments, and thus chose to use a two fold higher dosage. This may reflect phenotypic drift, or selective pressure affecting levels of Akt and Erk activity, although this is unknown. Similarly U0126 was

used at a two fold lower dosage compared with section 3.3.5, given that we observed substantial toxicity after 20µM treatment.

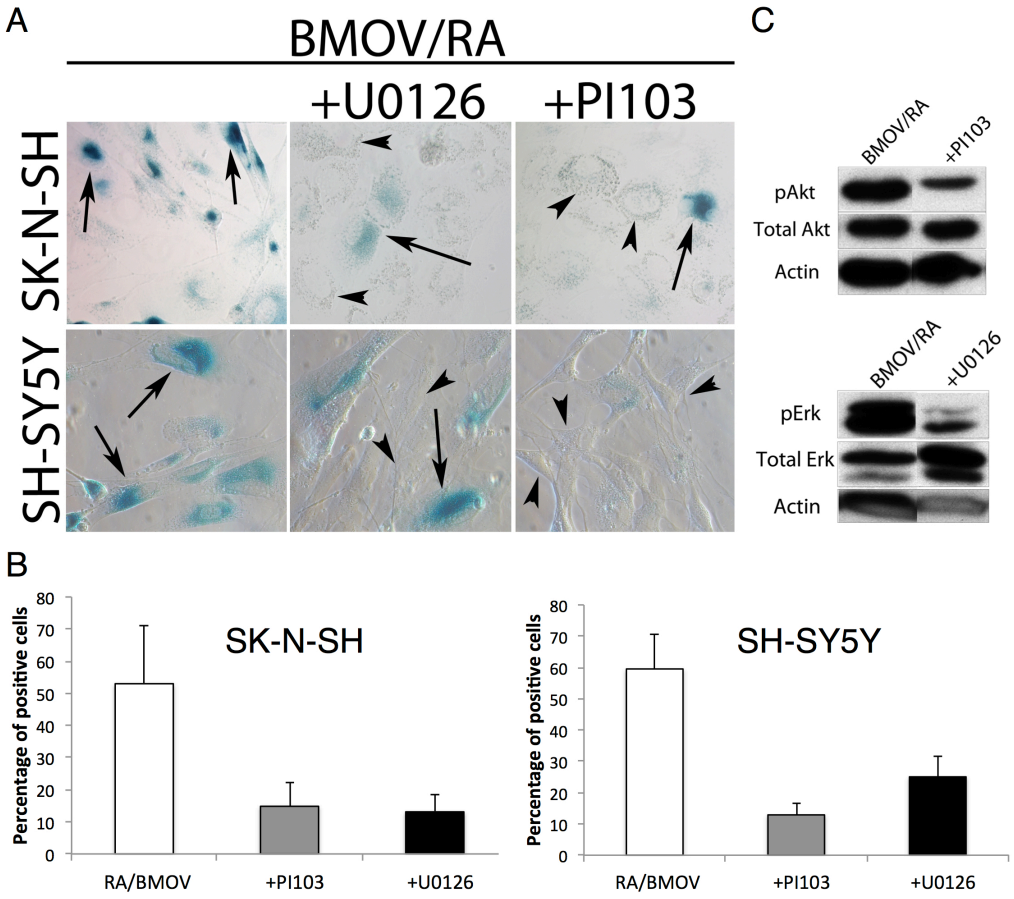

Figure 3.23. BMOV/RA induced senescence is Erk and Akt-dependent. Cells treated for 14 days with RA (5µM) and BMOV (20µM)/RA in the presence or absence of the MEK inhibitor U0126 (10µM) or the PI3K inhibitor PI103 (500nM) followed by a 14 (SK-N-SH) or a 21 (SH-SY5Y) day treatment-removal period and stained for SA-β-Gal activity. (**A**) Both PI103 and U0126 cause reductions in the number of SA-β-Gal positive cells (arrows) and sharp increases in the number of strongly negative cells (arrowheads). (**B**) Means and SEMs of the proportion of SA-β-Gal positive cells (N=3). (**C**) Immunoblot showing affect of both inhibitors on BMOV/RA induced Akt and Erk activation following 1 day of treatment. A = 40x objective magnification.

Figure 3.24. Compound PI103/U0126 treatment does not alter cellular morphology. Cells treated for 14 days (Day 0) followed by 7 and 14 days of culture without treatment. Treatments as in figure 4.23. 32x objective magnification.

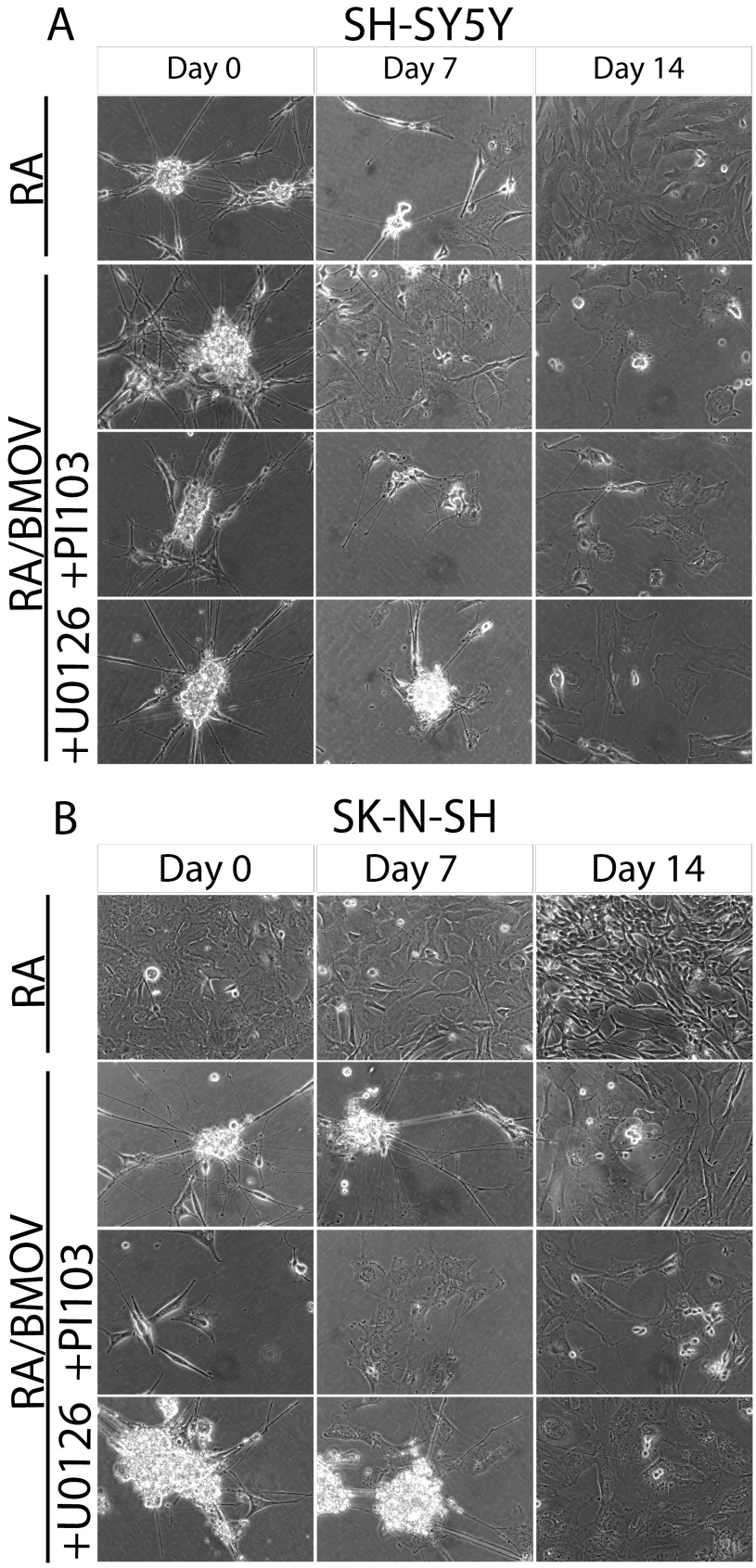
A
SH-SY5Y
Day 0
Day 7
Day 14
RA
RA/BMOV
+U0126 +PI103
B
SK-N-SH
Day 0
Day 7
Day 14
RA
RA/BMOV
+U0126 +PI103

3.4. Discussion

PTPs frequently function as negative regulators of RTK-driven signalling pathways that, when activated, can drive cancer cells to differentiate/undergo senescence (Alimonti et al., 2010b; Lin et al., 1998; Nogueira et al., 2008). We sought to test the hypothesis that broad inhibition of PTPs achieved with vanadium compounds, principally BMOV, would augment RA-mediated differentiation of NBL cells, given that such compounds have been shown to cause neuritogenesis, a cell-structural parameter of differentiation (Rogers et al., 1994), as well as activating PI3K/Akt signalling (Shioda et al., 2008), shown to have a role in RA-induced differentiation (López-Carballo et al., 2002). Indeed BMOV-induced comparable neurite outgrowth and upregulation of neural markers to that of RA, while increasing the effects of RA alone. However, more importantly, BMOV/RA treatment caused synergistic 'hyper-activation' of both Akt and Erk signalling, both of which were shown to be involved in stimulating differentiation/cell senescence that persisted in the absence of treatment, unlike RA, and appears independent of PTEN inhibition.

Pro-senescence treatment has been suggested as a potential therapeutic modality based on the well-established issues of conventional chemotherapy, including severe toxicity-related side effects and acquired resistance, as well as intransigence at clinical presentation (Nardella et al., 2011). The most common form of senescence exhibited by cancer cells/precancerous lesions is OIS (Braig and Schmitt, 2006; Collado and Serrano, 2010), resulting from increased levels/constitutive activation of oncogenic kinase signalling, leading to the induction of senescence through a DNA damage response involving p53/$p16^{INK4A}$ (Lin et al., 1998; Michaloglou et al., 2005; Oikonomou et al., 2009; Wajapeyee et al., 2008). While there is evidence that this phenomenon contributes to the outcome of cancer therapy (Schmitt et al., 2002; Wu et al., 2007), it is often circumvented due to mutations in both p53 and $p16^{INK4A}$ that frequently occur in cancer. Furthermore senescence might only be activated following excessive oncogenic activity (Sarkisian et al., 2007), which might otherwise be tightly regulated in cancer cells, and achieving such activation is difficult given that most forms of targeted therapy rely on target inhibition rather than activation. We have shown that PTP inhibition,

although not sufficient alone, can synergise with RA in the activation of Akt and Erk signalling to drive cell senescence. We hypothesize that this effect is directly related to the level of Akt/Erk activation, given that both BMOV and RA are capable of inducing such activation at lower levels alone but fail to efficiently induce irreversible differentiation/senescence. Furthermore this effect appears distinct to a recently characterised novel form of senescence entitled PICS (Alimonti et al., 2010b), achieved through activation of Akt concomitant to PTEN inhibition. In contrast to PICS, BMOV/RA-induced senescence is effective in the absence of heterozygous PTEN mutations (which are infrequent in NBL), and occurs independently of p53 and mTOR.

The effects of BMOV/RA are potentially valuable to NBL therapy. Tumour relapse is arguably the most significant barrier to effective therapy, given that a plethora of compounds have been shown to effectively induce tumour regression in solid tumours including NBL, but fail to prevent relapsed tumour growth. Thus eradication based on a therapy whose effects are apparent following treatment removal could potentially prevent relapse. To our knowledge little if any research has focused on the effects of RA-treatment following the termination of therapy, raising a significant issue that apparently growth-arrested cells might return to a proliferative state in the absence of on-going treatment. Although there are inherent risks associated with the activation of RTK-driven signalling, we have found little evidence for negative side effects. For instance, BMOV/RA fails to induce hyper-proliferation associated with OIS, which might be expected to occur following the activation of both Akt and Erk given that both are involved in stimulating proliferation/cell-survival (Roberts and Der, 2007; Vivanco and Sawyers, 2002). This argues against the obvious issue that attempting to activate oncogenic signalling would potentially unleash uncontrolled proliferation in bulk tumour cells. Furthermore BMOV/RA causes little if any evidence of cytotoxicity, a commonly dose-limiting factor in the administration of chemotherapy. Of particular note is the independence of p53 to BMOV/RA-induced cell senescence, despite the fact that the induction of cell senescence as well as apoptosis frequently centres on p53 induction. This is an important point given that relapsed and thus treatment-resistant NBL is frequently characterised by p53 mutations (Carr-Wilkinson et al.,

2010), while p53 is also often inactivated by other means (Tweddle, 2003). Lastly this approach may be an effective means of therapy given that it relies on, rather than antagonizes the molecular make up of a tumour, i.e. further stimulating pathways that drive tumour maintenance to exploit fail-safe mechanisms, as opposed to inhibiting growth/survival-signalling kinases, which ultimately results in selection of resistant cells and/or off-target effects (Balmanno et al., 2009).

One caveat is that BMOV/RA relies on the effectiveness of RA. Although BMOV appears to augment the actions of RA we found no evidence that it can sensitize RA-resistant cells to RA-mediated differentiation, nor does this effect occur in all NBL cell lines which exhibit increased Akt activity, suggesting that further studies are needed to examine the mechanisms of resistance to such differentiation/senescence, and the transcriptional changes associated with RA treatment that might synergise with RA/BMOV-induced Akt activation to enhance senescence.

The effects of BMOV/RA treatment and RA alone also exhibited variability. For instance initial experiments (e.g. see figure 3.16) showed marked differences in the propensity of RA and BMOV/RA treated cells to undergo senescence, whereby cells treated with RA alone would fully revert back to proliferative neuroblasts with few if any senescent cells. In contrast later experiments (e.g. see figure 3.23) found less evidence for clear-cut differences in senescence responses, and RA-treated cells more closely resembled BMOV/RA treated cells (esp. in SH-SY5Y). While the reasons for this are unclear, this may relate to gradual changes in endogenous and BMOV/RA-mediated Akt and Erk stimulation, which may be due to selective pressures in cultured cells, and/or phenotypic drift experienced with cell lines. However put another way this perhaps argues in favour that increased levels of Akt signalling can induce senescence, as such an effect occurs following stimulation with RA alone when this treatment causes abnormally high Akt activity. One further caveat is that while initial experiments based on the effects of U0126/LY294002 suggested that both Akt and Erk were involved in morphological differentiation induced by both RA and BMOV, the later experiments (shown here) failed to find evidence for differences in morphology following U0126/PI103 treatment. In the case of the latter, the effects of LY294002 aren't always clear given its propensity for

off-target inhibition, thus PI103 is perhaps a more reliable inhibitor especially given that it exerts activity on both PI3K and mTOR (Fan et al., 2006). However these differences may also be related to inhibitor dosage, which was used at a maximum limit in earlier experiments; this was designated unfeasible in later experiments however due to low seeding density and high toxicity, which would have limited the number of cells to assay following termination of experiments, but one might predict a more pronounced effect on senescence if such inhibitors were used at two fold higher doses.

Certain issues still remain regarding BMOV/RA-induced senescence in comparison to previously published findings. It is unclear how BMOV/RA-induced senescence occurs in the absence of p53/$p16^{INK4A}$, given that these proteins are frequently involved in OIS as well as PICS. It is also noteworthy that BMOV/RA-induced senescence occurs following strong activation of Erk, given that MEK/Erk signalling has been cited as a mechanism of RA-resistance following mutational inactivation of *NF1* in NBL (Hölzel et al., 2010). However as previously discussed this phenomenon might be related to the duration and level of activation of Erk (von Kriegsheim et al., 2009). Lastly PI3K has been recently shown to inhibit senescence downstream of Ras (Kennedy et al., 2011), while clearly Akt and Erk are co-activated by BMOV/RA treatment with little consequence. However it is of course possible that such effects are entirely cell-type dependent.

The apparent causal role of Akt signalling in this senescence response complicates the contention that Akt only contributes negatively to disease progression in NBL by controlling proliferation/cell-survival (Bender et al., 2011; Opel et al., 2007). Targeted inhibition of Akt, which has been argued as a potential strategy against NBL tumours (Li et al., 2010; Li and Thiele, 2007), may be an effective means of tumour eradication. However tumours with low Akt activity may also benefit from augmentation of Akt, given that this could stimulate a senescence response. Furthermore tumours with high Akt may also benefit from increased Akt activity if this senescence response is simply related to a threshold of Akt activity. This may already be a consequence of RA treatment in some tumours, although there is no formal proof for this. Although caution is certainly required in suggesting that a pathway that frequently controls proliferation/survival should be augmented,

this approach is appealing in some ways as it may avoid problems of toxicity associated with the inhibition of a fundamental signalling pathway such as PI3K/Akt, as well as compensation limiting the effectiveness of Akt inhibition (Chandarlapaty et al., 2011). Furthermore Akt inhibition might limit the effectiveness of RA in inducing irreversible growth arrest (which could otherwise be augmented by BMOV), although this could be avoided by confining BMOV/RA treatment to MRD. Thus in sum the effectiveness of BMOV/RA certainly warrants pre-clinical testing of such a treatment combination against NBL tumours, which despite recent advances in the understanding of pathogenesis is still frequently resistant to current treatments. Importantly a number of related vanadium compounds have been shown to be effective against solid tumours in pre-clinical testing (Bishayee et al., 2010), as well as being well tolerated in human clinical studies (Thompson et al., 2009), urging their use in combination with RA treatment to potentially further improve NBL patient survival (Matthay et al., 2009; Matthay et al., 1999).

Chapter 4. The effects of vanadium-based tyrosine phosphatase inhibitors on cell death

4.1. Introduction

As previously mentioned, conventional chemotherapy involves the induction of wide scale DNA damage in rapidly dividing tumour cells, inducing selective cytotoxicity. However this is often associated with considerable side effects related to non-specific toxicity e.g. due to off target effects on dividing cells of the gastrointestinal tract and hair follicles for instance. Thus since the discovery of cancer-causing oncogenes in the early 1980s, drug discovery has focused on targeted therapy of proteins driving tumour progression, culminating in the FDA approval of the first targeted therapy Trastuzumab (Herceptin) in 1998, a monoclonal antibody that interferes with the HER2/neu receptor in breast cancer. This has met with some remarkable successes, for example the use of the BCR-ABL fusion protein tyrosine kinase inhibitor Imatinib mesylate (Gleevec), which causes remission of chronic myeloid leukaemia (CML) in as high as 90% of cases.

However this has considerable challenges in tumours of polygenic origin (the majority of tumours), which do not present with one single target driving tumour progression. Similarly although the phenomenon of oncogene addiction, whereby cancer cells become dependent on particular proteins for survival, has been noted to occur in tumours (Weinstein and Joe, 2008), redundancy between growth/survival signalling pathways often mitigates the effects of targeted therapy. Perhaps most importantly tumour cells often develop resistance to targeted therapy, both through Darwinian selection and direct adaptation, rendering drugs ineffective and causing relapse. This has been elegantly demonstrated with Trastuzumab by the recent finding that the tyrosine kinase SRC is a key node in both *de novo* and acquired resistance to this drug, controlling alternative survival pathways normally negatively regulated through dephosphorylation by the tumour suppressor PTEN (Zhang et al., 2011). Conversely, inhibition of the survival/growth-promoting kinase Akt has been shown to relieve feedback suppression of multiple tyrosine kinase receptors including HER3 (Chandarlapaty et al., 2011). Lastly resistance can develop through acquired mutations in unrelated proteins that confer a selective advantage, such as in NBL where loss of the tumour suppressor NF1 has been shown to mediate resistance to RA (Hölzel et al., 2010; Huang et al., 2009). A common theme in all of

these studies is the targeting of multiple kinases to alleviate compensatory survival signalling. Although this strategy may appear effective it is presumably subject to the same limitations of resistance and adaptation mechanisms, as well as potentially incurring problems due to targeting multiple pathways required for normal homeostasis and development, e.g. PI3K/Akt.

Given that a substantial majority of targeted therapies are aimed either directly or indirectly at tyrosine-kinases, the PTP family is perhaps an overlooked pool of drug targets. This is not without its reasons, given the initial hypothesis that PTPs would most likely represent tumour suppressors due to their ability to negatively regulate growth-factor receptor driven signalling pathways. However findings such as that of MacKeigan *et al.* that as much as 32% of the PTP family promote cell-survival signalling in cancer cells (MacKeigan et al., 2005), has highlighted the PTP family as a growing family of potential targets (Easty et al., 2006).

Since these early discoveries, a number of PTPs have emerged as *bona fide* cancer-promoting genes that are truly viable drug targets. For instance, SHP2, PTP1B and PTPH1 can all function in a positive manner to increase tumour growth (see 1.4.3). Lastly a pro-tumorigenic function of the dual-specificity phosphatase DUSP26 was recently highlighted by its ability to inhibit p53 tumour suppressor function in NBL (Shang et al., 2010). With the exception of PTPH1, selective inhibitors have been developed for all of these phosphatases, making them tempting targets for novel therapies. Although PTP targeting is a relatively untapped therapeutic strategy, it would obviously be subject to the same limitations as the targeting of tyrosine kinases, although perhaps suffering less from non-specific toxicity. Thus an appealing hypothesis is the notion that PTP inhibition could engage apoptotic pathways by paradoxically stimulating growth-factor receptor signalling cascades. Although there is little evidence for this occurring in cancer, numerous examples exist whereby over-activation of proteins normally engaged in survival mechanisms can cause cell death. For instance the increasing expression of Mycn, a transcription factor with various survival/growth-promoting roles when amplified in NBL, can paradoxically sensitise NBL cells lacking Mycn amplification to apoptosis induced by chemotherapy (Gamble et al., 2011; Peirce, 2009). The serine/threonine kinase Akt, which controls

numerous survival pathways in most human cancers, has been shown to paradoxically sensitise cells to apoptosis mediated by reactive oxygen species through inhibition of FoxO transcription factors and their ROS-inhibiting targets (Nogueira et al., 2008). This perhaps represents the most salient paradox of cancer-survival signalling, as inhibition of FoxO transcription factors has been considered the primary mechanism by which Akt promotes cell-survival (Brunet et al., 1999), yet FoxOs have also been shown to maintain the survival of tumour-initiating cells in CML, conferring resistance to Imatinib (Naka et al., 2010; Tothova et al., 2007).

Thus we hypothesise that the inhibition of PTPs may both identify novel regulators of cell-survival within this enzyme group, as well as potentially elucidating mechanisms by which the activation of kinases can actually promote cell death, uncovering alternative methods to targeted therapy whereby one can exploit the Achilles heal of cancer-promoting enzymes and thus work with rather than against deregulated signalling given its ubiquitous presence in cancer.

4.2. Experimental procedures

4.2.1. Immunoblotting for oxidized PTEN

The detection of oxidised and reduced forms of PTEN was achieved as previously described (Lee, 2002). Specifically SDS-PAGE gels were made with 7.5% acrylamide to facilitate band separation at the 40-70kDa range. Cells were lysed in the usual manner except that 40mM N-ethylmaleomide (NEM) was added to lysis buffer to block free sulfhydryls, i.e. preventing reduction of oxidised PTEN. Following clarification lysates were then added to standard loading buffer without β-mercaptoethanol and separated without boiling in order to prevent reduction.

4.2.2. Isogenic Mycn cell lines

The Tet21N cell line is a variant of the SHEP cell line, itself a subclone of SK-N-SH cells, stably expressing Mycn using the Tet Off system (Lutz et al., 1998). Briefly the Tet-Off system was developed for the reversible activation of protein expression by binding of the tetracycline transactivator (tTA) to DNA at a ‘tet’ Operator, which activates a coupled promoter containing a tetracycline response element (TRE)

resulting in gene expression (Gossen and Bujard, 1992). Addition of tetracycline to culture medium prevents binding of tTA to the Mycn TRE, preventing promoter transactivation. The second Mycn inducible cell line SK-N-AS MycnER works in the opposite fashion. Specifically this cell line stably expresses a fusion protein of Mycn and the oestrogen receptor, which can be activated by binding of the oestrogen analogue 4-Hydroxytamoxifen (4-OHT), activating transcription of Mycn after addition of 4-OHT to culture medium (Koppen et al., 2007). The third isogenic cell line is simply a variant of the Mycn non-amplified cell line ACN (Thiele, 2006), that can stably expresses Mycn under the control of the CMV promoter at 3 different levels, ACN-0 (empty vector), ACN-5 (Mycn low) and ACN-10 (Mycn high) cell lines (Gualdrini et al., 2010), although we noted no difference in expression levels between ACN-5 and ACN-10.

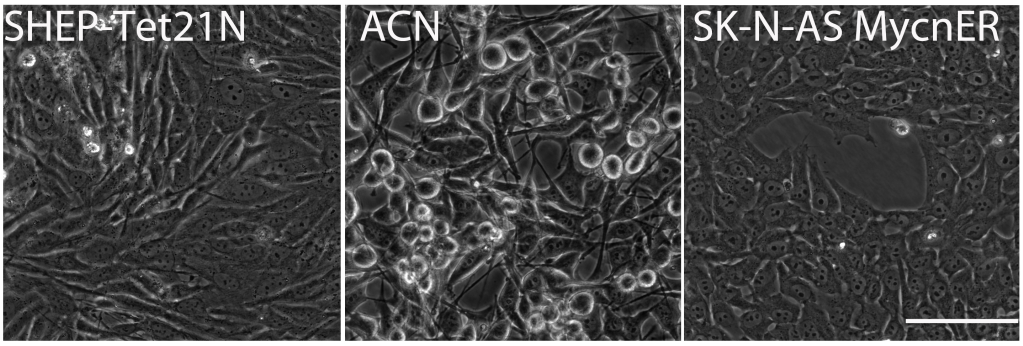

Figure 4.1. Isogenic Mycn expressing cell lines. Cell lines Tet21N, ACN and SK-N-AS MycnER have been engineered to either stably or conditionally express Mycn. Scale bar = 10 microns

4.3.3. Detection of intracellular ROS and glutathione

Fluorescent dyes activated by ROS are a commonly used means of intracellular ROS detection (Wardman, 2007). Perhaps the most widely used die is 2',7'-Dichlorodihydrofluorescein ($DCFH_2$), which has been in existence for over 40 years (Chen et al., 2010c; Eruslanov and Kusmartsev, 2010). This method of ROS detection is relatively simple (**Figure 4.2**). The non-fluorescent lipophillic $DCFH_2$ is membrane permeable in its deacetylated form $DCFH_2$ diacetate ($DCFH_2$-DA). Following addition to culture medium the $DCFH_2$-DA compound diffuses across the phospholipid cell membrane (1), where it is targeted by endogenous esterases to yield the deacetylated membrane-impermeable polar form $DCFH_2$ (2), which is oxidised by intracellular ROS to yield the fluorescent molecule 2'-7'-dichlorofluorescein (DCF)

(4), losing 2 electrons in the process. Although used as a generic ROS detector, $DCFH_2$ is not oxidised by all species, for instance the superoxide ($O_2^{\cdot-}$) anion, and is most commonly used for the detection of H_2O_2 (Chen et al., 2010c).

Dihydrorhodamine (DHR) 123 was used as an alternative to DCFDA for the detection of ROS. DHR 123 works on the exact same principle as DCFDA, whereby intracellular H_20_2 oxidises the non-fluorescent chemical DHR 123 into the fluorescent molecule rhodamine 123, which emits fluorescence at 534nm when excited at 502nm (Emmendörffer et al., 1990). Importantly DHR123 has been suggested to be more sensitive in the detection of ROS when compared with DCFDA. Briefly cells were seeded onto a 96 well plate at high density ($5x10^4$). Cells were allowed to adhere to their surface, and then treated for 4 hours with compounds of interest. Following treatment, cells were washed with pre-warmed HBSS then incubated with 10µM DHR 123 diluted in DMSO in fresh HBSS for 30 minutes at 37°C. Following this DHR loading, cells were washed with HBSS, then replaced with fresh HBSS and fluorescence was immediately read using a FLUOstar OPTIMA plate reader (BMG Labtech, Offenburg, Germany) microplate reader at an excitation/emission ratio of 492/520.

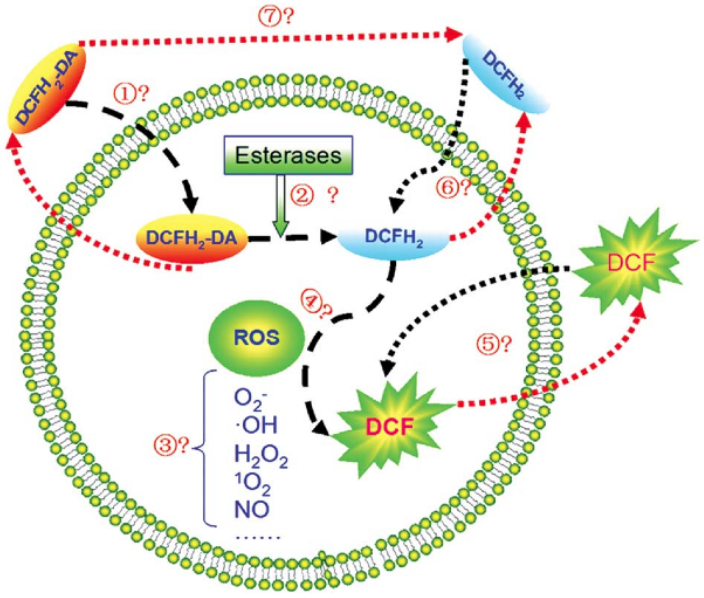

Figure 4.2. Mechanism of ROS detection by DCF fluorescence. $DCFDH_2$-DA enters the cell membrane (1) where it is deacetylated by esterases (2) and oxidised to DCF by intracellular ROS (3), generating a fluorescent signal (4). Note that controversies exist such as which ROS target $DCFDH_2$ (3), the leakage of DCF by diffusion (5) as well as the membrane impermeability of $DCFH_2$ (6) and whether deacetylation may occur prior to cell entry (7), reflecting general uncertainties concerning the mechanism of action of such probes. Taken from (Chen et al., 2010c).

Monochlorobimane was used for the detection of intracellular glutathione (GSH). MCB enters into the cell forming a fluorescent GSH-MCB product dependent on the glutathione-S-transferase activity, which catalyses the conjugation of GSH. GSH-MCB is thus indicative of the relative levels of cellular GSH (Kamencic et al., 2000). Briefly cells were seeded in 96 well plates and treated as previously. However following treatment, 50µM MCB diluted in DMSO was added to the culture medium and fluorescence was read immediately at an excitation/emission ratio of 426/490.

4.2.4. Examination of apoptosis following plasmid overexpression

To examine the influence of Akt on BMOV-induced toxicity, we overexpressed plasmids containing a dominant negative HA-Akt DN (K179M) (Zhou et al., 2000) and a constitutively active myr-Akt Delta4-129 (Kohn et al., 1996) form of Akt, a gift of Dr. Mien-Chie Hung (Addgene plasmid 16243) and Dr. Richard Roth (Addgene plasmid 10841) respectively. Due to the absence of selectable marker genes, cells were co-transfected with a CAG-H vector (see Chapter 3) containing the *HLH* gene conferring resistance to the antibiotic hygromycin B. One-day post transfection cells were selected by the addition of hygromycin B to the culture medium (400µg/µl) for 72 hours, then re-plated onto new dishes and treated as normal for 72 hours. This method allowed significant enrichment for transfected cells (**Figure 4.3**).

In order to achieve maximal transfection, the lipid-based transfection reagent Lipofectamine™ 2000 (L2K) (Invitrogen, Carslbad, CA) was used. Briefly L2K was diluted in reduced serum Opti-MEM medium and allowed to incubate for 5 minutes. DNA was diluted at a ratio of 2:3 DNA: L2K in an equal volume of Opti-MEM and both mixtures were combined and incubated for 20 minutes before addition to the culture medium. Media was removed 12-16 hours following transfection.

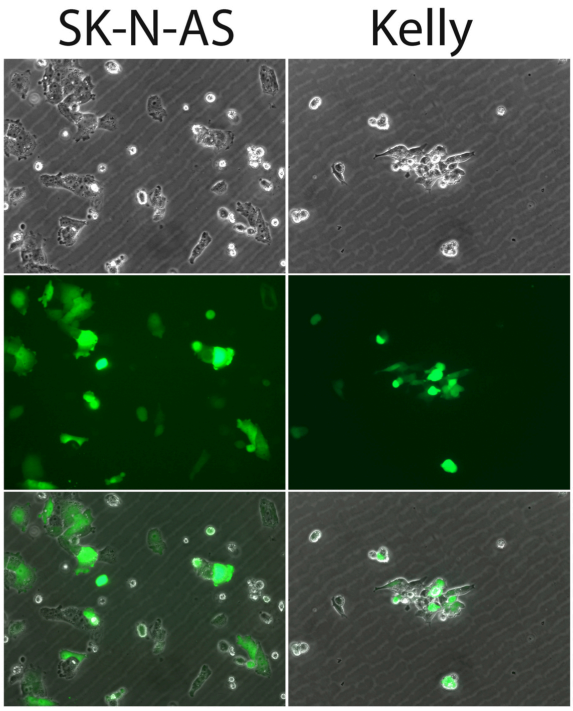

Figure 4.3. Enrichment cells over-expressing plasmid based on acute antibiotic selection. Cells were co-transfected with a vector encoding GFP and a vector containing the hygromycin resistance gene then acutely selected for 48 hours using hygromycin B (400µg/µl) followed by trypsinisation and reseeding. Surviving cell populations are highly enriched for GFP positive and thus transfected cells.

4.2.5. Detection of autophagy

The detection of macroautophagy (autophagy) was achieved through 3 methods. The first made use of a plasmid encoding a GFP-LC3 fusion protein (A kind gift of Dr. Toren Finkel, Addgene plasmid 24920), which facilitates the detection of autophagy due to LC3 becoming conjugated to phosphatidylenimine (PE) during the induction of autophagy and its localisation transitioning from a cytosolic to an autophagosome membrane distribution, thus becoming punctate in appearance (Elgendy et al., 2011). Here cells were transiently transfected, fixed in 4% paraformaldehyde and photographed under blue excitation. The second method involved the vital dye acridine orange, which becomes protonated under acidic conditions, leading to orange staining when subjected to excitation by blue light (Mains and May, 1988). Here cells were treated for 15 minutes with acridine orange (5µg/ml) diluted in water and fixed in 4% paraformaldehyde. Cells were then photographed under both green and red emission. Although red light emitting acidic vesicles should be detected under blue light, we examined fluorescence under each excitation beam

and did not detect any red signal under blue light. Thus vesiculation after excitation with green light was took as indicative of autophagy. Lastly the conjugation of LC3-I to LC3-II was detected by immunoblotting, whereby LC3-II migrates faster than LC3-I giving rise to two distinct bands. Here cells were treated with lysosomal peptide inhibitors E64d (4µg/ml) and pepstatin-A (2µg/ml) to block endogenous turnover of LC3-II in the autophagosome for 4 hours, followed by treatment with chemical of interest for 12 hours. Cells were then lysed and subjected to SDS-PAGE using a 15% acrylamide gel to facilitate detection of bands less than 25kDa.

4.4. Results

4.3.1. Vanadium compounds selectively induce apoptosis in a cell line-dependent manner

Undoubtedly the most common approach to chemotherapy is the selective targeting of cancer cells through their reliance on survival mechanisms, for instance oncogene addiction (Weinstein, 2002; Weinstein and Joe, 2008), resulting from constitutive activation of growth factor signalling. Although traditionally viewed as positive regulators of programmed-cell death through dampening growth factor signalling, PTPs have been shown to be largely responsible for cell survival with an RNAi screen in the cervical cancer HeLa cell line identifying 33% of phosphatases as contributing positively to cell survival (MacKeigan et al., 2005). Thus we sought to see if vanadium compounds could act in a similar manner to conventional chemotherapeutics by initiating a cytotoxic response selectively in neuroblastoma cells.

We noted previously that LAN-5 cells displayed evidence of morphological apoptosis in response to VA as well as undergoing neuritogenesis (See section 3.1). Thus we sought to confirm this by analysing the sub-G1 fraction of cells (a marker of DNA fragmentation following apoptosis) after treatment with VA. VA treatment of LAN-5 cells significantly increased apoptosis while both SK-N-SH and SH-SY5Y cells were unaffected (**Figure 4.4, A**). This effect was partially reduced by concurrent treatment with RA, suggesting it is unrelated to differentiation and for instance neurotrophin dependence (Encinas et al., 2000b). VA also failed to induce cell death in transformed cells (293T, COS7) as well as glioma (C6) and pheochromocytoma

(PC63) cells (**Figure 4.4A**). This suggests VA induces highly selective cytotoxicity for NBL cells, given that (1) pheochromocytoma is a neuroendocrine, neural crest derived tumour likely originating from a common precursor to NBL, and (2) that glioblastoma is a tumour of neuronal origin. Similarly non-transformed MEFs were unresponsive to VA treatment, reinforcing the selectivity of the effect on NBL and showing that these normal, non-immortalised cells are resistant to BMOV (**Figure 4.4, B**).

Further testing revealed that multiple cell lines (KCNR, Kelly, IMR-32) also responded to VA with cell death, with 5µM dosage significantly abrogating cell survival (**Figure 4.4, C**). Importantly this effect appeared selective for a subset of NBL cell lines, as cells that were unresponsive to VA (SK-N-DZ, SK-N-AS) failed to undergo cell death at doses up to 10 fold higher (data not shown). Crystal violet staining for viable cells revealed a near complete loss of surviving cells following 6 days of treatment with the alternative vanadium compound BMOV (**Figure 4.4, D**). VA was also observed to induce morphological evidence of apoptosis, causing picnotic nuclei as evidenced by DAPI staining (**Figure 4.4, E**) and positive staining for propidium iodide that preferentially marks cells that have lost membrane integrity, indicating late-stage apoptosis and/or necrosis.

To briefly summarise, both BMOV and VA cause cytotoxicity in a subset of NBL cell lines by mechanisms distinct from non-specific cell stress, e.g. sparing non-NBL cell types, and indicating both PCD and necrosis as possible contributing forms of cell death. We next sought to characterize this response further by examining the mechanism of cell death. Chemotherapeutic targeted drugs often induce cell death via apoptosis, a mechanism of PCD in which cells undergo distinct morphological changes including membrane blebbing, chromatin condensation, nuclear fragmentation (karyorrhexis) and cell shrinkage. PCD and apoptosis generally occur through activation by proteolytic cleavage of caspases, where stimuli activate initiator caspases (2, 8, 9, 10) that lead to activation of effector caspases (3, 6, 7).

Figure 4.4. Vanadium compounds induce cytotoxicity in a cell-line specific manner selectively in NBL cells. **(A)** Sub G1 analysis showing increases in the percentage of apoptotic cells in LAN-5 cells treated for 6 days with VA (5μM), an effect reduced by co-treatment with RA. Increased sub G1 is not exhibited by non-cancerous transformed control cells (COS-7, 293T) and neuroendocrine (PC-63) and glial (C6) tumour control cells. **(B)** BMOV (10μM) exerts no cytotoxicity against untransformed wild-type mouse embryonic fibroblasts treated for 6 days. **(C)** VA-induced cytotoxicity is shared with BMOV in distinct NBL cell lines (IMR-32, KCNR, Kelly), whereas other NBL cell lines (SK-N-DZ, SK-N-AS) are unresponsive to both inhibitors after the same treatment period (3-6 days)/dosage (10μM). **(D)** Crystal violet staining of fixed cells treated for 6 days with 5μM VA revealing gross reductions in cell survival. **(E)** DAPI and propidium iodide staining revealing morphological apoptosis characterized by picnotic nuclei (DAPI – arrows and insets) and late-stage apoptosis/necrosis (PI – arrow heads) in cells treated for 3 days with BMOV (10μM). Scale bar = 10 micrometers.

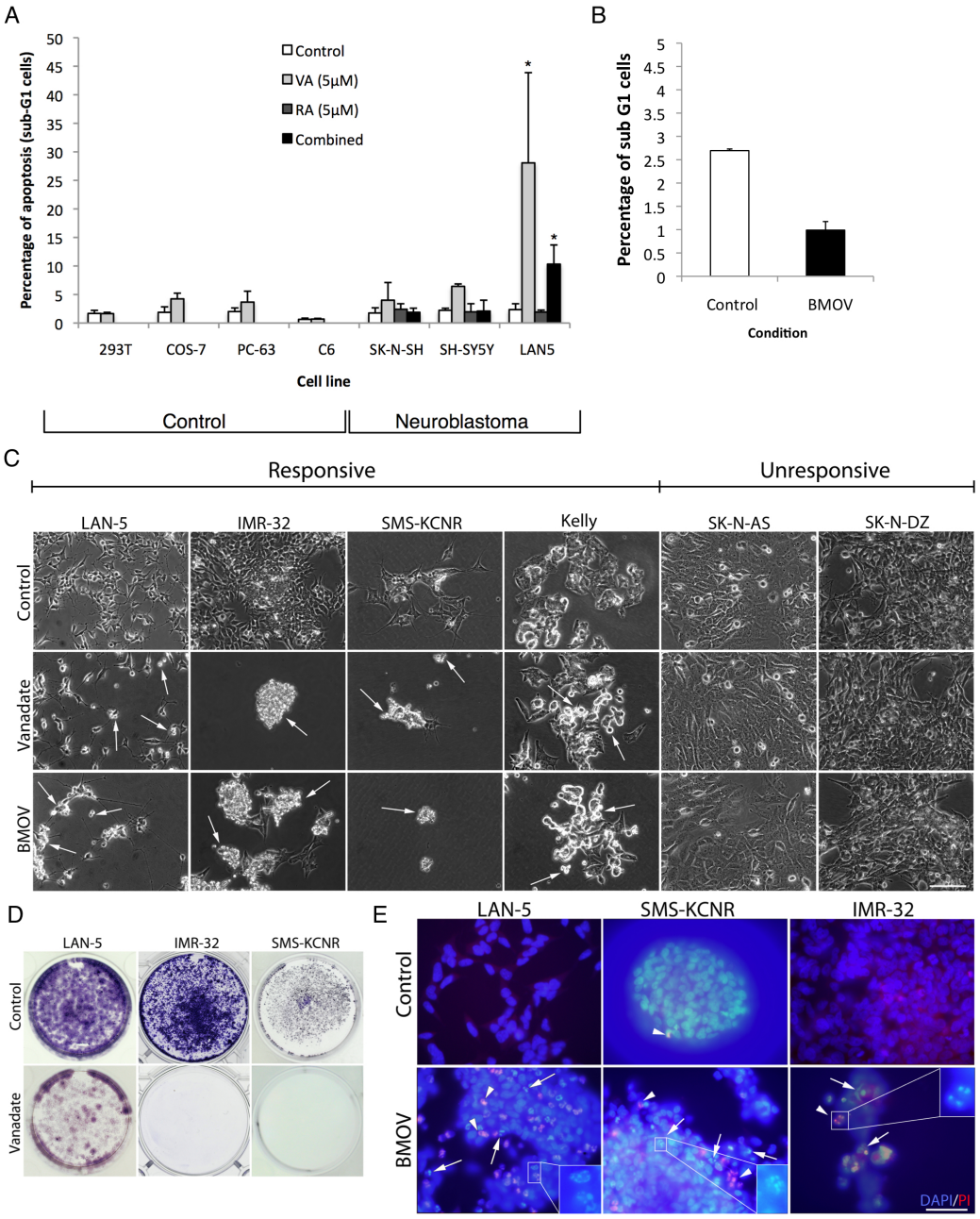
A
Percentage of apoptosis (sub-G1 cells)
Control
VA (5μM)
RA (5μM)
Combined
293T
COS-7
PC-63
C6
SK-N-SH
SH-SY5Y
LAN5
Cell line
Control
Neuroblastoma
B
Percentage of sub G1 cells
Control
BMOV
Condition
C
Responsive
Unresponsive
LAN-5
IMR-32
SMS-KCNR
Kelly
SK-N-AS
SK-N-DZ
Control
Vanadate
BMOV
D
LAN-5
IMR-32
SMS-KCNR
Control
Vanadate
E
LAN-5
SMS-KCNR
IMR-32
Control
BMOV
DAPI/PI

Thus we examined whether the effector caspase 3 was cleaved following treatment with BMOV in those NBL cell lines that respond via cell death. Immunostaining for cleaved caspase 3 revealed an increase in the proportion of cells expressing cleaved caspase 3 in LAN-5, IMR-32, Kelly and KCNR NBL cells. This increase however was fairly modest, and did not appear to recapitulate the extent of cell death after BMOV treatment (**Figure 4.5, A**). Activated caspase-3 positivity was observed to roughly correlate with propidium iodide staining suggesting that cell death was occurring predominantly via caspase activation but to a lesser extent via caspase-independent PCD and/or necrosis (**Figure 4.5. A**).

Given that we observed propidium iodide positive cells and cells exhibiting morphological apoptosis (picnotic nuclei) in cases were caspase 3 activation was infrequent, we sought to examine whether BMOV induced-cell death was dependent on caspase activation using Z-VAD-FMK, a pan-caspase inhibitor that irreversibly binds to the caspase active site (Slee et al., 1996). Compound treatment with zVAD-FMK partially but significantly blocked BMOV-induced death in KCNR cells (**Figure 4.5, B**). However a significant sub G1 fraction remained in the presence of Z-VAD-FMK, suggesting either that this inhibitor was not achieving full efficacy and thus some apoptosis was still occurring, or that one component of BMOV induced-cell death may be PCD occurring independently of caspases (Kroemer and Martin, 2005; Lockshin and Zakeri, 2004; Tait and Green, 2008).

One of the most common mechanisms of PCD induced by chemotherapeutic agents occurs via stress signalling/activation of the DNA damage response leading to stabilization and activation of p53 (Junttila and Evan, 2009). While p53 is generally wild type at presentation in NBL (Chen et al., 2007), it can be frequently inactivated via mechanisms including post-translational squelching caused by MDM2 (Van Maerken et al., 2011) and mutations acquired during tumour remission causing relapse (Carr-Wilkinson et al., 2010). Thus we examined whether BMOV was causing cell death through genotoxic stress induced by stabilization and activation of p53. Immunoblotting revealed that standard and two-fold higher doses of BMOV did not lead to upregulation of p53 (**Figure 4.5, C**). In fact p53 was undetectable in three lines that respond to BMOV via cell death (LAN-5, KCNR, IMR-32) and only detectable in Kelly cells, but at basal levels. Similarly we observed no effect of the

p53 inhibitor Nutlin (data not shown). This suggests that BMOV-induced cell death is independent of p53.

Stress and damage responses also commonly activate the p38 MAPK family, which positively regulate cell death (Xia et al., 1995). Thus we asked the question of whether BMOV-induced cell death was the result of p38 MAPK activation. Immunoblotting revealed that BMOV did not cause increased activation of p38 MAPK in any cell line (**Figure 4.5, D**), further suggesting that BMOV does not exert its cytotoxic effects via activation of a general cell stress response.

In sum, both VA and BMOV induce cell death in a cell-line specific manner, causing significant increases in morphological cell death/DNA fragmentation at a dosage that is tolerated in genetically distinct NBL cells as well as non-neuroblastoma transformed and tumour cells and normal non-tumour cells. Furthermore this cytotoxic response elicits morphological apoptosis and necrosis that activates cleaved caspase 3. However, a caspase inhibitor study suggests that caspase-independent PCD is also a significant component. Lastly, BMOV fails to activate either p53 or p38 MAPK, suggesting that this cytotoxic effect is not simply due to non-specific genotoxic stress. BMOV could thus potentially target NBL tumours having mutations in the p53 pathway, a frequent obstacle to chemotherapy.

4.3.2. Decreasing cell adhesion increases cell death in BMOV-unresponsive cells and reduces SRC kinase levels

Both SRC and FAK have been shown to contribute to cell survival in NBL, where joint inhibition was found to cause cytotoxicity due to decreased adhesion and apoptosis through detachment from the extra-cellular matrix (anoikis) (Beierle et al., 2010). Similarly FAK is a target of Mycn, where increased expression of Mycn causes increases in the levels of FAK (Beierle et al., 2007) and is thus considered a good target for therapy (Gillory and Beierle, 2010). Caspase-8 was shown to promote SRC-mediated adhesion in NBL, explaining its lack of tumour-suppressive function (Finlay and Vuori, 2007), while joint activation of FAK and SRC have been found to promote α5β1 and α4β1 integrin-stimulated NBL cell motility (Wu et al., 2008).

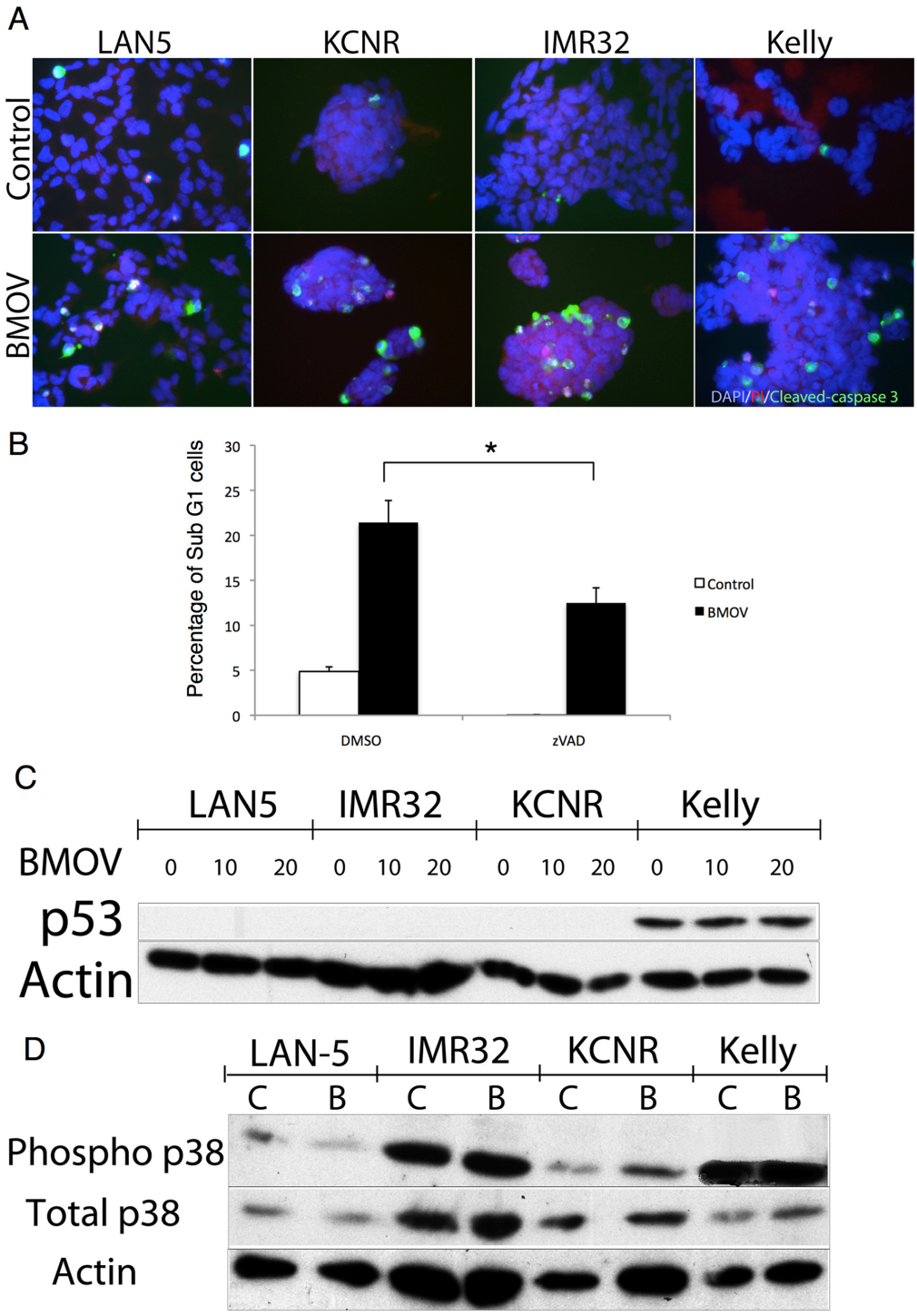

Figure 4.5. VA/BMOV induced cell death involves caspase activation but does not induce genotoxic stress signalling. (**A**) ICC illustrating cleavage of caspase 3 following 48 hour treatment with BMOV (10µM), note that caspase-3 activation generally fails to co-localise with propidium iodide staining indicating both necrosis and apoptosis. (**B**) KCNR cells treated for 2 hours prior too and 48 hours during BMOV (10µM) treatment with the pan-caspase inhibitor z-vad-FMK (20µM), which significantly reduces BMOV-induced cell death (sub G1 DNA content). (**C**) 24-hour BMOV treatment fails to induce the expression of p53 or activate p38 MAPK signalling (**D**) illustrating that BMOV-induced cell death is independent of genotoxic stress signals. C shows mean and SEM with independent samples student's t tests. D = 10µM BMOV.

Both SRC and FAK are subject to regulation through reversible tyrosine phosphorylation where a number of PTPs play a direct role both positively and negatively regulating FAK/SRC activity. For instance PTP-PEST (PTPN12) has been shown to dephosphorylate SRC at Y416, preventing the phosphorylation of villin 1 and negatively regulating cell migration/invasion (Mathew et al., 2008). PTEN has recently been shown to directly dephosphorylate SRC, negatively regulating its activity contributing to tumour regression during chemotherapy (Zhang et al., 2011). Conversely PTPRA has been found to dephosphorylate SRC on Y527 through its interaction with integrin α5β3, activating SRC and positively regulating the association of FAK and SRC (Harder et al., 1998). PTP1B has been demonstrated to activate SRC, an event necessary for transformation of human breast epithelial cells by ErbB2 (Arias-Romero et al., 2009).

The PTP family has a well-defined role in cell adhesion (Gebbink et al., 1993), while treatment with vanadium compounds has been shown to modulate cell adhesion (Edwards et al., 1991). Given the fact that both SRC and FAK are subject to regulation by PTPs, and are involved in regulating cell adhesion, motility and invasion in tumour cells and contribute positively to cell survival in NBL, we hypothesized that BMOV may alter their activation, causing cell death through anoikis. Indeed KCNR cells are among the least adhesive of the panel of tested NBL cells and the most sensitive to BMOV induced-cytotoxicity, while SK-N-AS cells are at the opposite end of the spectrum, representing highly substrate adherent cells with a high tolerance to BMOV treatment. Thus we examined the expression and phosphorylation status of both FAK and SRC in both BMOV-sensitive (LAN-5, KCNR) and BMOV-unresponsive (SK-N-AS) cells.

Immunoblotting revealed large differences in the expression of SRC and FAK in BMOV-responsive cells versus unresponsive cells, with SK-N-AS expressing high levels of endogenous, phosphorylated FAK and SRC compared to low levels in KCNR/LAN5 cells (**Figure 4.6**). BMOV treatment was found to further decrease both total and phosphorylated SRC levels in all cell lines. Due to the high level of SRC expression/activation in SK-N-AS cells the effect of BMOV was negligible, however in the case of both LAN-5/KCNR treatment with BMOV reduced the expression of total and activated SRC to undetectable levels.

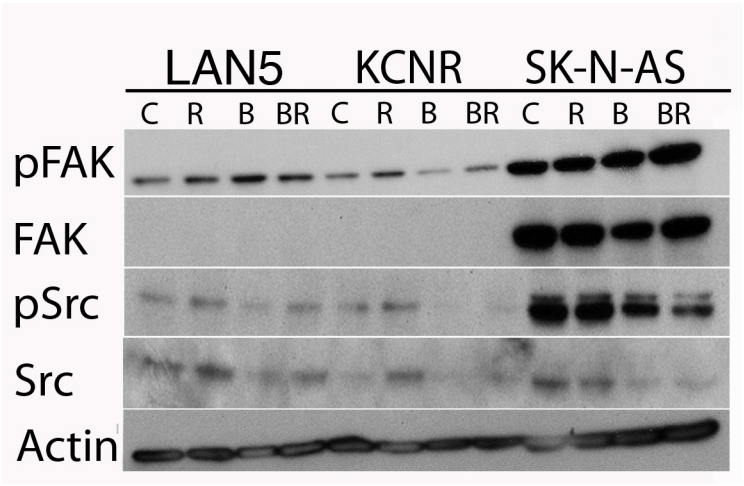

Figure 4.6. High expression of total and activated FAK and SRC in BMOV-unresponsive SK-N-AS cells. In each cell line BMOV (B) (10μM) treatment decreased levels of SRC protein and phospho-SRC, without significantly affecting FAK**.** Cells were treated for 24 hours. C – control; R – RA; BR = BMOV/RA. Experiment carried out with M. Attwood under direct supervision of O.Clark.

Based on this evidence we hypothesized that high expression of endogenous activated SRC may form a mechanism of resistance to BMOV. This might potentially explain why SK-N-AS cells, which express high levels of SRC, are BMOV-unresponsive, while KCNR cells, which express low levels of SRC that is further decreased by BMOV, are sensitive to its cytotoxic effects. Both low expression of FAK/SRC and sensitivity to BMOV may be related to a relative lack of substrate adherence in KCNR cells versus SK-N-AS, given that inhibition of SRC/FAK causes anoikis (Beierle et al., 2010). Thus we attempted to test this by seeding cells onto non-tissue culture treated dishes, which lack a hydrophilic surface and therefore fail to facilitate adhesion to the substratum. Although SK-N-AS cells were able to adhere to non-treated plastic, they exhibited a morphology more closely resembling that of adherent KCNR cells when seeded onto treated plastic in terms of a propensity to form loosely adherent spheroid structures and a more fusiform phenotype (**Figure 4.7, A)**.

Indeed seeding cells onto non-treated plastic greatly reduced the levels of endogenous FAK and SRC in SK-N-AS cells in terms of both activated and total protein expression, resembling levels of KCNR cells seeded onto treated plastic (**Figure 4.7, B, C**). Activated FAK was also observed to decrease following BMOV treatment only in SK-N-AS cells seeded onto non-treated plastic, highly suggestive of the fact that preventing substrate adherence increases the effect of BMOV

treatment. However In these experiments BMOV-sensitive KCNR cells were observed to increase FAK activation slightly following BMOV treatment in both substrate adherent and non-adherent conditions, suggesting that decreased FAK activation was not a determinant of cytotoxicity to BMOV. Levels of both activated and total SRC remained low in KCNR cells regardless of seeding surface. Thus preventing adequate substrate adhesion in SK-N-AS cells led to a profile of FAK/SRC expression and activation that closely resembled that of KCNR cells at basal levels, reducing protein expression and conferring sensitivity to BMOV-induced changes in activation.

We next sought to see if the observed changes in FAK/SRC expression correlated with changes in sensitivity to the cytotoxic effects of BMOV. Sub-G1 analysis was carried out following BMOV treatment of cells seeded onto both treated and non-treated surfaces. As expected SK-N-AS cells failed to undergo increases in the percentage of sub-G1 cells when seeded onto treated plastic, in contrast to KCNR cells that underwent significant cell death. However, modulating the substrate adherence by seeding onto non-treated plastic significantly increased the percentage of apoptotic SK-N-AS cells treated with BMOV (**Figure 4.8**). Importantly, untreated cells did not significantly undergo apoptosis although we did note a modest increase, arguing against the explanation that preventing adhesion simply reduces cell survival. Although KCNR cells did not further increase their sensitivity to BMOV, this may reflect the fact that the levels of FAK/SRC are already very low. Similarly the high rate of death seen in untreated KCNR cells seeded onto non-treated plastic may reflect their reduced capability to survive in suspension, where BMOV may mimic this process by inducing anoikis.

To briefly summarize, cells unresponsive to BMOV (SK-N-AS) express high levels of endogenous activated SRC and FAK compared with BMOV-sensitive cells (KCNR). Treatment with BMOV causes reductions in the levels of activated SRC in KCNR cells, which are mimicked in SK-N-AS cells when their substrate adherence is partially attenuated. This correlates with an increase in the sensitivity to BMOV induced-cytotoxicity. Thus we hypothesized that the ability of BMOV to induce cytotoxicity may be a direct result of its ability to decrease the level of activated SRC. Here high endogenous levels of activated SRC in SK-N-AS versus KCNR cells can explain resistance to BMOV. Thus we tested this hypothesis by conducting sub-G1

analysis on cells treated with BMOV in combination with the SRC inhibitor PP2, predicting that compound inhibition of SRC would augment BMOV induced-cytotoxicity owing to more effective inhibition. Furthermore PP2 should mimic the effects of BMOV, achieving increased cytotoxicity in KCNR cells compared with SK-N-AS cells.

Although KCNR cells exhibited increased sensitivity to the SRC inhibitor PP2, treatment alone failed to induce significant increases in cell death (**Figure 4.9, A**). Similarly compound treatment of KCNR cells failed to significantly increase cell death in KCNR cells compared with cells treated with BMOV alone. Although SK-N-AS cells were observed to significantly increase the number of sub-G1 cells following compound treatment with PP2/BMOV, despite not undergoing significant cell death with either inhibitor alone, this failed to mimic the levels seen in KCNR cells treated with BMOV and was also exhibited by the inactive PP2 analogue PP3 (**Figure 4.9, B**).

This evidence suggests that inhibition of SRC is not the primary determinant of BMOV induced-cytotoxicity, as inhibition of SRC did not recapitulate the effects of BMOV, nor did it significantly increase its efficacy. Nevertheless, with KCNR, we did observe a slight increase in cell death with both PP2 alone and PP2/BMOV treatment. It could be argued therefore that BMOV is already achieving near maximal inhibition of SRC, and remaining cell survival is largely through other mechanisms. Thus PP2 may not be able to greatly alter the biochemical response of

NBL cells in terms of the relative level of total to phosphorylated SRC. However, subsequent experiments demonstrated high variability and in some cases undetectable expression of activated SRC at endogenous levels, raising doubts over the initial hypothesis that SRC activation confers survival in NBL cells. We sort to further test this hypothesis, by examining whether overexpression of dominantly active SRC would attenuate BMOV-induced cell death, however we did not obtain any consistent effects in such experiments (data not shown). Thus taken together this data argues against SRC-inhibition being the primary determinant of BMOV-induced cytotoxicity

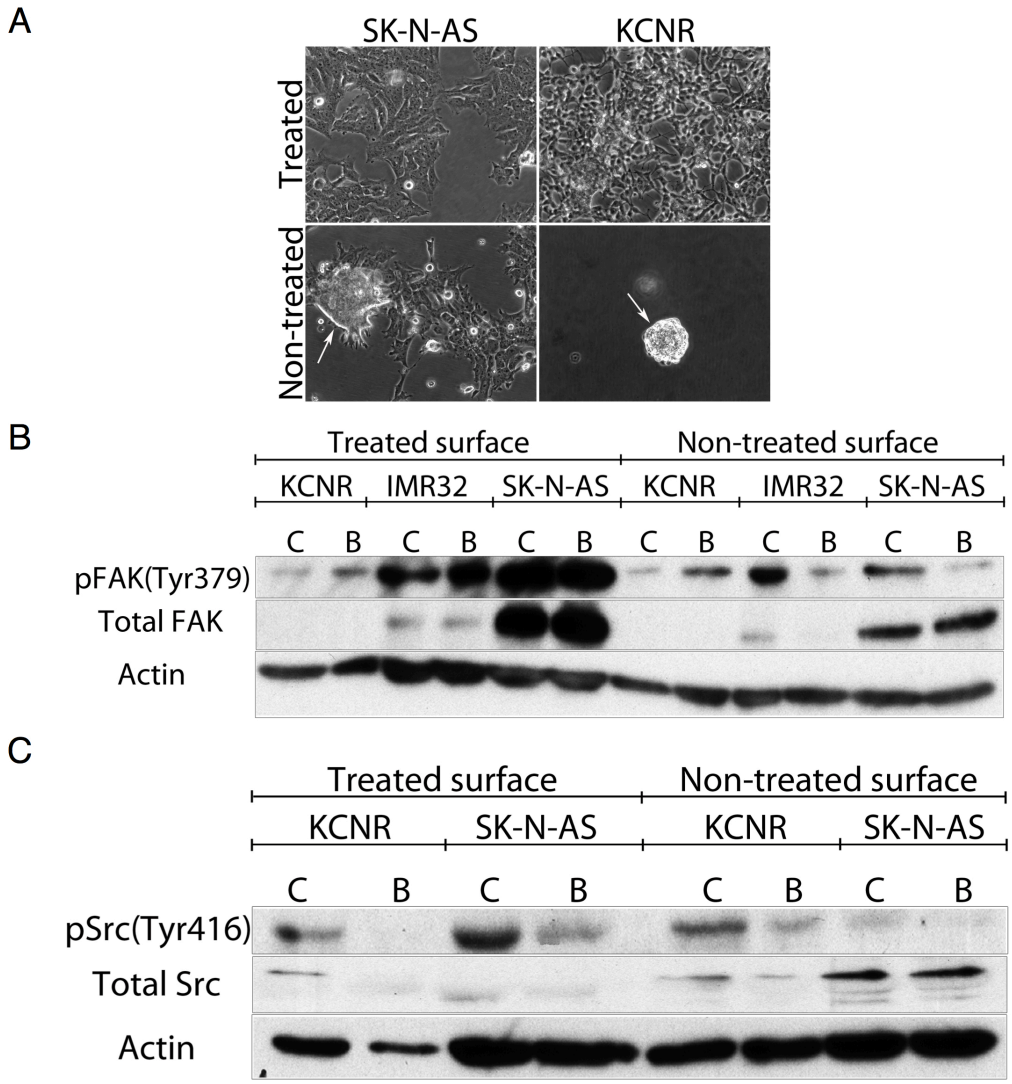

Figure 4.7. The effects of adhesion on the regulation of SRC/FAK by BMOV. Cells were cultured on tissue culture plastic suitable to facilitate adherence (treated) or normal plastic to prevent adhesion to the substratum (non-treated) (**A**). Loss of adhesion dramatically reduced the levels of both total and phosphorylated FAK protein and sensitised cells to the dephosphorylation of FAK induced by BMOV in SK-N-AS and IMR32 cells, but did not affect KCNR cells (**B**). BMOV caused a decrease in phosphorylated SRC, which was further augmented in SK-N-AS cells by the loss of adhesion (**C).**

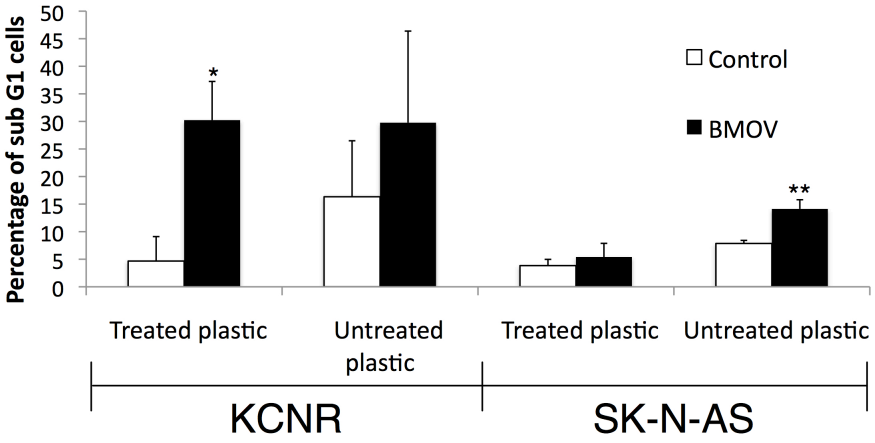

Figure 4.8. The effects of adhesion on sensitivity to BMOV. Cells were seeded onto treated and non-treated plastic and analysed for sub-G1 DNA content after 3 days of treatment with BMOV (10μM). The loss of adhesion following seeding onto untreated plastic in SK-N-AS cells significantly increased their sensitivity to BMOV. Mean and SEM of 3 independent experiments.

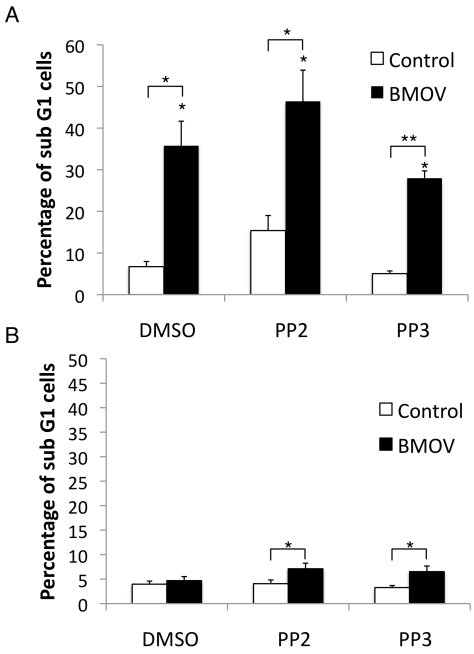

Figure 4.9. Treatment of KCNR (A) and SK-N-AS (B) cells with the SRC inhibitor failed to neither mimic the effects of BMOV nor significantly increase it effectiveness. Cells were treated for 3 days with BMOV (10μM) prior to sub-G1 analysis. Although PP2 (10μM) did cause cytotoxicity in KCNR cells and not SK-N-AS this did not obtain statistical significance in independent samples t-tests. Similarly PP2 increased the efficacy of BMOV but again this did not obtain significance (KCNR) or was also exhibited by the inactive analogue PP3 (10μM) (SK-N-AS). *= $p<0.05$; **=$p<0.005$. Graph shows means and SEM. Asterisk above bars represents condition versus DMSO control.

4.3.3. BMOV upregulates Mycn protein levels independently of the PI3K/Akt/mTOR signalling pathway

Amplification of Mycn, which occurs in approximately 22% of patients, is currently the only genetic marker allowing patient stratification in NBL, where high expression contributes to tumour progression, treatment failure and reduced likelihood of survival (Cohn and Tweddle, 2004; Schwab, 2004). Thus targeting Mycn to prevent tumour progression has been the subject of much research (Cohn and Tweddle, 2004). However as a transcription factor Mycn has often been regarded as undruggable. Thus efforts have instead focused on either targeting Mycn through its regulatory pathways or through its targets (Bell et al., 2010; Gustafson and Weiss, 2010).

Mycn protein is subject to multiple levels of regulation including, but not limited to, post-translational modification. Here growth factor signalling pathways positively regulate Mycn levels by preventing its degradation (Gustafson and Weiss, 2010). For example, PI3K has been shown to stabilize Mycn by blocking glycogen synthase kinase 3β (GSK3β)-mediated phosphorylation and increasing its levels *in vitro*, where inhibition of PI3K reduces Mycn levels (Chesler et al., 2006). Similarly mTOR downregulates protein-phosphatase 2A (PP2A) preventing dephosphorylation and ubiquitin targeting of MYCN and thus promoting its stabilisation, where inhibition of mTOR has been shown to downregulate Mycn protein expression and inhibits NBL growth both *in vitro* and *in vivo* (Johnsen et al., 2008).

We previously noted that Mycn protein expression was modestly increased by BMOV treatment in lines with Mycn amplification (See Chapter 3). Given that BMOV activates Akt, suggestive of PI3K stimulation, one might predict increased stabilization of Mycn. However we also noted that Mycn-amplified cell lines are particularly sensitive to BMOV (LAN-5, IMR-32, Kelly, KCNR) while we did not observe BMOV-induced cytotoxicity in any non-Mycn amplified cell lines. Thus we sought to characterize BMOV-induced upregulation of Mycn in terms of the responsible signalling changes and its role in BMOV-induced cell death.

In order to test the hypothesis that increased Mycn protein expression was due to increased activation of PI3K/Akt, we used the PI3K inhibitor LY294002 in combination with BMOV to test whether this would block changes in Mycn

expression. In line with earlier findings Mycn protein levels were observed to increase after BMOV treatment in three NBL cell lines that exhibit cytotoxicity in response to BMOV (LAN-5, Kelly, KCNR). However we observed similar increases in the presence of LY294002 (**Figure 4.10, A**) in both LAN-5 and Kelly cells although levels were slightly reduced in KCNR. Surprisingly, we observed a paradoxical increase in the levels of phosphorylated Akt (pAkt) after treatment with LY294002. Combination treatment of cells with both BMOV and LY294002 caused increases in pAkt in a dose dependent manner, causing dramatic increases at 20μM. Similarly LY294002 failed to block endogenous Akt activation and instead caused slight increases in pAkt (KCNR and Kelly). Although these counterintuitive effects of LY294002 precluded the test of our original hypothesis, this data does argue against increases in Mycn being the result of BMOV-induced stimulation of PI3K, given that Mycn levels did not increase despite large increases in the level of pAkt after combined BMOV/LY294002 treatment, and even decreased in some instances.

Thus in order to address this question further, we conducted a similar experiment with the second-generation dual PI3K/mTOR inhibitor PI-103, which has shown high efficacy and selectivity towards its targets at nanomolar concentrations (Fan et al., 2006). Treatment with PI-103 effectively abolished activation of both Akt and the mTOR target 4E-BP1, both in the presence and absence of BMOV. However despite this, increases in Mycn expression remained broadly similar in both pattern and level, increasing after BMOV treatment and remaining at untreated levels in PI-103-treated cells (**Figure 4.10, B**).

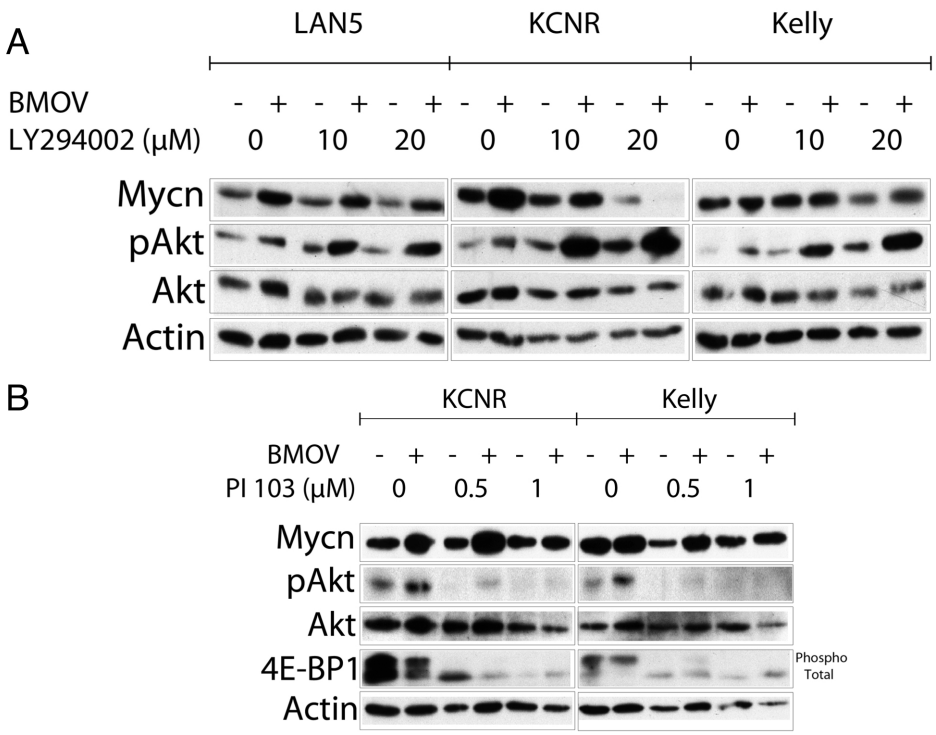

Figure 4.10. BMOV upregulates Mycn protein expression independently of PI3K and synergistically activates Akt in the presence of LY294002. **(A)** 24-hour BMOV (10μM) treatment causes an increase in Mycn in three NBL cell lines sensitive to its cytotoxic effects. Paradoxically, increased Akt activation is seen with increasing PI3K inhibitor LY294002 (10-20μM), paralleling decreasing MYCN levels. **(B)** BMOV induced-increases in Mycn occur in the absence of PI3K/mTOR activation, inhibited by constant treatment with the dual PI3K/mTOR inhibitor PI-103 (0.5-1μM). Akt and 4E-BP1 were used to assess activation of PI3K and mTOR respectively due to their status as downstream effectors.

The finding that LY294002 in combination with BMOV increases the levels of phosphorylated Akt beyond those seen with BMOV treatment alone raises a substantial paradox, given that LY294002 is a well-established inhibitor of PI3K. LY294002 is generally classified as a 'dirty' inhibitor due to its effects on other kinases independent of PI3K. The effectiveness of mTOR inhibitors such as rapamycin has been attributed to their propensity to inhibit activation of S6 kinase 1 (S6K1) downstream of mTOR (Zoncu et al., 2011), the phosphorylation and activation of which causes negative feedback signalling to PI3K dampening and thus regulating excessive output of the PI3K/Akt/mTOR pathway (O'Reilly et al., 2006). Thus we hypothesised that LY294002 may inhibit S6K1, which when coupled with the activation of PI3K/Akt by BMOV would remove negative feedback regulation resulting in increased activation. Thus we conducted immunoblotting towards

phosphorylated S6 ribosomal protein, which is directly phosphorylated by S6K1 as a means of examining S6K1 activation following treatment with BMOV both alone and in combination with LY294002. Indeed while BMOV alone was observed to activate S6K1, correlating with increased activation of Akt as expected (i.e. downstream of mTor), concurrent treatment with LY294002 effectively inhibited S6K1 activation to within control levels, which correlated with an increase in the activation of Akt (**Figure 4.11**).

Taken together these findings indicate that BMOV-induced upregulation of Mycn occurs independently of the PI3K/Akt/mTOR pathway, despite its activation by BMOV and its regulatory effect on Mycn levels in NBL cells. However this also presents an interesting paradox, namely that BMOV induced cell death occurs in the presence of heightened Mycn protein levels, as well as increased PI3K activity. Thus we hypothesized that rather than being an unrelated consequence of BMOV treatment, increased Mycn protein expression may actually be detrimental to cell survival. This is an appealing hypothesis given that only those NBL cell lines harbouring Mycn amplification are responsive to the cytotoxic effects of BMOV. This is also pertinent given that forced expression of Mycn can confer sensitivity to chemotherapeutics, although this phenomenon is only apparent in NBL cells lacking Mycn amplification (Hogarty, 2003). Lastly of note is the finding that combined treatment with BMOV/LY294002 paradoxically activates Akt to a greater extend than BMOV alone potentially due to the inhibition of S6K1, which represents a negative influence on PI3K activity downstream of Akt/mTOR. Given that LY294002 has been reported to exhibit very low affinity for S6K1 (Vlahos et al., 1994), one possibility is that this compound is achieving inhibition of the mTORC1 complex in a similar manner to rapamycin, thus still allowing phosphorylation of Akt at serine 473 by mTORC2. Here BMOV may act synergistically by attenuating inhibition of PI3K by LY294002, for instance activating Akt through inhibiting PTPs that negatively regulate its activity, or activating mTORC2 that would lead to phosphorylation of Akt independent of PI3K. This possibility remains to be tested however.

4.3.4. Mycn is not required for BMOV induced-cytotoxicity nor does it sensitize cells to BMOV

Mycn is thought to increase tumour aggressiveness by stimulating quiescent cells to re-enter the cell cycle, shortening cell cycle progression time and increasing detachment from the extracellular matrix (see section 1.2). However, paradoxically Mycn also has a role in the induction of apoptosis. For instance, conditional

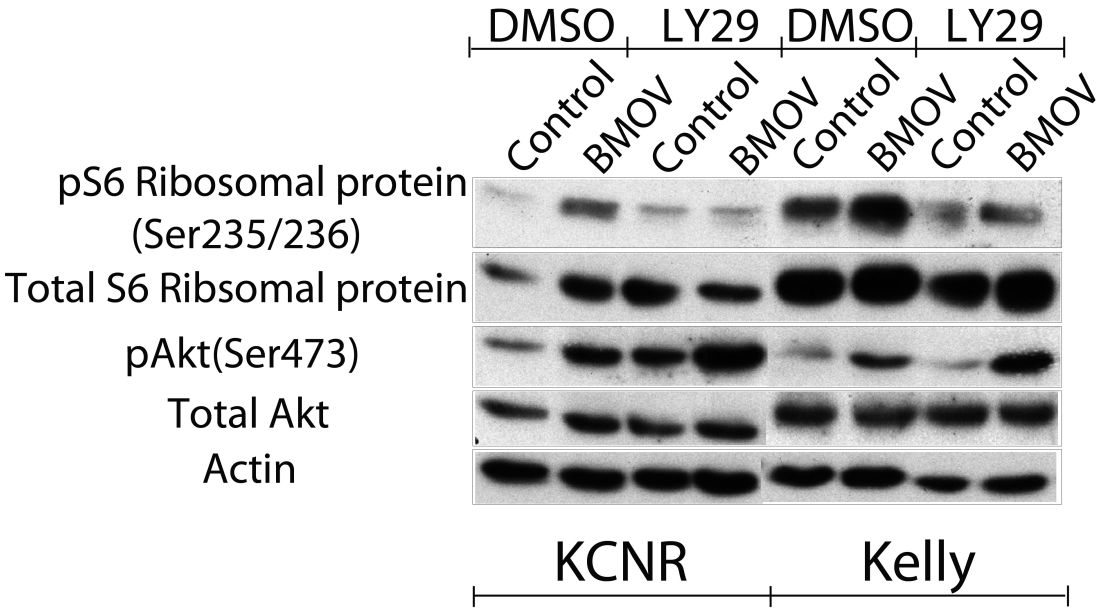

Figure 4.11. BMOV/LY294002 inhibits S6 kinase. Cells treated for 24hr with BMOV (10µM) and LY294002 (5µM). While BMOV activates S6 kinase alone (as shown by phosphorylation of its target S6 ribosomal protein), combined treatment with LY294002 inhibits this activation removing negative feedback of PI3K and thus correlating with increased Akt activation.

overexpression of Mycn in a non-Mycn amplified NBL cell line was shown to sensitize cells to chemotherapeutic-induced apoptosis (Fulda et al., 2000; Fulda et al., 1999). Similarly induction of Mycn expression by the p53 inhibitor Nutlin-3 was shown to enhance chemosensitivity (Peirce, 2009). Thus NBL cells with amplified Mycn may require aberrant PCD signalling in order to survive in the face of high-level Mycn expression (Hogarty, 2003).

Based on this evidence, we decided to test the hypothesis that BMOV-induced upregulation of Mycn sensitizes cells to its apoptotic effects. Thus we used the isogenic cell line SH-EP Tet21N (Tet21N), which has been engineered to conditionally express Mycn in the absence of tetracycline using the tet on/tet off system (Lutz et al., 1998). Indeed Tet21N cells appeared hypersensitive to BMOV

treatment specifically in the Tet-Off/Mycn+ condition, i.e. absence of tetracycline (**Figure 4.12, A**). Crucially BMOV had no visible effect on the survival of Tet21N cells in the Tet-On/Mycn- condition i.e. in the presence of tetracycline, nor did tetracycline itself display any effects on cell survival. Crystal violet staining for cell viability revealed a statistically significant decrease in cell survival following BMOV treatment only in the Mycn+ condition (**Figure 4.12, B**). However we failed to confirm the conditional suppression of Mycn expression by immunoblotting (**Figure 4.12, C**), thus suggesting that the protective effect of tetracycline does not result from its suppression of Mycn expression. Therefore although this represents another example of cell death induced by BMOV associated with the expression of MYCN, it does not provide evidence that increasing Mycn expression in this cell line sensitizes cells to BMOV induced apoptosis, as we failed to conditionally suppress Mycn expression.

To investigate this hypothesis further, we took advantage of an NBL cell line, ACN, that has been engineered to stably express Mycn at different levels using different plasmid expression vectors, namely ACN-0, expressing vector alone, ACN-5, expressing a vector encoding Mycn, and ACN-10, expressing a vector encoding Mycn at a greater level of expression. We confirmed the levels of Mycn protein expression by immunoblotting, however we failed to detect a difference between the levels of Mycn protein in ACN-5 and ACN-10 cells, but did detect increased expression of Mycn in both compared with ACN-0 (**Figure 4.13, A**). However, we observed minimal differences in sensitivity to BMOV between ACN-0, ACN-5 and ACN-10 cells (**Figure 4.13, B**). In fact all three isogenic versions of ACN responded to BMOV with significantly reduced cell survival, despite no detectable expression of Mycn in ACN-0 cells (**Figure 5.13, C**). This provides evidence against the hypothesis that an upregulation of Mycn protein level is required for BMOV induced-cytotoxicity, given that ACN cells without Mycn amplification are BMOV sensitive. However it does not exclude the possibility that BMOV can exert cytotoxicity via different mechanisms, one of which is through an upregulation of Mycn.

Thus we sought to further answer this question using isogenic SK-N-AS-nMycER cells, which have been engineered to stably express Mycn fused to an oestrogen responsive domain capable of binding to 4-OHT to stimulate Mycn activity

(Koppen et al., 2007). As earlier findings indicated that the non-Mycn-amplified SK-N-AS cells were unresponsive to BMOV (Section 4.3.1), SK-N-AS-nMycER cells are well suited to answer the question of whether increasing Mycn expression sensitizes NBL cells to BMOV. However, we did not detect differential sensitivity to BMOV following treatment with 4-OHT (**Figure 4.14, A, B**). We confirmed that treatment with low dose 4-OHT increased the levels of Mycn protein (**Figure 4.14, C**). This therefore again argues against the hypothesis that BMOV induced-cytotoxicity relies on Mycn, given that forced expression of Mycn in SK-N-AS cells did not confer sensitivity.

Lastly we sought to once again test the hypothesis that conditionally expressing Mycn in the Tet21N cell line would sensitize cells to BMOV using an alternative source of an identical cell line (a kind gift of Manfred Schwab, University of Heidelberg). Although in this case tetracycline treatment suppressed the expression of Mycn after 24 hours (**Figure 4.15, A**), we observed the opposite effect of BMOV on cell death when compared with the first Tet21N cell line, namely that conditional expression of Mycn appeared to exert a protective effect (**Figure 4.15, B**), reducing the degree of cell death.

In sum, we have shown that while upregulation of Mycn protein expression is a consequence of BMOV treatment that correlates with cytotoxicity, it is unlikely to be a causative factor. Although a version of Tet21N cells expressing Mycn was sensitive to BMOV, tetracycline appeared to suppress this effect independently of Mycn levels. Conversely an alternative Tet21N cell line responded to BMOV only in the presence of tetracycline and the absence of Mycn. Similarly SK-N-AS cells remained unresponsive to BMOV regardless of Mycn expression, and Mycn expression was not required for sensitivity to BMOV in the non-Mycn amplified cell line ACN. However one potential caveat of these experiments is the use of isogenic cell lines engineered to express Mycn though lacking in Mycn amplification. This situation may be entirely different than that of Mycn amplified cell lines, in which high Mycn levels likely result may result in Mycn addiction, as has been evidenced with other proto-oncogenes (Weinstein and Joe, 2008). In the same vein cytotoxicity due to enforced Mycn expression has been suggested to be p53-dependent, relying on a DNA damage response, which is not induced by BMOV (Petroni et al., 2011).

This means that while forced expression of Mycn may not necessarily enhance chemosensitivity, interference with correct regulation of Mycn protein expression may alter the ability of NBL cells to survive, although this remains to be proven.

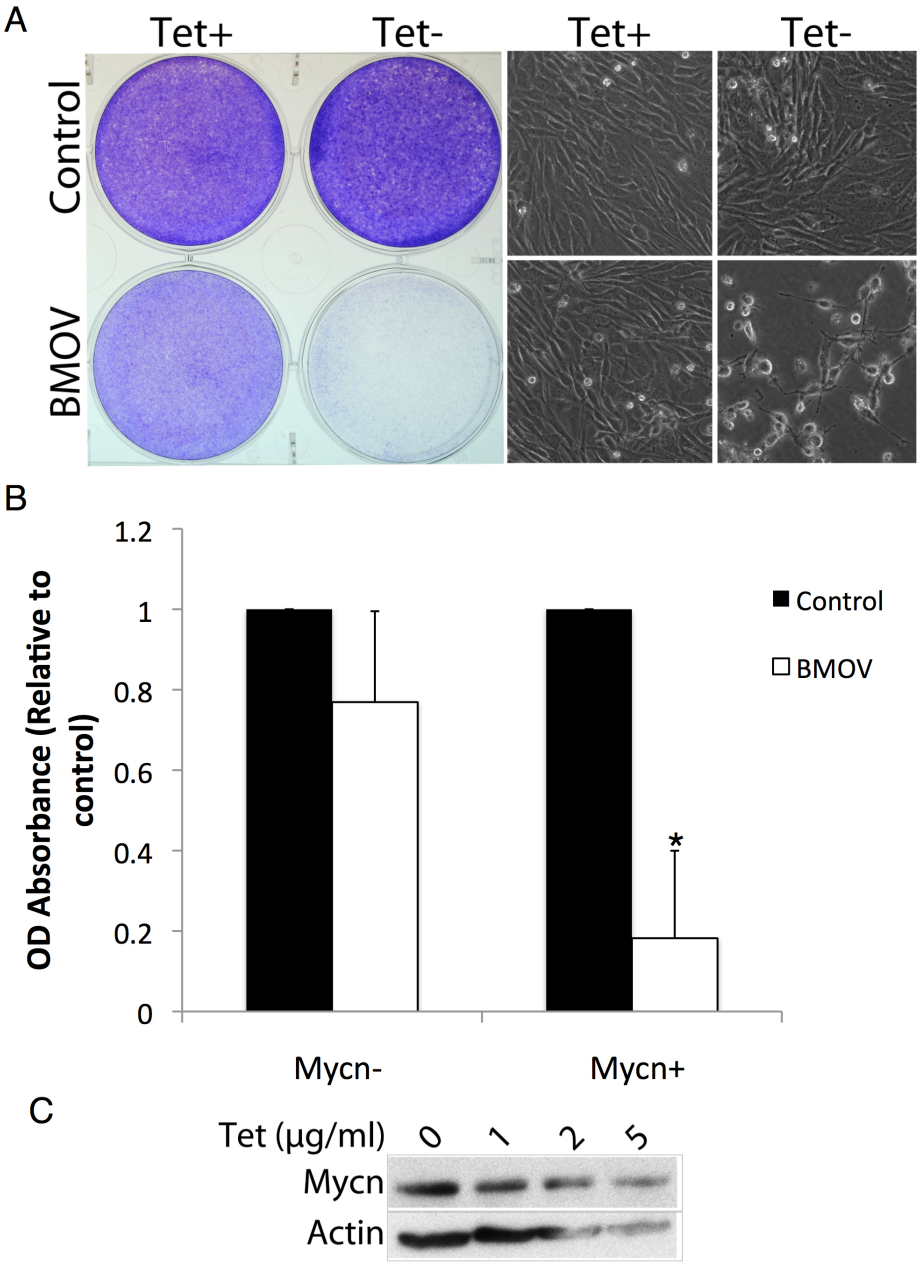

Figure 4.12. Tetracycline treatment enhances BMOV induced-cytotoxicity in the isogenic cell line Tet21N without inducing MYCN. (A) Crystal violet staining/phase contrast images of SH-EP Tet21N cells pretreated for 48 hours with tetracycline (2.5µg/ml) following 3 days of BMOV treatment (10µM) revealing gross reductions in cell survival in the Tet-Off/Mycn-On condition only. **(B)** Independent samples t-tests of OD absorbance following solubilisation of crystal violet staining of Tet21N cells treated with BMOV (10µM) for 3 days showing a statistically significant reduction in cell survival only in the Tet-Off/Mycn-On condition (*=$p<0.05$). Error bars denote standard deviation. **(C)** Immunoblot for Mycn demonstrating the presence of Mycn in the absence of tetracycline and a lack of increase in Mycn expression at increasing doses of tetracycline.

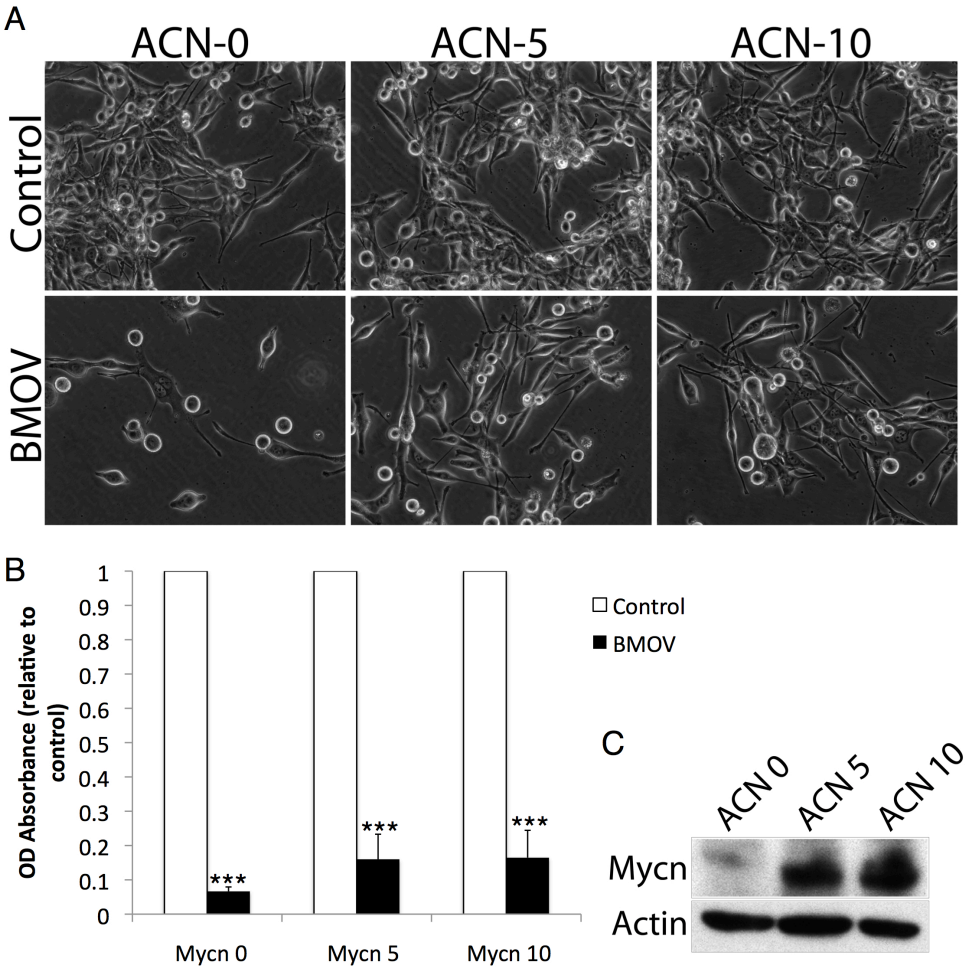

Figure 4.13. The non-Mycn-amplified cell line ACN is sensitive to BMOV, which is not enhanced by forced expression of Mycn. (A) Phase-contrast images of ACN cells treated for 3 days with BMOV (10µM) showing reductions in the number of viable cells independently of isogenic Mycn expression. **(B)** Following 3 days treatment, cells were crystal violet stained dye was solubilised to obtain a gross read out of the number of viable cells. Independent samples t-tests revealed BMOV (10µM) significantly reduced cell numbers in both Mycn expressing and non-expressing cells. (***=p<0.001). Error bars denote standard deviation. **(C)** Immunoblot for Mycn confirming increased protein expression in ACN-5/10 cells compared with ACN-0 expressing vector alone.

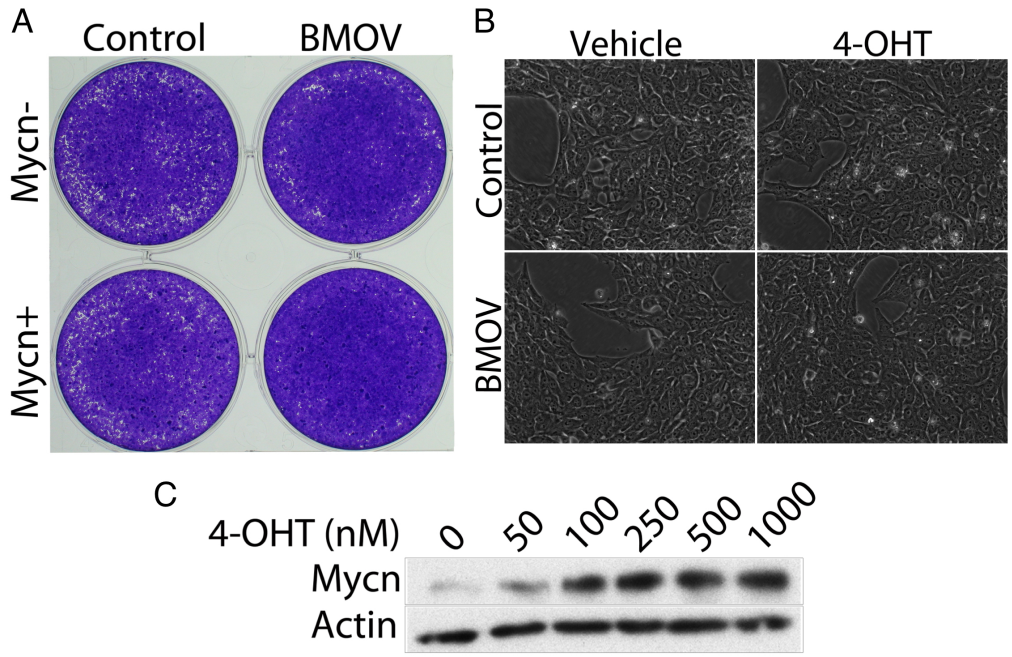

Figure 4.14. Forced expression of Mycn in an isogenic version of SK-N-AS cells does not cause sensitivity to BMOV. Crystal violet stained **(A)** and phase contrast **(B)** images of SK-N-AS nMycER cells treated for 3 days with BMOV (10μM) following 48 hours pre-treatment with 4-OHT (250nM) revealing an absence of cytotoxicity in either +/- Mycn conditions. **(C)** Immunoblot for Mycn confirming increases in protein expression following 48 hours treatment with 4-OHT in a dose-dependent manner.

4.3.5. BMOV-induced cell death is enhanced both by inhibition and augmentation of Akt activation

We previously found that BMOV was capable of activating both Akt and Erk as a single agent (See Chapter 3). Both of these signalling effectors are capable of inducing cell death or survival depending on multiple factors such as level and duration of stimulation, differentiation status and cell type. For instance, activation of Akt has been shown to induce cell death in the presence of heightened reactive oxygen species (ROS) production (Nogueira et al., 2008). Similarly inhibiting Akt as a means of targeted therapy has been shown to positively affect cell survival by relieving negative feedback of growth factor signalling (Chandarlapaty et al., 2011) and also inducing coping mechanisms such as autophagy (Fan et al., 2010). This is of particular interest given that the PI3K/Akt pathway is frequently mutated in human cancer and a commonly sought after target of therapy (Hennessy et al., 2005). This is also true of NBL, where Akt activity has been shown to contribute negatively to tumour progression (Opel et al., 2007). Inhibition of Akt has also been shown to

reduce tumour growth *in vitro* and *in vivo* (Li et al., 2010) and inhibition of PI3K has been shown to synergistically enhance existing chemotherapeutics (Bender et al., 2011).

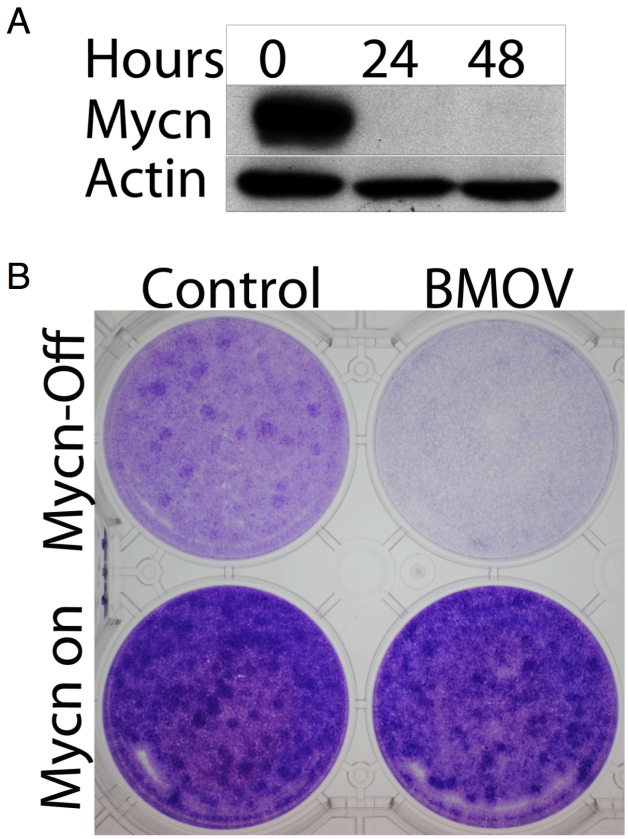

Figure 4.15. Conditional suppression of Mycn in Tet21N cells does not sensitize cells to BMOV. Tetracycline treatment (2µg/µl) causes suppression of Mycn levels after 24 hours (**A**), however in comparison to previously tested Tet21N cells (Figure 5.12), here BMOV induces cytotoxicity in the presence of tetracycline, which in this case is in the absence of Mycn, as shown by crystal violet staining of viable cells following 48 hours treatment (**B**).

Similarly Erk activation has been shown to mediate cell survival of neuronal cells (Scuteri et al., 2010) and cancer cells (Kim et al., 2005) as well as mediating resistance to chemotherapy (Balmanno et al., 2009). This is again not surprising given that Erk is commonly activated in human cancer via mutations in its upstream effectors Ras, MEK and RAF (Montagut and Settleman, 2009). However activation of Erk has been shown to cause cell death induced by chemotherapeutics such as the commonly used platinum based 'front line' agent cisplatin (Woessmann et al., 2002). This dichotomy of responses to Erk stimulation has been shown to depend on the

duration of activation (Marshall, 1995) due to differential interactions with downstream substrates (von Kriegsheim et al., 2009).

Given that BMOV causes cell death in the presence of activated Akt and Erk, we hypothesized that stimulating both of these enzymes in NBL cells reduces cell survival. Thus we tested this by using inhibitors of MEK/Erk (U0126) and PI3K/Akt (LY294002) and examining sub-G1 cells as a marker of apoptosis. First generation inhibitors have often been criticized due to off-target effects. Thus we used both U0126 and LY294002 at low doses (5µM versus 10-20µM standard dose), although the effects of LY294002 are of course complicated by the fact that it was previously found to paradoxically increase the activation of Akt in the presence of BMOV (See Section 5.3.3). Thus rather than inhibiting Akt, combined BMOV treatment actually results in its stimulation.

Low dose treatment with both LY294002 and U0126 had no visible cytotoxic effect alone, however remarkably we found that at the same dosage, compound treatment of both U0126 and LY294002 induced synergistic gains in cell death (**Figure 4.16, A**). This effect was less dramatic for U0126, which only caused modest gains in sub-G1 when compared to BMOV alone in both KCNR and LAN-5 cells, although significantly enhancing cell death when compared to untreated cells in LAN-5 despite a lack of response to BMOV. However LY294002 significantly enhanced the effects of BMOV alone in both cell types. We reasoned that given the similarity between the effects of the Ras/RAF/MEK/Erk and PI3K/Akt/mTOR pathway, redundancy might exist, causing compensatory survival signalling by Akt in the presence of inhibited Erk for instance (Balmanno et al., 2009). However combined treatment of U0126/LY294002/BMOV did not increase the effects of either inhibitor alone, suggesting a reliance on signalling through one of these pathways as a survival mechanism. Importantly compound treatment with U0126/LY294002 alone had no effect on cell death, arguing against the possibility that cell death caused by BMOV/LY294002 is simply the result of non-specific stress caused by multiple compound treatments. We confirmed the presence of biochemical inhibition of Erk (U0126) and activation of Akt (LY294002) following compound treatment with BMOV (**Figure 4.16, B**).

We next sought to examine whether interfering with the regulation of major growth factor signalling pathways in the presence of a cytotoxic stimuli (BMOV) was causing non-specific cell death. However sub-G1 analysis of cell death following treatment of primary wild-type MEFs revealed a complete absence of toxicity induced by combination BMOV/LY294002 or BMOV/U0126 treatment (**Figure 4.16, C**). This again argues against the notion that the combination of these compounds is simply exerting a battery of changes in intracellular signalling causing non-specific cell stress and cytotoxicity.

LY294002 increases the cytotoxicity of BMOV. However we initially sought to find out whether inhibiting Akt activation induced by BMOV would attenuate its cytotoxic potential. LY294002 was earlier shown to paradoxically augment Akt activation in the presence of BMOV, thus arguing in favour of this being a mechanism of BMOV induced cell death. However we wished to confirm this by answering the earlier question of whether inhibition of Akt could block the effects of BMOV. Thus we conducted similar experiments with PI-103, a dual PI3K/mTOR inhibitor that effectively inhibits PI3K at nanomolar concentrations (Fan et al., 2006). We found that treatment of KCNR cells with PI-103 caused a cytotoxic response as shown by an increased percentage of sub-G1 cells that was significantly augmented after combined treatment with BMOV (**Figure 4.17, A**), at doses that effectively inhibited Akt activation (**Figure 4.17, B**). Here increases in sub-G1 were additive, as both BMOV and PI-103 increased the percentage of sub-G1 cells to ~20%, whereas combined PI-103/BMOV treatment raised the percentage to ~50%. Similar to both LY294002 and U0126, combined treatment of cells with PI-103 and BMOV did not induce non-selective toxicity, as the levels of sub-G1 cells in MEFS were unaffected (**Figure 4.17, C**).

This presents a possible paradox in that both PI-103 and LY294002 cause similar increases in cell death in the presence of BMOV, despite having converse effects on the status of Akt signalling, blocking and stimulating it respectively. Thus we sought to examine whether an alternative compound that stimulated Akt would recapitulate the effects of BMOV/LY294002. Thus we conducted the same

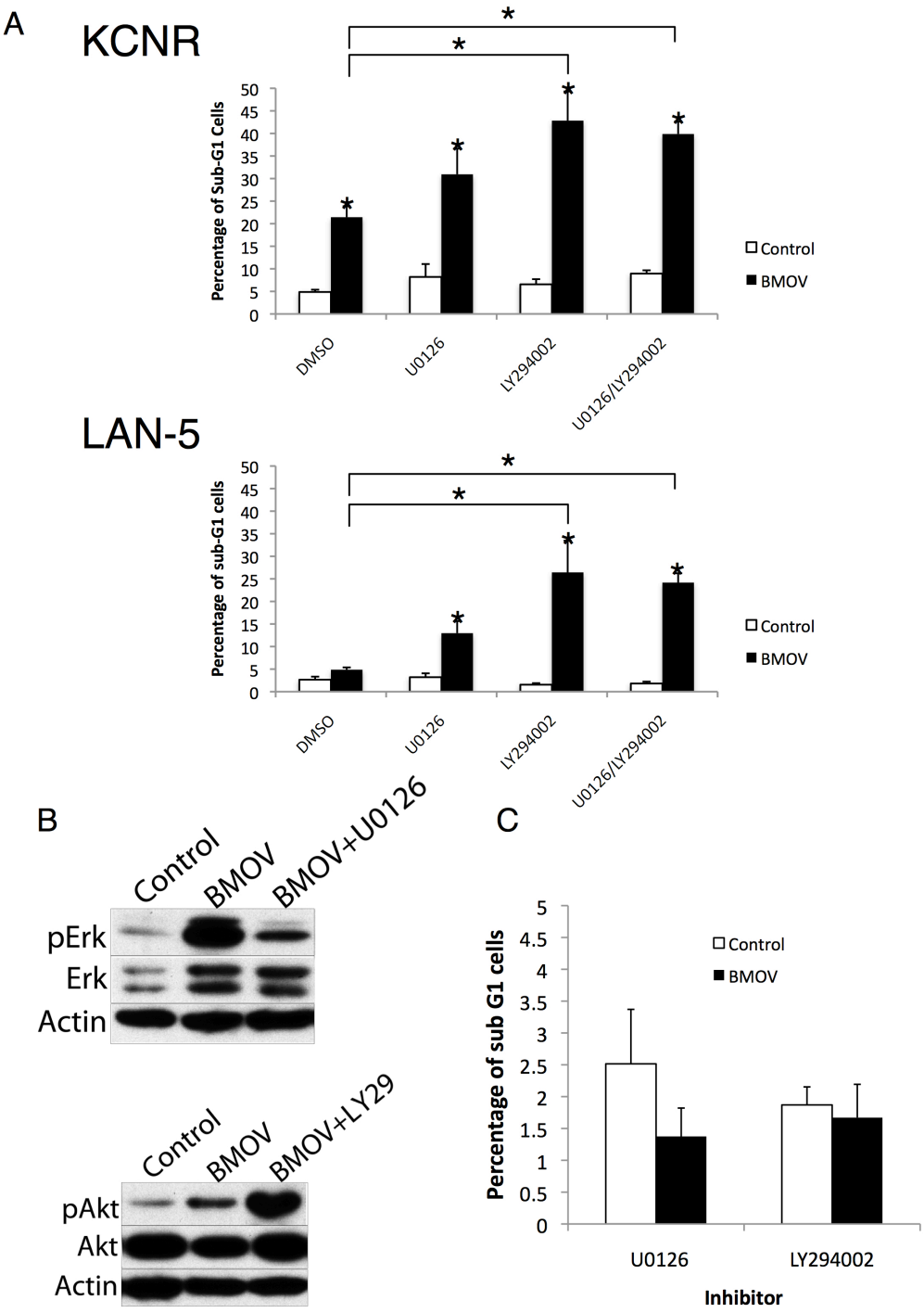

Figure 4.16. MEK inhibition and Akt stimulation enhance BMOV-induced cytotoxicity. (**A**) Sub G1 analysis of cells treated for 48 hours with BMOV (10µM), U0126 (5µM) and LY294002 (5µM) indicating both compounds increase the effects of BMOV on cell death. (**B**) Immunoblot of KCNR cells treated for 24 hours with BMOV, U0126 and LY294002 (LY29) indicating the U0126 inhibits BMOV-induced Erk activation while LY294002 augments BMOV-induced Akt activation. (**C**) Neither U0126 nor LY294002 in combination with BMOV cause toxicity to non-tumour control mouse embryonic fibroblasts as shown by sub G1 analysis.

experiment using the specific inhibitor of mTOR rapamycin. Rapamycin has been shown to increase the activation of Akt due to a lack of mTOR mediated-inhibition of S6 kinase 1, which itself inhibits PI3K in a negative feedback loop (O'Reilly et al., 2006), and has been used to augment Akt signalling in contexts where this may induce cytotoxicity (Nogueira et al., 2008).

In line with previous reports, rapamycin was not cytotoxic alone and did not cause a significant increase in the percentage of sub-G1 cells. However combined treatment with BMOV increased the effects of BMOV on the proportion of sub-G1 cells by ~15%, although this was not significant (**Figure 4.17, A**). However we observed that combined treatment of KCNR cells with BMOV and rapamycin actually caused very little change in the status of Akt phosphorylation at the given doses (**Figure 4.17, B**). This suggests that inhibition of mTOR in KCNR cells has a negligible effect on PI3K activation, and thus does not allow us to distinguish whether increases in Akt activation result in increased cell death in the presence of BMOV. Lastly while PI-103/BMOV caused large increases in cell death in NBL cells, treatment caused no observable toxicity in non-tumour cell MEFs (**Figure 4.17, C**).

In sum, we hypothesized that BMOV-induced activation of Akt and Erk may be the determinant of cell death; we have shown that prevention of this activation actually enhances the effectiveness of BMOV. However paradoxically we also found that stimulating Akt with a putative PI3K inhibitor similarly enhances the effectiveness of BMOV. This suggests two possibilities. Firstly activation of Erk and to a greater extent Akt may be an effective coping strategy that NBL cells employ in order to limit the cytotoxicity of BMOV, that when inhibited significantly attenuates resistance to cell death. This is evidenced by the fact that inhibiting both Erk and Akt using U0126 and PI-103 respectively increases cell death. However a second possibility is that aberrant signalling of growth stimulatory pathways caused by BMOV is responsible for BMOV induced cell death. This is arguably a more likely possibility given that both increasing and decreasing the levels of Akt stimulation using LY294002 and PI-103 respectively caused a similar increase in cell death. Thus inhibiting and activating Akt may cause cell death via opposing mechanisms, highlighting a need for finely tuned PI3K/Akt signalling for cell survival.

4.3.6. BMOV induced-cytotoxicity is abrogated by blocking the production of ROS and is augmented by attenuating ROS protection

ROS such as the superoxide anion, hydroxyl radicals and hydrogen peroxide are natural by-products of intracellular redox reactions that can induce cell stress through oxidative damage of lipids, proteins, carbohydrates and nucleic acids. ROS can also participate in intracellular signal transduction functioning as second messengers and cause enzymatic inhibition through nucleophilic attack of sulphydryl groups on cysteine residues (Davies, 1995). ROS have been shown to contribute to apoptosis triggered by chemotherapeutics in NBL (Marengo et al., 2005), and insensitivity to ROS is a putative mechanism of chemotherapeutic resistance in Mycn amplified NBL (de Tudela et al., 2010).

ROS are frequently responsible for regulation of growth factor signalling including activation of MAPK (Wu et al., 2009), activation of Akt (Crossthwaite et al., 2002), inhibition of FAK (Chiarugi et al., 2003) and inactivation of SRC (Tang et al., 2005), with various consequences including apoptosis and differentiation. PTPs are also major targets of ROS (den Hertog et al., 2005; Groen, 2005), contributing to inhibition through oxidation of their active site cysteine. Similarly vanadium based PTP inhibitors have been shown to generate ROS with this being a putative mechanism of action and a crucial factor in determining the sensitivity of cancer cells to vanadium-induced apoptosis (Wang et al., 2010; Zhang et al., 2003), although this may vary between vanadium-based compounds (Krejsa et al., 1997; Krejsa and Schieven, 1998).

Thus given their ability to cause apoptosis through oxidative stress, to regulate signalling of Akt/Erk/SRC, form as a consequence of PTP inhibition by vanadium compounds and themselves potently inhibit PTPs, ROS represent a highly relevant candidate for investigation into the molecular basis of cytotoxicity of BMOV. We first sought to determine the level of intracellular ROS following BMOV treatment in BMOV-sensitive NBL cells, using the fluorescence-based ROS dye DCFDA, which ultimately forms the highly fluorescent molecule DCF through oxidation by ROS, generating a fluorescent signal corresponding to the levels of intracellular ROS (Eruslanov and Kusmartsev, 2010) (see Figure 4.2).

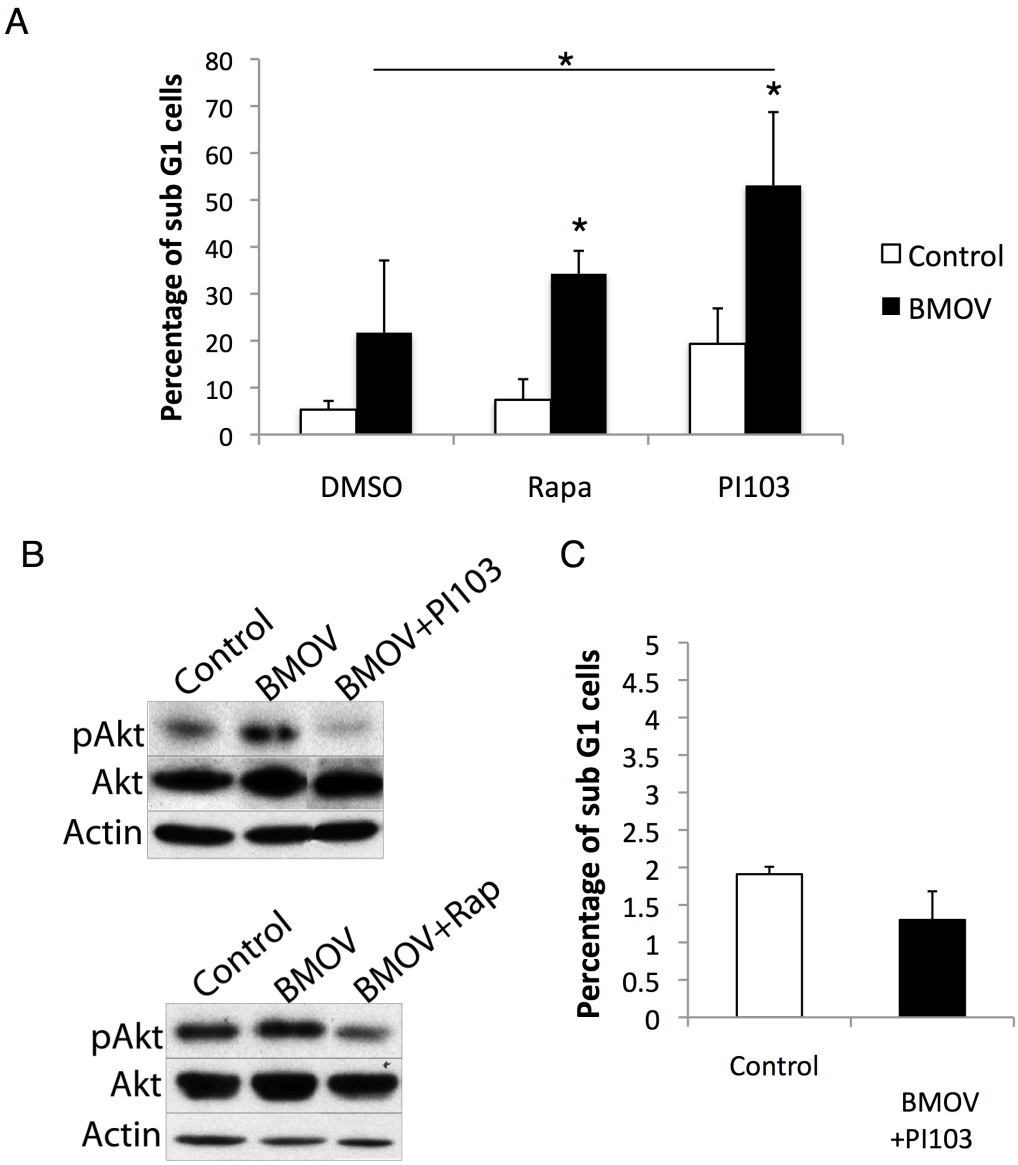

Figure 4.17. Inhibition of PI3K and mTOR enhance BMOV-induced cell death. (**A**) Sub-G1 analysis showing the effects of the PI3K/mTOR inhibitor PI-103 (500nM) and the mTOR inhibitor rapamycin (100nM) on KCNR cells, both of which increased BMOV-induced cell death. (**B**) Immunoblot of KCNR cells treated with BMOV and PI-103, which inhibits Akt phosphorylation, and Rapamycin (Rap) which failed to increase Akt phosphorylation. (**C**) PI-103/BMOV-induced toxicity is specific to NBL cells, as MEFs do not increase the levels of sub-G1 cells.

Short-term treatment with BMOV in Kelly cells was observed to cause modest increases (50%) in DCF signal intensity beyond untreated control cells at standard dosage capable of inducing cell death (10µM) while inducing greater changes with increasing dosage (200µM) more in line with that generated from a positive control treatment of pervanadate, which has been suggested to generate much higher levels

of ROS than BMOV through irreversible inactivation of PTPs (Krejsa et al., 1997) (**Figure 4.18**). However, figure 5.18 is just a representative example and in fact we noted very high variability in this assay, making statistical comparisons difficult. The laboratory has not yet been able to understand or control this variability. Furthermore given the high level of fluorescence in untreated control cells, changes induced by low dose BMOV may be too subtle for detection in this assay.

Thus we attempted identical experiments using an alternative fluorescent dye DHR 123, which has been suggested to exhibit greater sensitivity than DCF (Emmendörffer et al., 1990). Here BMOV treatment again induced modest (30%) but significant increases in fluorescence intensity beyond that of untreated control cells in both Kelly and SK-N-AS cells, despite the latter exhibiting little phenotypic response to BMOV (**Figure 4.19**). We previously observed a synergistic increase in BMOV-induced cytotoxicity with the PI3K inhibitor LY294002 (LY29), despite no evidence of PI3K inhibition when used in combination with BMOV (see section 5.3.5). Both LY29 and the inactive analogue LY303511 have been demonstrated to induce toxicity independent of the PI3K/Akt pathway by stimulating intracellular H_20_2, which in turn activates MAPKs leading to tumour necrosis factor (TNF)-related apoptosis-inducing ligand (TRAIL)-mediated cell death (Shenoy et al., 2009).

Thus we sought to examine whether LY29 was further increasing ROS following BMOV treatment, leading to enhanced cytotoxicity. Similarly we used in the same manner L-buthionine-*S,R*- sulfoximine (BSO), which depletes cells of the antioxidant glutathione by inhibiting an enzyme involved in its production by γ-glutamylcysteine synthetase. BSO would be expected to increase ROS (Marengo et al., 2008). Interestingly LY29 induced significant increases in ROS alone in Kelly cells, beyond that of BMOV (**Figure 4.19**). However while BSO did not induce statistically significant increases in ROS, contrary to previous reports (Marengo et al., 2008). Compound BSO/BMOV treatment did cause higher ROS levels than BMOV treatment alone, although this did not attain statistical significance (**Figure 4.19**).

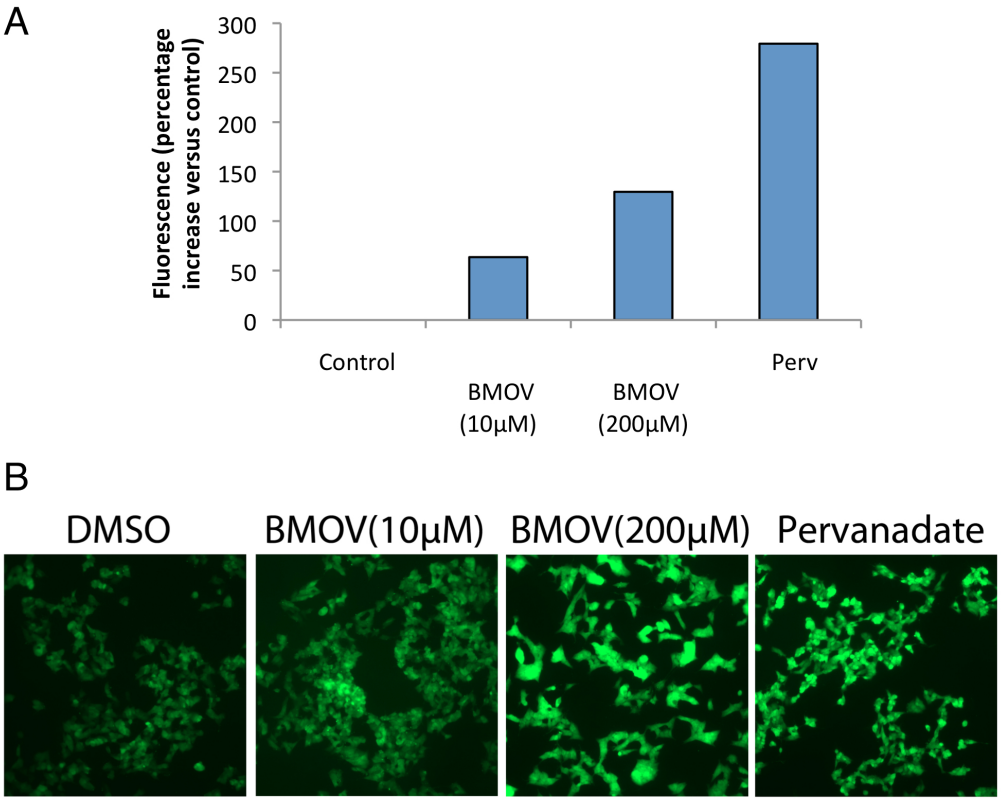

Figure 4.18. BMOV induces increases in ROS. Representative graph of DCF fluorescence signal normalized to untreated control cells (**A**) and microscopic (10x objective) images (**B**) of Kelly NBL cells treated for 2 hours with BMOV (10 and 200µM) or for 10 minutes with pervanadate (1mM) in one single experiment.

Given that antioxidant defence systems have been shown to positively maintain the survival of cancer cells, mediating therapeutic resistance (Denicola et al., 2011; Diehn et al., 2009; Raj et al., 2011), we sought to examine whether BMOV treatment alone or in combination with LY29 or BSO affected levels of ROS detoxification by examining relative amounts of GSH following treatment using the fluorescent GSH dye MCB. Indeed following 14 hours of treatment, a period of time that preceded cell death, all treatments were found to significantly reduce the levels of GSH relative to untreated control cells in both Kelly and SK-N-AS cells (**Figure 4.20**). While reductions in MCB signal intensity were low in cells treated with BMOV alone, combination treatment of BSO/BMOV caused much larger decreases, over and above that of BSO alone.

In order to determine whether increases in ROS production were responsible for BMOV induced-cytotoxicity, we conducted viability analysis of cells treated with

BMOV in the presence of the reducing agent NAC in order to block ROS production. BMOV was found to cause a 50% reduction in the number of viable LAN-5 cells after 6 days of treatment. However, compound treatment with low dose NAC almost completely abolished this reduction in viability, with BMOV treated cells returning to levels of vehicle treated control (**Figure 4.21, A**). This effect however did not extend to KCNR cells, in which treatment with NAC further increased the cytotoxicity of BMOV. During these initial studies we observed substantial toxicity at commonly used doses of NAC, precluding higher dose analysis. However, pH adjustment of NAC prior to its addition substantially reduced its own toxic effects in KCNR cells, allowing analysis of higher dose treatment. Here sub-G1 analysis using higher dose NAC revealed a near complete blockade of the cytotoxic effects of BMOV, where compound treatment significantly abolished BMOV induced increases in apoptotic cells (**Figure 4.21, B**). Similarly NAC treatment significantly decreased BMOV/LY29-induced cytotoxicity, although this did not fully return to the levels of untreated control cells (**Figure 4.21, C**).

The ability of the reducing agent NAC to abrogate the effects of BMOV on cell death is suggestive of a functional role for ROS in BMOV induced-cytotoxicity. Thus we sought to examine whether preventing protection from ROS would augment the effects of BMOV. Importantly glutathione has been found to be upregulated in tumour cells, where BSO has been shown to enhance the efficacy of multiple chemotherapeutics by increasing basal ROS levels in multiple tumours including NBL (Lewis-Wambi et al., 2008; Marengo et al., 2008). Sub-G1 analysis revealed that BSO significantly augmented BMOV-induced cytotoxicity in KCNR cells (**Figure 4.22 A**). This response occurred at doses of BSO far lower than commonly used, and ones that induced no visible toxicity alone. This suggests a synergism between BSO and BMOV. Importantly, compound treatment of primary wild-type MEFs failed to stimulate apoptosis, suggesting this sensitivity to enhanced ROS levels in the presence of BMOV/BSO is a feature of tumour cells as previously documented (Wang et al., 2010). Lastly we wished to examine whether GSH was indeed counteracting the effects of BMOV by performing a rescue experiment in which cells were treated with BMOV in the presence of GSH ethyl ester, in order to increase/prevent BMOV-induced decreases of GSH. Indeed the addition of GSH ethyl ester significantly

blocked BMOV-induced toxicity in KCNR cells, suggesting a causal role for inhibition of GSH synthesis.

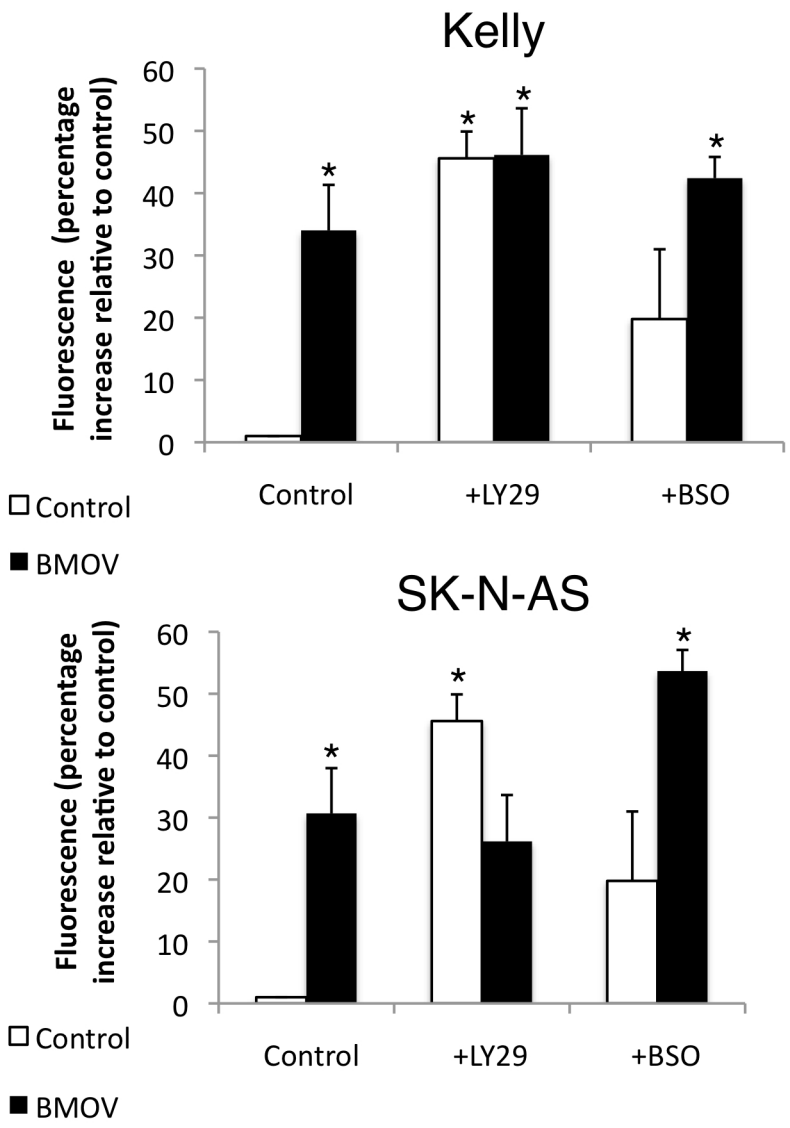

Figure 4.19. BMOV and LY29 cause significant increases in ROS. DHR fluorescence intensity normalized to untreated control cells following 4 hours treatment with BMOV (10µM), LY29 (5µM), or 4 hours following 24 hours pre-treatment with BSO (10µM). While BSO did not induce significant ROS production, combined treatment with BMOV did cause modest increases in ROS levels beyond BMOV alone. Mean from 3 independent experiments each with triplicate samples; Error bars denote SEM; independent samples t-tests.

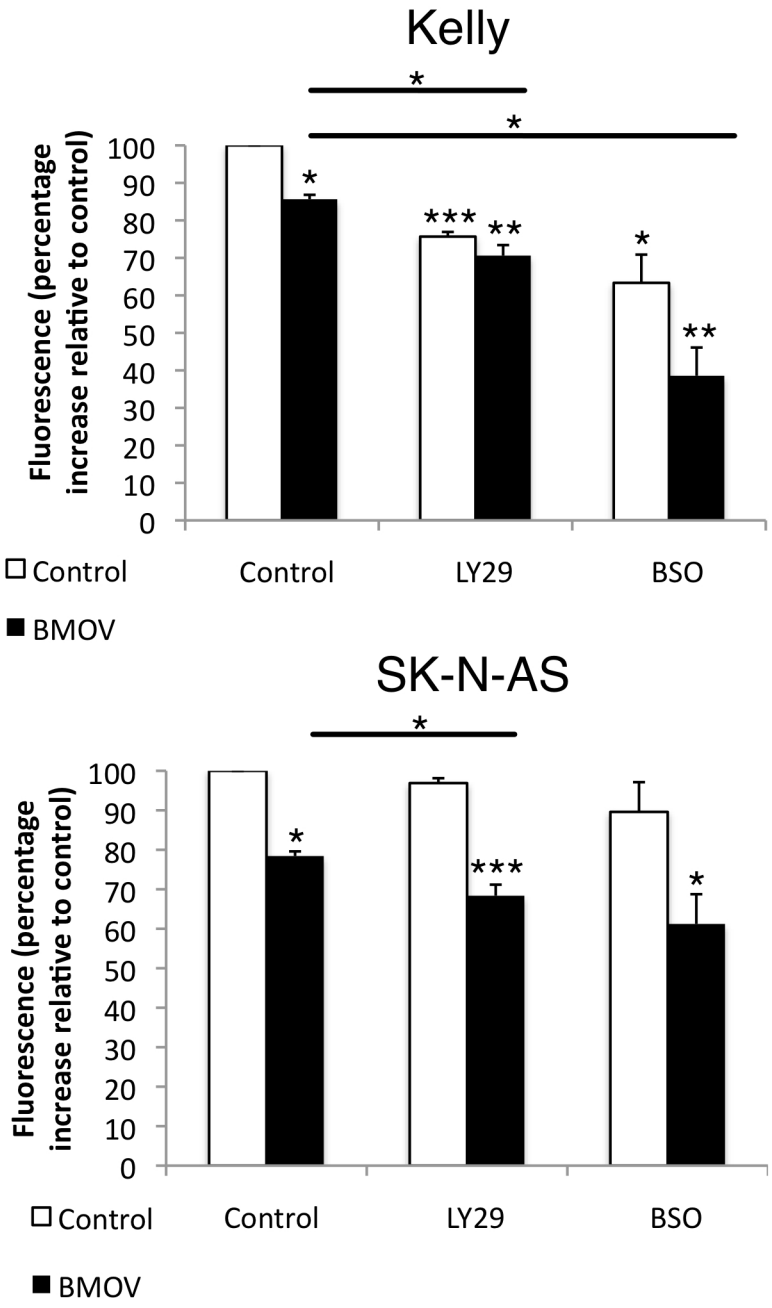

Figure 4.20. BMOV, LY29 and BSO cause reductions in the level of GSH as measured by decreases in fluorescence intensity of MCB. Cells treated for 14 hours with BMOV (10µM) and LY29 (5µM) or 14 hours following 12 hours pre-treatment with BSO. Mean signal intensity relative to untreated control cells from 5 independent experiments each containing 3 independent samples. Graphs show means and SEM with independent samples t-tests.

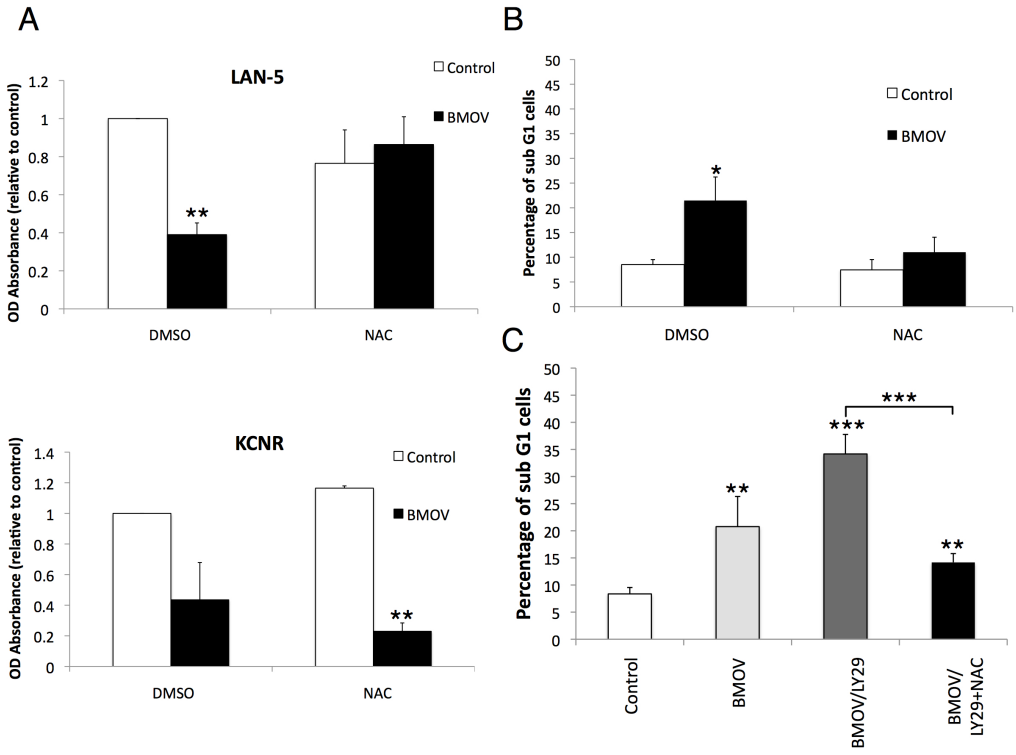

Figure 4.21. Preventing ROS production NAC attenuates BMOV-induced increases in apoptosis. (A) LAN-5 and KCNR cells treated for 6 and 3 days with BMOV (10µM) in the presence or absence of concurrent NAC treatment (100µM). Following crystal violet staining dye was solubilised to assess gross cell viability, showing attenuation of BMOV induced cytotoxicity by NAC in the case of LAN-5 only. **(B)** KCNR cells treated for 3 days with BMOV (10µM) in the presence or absence of concurrent NAC (5mM, pH 7.2) treatment were subjected to flow cytometry analysis of sub G1 content revealing a significant reduction in the cytotoxic effects of BMOV by NAC. (**C**) As (B) except for LY29 (5µM)/BMOV treatment.

In sum, BMOV is capable of causing increases in intracellular ROS as well as decreases in GSH. While these are modest and non-selective, i.e. occurring in unresponsive SK-N-AS cells, they appear at least partly causative in BMOV-induced cytotoxicity, since blocking ROS with the reducing agent NAC prevents increases in cell death. Furthermore, reducing ROS protection using the glutathione inhibitor BSO enhances the efficacy of BMOV, although this may be through preventing reduction of vanadate to vanadyl (see section 4.4). Lastly, synergistic increases in cell death caused by compound BMOV/LY2942002 treatment similarly appear ROS-dependent as they're significantly blocked by NAC and correlate with further decreases in GSH and increases in ROS.

4.3.7. BMOV causes additive reductions in cell survival in conjunction with PI3K/mTOR inhibition by preventing the induction of autophagy

Macroautophagy (autophagy) is a lysosomal degradation pathway for the breakdown of intracellular organelles and macromolecules. It functions predominantly as a survival pathway, recycling cellular components in periods of nutrient deprivation or stress, to maintain metabolic homeostasis. Autophagy has long been considered a 'double-edged sword' in cancer, due to its converse functions in promoting and suppressing cell survival (White and Dipaola, 2009). For instance, tumour cells capable of circumventing apoptosis can survive long periods of stress/deprivation by activating autophagy, in the absence of adequate nutrition and sustainable mitogenic signalling. However paradoxically autophagy defects such as loss of the essential gene *beclin1* are often observed in many cancers, and in contrast to its pro-survival functions, autophagy can cause autophagic cell death (Kroemer and Levine, 2008), thought to be an alternative form of PCD distinct to apoptosis (Bröker et al., 2005).

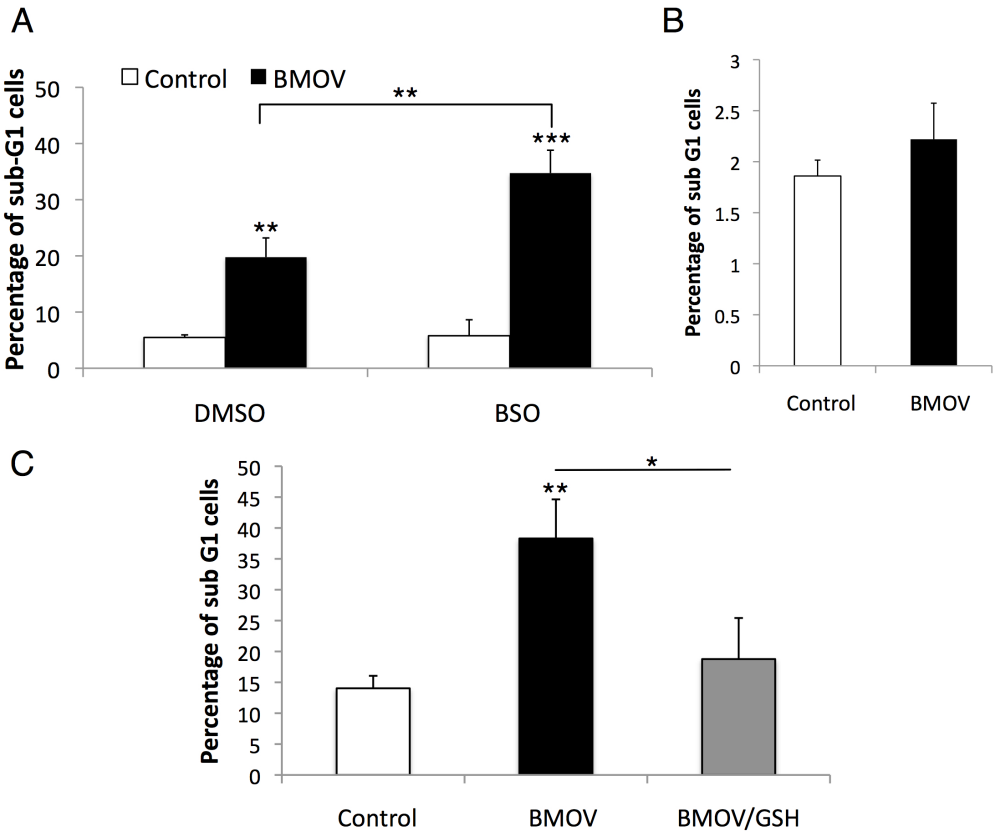

Figure 4.22. BMOV-induced toxicity in KCNR cells is augmented by inhibition of GSH synthesis. (**A**) Cells treated for 3 days with BMOV (10μM) or BMOV/BSO (10μM) and analysed fro sub-G1 content by flow cytometry. (**B**) BMOV/BSO treatment is non-toxic in non-tumour cell MEFs treated or the same period with BMOV/BSO (BMOV on graph). (**C**) BMOV-induced increases in sub-G1 KCNR cells are significantly blocked by the addition of GSH ethyl ester (2mM) (referred to in graph as GSH).

There have been a number of recent elegant demonstrations of this phenomenon. For instance, Yang *et al.* showed that pancreatic tumours rely on autophagy for survival, exhibiting high basal rates of autophagy which when inhibited using chloroquine, elevated ROS/DNA damage and growth suppression both *in vitro* and *in vivo* (Yang et al., 2011). Similarly expression of oncogenic Ras triggers autophagy, which when rendered defective causes mitochondrial damage and reduced oxygen consumption, suggesting autophagy maintains mitochondrial functionality required for survival under starvation (Guo et al., 2011). Conversely Elgendy *et al*. showed that the induction of autophagic proteins noxa and beclin-1 by oncogenic Ras actually triggers autophagic cell death independent of caspase activation (Elgendy et al., 2011). Indeed such Ras driven autophagic cell death has been demonstrated to be a feature of NBL tumours, and cited as a possible mechanism of spontaneous regression given that high Ras expression is actually a positive prognostic marker in NBL (Kitanaka et al., 2002).

Adding further confusion to the matter, Fan *et al.* recently showed that the inhibition of the PI3K/Akt/mTOR, which drives proliferation/survival in therapy-resistant glioma, actually promotes autophagy as a survival/coping mechanism (Fan et al., 2010). Here it was shown that the dual PI3K/mTOR inhibitor PI-103 as well as the mTOR inhibitor rapamycin caused the induction of autophagy, inhibitors of which caused apoptosis in a cooperative manner. Importantly chloroquine synergised with a novel PI3K inhibitor *in vivo* to cause tumour regression. While taken together these findings are paradoxical, i.e. one would predict autophagy to be activated by PI3K/Akt in order for cancer cells to survive unrelenting mitogenic signals in the face of sparse nutrition, this points to the possibility that autophagy may contribute to cell survival following inhibition of growth factor signalling, a common target of therapy.

We previously demonstrated additive increases in cell death when the dual PI3K/mTOR inhibitor PI-103 was used in combination with BMOV (section 4.3.5). However this again presented a paradox given that increasing Akt also led to synergistic cell death, possibly suggesting that an alternative mechanism i.e. one independent of canonical downstream PI3K/Akt targets, may be mediating these effects. Thus we hypothesised that PI-103 may in similarity to its effects on glioma

cells cause the induction of autophagy as a survival mechanism in the presence of inhibited PI3K/mTOR, which may be suppressed by BMOV due to its putative activation of various RTK-driven growth factor signalling pathways, leading to enhanced cell death. Thus we sought to examine the role of autophagy in this context.

Microtubule-associated protein 1A/1B-light chain 3 (LC3) is expressed diffusely throughout the cytoplasm. During autophagy, autophagosome engulfment causes conjugation of cytosolic LC3 (LC3-I) to PE, forming LC3-III and resulting in its autophagosome-membrane recruitment and punctate distribution (Mizushima et al., 2010). Thus the expression pattern of GFP-tagged LC3 is indicative of the activation of autophagy, i.e. due to transitioning from diffuse to punctate GFP localisation.

We first sought to examine whether PI-103 causes autophagy in U87 glioma cells as shown by punctate LC3, in line with recent reports (Fan et al., 2010). However we failed to detect any gross changes in the proportion of punctate GFP cells in PI-103 treated U87 cells transfected with GFP-LC3 (**Figure 4.23, A**). Increased punctate GFP was neither observed in BMOV treated cells nor cells treated with the alternative PI3K inhibitor LY294002, ruling out the explanation that PI-103 was actually suppressing autophagy. Similarly the NBL cell line Kelly also failed to show any evidence of increased punctate GFP in any treatment condition (**Figure 4.23B**), and neither cell type showed a degree of puncta that matched other reports e.g. Fan *et al.*

This suggests that autophagy may not be being activated in either glioma or NBL cells in response to PI3K inhibition. However given that this goes against recent reports, we sought to confirm this using an alternative method. Thus we used the green fluorescent dye acridine orange, which becomes protonated in response to lysosomal acidification, emitting a signal that can be preferentially detected at 588nm, i.e. increasing punctate red staining in the presence of autophagy (Mains and May, 1988). In contrast to LC3-GFP, acridine orange reliably detected the presence of autophagy in PI-103 treated U87 cells (data not shown), thus this method was used to test the original hypothesis that PI-103-induced autophagy may occur in NBL cells.

Indeed Kelly cells actually displayed high rates of basal autophagy, as shown by acridine orange staining, although this was not affected by PI3K inhibition using PI-103 or Akt-stimulation using LY29 (**Figure 4.24**). Remarkably BMOV treatment suppressed the induction of autophagy both in basal situations and in response to PI-103 treatment. However a significant caveat is that we failed to detect red staining following excitation with blue fluorescent light, which has been suggested to be specific for acidic organelles such as autophagosomes. Instead staining was detected by red emission following green excitation, which could be potentially indicative of RNA. However the punctate staining observed in the red channel, which exhibited greater signal intensity than diffuse red staining suggests that we may indeed be detecting acidic vesicles on this channel. The only other possible explanation for this pattern of staining is that acridine orange may in this case be detecting RNA stress granules, which have been shown to occur following transformation by an ALK fusion protein (Fawal et al., 2011), although this seems less likely.

As previously mentioned the staining of autophagic vesicles by acridine orange shown above may be artifactual, or may represent RNA granules. Furthermore acridine orange is considered by some to be insufficient evidence of autophagy given that this procedure stains acidic vesicles only, which include lysosomes as well as autophagosomes (Mizushima et al., 2010). Thus to retest the hypothesis that BMOV may suppress PI-103-mediated induction of autophagy by a different assay, we conducted immunoblotting for LC3. As previously mentioned during the formation of autophagosomes, LC3 becomes conjugated to PE to form LC3-II, which can be visualised as a distinct band that migrates slightly faster than LC3-I during SDS-PAGE due to its hydrophobicity. We were able to detect both forms of LC3 (I/II) by SDS-PAGE in untreated NBL cells. As hypothesised, treatment with PI-103 caused an induction of autophagy as shown by an increase in the level of LC3-II, as did a positive control of rapamycin, which should cause autophagy through inhibition of mTOR. Remarkably BMOV was able to suppress both rapamycin and PI-103-mediated increases in LC3-II, causing levels to return to that of untreated control cells (**Figure 4.25**).

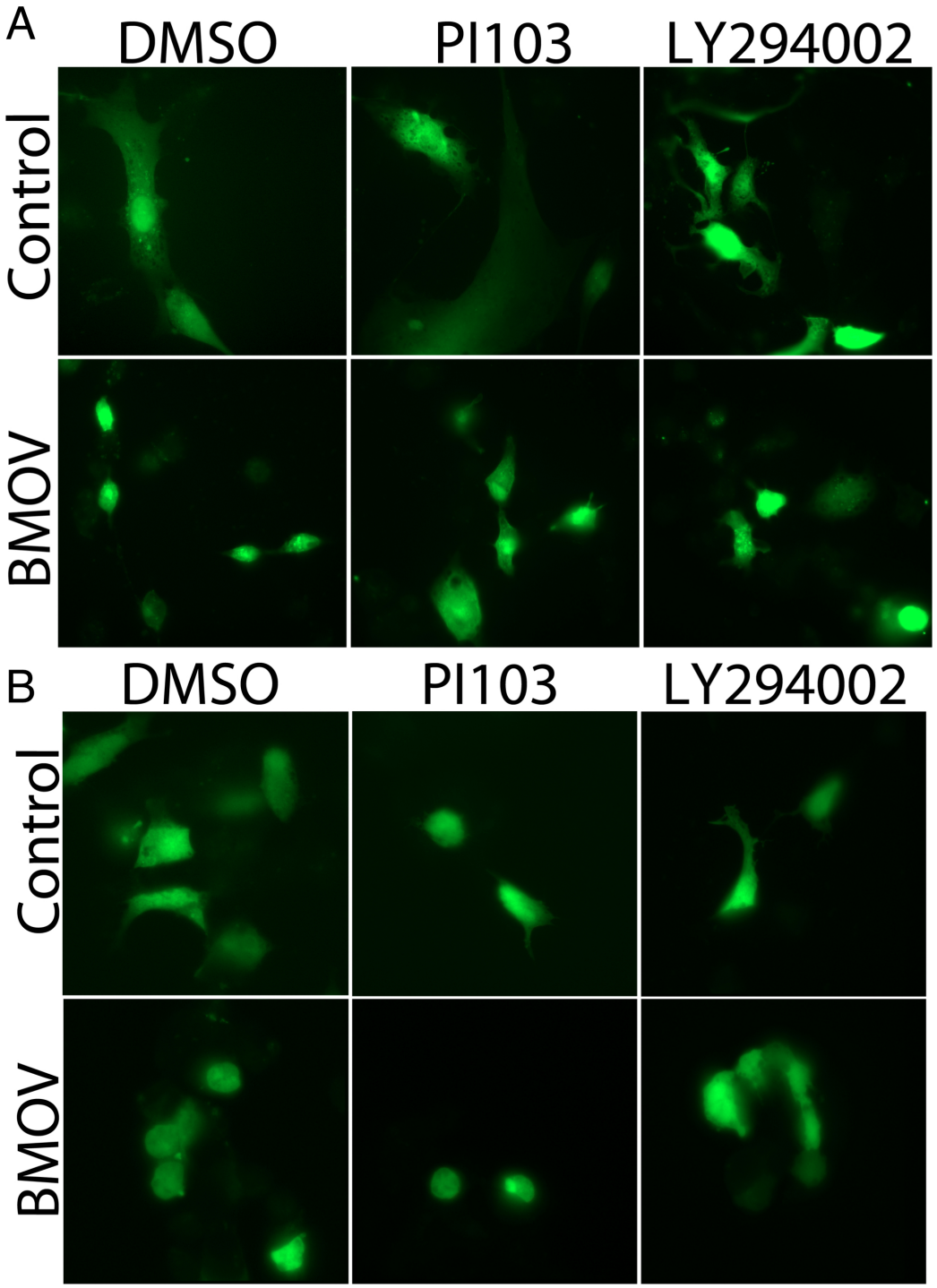

Figure 4.23. LC3-GFP revealing a lack of autophagy in both U87 glioma and Kelly neuroblastoma cells in response to PI3K/mTOR inhibition. Cells were transiently transfected with a GFP tagged LC3 expression vector 24 hours prior to inhibitor treatment, however, neither U87 (**A**) nor Kelly (**B**) cells exhibited punctate GFP expression after 72 hours of treatment with PI-103 (500nM), LY294002 (5μM) or BMOV (10μM). Magnification = 63x objective lens. B = 2x enlargement. DMSO = vehicle control.

Thus this provides tentative evidence that at least one mechanism by which BMOV may be enhancing the efficacy of PI-103 is by attenuating autophagy activated by PI3K/mTOR inhibition, and thus preventing autophagic cell survival by stimulating alternative growth factor signalling pathways e.g. RAF/MEK/Erk. This parallels similar findings in glioma (Fan et al., 2010).

4.3.8. The effects of BMOV on apoptosis appear independent of PTEN

We previously documented VA/BMOV mimetic effects of the specific PTEN inhibitor VO-OH Pic in terms of synergistically activating Erk and Akt signalling in combination with retinoic acid, as well as inducing neuritogenesis at micromolar ranges (See section 3.3.7). However given the lack of effect at nanomolar ranges, at which this inhibitor has previously been documented to specifically inhibit PTEN over other phosphatases (Alimonti et al., 2010b; Rosivatz et al., 2006), we were reluctant to conclude that PTEN is the primary determinant of the response of NBL cells to vanadium compounds.

Nevertheless, in order to falsify this hypothesis, we wished to examine the response of NBL cells that undergo cell death when treated with vanadium compounds to the PTEN inhibitor VO-OH Pic. Thus we tested its effects over short-term treatment periods on KCNR cells. Treatment of NBL cells with VO-OH Pic matched the effects of BMOV in inducing cytotoxicity at a similar concentration range (**Figure 4.26**). In fact VO-OH Pic was shown to induce broad and acute cell death at concentrations in which BMOV had little effect, as shown by cell morphology. However, crucially, VO-OH Pic failed to induce cell death at concentrations lower than 5μM, a ten fold higher dose than that used in previous publications, suggesting this effect may not be due to specific PTEN inhibition but more broad PTP inhibition by vanadate delivery and/or the production of ROS.

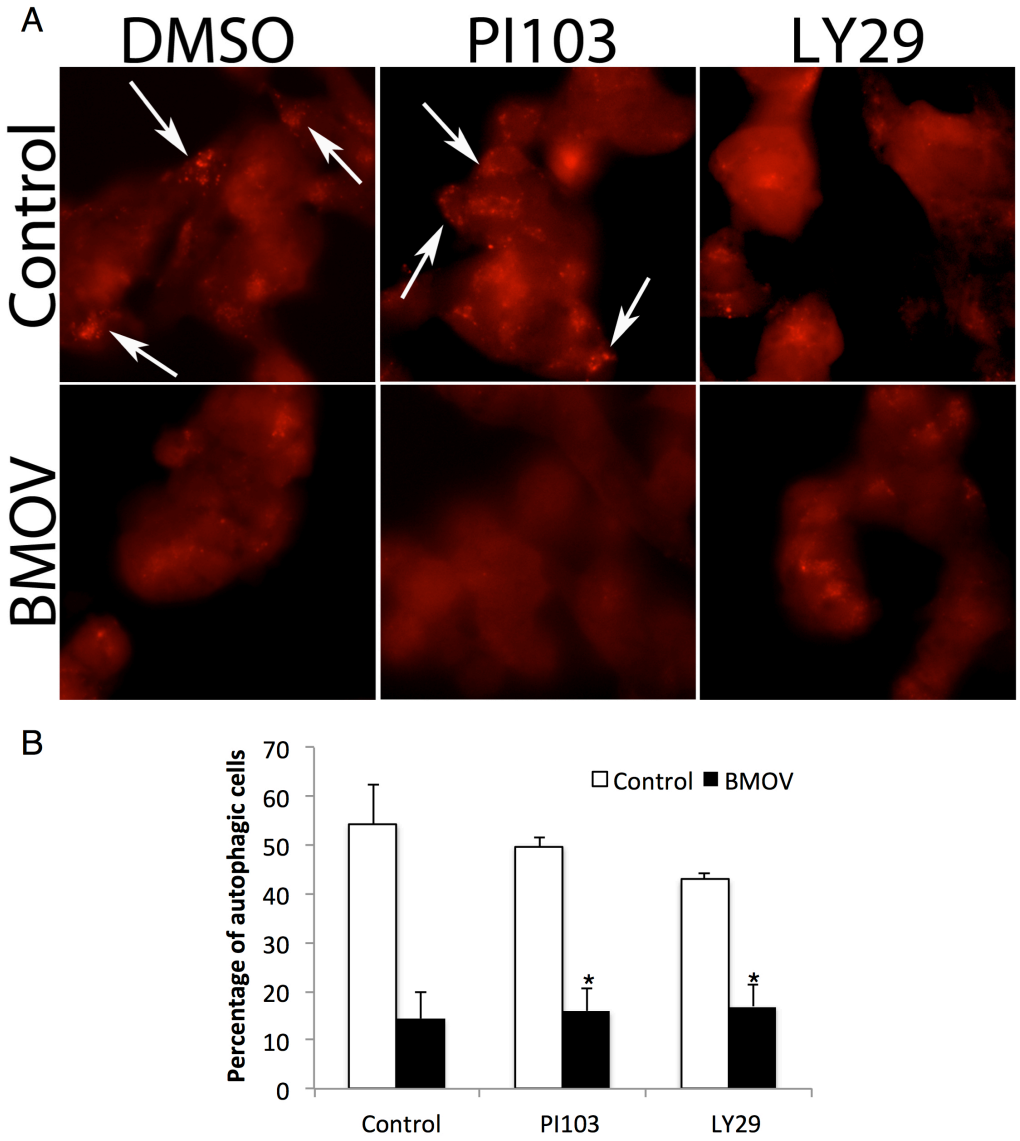

Figure 4.24. BMOV may suppress autophagy as shown by acridine orange staining. (A) Kelly NBL cells treated for 3 days with PI-103 (500nM) or LY29 (5µM) with and without BMOV (10µM), then stained with acridine orange (5µg/ml) for 15 minutes and photographed when excited with green light. Potential autophagosomes (arrows) were detected in all conditions but were significantly suppressed following BMOV treatment. 63x objective magnification. (**B**) Mean percentage of autophagosome-containing cells, as judged by the presence of at least 10 red puncta (white arrows in A). Error bars denote SEM (N=2).

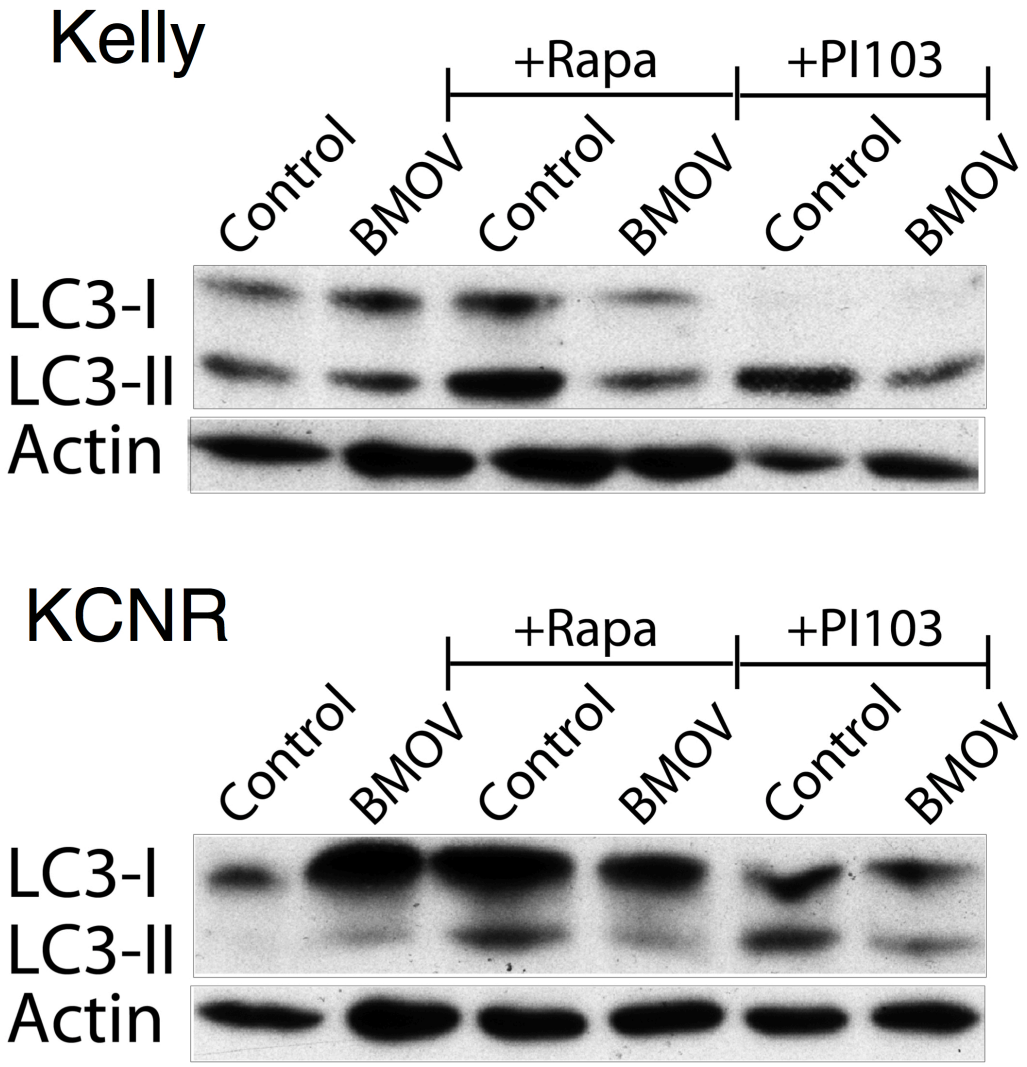

Figure 4.25. BMOV inhibits PI-103/Rapamycin-induced increases in LC3-II. The Induction of LC3-II indicative of autophagy can be visualised as a distinct band below LC3-I. 15-hour treatment with both PI-103 (1μM) and rapamycin (200nM) caused significant increases in LC3-II, which were completely blocked by concomitant treatment with BMOV in both Kelly (**A**) and KCNR (**B**) cells. Note that PI-103 also decreases LC3-I, which is not abrogated by BMOV, however it is unknown whether restoration of LC3-I is required to suppress autophagy.

We previously demonstrated a synergistic induction of cell death in NBL cells treated with BMOV following depletion of GSH using BSO (See section 4.3.6), despite minimal evidence of increased ROS following compound BSO/BMOV treatment. To further explore the possibility that inhibition of PTEN may be a determinant of the cytotoxic response of NBL cells to BMOV, we examined whether PTEN inactivation by oxidation may account for the combined effects of BMOV/BSO. As previously discussed, oxidation of the PTP active-site cysteine (Cys) is a major mechanism by

which PTPs are physiologically inhibited by ROS (See section 1.4). PTEN itself has been shown to be subject to reversible oxidation. For instance, Lee *et al.* demonstrated that hydrogen peroxide (H_2O_2) treatment of PTEN *in vitro* caused inactivation via oxidation due to cross-linking between the conserved active site Cys^{124} with Cys^{71} (Lee, 2002), a process that is negatively regulated by thioredoxin. More importantly GSH was recently shown to negatively regulate PTEN oxidation by directly reducing oxidised PTEN in mammalian cells (Kim et al., 2010). Here genetic knockdown of the catalytic subunit of glutamate cysteine ligase (GCL_c), a rate-limiting enzyme in GSH synthesis, increased oxidation of PTEN and phosphorylation of Akt following growth factor stimulation.

Thus we reasoned that given the evidence that BMOV is capable of stimulating growth factor-receptor driven signalling pathways (e.g. PI3K/Akt) most likely by PTP inhibition, combined treatment with BSO may augment this effect by preventing the reduction and thus activation of PTEN, contributing to its inhibition and thus further boosting PI3K/Akt signalling. Crucially this would predict that, A) BSO treatment causes the inactivation of PTEN, which could be further inhibited by BMOV treatment explaining the cytotoxicity of BSO/BMOV, B) BSO-induced PTEN inactivation augments BMOV driven PI3K/Akt activation, which may also contribute towards cell death if PTEN inhibition/Akt activation is causatively linked to BMOV induced toxicity.

In order to examine oxidation of PTEN in the presence of BSO, we conducted immunoblotting for PTEN under non-reducing conditions, which have been shown to identify both oxidised and reduced forms of PTEN due to their different migrational speeds during SDS-PAGE (Lee, 2002). BSO treatment of two NBL PTEN-expressing cell lines (KCNR/SK-N-SH) (see section 3.3.7) failed to cause PTEN oxidation as evidence by immunoblotting (**Figure 4.27, A**). Here only the reduced form of PTEN was detected. We also failed to detect oxidised PTEN following BMOV treatment, as well as combined BMOV/BSO treatment, suggesting that despite increasing ROS/decreasing antioxidant defences, neither compound was able to oxidise and inactivate PTEN. Importantly the detection of oxidised PTEN was verified using Hydrogen peroxide. Thus this suggests that augmentation of BMOV-induced cell death by BSO does not result from concomitant inactivation/inhibition of PTEN.

We next sought to examine whether BMOV/BSO treatment caused activation of PI3K/Akt. Immunoblotting for phosphorylated Akt also did not provide evidence for further significant activation of Akt induced by BMOV after combination treatment with BSO (**Figure 4.27, B**). Thus this provides further evidence that BSO treatment of NBL cells does not cause inactivation of PTEN, as this would most likely result in attenuation of PI3K/Akt suppression by PTEN and thus increased Akt activation in cells treated with BSO both alone and with BMOV. This also shows that the greatly enhanced cytotoxic effect of BSO/BMOV treatment is not the result of enhanced Akt stimulation.

In sum this data provides little evidence for the involvement of PTEN in the cytotoxic response of NBL cells to vanadium compound treatment. Although the PTEN inhibitor VO-OH Pic was able to induce cytotoxicity, this effect failed to extend to nanomolar doses. Of course this may reflect the wild type PTEN status of NBL cells, given the lack of evidence for genetic mutations/deletions in PTEN, as VO-OH Pic has been suggested to only induce cell senescence in cells harbouring hemizygous deletions of PTEN (Alimonti et al., 2010b), but NBL cell lines expressing low levels of PTEN (e.g. SK-N-AS/SK-N-DZ) were found to be unresponsive to either BMOV or VO-OH Pic treatment (data not shown). Similarly it has been argued that due to its hydroxypicolinic acid scaffolding, VO-OH Pic achieves selective inhibition by specifically binding to the wide active site cleft of PTEN, in contrast to BMOV that has been shown to deliver vanadate to the active site of generic PTPs (Mak et al., 2010). However it is difficult to conceive that NBL cells require a ten fold higher dose of VO-OH Pic to achieve PTEN inhibition at similar efficacy to other mammalian cells such as adipocytes/fibroblasts, as well as prostate cancer cells, which have all been shown to be subject to PTEN inhibition after 500nM VO-OH Pic treatment. It has been argued that VO-OH Pic would still selectively target PTEN at higher doses (R. Woscholski, personal communication), however it cannot be dismissed that here VO-OH Pic may simply also degenerate into vanadate and thus non-selectively inhibit PTPs. Thus in sum, PTEN does not appear to be the primary determinant of BMOV-induced cell death.

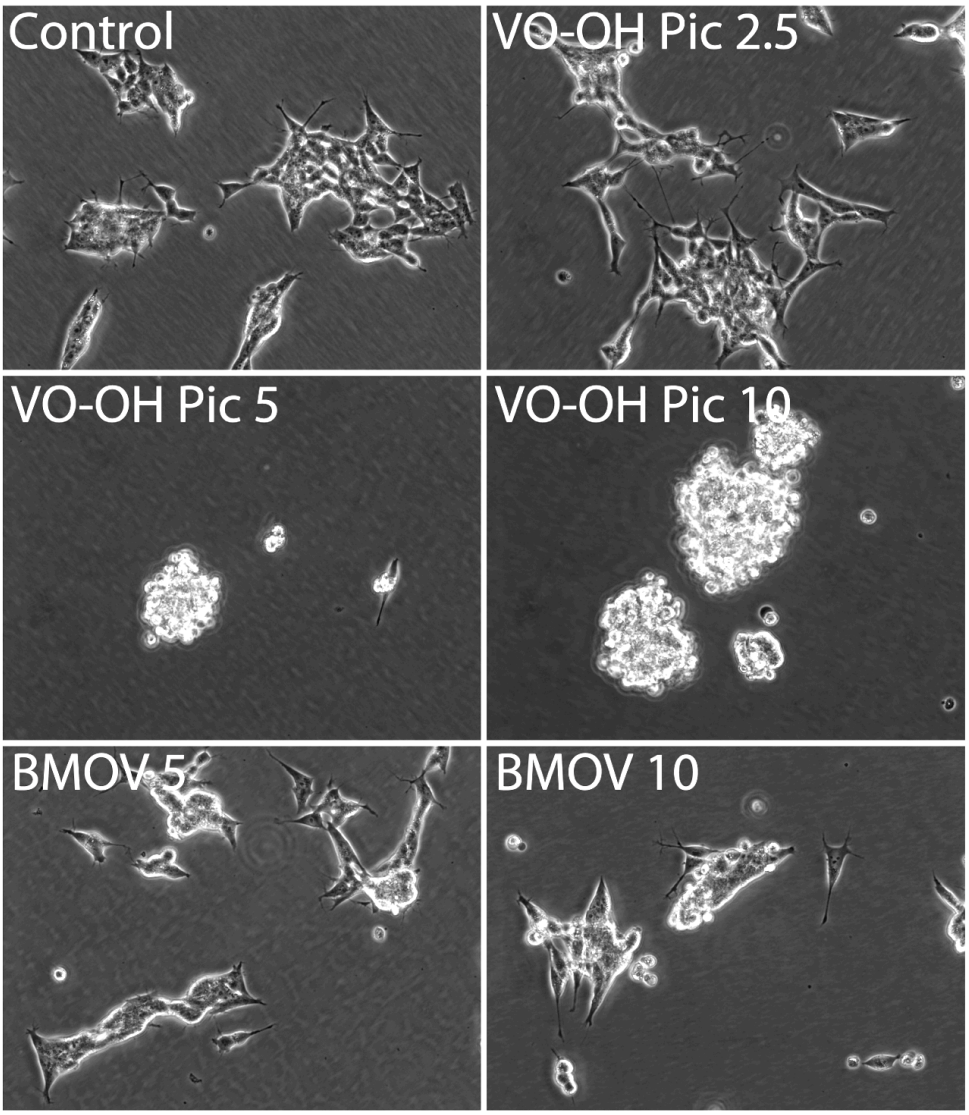

Figure 4.26. The PTEN inhibitor VO-OH Pic induces cytotoxicity similar to BMOV, but only above 2.5µM. KCNR cells were treated for 48 hours with various doses of the organovanadium compound BMOV and the selective PTEN inhibitor VO-OH Pic and cell death was analysed by grossly comparing morphology to that of untreated control cells. VO-OH PIC induced cytotoxicity more effectively than BMOV at a two fold lower dosage, however this effect failed to extend to the nanomolar dosages at which this inhibitor is commonly used. Magnification = 32x objective lens.

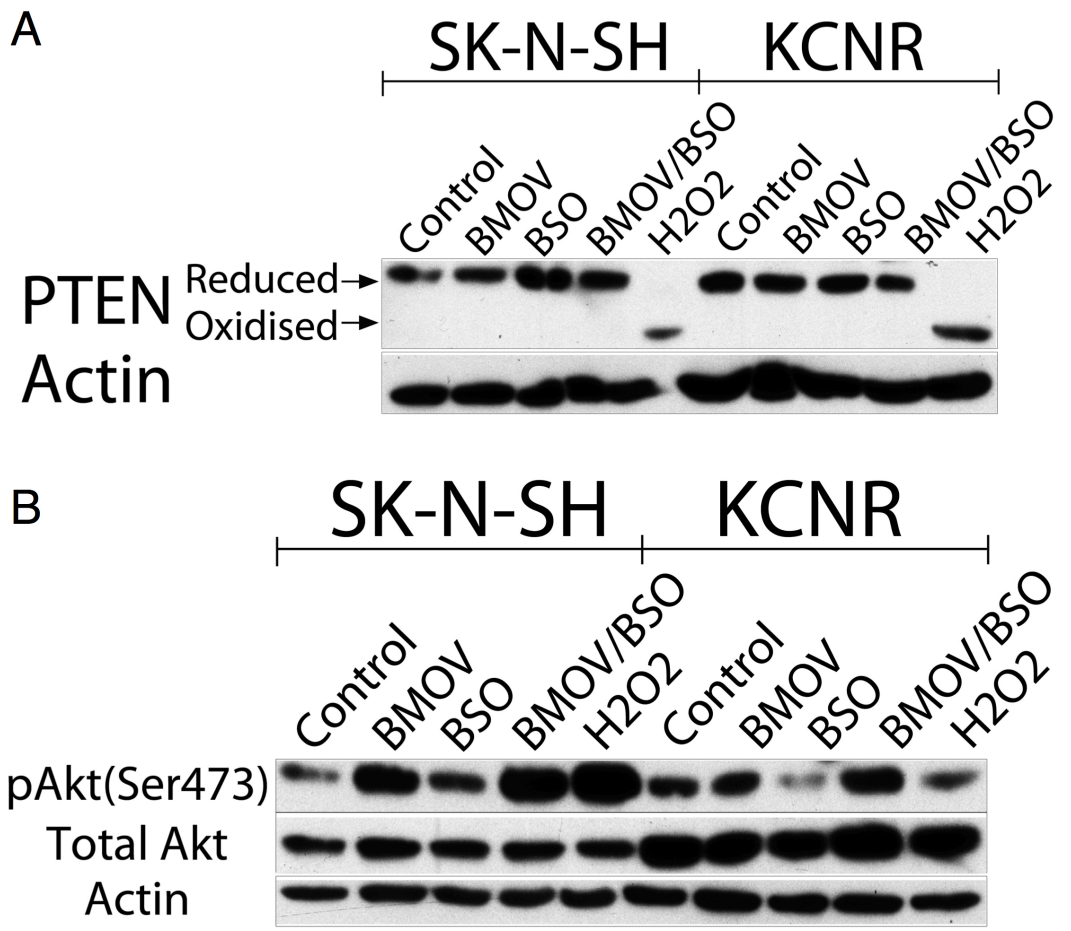

Figure 4.27. BSO treatment fails to neither inactivate PTEN by oxidation nor increase Akt stimulation. (**A**) Immunoblotting under non-reducing conditions reveals the presence of a lower band indicative of the oxidised form of PTEN following 5-minute stimulation with H_2O_2 (2mM) but not after 24-hour stimulation with either BMOV (10µM) or BSO (10µM) alone or in combination in PTEN expression KCNR and SK-N-SH cells. (**B**) Immunoblot showing a failure of BSO to increase BMOV stimulated Akt activation in both SK-N-SH and KCNR cells, although the latter also failed to be stimulated by H_2O_2 despite its ability to inactive PTEN.

4.3.9. Cytotoxicity by BMOV is not significantly induced by Akt activation or inhibition in BMOV-resistant cells

Contrary to its well characterised role as a pro-survival factor in a range of human cancers, Akt has been shown to have an 'Achilles heel' whereby increases in its phosphorylation lead to downstream deactivation of FoxO transcription factors and sestrin 3 (a FoxO target), resulting in reductions in the capability to detoxify cellular ROS, thus leading to oxidative apoptosis (Nogueira et al., 2008). We have shown that BMOV can induce increases in Akt phosphorylation and ROS production as well as decreases in the levels of a major antioxidant GSH, that has a crucial role in

countering increased ROS levels. Furthermore LY29 was observed to amplify the cytotoxic effects of BMOV while also increasing Akt phosphorylation and causing ROS increases and GSH decreases alone and in combination with BMOV. Lastly we failed to observe changes in Akt phosphorylation induced by BMOV in cells that failed to undergo phenotypic changes (SK-N-AS, SK-N-DZ), although the former were not resistant to BMOV mediated ROS increases. These results begged the question of whether ROS and Akt played a causal, cooperative relationship in BMOV-mediated cytotoxicity, whereby BMOV-mediated increases in Akt phosphorylation sensitises cells to the toxic effects of ROS, also increased by BMOV, by limiting ROS detoxification. Indeed such an effect has been demonstrated to result from rapamycin-mediated Akt phosphorylation and phenethyl isothiocyanate-mediated ROS production in ovarian cancer cells (Nogueira et al., 2008).

Thus we manipulated Akt activity in BMOV-unresponsive SK-N-AS cells by over-expressing plasmids encoding a dominant negative Akt mutant (DN Akt), which blocks Akt activation due to a point mutation in the ATP-binding domain (K179M) (Franke et al., 1995), as well as a dominant active version of Akt, which is constitutively active due to the presence of a SRC myristoylation signal (Myr Akt) (Kohn et al., 1996). We confirmed the expression of both plasmids following transient transfection and acute selection via immunoblotting for HA (Both plasmids were HA-tagged), although this was considerably higher for Myr Akt compared with DN Akt (**Figure 4.28**). Furthermore Myr Akt caused highly significant increases in Akt activity beyond control levels and relative to Akt protein levels (**Figure 4.28**).

We next conducted sub-G1 analysis of apoptosis following transient overexpression of DN/Myr Akt in SK-N-AS cells after BMOV treatment. Although Myr Akt was found to increase apoptosis following BMOV treatment, this did not attain statistical significance, in contrast to DN Akt, which actually enhanced the effects of BMOV to a greater degree than Myr Akt (**Figure 4.29**), similar to the effect of combined BMOV/PI-103 treatment. However this effect exhibited high inter-experimental variability.

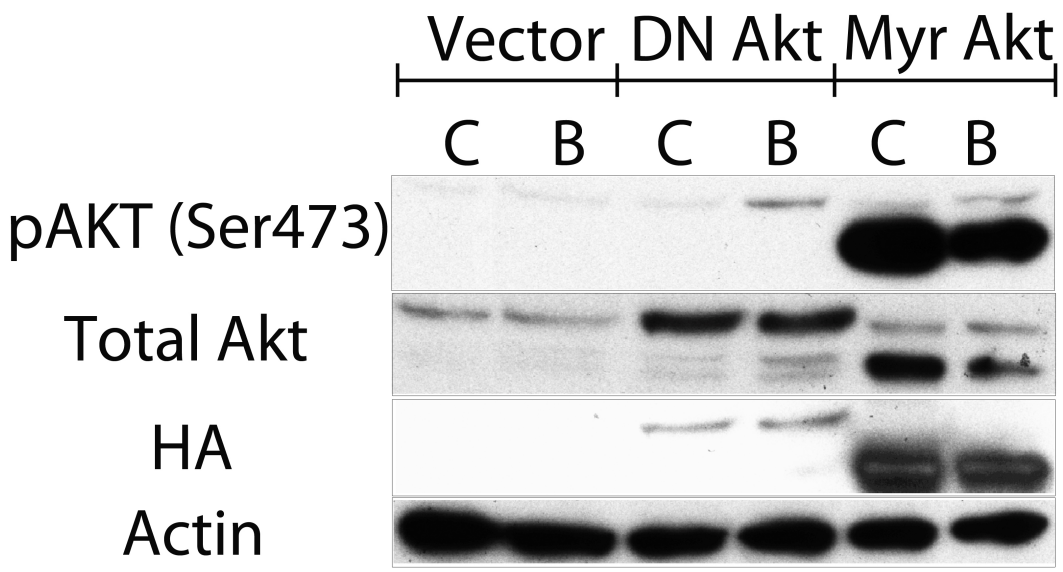

Figure 4.28. Immunoblotting for phosphorylated Akt and HA. SK-N-AS cells were co-transfected with either DN or Myr Akt and a vector encoding resistance to hygromycin B, followed by acute selection for 48 hours in the presence of hygromycin (400µg/ml), reseeding and 24 hour treatment with BMOV (10µM).

This suggests that high levels of Akt activation are associated, but not sufficient to sensitize cells to BMOV treatment, arguing against the hypothesis that BMOV-resistance is caused by low Akt activation.

4.4. Discussion

PTPs have been shown to contribute to cell survival and therapeutic resistance (MacKeigan et al., 2005), and individual PTPs such as DUSP26 and SHP2 have been highlighted as potential oncogenes in NBL (Bentires-Alj et al., 2004; Shang et al., 2010). Thus we sought to test the efficacy of PTP inhibition as a means of inducing selective apoptosis in NBL cells. In doing so we have shown that the broad PTP inhibitor BMOV causes selective apoptosis in a subset of NBL cell lines. This effect does not appear to involve either p53/p38 MAPK, as we did not detect induction or activation of these proteins respectively, although we did not examine p53 phosphorylation that may occur. Remarkably this effect is associated with enhanced activity of Akt, despite its normal role in mediating cell survival. Both apoptosis and Akt activity are dramatically enhanced by co-treatment with LY294002 due to apparent inhibition of negative feedback regulation of PI3K/Akt. Furthermore these effects were shown to result from a change in REDOX state, where BMOV was shown

to increase ROS and decrease the antioxidant GSH, while NAC/GSH-ethyl ester treatment abrogated apoptosis and inhibition of GSH synthesis augmented it. Lastly we hypothesised that resistance to BMOV exhibited by SK-N-AS cells might result from low levels of Akt activity, however constitutive activation of Akt failed to effectively sensitize cells to BMOV, although it did cause an increase in BMOV-induced apoptosis. Thus in sum these data suggests that BMOV is able to increase Akt activity and ROS production as well as target the ROS detoxification system to cause ROS-dependent apoptosis, showing that in contrast to the well known pro-survival functions of Akt, its activity is actually associated with cell death in this case.

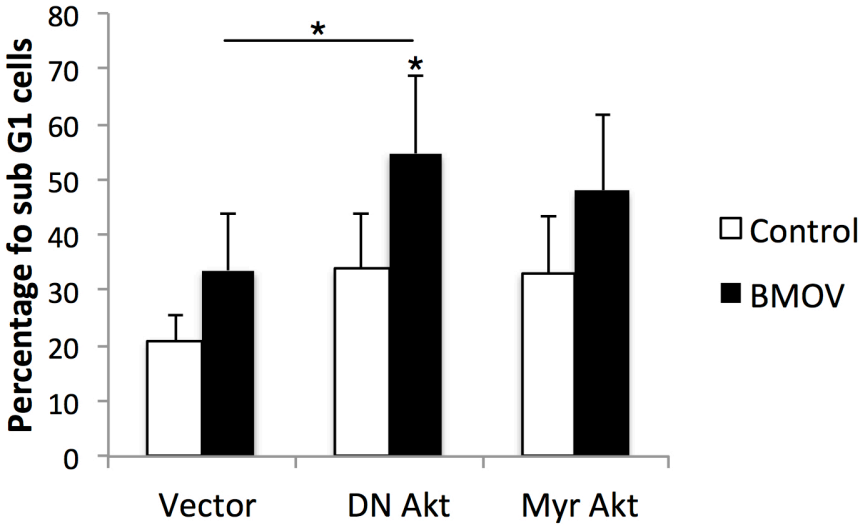

Figure 4.29. Overexpression of constitutively active Akt does not significantly sensitize BMOV-resistant SK-N-AS cells to apoptosis. Sub-G1 analysis of cells over-expressing either DN or Myr Akt treated for 3 days with 10µM BMOV. Myr Akt failed to significantly sensitize cells to BMOV treatment, although DN Akt did. Mean and SEM of 4 independent experiments.

The PI3K/Akt pathway is arguably the most important signalling pathway in tumour initiation and maintenance, governing diverse roles from cell survival, proliferation, migration and angiogenesis (Vivanco and Sawyers, 2002). The *PIK3CA* gene encoding the p110a catalytic sub-unit of PI3K is a frequent target of activating-mutations and amplification and the negative regulator of Akt PTEN is one of the most frequently mutated tumour suppressor genes identified to date (Salmena et al., 2008). This extends to NBL where Akt activation is a negative prognostic marker (Opel et al., 2007), and inhibition of both PI3K (Bender et al., 2011) and Akt (Li et al., 2010) have

emergent efficacy in NBL treatment. While PI3K/Akt inhibition is certainly worthy of consideration in NBL (Brodeur, 2010; Li and Thiele, 2007), it is not without caveats. First, there is considerable redundancy between both PI3K isoforms themselves (Foukas et al., 2010) and other signalling pathways such as MEK/Erk (Mendoza et al., 2011), which can directly compensate for each other by the activation of joint targets (She et al., 2010). In fact PI3K/Akt inhibition has been shown to directly result in an adaptive response by relieving negative feedback suppression of oncogenic RTKs such as HER2 (Chandarlapaty et al., 2011; Serra et al., 2011). Thus as with other kinase targets, therapeutic resistance as well as off-target effects associated with inhibition of such an integral pathway are obvious concerns (Zoncu et al., 2011).

The ability of an enzyme like Akt to regulate a diverse plethora of substrates potentially exposes it to an 'Achilles heel'. For instance, inhibition of FoxO transcription factors, although a key pro-survival function of Akt (Brunet et al., 1999), causes downregulation of sestrin 3, limiting ROS detoxification and resulting in apoptosis (Nogueira et al., 2008). This suggests that targets negatively regulated by Akt otherwise potentially maintain survival of cancer cells in the face of oxidative stress (Naka et al., 2010; Tothova et al., 2007), often induced by chemo and radiation therapy. This research highlights a potential strategy whereby increasing Akt activation may actually hinder cell survival when accompanied by increased ROS production. Indeed oncogenic transformation is accompanied by concomitant increases in molecules mediating ROS detoxification (Denicola et al., 2011), suggesting a requirement for antioxidants in the prevention of ROS-mediated cell death of tumour cells.

We have characterised such a dual function of BMOV, which through broadly inhibiting PTPs results in enhanced kinase activity of Akt, while also causing increases in ROS and reduced glutathione protection. This approach allows further modulation allowing increased efficacy. For instance, limiting the ROS defence system by compound treatment with BSO dramatically augments apoptosis induced by BMOV. Similarly although commonly described as a PI3K inhibitor, by preventing negative feedback suppression of PI3K through S6 kinase inhibition the compound LY294002 increases the effects of BMOV on Akt activity, also enhancing apoptosis. Remarkably these compounds though effective at inducing apoptosis in NBL cells show no

toxicity against non-neoplastic dividing cells, likely reflecting the fact that this approach specifically targets NBL cells due to their sensitivity to ROS and requirement for tightly regulated PI3K/Akt signalling. This latter point is reinforced by the fact that PI3K inhibition also enhances BMOV-induced apoptosis, providing tentative evidence that NBL cells rely on a finely balanced or 'just right' regulation of Akt activity for cell survival, evidence for which has been demonstrated in the case of Wnt signalling in colorectal cancer, dubbed the Goldilocks hypothesis (A. Clark, personal communication). However this may also simply reflect entirely different functions of Akt, for instance PI3K inhibition likely upregulates pro-apoptotic proteins enhancing most chemotherapeutic agents (Bender et al., 2011). We have also provided preliminary evidence that BMOV can suppress autophagy, a putative mechanism of cell survival in response to PI3K/mTOR inhibition (Fan et al., 2010), providing one possible mechanism for enhancement of cell death by PI-103/BMOV. This is an interesting subject for further investigation, given the lack of well-tolerated autophagy inhibitors and the suggestion that autophagy inhibition may be an effective form of therapy.

Importantly this approach may circumvent acquired therapeutic resistance, the most common limitation of targeted therapy, because BMOV treatment actually takes advantage of rather than working against the basal state of NBL cells, i.e. having increased Akt activity, and instead exploits an Achilles heel. The lack of a requirement for p53 in BMOV-induced apoptosis is also a useful feature, given that p53 often becomes mutated following chemotherapy, leading to relapse in NBL (Carr-Wilkinson et al., 2010). BMOV also targets a dependence on ROS homeostasis exhibited by cancer cells, which have much higher levels of ROS and therefore rely more heavily on antioxidant defences (Raj et al., 2011). One interesting point is that CSCs, whose existence has been hypothesised to drive tumour recurrence in NBL (Hansford et al., 2007), have been shown to rely more heavily on antioxidant defences against ROS (Diehn et al., 2009) as well as FoxOs (Naka et al., 2010) for survival, allowing us to speculate that this therapy may be particularly effective against CSCs in NBL.

An obvious caveat is that this approach is not equally effective in all NBL cell lines, as they exhibit differential sensitivity to BMOV. While the reasons for this need

to be investigated further, future studies may elucidate candidate PTPs that could be mediating therapeutic resistance, which may be more highly expressed and/or active in BMOV-resistant cells. Alternatively, this may simply reflect the known heterogeneity in the molecular make up of NBL tumours and their derived lines, whereby some tumour cells may rely on correct Akt and ROS regulation more than others.

One further caveat that was briefly raised is that the ability of NAC/GSH-ethyl ester to abrogate the effects of BMOV may simply reflect the propensity of these reducing agents to reduce oxidised and thus activated vanadium (V) TO (IV), lowering its potency (with the converse argument applying to BSO). While it is not possible to rule this out, there are a number of counter arguments. Firstly if BSO were to increase oxidised vanadium increasing its potency, one would expect an increase in Akt activation in BSO/BMOV treated cells versus BMOV treated cells alone, which was not observed. In the same vein we found no evidence for toxicity of BSO/BMOV on MEFs, which one would predict to occur if BSO simply altered the dosage of vanadium (as toxicity was observed with BMOV treatment greater than 50µM). Lastly the finding that BMOV increases ROS and decreases GSH also provides supporting evidence to the rescue experiments with NAC/GSH-ethyl ester, suggesting that an altered redox state is at least partially responsible for these effects.

It is also noteworthy that BMOV causes increases in the expression of Mycn. Given that Mycn is the best-characterised negative prognostic marker in NBL, one might expect that any agent capable of increasing Mycn levels might increase rather than reduce cell survival. While it is of course possible that increases in Mycn may play a causal role in apoptosis due to the well characterised effects of forced Mycn expression leading to apoptosis in NBL cells, we detected little direct evidence for this. It remains to be seen whether increasing Mycn in cells already harbouring amplified and thus high level Mycn results in either survival or apoptosis, but this could be tested using a knockdown approach. In sum the efficacy of BMOV treatment clearly warrants further investigation, including preclinical testing, and suggests that BMOV either alone or in combination with LY294002 or BSO, may represent an effective, novel therapy in NBL treatment.

Chapter 5. The expression profile of the PTP gene family in neuroblastoma cells and its relation to the effects of vanadium compounds

5.1. Introduction

Gene-expression analysis has become an important tool in providing preliminary evidence for causal roles of proteins in diverse cell biological processes. For example, the genes of important proteins, most notably 'house keeping' proteins with roles in general homeostasis, are expressed at higher levels than genes encoding proteins with a less crucial, or more specialised functions. Real-time (RT) qPCR is the most reliable method of analysing gene expression due to its sensitivity and therefore ability to detect low levels of mRNA, as well as its capacity for high-throughput analysis, increasing the possible power of experiments. As changes in gene expression are crucial to differences in cell growth, differentiation and survival, RT-qPCR is ideally suited to identify candidate proteins involved in tumorigenesis or tumour maintenance in cancer. For instance oncogenic transformation often results in increased expression of genes encoding receptor-tyrosine kinases, leading to increases in protein level and altered signal transduction (Blume-Jensen and Hunter, 2001). While targets of genomic amplification such as Mycn will show drastic changes in gene expression reflecting their importance in tumour cell survival (Schweigerer et al., 1990). Similarly, subtypes of tumours can be delineated based on the differential expression pattern of a gene set, as has been shown with TrkA and TrkB-expressing NBL tumours (Schulte et al., 2005).

As well as general changes associated with transformation, gene expression profiling has been conducted in NBL following treatment with differentiation induction agents such as RA (Yuza et al., 2003) and NGF (Oe et al., 2005), in order to identify candidate proteins mediating differentiation. For instance the upregulation of a given protein following treatment with RA may be causal, indicating that its expression is required to initiate/maintain differentiation, though this requires functional validation. As previously mentioned, for the most part PTPs have been regarded as a tumour-suppressor 'enriched' family given their negative regulation of oncogenic kinases. However such a view has become out-dated given that a substantial proportion of PTPs maintain a positive role in tumour initiation and progression by regulating cell survival and therapeutic resistance (MacKeigan et al., 2005). Furthermore, a recent report conducted gene-expression profiling on PTPs in

association with transformation by the HER2 oncogene in breast cancer, identifying numerous alterations in PTP expression both positive and negative as a result of HER2 modulation (Lucci et al., 2010).

So far little research has been carried out into the role of PTPs in NBL. One study that compared the expression of genes in NBL tumours to that of fetal neuroblasts, the cell-of-origin in NBL, only documented two PTPs, *PTPRD* and *PTPRK* that were differentially regulated. However, given that numerous reports have identified a host of PTPs as having roles in cancer (Julien et al., 2011), one might expect numerous gene expression alterations to take place between untransformed cells and NBL cells. Thus as a first, albeit preliminary step, we sought to analyse differences in PTP gene expression between normal nervous system tissue and a range of NBL cell lines, to highlight potential oncogenes and tumour suppressors. For instance, tumour suppressor PTPs could be acting as a barrier to tumorigenesis through mechanisms such as growth suppression and execution of apoptosis. Conversely other PTPs may be promoting tumour formation and progression e.g. by negatively regulating tumour suppressive proteins or through direct interaction with proteins involved in motility, proliferation or survival. Furthermore given that the phenotypic consequences of inhibition of the PTP family segregates NBL cell lines into neuritogenic, apoptotic and resistant groups (Chapters 3-4), we wished to understand whether certain PTPs may be differentially expressed within each cell group, highlighting possible effector pathways or mechanisms of therapeutic resistance.

5.2. Experimental procedures

5.2.1. qPCR array

For generating PTP gene expression profiles, we made use of a semi-automated qPCR platform generously made available to us by Dr. Rob Hooft van Huijsduijnen at Merck-Serono Pharmaceuticals AG, Geneva, Switzerland. This was a collaboration within the FP6 Network PTPNET. With the exception of the RNA isolation and the final data analysis, Dr. Fanny Schmidt carried out all of the RT-QPCR assays. 384 well plates were filled with Qiagen primers for the entire PTP family as well as four

different house-keeping genes (HKGs) - *Actin, Canx, Psmb3* and *Hbms*. Cross point or threshold cycle values (Ct), representing the number of cycles required to reach a set threshold of fluorescence intensity, were obtained for each sample by normalizing to the average of HKGs using the equation $2^{-\Delta Ct}$, where ΔCt = Ct (sample) – Mean Ct (reference genes). Ct values were extracted using Fast 7900 SDS 2.2.2 software (Applied Biosystems, Life Technologies, Carslbad, CA, USA). Results are displayed as a percentage of expression compared to the HKG set i.e. $\%2^{-\Delta Ct}$, e.g. a value of 100 denotes the same expression as the HGKs whereas 50 denotes a 2 fold lower expression level. All RNA was isolated in triplicate at different time points, with the exception of non-neoplastic neural tissue samples that were a kind gift of Mr. Simon Picker (adult cortex) and Dr. Francesca Menghi (Fetal – 26 weeks gestation/adult – 26 years cerebellum), and were originally either isolated from primary biopsy tissue or purchased commercially (BioChain, Hayward, CA, USA - CB6 (adult cerebellum), No. R1234039-50; CBF3 (fetal cerebellum), No. R1244039-50), respectively. Where applicable, non-neoplastic neural tissue expression was pooled, by combining values for each tissue type (adult and fetal cerebellum and adult cortex) and expressing a mean value for non-neoplastic neural tissue overall (referred to as brain), to generate a rough estimate of 'normal' e.g. non-neoplastic expression levels.

Although the Qiagen PTP primers have not been strictly normalised to each other in terms of efficiency, they are expected to be similar. For example, research by Viktoria Tchtchelnitksi compared similar qPCR data of murine PTPs against an exon array and obtained very comparable, relative gene expression profiles (V.Tchetchelnitski, UCL PhD Thesis).

5.2.2. Statistical analysis and clustering

Clustering analysis was completed using MeV software (V4.7) in collaboration with Mr Simon Picker (ICH, UCL). Clustering dendrograms were created by sub-grouping cell lines into non-neoplastic neural tissue (adult cortex, fetal cerebellum, adult cerebellum), glioblastoma (U118, T98G), unresponsive NBL (IPhNB1, SK-N-BE(2), SK-N-AS, SK-N-DZ), neuritogenic NBL (SK-N-SH, SH-SY5Y, LAN5) and apoptotic NBL (KCNR, IMR32, Kelly). Between subjects student's t-tests were computed for each comparison between NBL groups only, with a predetermined p value of 0.05.

5.3. Results

5.3.1. qPCR Expression profiling of PTPs in NBL cell lines

We previously hypothesised that the in line with recent evidence (Julien et al., 2011; MacKeigan et al., 2005), the PTP family would harbour a number of genes either crucial or detrimental to cell survival. This is a crucial question given the relative paucity of data concerning the role of PTPs in NBL. Thus we sought to analyse the expression of the entire PTP family in a range of NBL lines.

One main aim of this task was to highlight PTPs that are differentially expressed in NBL lines, depending on the response profiles of the cells to PTP inhibitors. For example, if a PTP is strongly expressed in BMOV-responsive lines and weakly in BMOV-unresponsive lines, then this might provide initial, indirect evidence for a role in the effects of BMOV treatment. Similarly this approach could potentially rule out a number of PTPs expressed at very low levels, given that they are unlikely to be targeted by vanadium. Lastly this approach could also generate hypotheses concerning the wider role of PTPs in NBL tumorigenesis, by highlighting candidate oncogenic and tumour-suppressive PTPs based on expression profiles in comparison to non-neoplastic tissue.

Thus we conducted qPCR on triplicate samples of every original NBL cell line (I.e. non-isogenic) used in the present study, including BMOV-responsive (SH-SY5Y, SK-N-SH, LAN5, IMR32, KCNR, Kelly) and BMOV unresponsive (SK-N-BE(2), SK-N-AS, SK-N-DZ, IPhNB1). Here responsiveness was defined based on phenotypic criteria established in chapters 4-5, whereby responsive cells undergo either apoptosis or neuritogenesis following 5-10µM treatments with either BMOV or VA, while unresponsive cells are phenotypically resistant at such doses. Furthermore as a comparison against a distinct neural tumour type, cell lines derived from the CNS solid tumour glioblastoma (T98G, U118) were included. This inclusion may help to rule out non-NBL specific PTPs as well as highlighting more general changes in expression in cancer. Lastly as a comparison, central nervous system tissue isolated from both fetal and adult cerebellum as well as adult cortex was included. Although not an ideal point of comparison, given the sympathoblastic origin of NBL, one might

expect reduced expression for instance of a tumour-suppressor gene in tumour derived neuroblasts when compared with normal nervous system tissue.

In sum, the proceeding analysis has provided a platform by which to generate hypotheses concerning the role of individual/sub groups of PTPs in NBL tumorigenesis and the response to PTP inhibition, by highlighting differentially expressed PTPs in sub groups of NBL, as well as in NBL tumours when compared to normal central nervous system **(Table/figure 5.1)**. The specific conclusions of this analysis and its relation to experimental results from chapters 3-4 will be discussed in the remainder of this chapter.

5.3.2. Relative expression of PTPs in NBL compared with known alterations in human cancer

In order to assess the general relevance of this expression profiling data set, we sought to compare our analyses with known alterations in human cancer. Clearly a large number of PTPs have been demonstrated to be involved in positive and negative aspects of tumorigenesis/ tumour maintenance (Julien et al., 2011; Ostman et al., 2006), however for the most part it is unclear whether these PTPs are involved in NBL pathogenesis. Similarly, to our knowledge this is the first gene expression analysis of the entire PTP gene family in NBL to date, thus an indication of PTPs that are significantly up/downregulated when compared with non-neoplastic tissue may at least hint at the involvement of novel PTPs. Firstly we sought to identify potentially oncogenic PTPs by indexing PTPs that were upregulated in one or more NBL cell lines in comparison to pooled non-neoplastic neural tissue (adult cortex/cerebellum, fetal cerebellum). In total we identified 15 PTPs that were expressed more highly in tumour samples compared with non-neoplastic neural tissues (**Figure 5.2**).

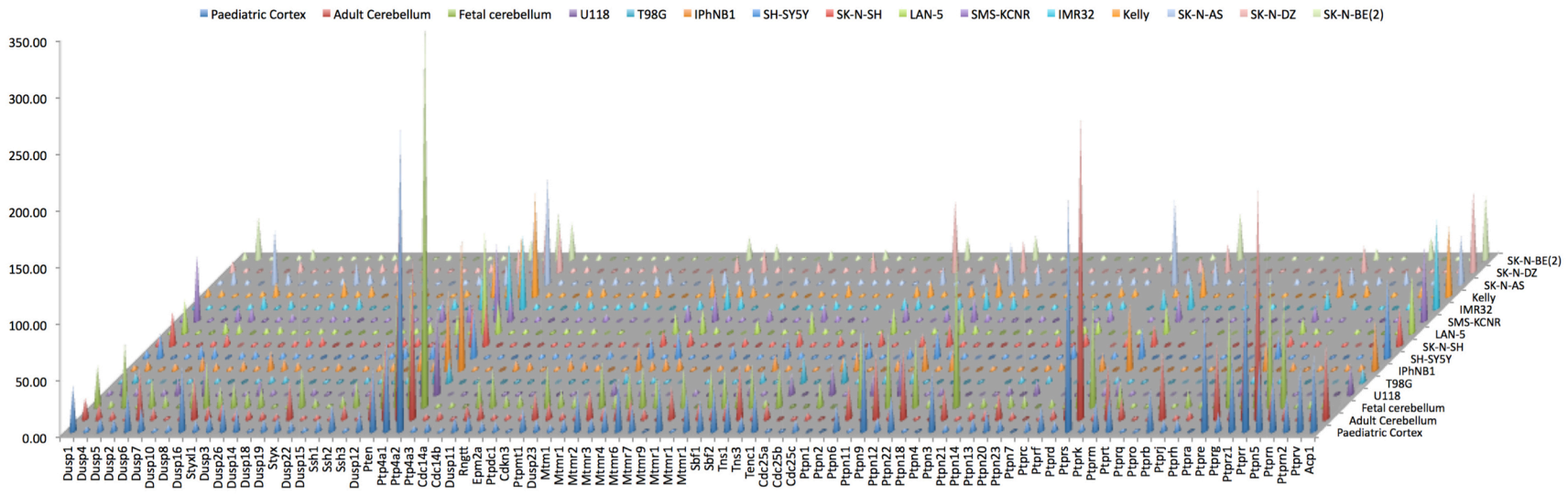

Figure 5.1. Two-dimensional graph depicting differential expression of PTP gene family in non-neoplastic nervous system, glioblastoma and neuroblastoma cell lines. Peaks depict high expression relative to HKGs possibly indicative of cancer-promoting/BMOV-resistance mediating PTPs, while hills denote PTPs that presumably have little involvement in NBL-cell survival. NBL cell lines are grouped according to response to BMOV.

	Adult Cortex	Fetal cerebellum	Adult Cerebellum	T98G	U118	IPhNB1	SK-N-BE	SK-N-AS	SK-N-DZ	SH-SY5Y	SK-N-SH	LAN5	KCNR	IMR32	Kelly
Dusp1	40.77	18.76	36.62	1.97	3.42	3.81	6.39	2.75	8.83	6.58	5.95	2.54	5.50	4.50	6.96
Dusp4	3.61	13.05	4.49	7.31	19.23	7.90	38.08	11.14	2.52	20.71	30.23	29.90	58.12	2.18	4.71
Dusp5	12.02	6.85	57.40	2.47	4.29	0.94	2.13	3.05	0.44	0.53	2.94	0.96	1.00	0.97	1.43
Dusp2	9.98	2.11	2.30	0.00	0.00	5.67	0.09	0.15	1.33	3.04	0.53	0.43	0.40	0.05	2.16
Dusp6	36.26	43.48	25.07	0.04	4.10	0.35	3.45	47.25	0.20	11.10	3.71	9.42	12.47	3.46	4.08
Dusp7	21.92	9.15	9.38	2.85	14.97	12.29	9.16	9.81	8.92	8.47	9.39	7.19	12.04	10.99	11.93
Dusp10	2.21	0.97	0.39	0.06	0.00	5.52	0.07	0.80	1.14	0.02	0.01	0.11	0.61	0.86	3.69
Dusp8	5.38	4.34	21.77	3.21	28.49	2.31	1.67	3.27	1.14	4.10	1.57	4.05	2.74	7.39	2.18
Dusp16	57.25	37.66	40.28	0.15	1.77	7.71	2.41	0.70	4.78	5.52	1.35	5.10	5.61	0.95	1.95
Styxl1	9.26	11.55	17.15	0.10	0.37	2.84	1.39	5.04	0.48	1.63	0.71	2.01	1.03	1.37	1.69
Dusp3	14.79	13.94	20.64	2.63	2.08	16.72	4.39	18.60	4.32	4.41	3.62	1.44	1.58	6.37	14.21
Dusp26	26.07	6.06	14.08	5.11	13.18	9.25	4.32	8.63	6.48	3.39	6.39	3.40	3.35	3.28	4.19
Dusp14	20.03	8.01	18.07	4.76	3.88	6.53	3.17	6.46	7.71	2.37	7.03	3.13	3.15	9.50	9.17
Dusp18	1.34	6.55	0.88	0.05	0.01	1.03	0.04	0.12	0.09	0.14	0.17	0.01	0.05	0.57	0.14
Dusp19	9.90	4.16	2.14	0.16	0.20	1.62	0.61	1.47	0.97	0.45	0.35	0.18	1.01	0.69	3.38
Styx	12.26	33.95	33.96	1.42	5.18	5.77	3.51	15.32	2.61	2.16	4.68	1.71	1.75	4.89	4.18
Dusp22	8.05	2.68	6.59	0.68	0.74	0.09	0.44	1.07	0.79	0.46	0.69	0.20	0.20	0.10	0.06
Dusp15	2.91	3.31	1.55	0.06	0.01	3.35	0.21	0.34	2.00	1.12	1.38	2.09	1.65	1.32	0.55
Ssh1	9.58	2.55	9.26	4.13	8.80	4.29	2.34	3.53	3.55	3.82	5.49	3.99	2.58	2.46	1.40
Ssh2	23.79	12.84	23.78	2.54	1.04	5.44	2.88	6.54	6.28	9.67	6.50	8.88	17.39	8.32	5.08
Ssh3	2.55	1.41	3.61	0.87	0.41	0.14	0.21	1.18	0.02	0.38	0.77	0.23	0.25	0.08	0.03
Dusp12	18.66	34.16	46.53	4.06	5.51	17.59	16.45	17.03	20.11	12.47	4.82	15.80	17.64	30.02	35.43
Pten	57.03	69.07	116.26	0.39	0.81	7.53	2.55	22.80	0.70	4.26	1.84	3.80	3.05	6.10	12.68
Ptp4a1	83.44	174.29	115.67	26.30	58.02	69.75	40.43	52.88	48.95	43.70	36.95	88.65	67.81	57.22	52.80
Ptp4a2	267.75	143.18	347.09	21.27	78.77	116.67	32.87	95.07	37.84	43.69	39.23	28.20	25.14	65.92	91.20
Ptp4a3	3.98	4.22	2.06	0.16	0.00	2.14	3.46	3.16	2.47	1.08	0.32	1.54	1.18	3.81	3.08
Cdc14a	7.60	6.24	3.31	0.57	0.89	1.65	4.26	1.32	3.91	1.65	1.31	3.06	3.34	1.73	2.87
Cdc14b	2.46	0.99	0.45	0.12	0.06	0.12	0.20	0.63	0.07	0.15	0.09	0.02	0.04	0.32	0.02
Dusp11	11.91	12.40	26.35	0.22	0.28	7.95	0.55	4.68	0.48	0.49	0.25	0.66	0.70	6.07	7.31
Rngtt	14.83	15.72	32.92	0.81	1.12	7.02	2.30	5.29	3.15	2.86	1.52	3.00	2.74	6.06	7.08
Epm2a	8.35	3.89	9.81	0.49	1.34	1.06	2.02	0.88	1.58	3.18	1.35	1.97	1.15	1.71	0.84
Ptpdc1	7.83	3.91	10.33	0.34	0.98	2.27	2.73	1.69	5.53	3.10	1.17	3.30	5.25	3.56	1.25
Cdkn3	0.97	4.10	1.28	0.00	0.00	8.97	0.02	6.24	0.01	0.01	0.00	0.01	0.01	6.10	4.08
Ptpmt1	19.95	23.66	37.24	0.59	0.39	7.41	0.85	11.44	0.44	0.58	0.43	1.17	1.06	5.53	9.35
Dusp23	9.85	15.00	14.81	0.66	1.83	4.27	0.00	0.64	0.04	5.65	3.27		0.00	0.01	0.02
Mtm1	5.36	5.57	7.96	0.00	0.00	0.34	0.00	0.31	0.00	0.00	0.00	0.00	0.00	0.19	0.12
Mtmr1	11.37	5.85	9.14	0.04	0.04	1.89	0.13	1.95	0.14	0.16	0.08	0.16	0.15	2.23	1.79
Mtmr2	35.46	27.13	41.09	8.08	11.96	20.70	19.44	11.97	13.76	17.54	12.94	17.59	14.66	7.50	19.16
Mtmr3	11.98	9.45	10.40	1.56	3.01	7.41	2.15	2.15	2.80	2.70	2.01	2.02	2.59	3.21	3.38
Mtmr4	22.01	16.82	30.50	4.13	6.05	10.16	12.64	11.33	19.30	23.07	11.81	20.94	26.22	22.65	10.12
Mtmr6	46.30	17.82	36.29	1.59	2.31	11.52	2.35	6.46	3.68	1.72	1.58	4.97	4.25	10.19	8.54
Mtmr7	23.64	8.69	25.92	0.00	0.01	1.23	1.16	0.24	1.72	0.68	0.19	0.19	1.84	0.51	2.00
Mtmr9	0.45	0.26	0.50			0.15	0.00	0.15	0.01	0.00	0.00	0.01	0.00		0.19
Mtmr11	44.82	28.80	33.91	2.07	3.65	3.66	7.56	5.41	8.35	10.01	6.04	11.68	10.22	4.73	4.83
Mtmr12	1.21	0.69	0.21	0.14	0.13	0.06	0.02	0.79	0.05	0.05	0.02	0.11	0.13	0.11	0.10
Mtmr10	35.63	13.54	31.62	2.30	4.03	4.23	3.11	3.98	3.59	2.41	2.93	2.39	2.30	3.09	4.49
Sbf1	27.28	11.05	32.22	0.31	0.78	0.60	0.60	2.23	0.98	1.19	0.95	0.98	1.11	2.05	1.62
Sbf2	40.55	13.84	20.30	8.73	10.26	13.58	8.31	3.87	17.62	16.29	13.12	19.76	14.97	6.45	10.60
Tns1	33.71	47.38	36.03	0.78	3.15	3.94	2.67	3.48	4.22	4.59	2.23	3.55	4.41	2.69	1.60
Tns3	13.53	5.86	5.87	0.00	0.08	0.91	0.56	4.09	0.40	0.72	1.39	0.70	0.34	0.84	1.73
Tenc1	38.61	14.16	34.35	23.98	18.52	1.65	0.25	2.70	3.62	1.32	8.89	2.95	2.66	3.11	1.82
Cdc25a	1.44	0.33	0.45	0.51	0.13	0.01	0.02	0.89	0.00	0.02	0.59				
Cdc25b	0.71	1.28	0.41	0.19	0.12	12.20	0.37	2.80	1.20	1.41	0.36	1.35	1.93	9.20	9.54
Cdc25c	9.48	5.22	22.73	24.27	27.20	16.58	19.58	14.90	63.02	15.04	13.02	22.46	14.91	8.92	13.97

Ptpn1	0.07	0.41	0.03	1.92	1.47	1.46	2.35	1.98	3.62	2.08	1.22	1.15	1.94	2.99	4.10
Ptpn2	0.10	0.07	0.17			0.10	0.00	0.06	0.00	0.00			0.00	0.07	0.05
Ptpn6	23.64	31.05	68.58	5.80	18.03	8.67	4.35	8.60	8.64	8.32	9.25	4.15	10.06	9.45	10.18
Ptpn11	2.13	0.58	1.00	0.00	0.00	0.68	0.01	0.02	0.28	0.01	0.01	0.02	0.01	0.04	3.06
Ptpn9	92.92	57.55	65.85	7.43	35.77	25.18	20.54	35.95	26.85	24.05	19.08	22.01	20.65	19.41	20.62
Ptpn12	11.91	7.58	8.79	1.29	2.73	3.40	4.94	5.00	3.78	5.87	3.43	6.99	5.71	6.33	3.98
Ptpn22	31.75	62.73	59.49	0.33	1.83	17.46	1.63	18.37	1.82	3.56	0.88	1.38	1.70	11.20	8.58
Ptpn18	2.07	1.46	5.62	0.27	6.35	0.01	0.10	0.01	0.11	0.00	0.27	0.20	0.55	0.01	0.01
Ptpn4	0.48	0.29	0.33	0.02	0.04	0.18	0.11	0.33	0.31	0.03	0.02	0.07	0.06	0.33	0.07
Ptpn3	54.02	26.15	141.70	0.72	0.35	2.75	3.27	3.01	2.21	2.86	1.37	3.06	3.76	3.29	2.61
Ptpn21	5.52418	1.95736	3.10907		0.00	0.16	0.08	2.25	0.00	0.00	0.02	0.00	0.04	2.78	0.31
Ptpn14	7.04	7.53	7.85	0.18	1.01	1.85	1.02	2.65	0.54	2.45	1.15	2.17	2.14	1.57	1.19
Ptpn13	11.30	7.96	3.20	4.30	6.94	0.15	0.07	6.86	0.12	0.23	8.15	0.04	0.03	0.71	0.08
Ptpn20	17.92	23.91	10.23	0.32	0.22	4.33	1.29	5.38	3.29	1.47	0.71	6.59	1.47	6.39	8.10
Ptpn23	10.32	5.89	9.23	5.21	13.07	6.24	3.96	3.52	7.43	11.81	10.99	11.20	10.81	6.37	6.61
Ptpn7	0.08	0.06	0.07				0.04		0.06			0.02			
Ptprc	9.41	1.70	6.15	0.01	0.01		0.06	74.86	0.01	0.01	0.01	0.01		0.05	
Ptprf	22.19	8.21	2.70	1.48	1.29	14.48	4.11	12.92	12.06	5.20	6.14	2.54	3.19	16.98	6.63
Ptprd	8.64	39.76	38.13	0.01	2.15	0.15	0.30	0.34	1.43	0.28	0.11	0.10	0.10	0.73	0.46
Ptprs	211.17	273.02	93.94	4.09	5.80	59.26	41.34	20.25	24.83	26.52	17.73	24.96	23.53	27.22	27.58
Ptprk	6.77	5.13	5.52	2.48	13.58	0.65	0.22	4.10	1.68	0.01	0.27		0.01	0.53	1.21
Ptprm	27.09	47.75	22.34	0.92	3.14	0.33	0.04	1.02	0.30	0.17	0.35	1.24	0.67	0.59	1.16
Ptprt	32.28	19.53	2.97		0.01	0.24	0.03	0.02	0.02	0.02			0.03	0.13	
Ptprq	1.70	1.11	0.8882	0.42	0.14	1.81	2.04	1.44	0.78	1.70	0.43	0.07	1.58	3.57	4.83
Ptpro	1.29	1.18	0.20	0.00	0.01	0.02	0.01		0.03	0.00		0.00	0.06	0.01	0.09
Ptprb	37.67	61.12	2.30	0.00	0.21	2.07	2.74	4.53	2.68	1.86	0.12	0.43	1.08	3.90	2.67
Ptprj	9.80	3.16	14.71	0.02	0.01	0.09	0.20	0.16	0.02	0.02	0.21	0.02	0.02	0.02	0.02
Ptprh	9.75	6.62	4.78	0.00	0.00	0.33	0.00	1.16	0.00	0.00	0.00	0.00	0.00	0.11	0.28
Ptpra	0.27	0.05	0.17	0.24	0.58	1.17	0.28	0.32	0.62	0.07	0.06	0.16	0.59	0.01	0.68
Ptpre	112.46	67.45	84.20	4.21	11.45	25.77	9.24	14.59	22.47	18.50	8.44	13.52	14.12	16.49	20.60
Ptprg	17.07	11.74	9.69	0.11	2.82	0.18	0.83	3.06	0.01	1.57	3.03	3.81	2.31		0.10
Ptprz1	67.60	85.79	50.08	3.38	10.09	6.66	1.52	6.31	3.94	1.01	4.17	1.07	1.16	7.92	10.73
Ptprr	159.75	206.58	116.85		0.01	1.01		0.08	0.01					0.03	
Ptpn5	62.49	28.83	99.21	0.03	1.26	3.43	19.72	11.79	4.08	0.66	1.62	2.75	1.84	1.60	3.47
Ptprn	51.64	12.54	1.53	0.00	0.00	1.11	0.02	0.03	1.55	0.18	0.01	0.28	0.11	0.02	
Ptprn2	33.96	1.72	4.90	0.01	0.00	4.71	1.98	2.62	1.19	1.70	0.17	0.37	1.65	4.04	8.30
Ptprv	58.28	14.37	6.82	0.09	0.11	4.84	2.94	0.12	3.69	3.77	0.56	1.53	1.78	2.12	1.94
Acp1	66.53	66.84		12.56	26.86	44.45	55.94	42.68	71.48	70.51	32.18	50.75	66.34	79.58	61.33

Table 5.1. Expression profile of PTPs in glioblastoma and NBL as well as in brain and cerebellar tissue. Values indicate mRNA levels relative to the expression of 4 HKGs (%). Blue cells ≥5<10; Green cells ≥10<20; Red cells ≥20. Missing values indicate an undetectable PCR product after 40 cycles. Samples are grouped by non-neoplastic neural tissue (adult cortex/cerebellum, fetal cerebellum), glioblastoma (T98G, U118), NBL vanadium unresponsive (IPhNB1, SK-N-AS, SK-N-DZ, SK-N-BE(2)) and NBL responsive (SH-SY5Y, SK-N-SH, LAN5, KCNR, IMR32, Kelly), as defined in experimental procedures.

Although these PTPs were rarely uniformly upregulated, this may suggest that certain PTPs may be involved in the formation or survival of genetically distinct NBL tumours. Thus 14 PTPs were shown to be overexpressed in one or more cell lines versus brain. However excluding glioblastoma, only 6 PTPs remained in this data set,

namely *PTPRC, PTPRF, CDC25b, CDKN3, DUSP3* and *DUSP10*. This provides a relatively small number of potentially oncogenic PTPs suitable for further investigation.

We reasoned that as well as overexpressed PTPs, genes that were highly expressed in NBL cell lines regardless of non-neoplastic neural tissue expression may also harbour functions in NBL, i.e. reliance for cell survival, given that high expression is generally indicative of an important function e.g. HKGs. Thus we sought to examine PTPs with high expression levels (e.g. 20% of HKGs). Although not surprisingly this yielded a large number of PTPs, exclusion of PTPs highly expressed in less than two cell lines yielded a much smaller group, containing *PTP4A1, PTP4A2, MTMR4, PTPN9, PTPRS, PTPRE* and *ACP1* (**Figure 5.3**). Thus such PTPs may also be vital to NBL cells reflecting their broader expression in the nervous system. Interestingly *PTPRS*, a type IIa PTP was expressed at very high levels uniformly throughout NBL cell lines, despite very low expression of the highly homologous type IIB *PTPRD*.

Lastly we sought to highlight possible tumour-suppressive PTPs by indexing PTPs with an expression value less than that of control tissue in one or more NBL cell lines. Clearly this is a pertinent question given that as negative regulators of oncogenic kinase signalling, PTPs were originally hypothesised as putative hallmark tumour suppressors. However, the identification of *bona fide* tumour suppressors has been less successful than envisaged, and no such genes have been identified in NBL to date. We found that 24 PTPs were expressed at very low levels in comparison to control tissue (**Figure 5.4**), including genes for which a tumour suppressive role has been demonstrated in other cancers such as *PTPRD* and *PTPRJ* (see below). Of note is that two PTPs, *PTPRK* and *PTPN18* were expressed at low levels in NBL cells only and thus excluded from this data set that included glioblastoma. However this identification is potentially more useful as these genes may function as tumour suppressors specific to NBL.

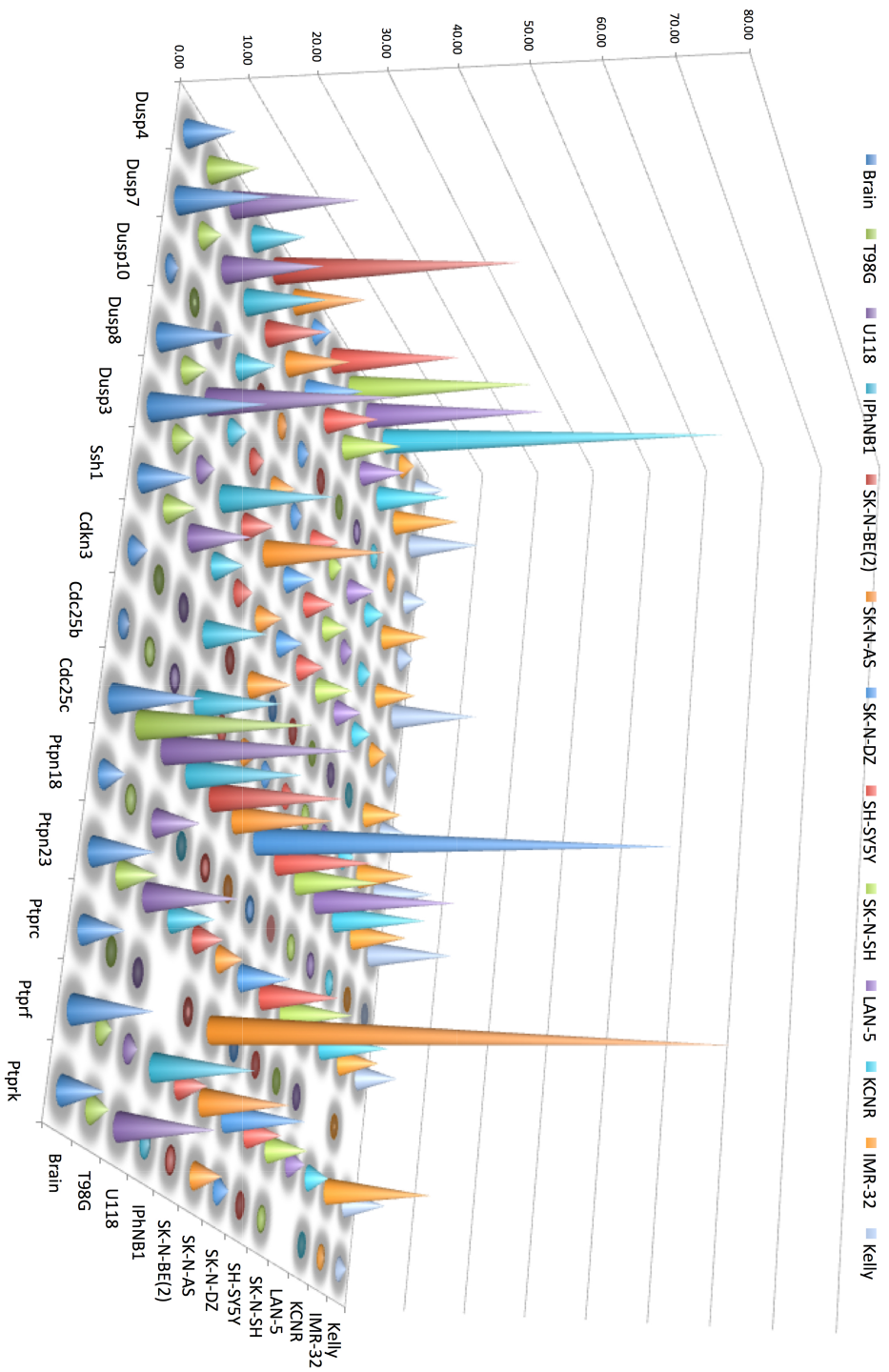

Figure 5.2. Highly expressed PTPs in NBL versus non-neoplastic neural tissue. Graph depicting gene expression levels of individual PTPs with higher expression values relative to 4 HKGs when compared with pooled central nervous system tissue. Note that glioblastoma cell lines (T98G, U118) are also shown as a comparison to NBL.

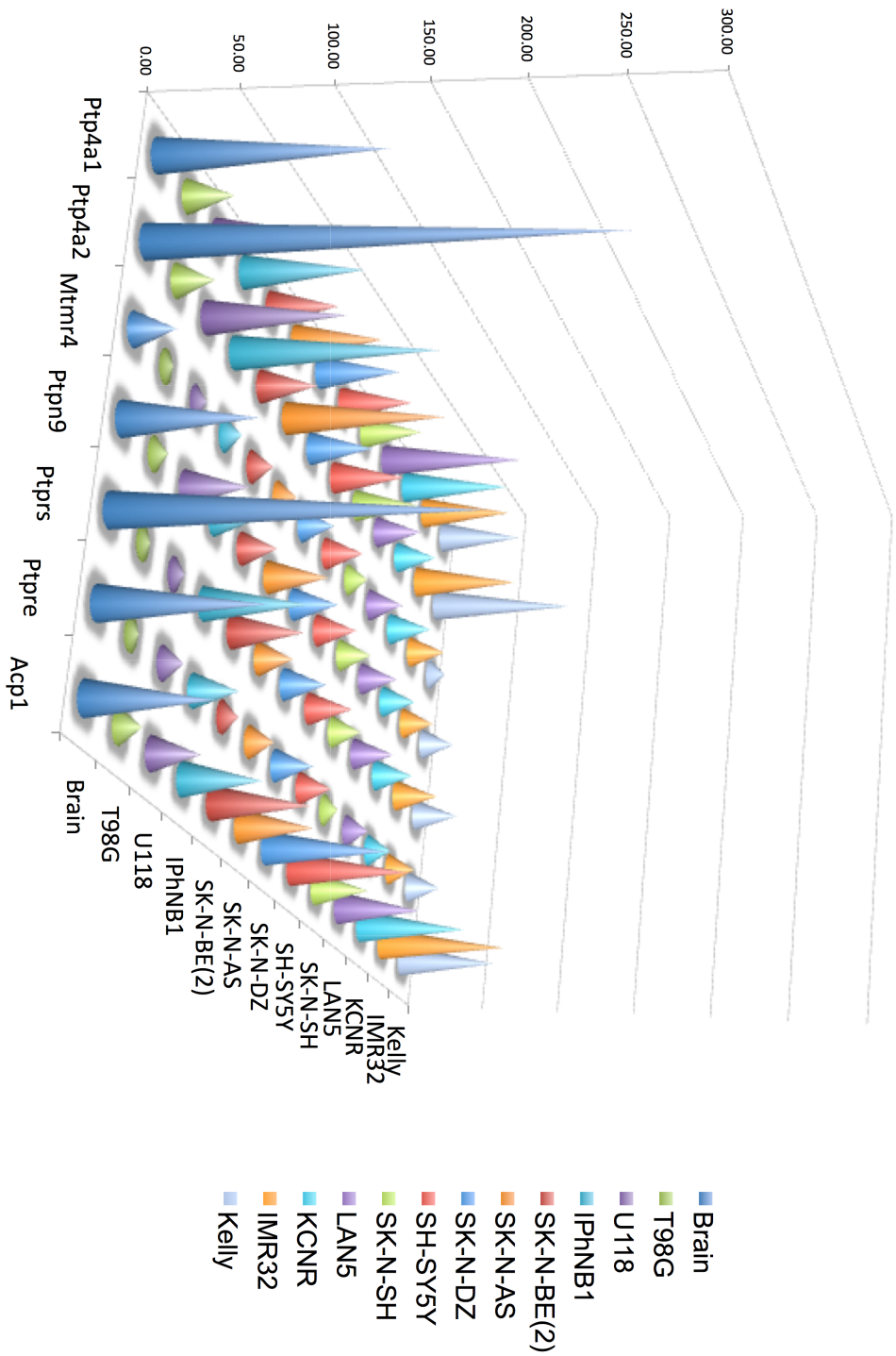

Figure 5.3. Highly expressed PTPs in multiple NBL cell lines. Graph depicting PTPs that are expressed over a cut off value of 20% of 4 HKGs in two or more NBL cell lines. Note that glioblastoma lines (T98G, U118) were included as a comparison.

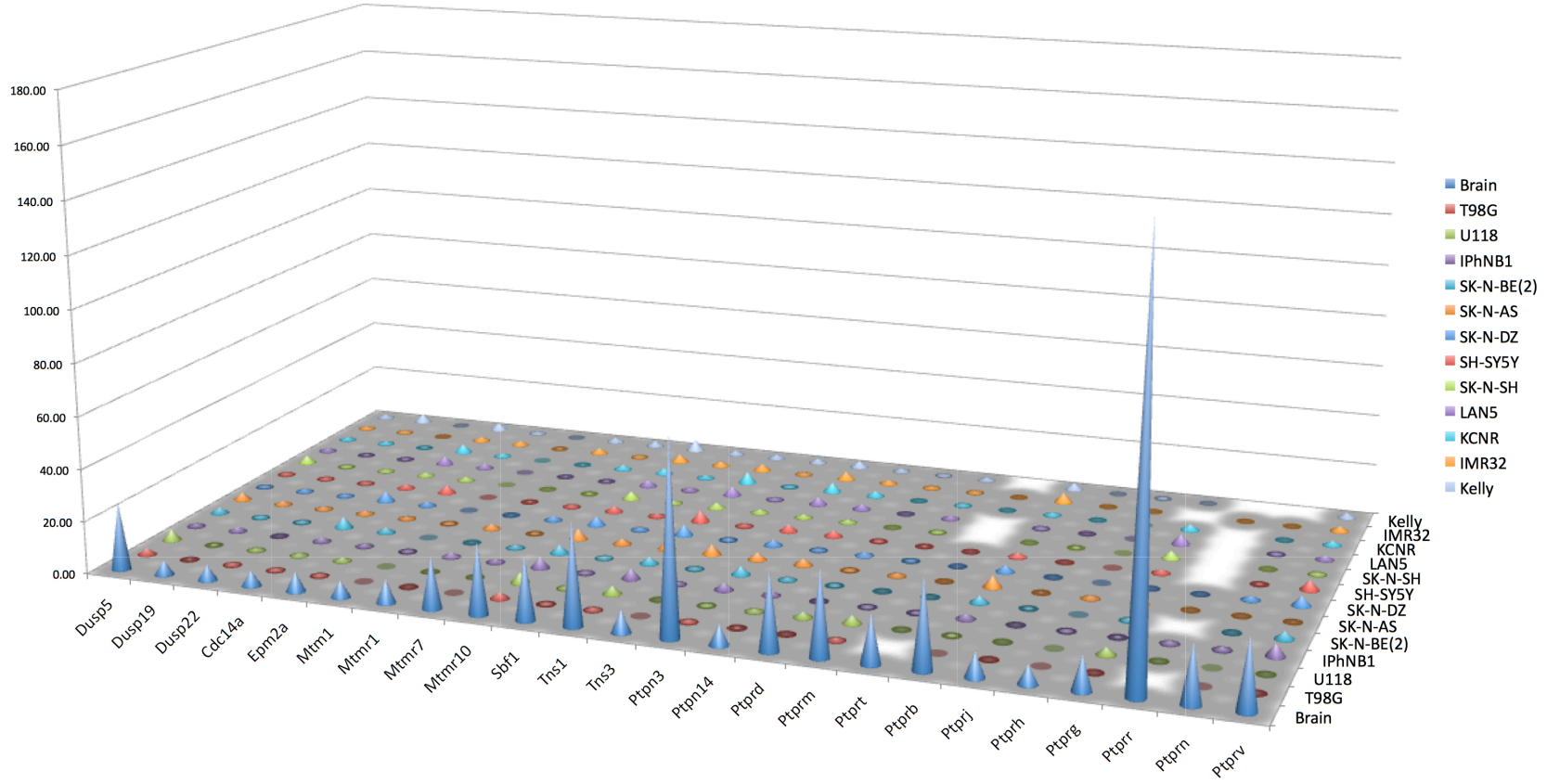

Figure 5.4. Low-level expression of PTPs in NBL. Graph depicting PTPs that are expressed at comparatively low levels versus non-neoplastic neural tissue. Note that all genes were included where expression was lower than pooled non-neoplastic neural tissue values in one or more NBL cell lines. Expression is relative to 4 HKGs.

Thus in sum we have identified a number of PTPs that are differentially regulated in NBL when compared with a reasonably matched (albeit non SA) comparison tissue type. On one hand we have identified PTPs that are either upregulated in NBL cell lines, or expressed at very high levels, suggesting a potentially oncogenic or at least important role in NBL cell function. On the other we have shown that a number of PTPs are expressed at very low levels, despite expression in the nervous system, suggestive of a potential tumour suppressive function in NBL. Interestingly a number of such genes have already been identified as being differentially expressed or even functionally involved in other human cancers, and in some cases linked to the regulation of signal transduction (**Table 5.2**). This bolsters the suggestion that such genes may be important in NBL pathogenesis, and are thus highly pertinent candidates for functional analysis.

For instance we observed overexpression of the DSPs *DUSP7, DUSP3, DUSP4* and *CDKN3*, all of which have been observed to be similarly overexpressed in a range of other cancers (Henkens et al., 2008; Lee et al., 2000; Levy-Nissenbaum et al., 2003a; Levy-Nissenbaum et al., 2003b; Wang et al., 2003). Perhaps of more interest is the very high expression of the phosphatase of regenerating liver (PRL) family genes *PTP4A1/2*, which have been shown by numerous groups to be upregulated in a number of cancers, where they are thought to contribute to growth and metastasis for instance by the regulation of Rho family GTPases (Fiordalisi et al., 2006; Peng et al., 2004; Polato et al., 2005; Zeng et al., 2003). Studies have also shown that targeting PRLS with inhibitors, RNAi and monoclonal antibodies has significant anti-cancerous effects (Guo et al., 2008; Pathak et al., 2002; Stephens et al., 2008).

A significant number of RPTPs were expressed at high or low levels in our NBL screen. For instance, we observed lower expression versus non-neoplastic neural tissue of *PTPRG* and *PTPRH,* extending similar observations from other cancers (Nagano et al., 2003; van Doorn et al., 2005). Of note was the low expression of *PTPRJ*, a fairly well defined tumour-suppressor (Ruivenkamp et al., 2002), which has also been shown to directly interact with Erk as well as negatively regulating Akt signalling (Omerovic et al., 2010; Sacco et al., 2009). Similarly low expression of *PTPRK* was also observed in line with similar findings of mutations and loss of heterozygosity (LOH) (Nakamura et al., 2003; Zhang et al., 1998). Low expression of

PTPRK has also been reported in primary NBL tumours (De Preter et al., 2006), and is clearly an interesting target for functional analyses given its proven ability to negatively regulate β-catenin (Novellino et al., 2008), which has been suggested to play a role in NBL pathogenesis (Maris et al., 2007).

PTPRT was also expressed at low levels in this screen, which was one of the first RPTPs to be shown to have a tumour suppressor function in colorectal cancer (Wang et al., 2004), and has also been shown to dephosphorylate STAT3 as well as controlling cell adhesion (Yu et al., 2008; Zhang et al., 2007), suggesting similarity to *PTPRD* (See Chapter 3). One last noteworthy mention is the remarkably high expression of *PTPRS*. As mentioned *PTPRS* is a type IIa RPTP from the same family as *PTPRD*, both of which are generally expressed at similar levels and share functional homology (Pulido et al., 1995). Although little work has been done on the role of PTPσ in cancer, numerous studies hint at a possible role in NBL. For instance PTPσ was shown to directly dephosphorylate receptors for the neurotrophins, suppressing NGF-dependent neurite outgrowth, a process that could be detrimental to NBL cell differentiation (Faux et al., 2007). Similarly a recent study documented the role of PTPσ in synaptic organisation through its interaction with TrkC (Takahashi et al., 2011). Although not as well defined as TrkA/B, TrkC expression has been suggested to contribute favourably to NBL prognosis (Brodeur et al., 2009), as has been shown for breast cancer (Blasco-Gutierrez, 2007). Thus this RPTP is certainly an interesting target for functional analysis.

PTP	**Alteration in neuroblastoma (relative to brain)**	**Alteration in human cancer**	**Cancer type**	**Known signalling events**
Dual specificity phosphatases				
ACP1	High expression	-	-	-
DUSP3	Overexpression	Overexpression (Henkens et al., 2008)	Cervical	-
DUSP4	Overexpression	Overexpression	Breast	-

		(Wang et al., 2003)		
DUSP5	Downregulation	-	-	-
DUSP7	Overexpression	Overexpression (Levy-Nissenbaum et al., 2003a; Levy-Nissenbaum et al., 2003b)	Leukaemia	-
DUSP8	Overexpression	-	-	-
DUSP10	Overexpression	-	-	-
DUSP19	Downregulation	-	-	-
DUSP22	Downregulation	-	-	-
CDC14a	Downregulation	-	-	-
CDKN3	Overexpression	Overexpression (Lee et al., 2000) Mutation (Yeh et al., 2000)	Breast/Prostate Liver	-
EPM2a	Downregulation	-	-	-
MTM1	Downregulation	-	-	-
MTMR1	Downregulation	-	-	-
MTMR4	High expression	-	-	-
MTMR7	Downregulation	-	-	-
MTMR10	Downregulation	-	-	-
PTP4A1	High expression	Overexpression (Stephens et al., 2008) Overexpression and metastasis (Wang et al., 2007)	Pancreatic Oesophageal and CRC	p130CAS cleavage, Rho GTPase activation and Akt signalling (Daouti et al., 2008), (Zeng et al., 2003), (Stephens et al., 2008)
PTP4A2	High expression	Overexpression (Stephens et al., 2008)	Pancreatic CRC	Akt and Erk signalling (Stephens et al.,

		Overexpression and association with metastasis (Zeng et al., 2003)		2008)
SBF1	Downregulation	-	-	-
TNS1	Downregulation	-	-	-
TNS3	Downregulation	-	-	-
Non-receptor PTPs				
PTPN9	High expression	-	-	-
PTPN3	Downregulation	Overexpression (Wu et al., 2006)	Gastric	-
PTPN14	Downregulation	Somatic mutation (Wang et al., 2004)	Breast, lung, gastric, CRC	-
PTPN18	Downregulation	Aberrant splicing (Guimarães et al., 2006)	Thyroid	-
PTPN23	Overexpression	-	-	-
Receptor PTPs				
PTPRB	Downregulation	Overexpression (Foehr et al., 2006; Goldmann et al., 2000; Muller et al., 2004)	Glioma and melanoma	-
PTPRC	Overexpression	-	-	-
PTPRD	Downregulation	Methylation, somatic mutation and microdeletion of 5'UTR (Veeriah et al., 2009), (Solomon et al., 2008), (Nair et	Glioma, melanoma, CRC, liver, head and neck, lung	STAT3 signalling (Veeriah et al., 2009)

		al., 2008)		
PTPRE	High expression	-	-	-
PTPRG	Downregulation	Somatic mutation, methylation and LOH (Cheung et al., 2008; Wang et al., 2004) Downregulation (Liu et al., 2002; van Niekerk and Poels, 1999; Vezzalini et al., 2007) Methylation (van Doorn et al., 2005; Wang and Dai, 2007)	Head and neck Breast, ovarian and lung Gastric and lymphoma	-
PTPRH	Downregulation	Downregulation (Nagano et al., 2003)	Liver	-
PTPRJ	Downregulation	LOH and missense mutation (Ruivenkamp et al., 2002) SNP and LOH (Ruivenkamp et al., 2002), SNP (Iuliano et al., 2004)	Colon, breast and lung CRC Thyroid	Erk1/2 interaction, p120 catenin signalling, ZO1 dephosphorylation, EGFR endocytosis (Kovalenko et al., 2000; Sacco et al., 2009; Tarcic et al., 2009)
PTPRK	Downregulation	Downregulation (McArdle et al., 2001; Zhang et al., 1998) LOH (Nakamura et al., 2003)	Melanoma Lymphoma	β-catenin-E-cadherin complex (Novellino et al., 2008)

PTPRM	Downregulation	Downregulation (Burgoyne et al., 2009; Sallee et al., 2006)	Glioma and melanoma	E-cadherin dependent adhesion (Hellberg et al., 2002)
PTPRN	Downregulation	-	-	-
PTPRR	Downregulation	-	-	-
PTPRS	High expression	Somatic mutation (Korff et al., 2008)	CRC	EGFR signalling
PTPRT	Downregulation	Somatic mutation (Wang et al., 2004)	CRC, gastric, lung	EGFR, paxillin and STAT3 signalling (Zhang et al., 2007; Zhao et al., 2010)
PTPRV	Downregulation	-	-	-
Class III phosphatases				
CDC25b	Upregulation	-	-	-
CDC25c	Upregulation	-	-	-

Table 5.2. Expression alteration of PTPs in NBL qPCR screen and their relation to published alterations/functional analyses in other cancers. Table documents the findings of the qPCR PTP screen, where applicable studies have been referenced documenting evidence of gene involvement in other cancer types. Expression levels are in comparison to CNS neural tissue, where high expression indicates that both NBL and non-neoplastic neural tissue expressed a given gene at similar levels, whereas overexpression (and conversely downregulation) denotes a difference between NBL and non-neoplastic neural tissue, although it should be noted that CNS tissue is distinct from SNS tissue (from which NBL is derived). Where known, an indication of possible molecular events concerning tumour function has been specified. LOH – loss of heterozygosity. CRC - Colorectal cancer. For further discussion see (Julien et al., 2011).

In sum a number of PTPs have been shown to be highly expressed, upregulated and downregulated in NBL in comparison to normal tissue. A number of such expression alterations agree with published data concerning the expression of PTPs in other human cancers. Furthermore a number of PTPs with roles in relevant biological processes such as regulation of motility, adhesion and signal transduction have been documented as functionally involved in cancer suppression/formation, allowing the

generation of hypotheses concerning functionality in NBL. As well as extending the findings of the known cancer phosphatome, the expression of PTPs whose function in cancer is currently unknown was also altered, hinting at further targets for exploration in NBL.

5.3.2. Clustering analysis

We previously documented stark differences in the responsiveness of NBL cell lines to PTP inhibition using BMOV/VA (See chapters 4-5). We wished to understand whether these differences might reflect actual expression levels of a particular subset of/individual PTPs, whereby comparatively high expression PTPs whose inhibition is required for BMOV/VA responsiveness may confer resistance to the effects of these compounds. Although the converse argument may also apply whereby high expression of PTPs may confer sensitivity, given that cells may rely on that high expression for survival/maintenance of an undifferentiated state. Thus we sought to conduct an unbiased clustering analysis based on our expression profile of 92 PTPs, grouping cell lines that were either unresponsive to BMOV, or those that responded to BMOV by either undergoing neuritogenesis or apoptosis, as well as non-neoplastic neural tissue and glioblastoma cells (GBM).

As expected we observed strong clustering of non-neoplastic neural tissue (group 1, light green bar) compared with all tumour lines, as well as clustering of GBM lines (group 2, blue bar) versus NBL lines, although this was not as dramatic (**Figure 5.5**). Interestingly we did observe weak clustering of neuritogenic NBL lines (group 4, yellow bar). However clustering was not particularly observed for either unresponsive NBL lines (group 3, red bar) or apoptotic NBL lines (group 5, dark green bar), which did not form unified subgroups. In fact half of the unresponsive NBL group segmented on the BMOV-responsive half of the dendrogram, at the opposite end to Non-neoplastic neural tissue/GBM cells, suggesting little deviation in their expression pattern compared with responsive cells.

Given that the extent of our qPCR profile was confined to only 92 genes, i.e. the PTP family only, which comprise a broad range of functions and substrates, we reasoned that this analysis was unlikely to reveal large differences between the entire PTP family within NBL cell lines, which share similar lineages. Thus we sought

to conduct a an unbiased statistical analysis comparing individual sub groups of NBL cells in order to identify individual PTPs whose differential expression might reflect differences in the responsiveness of cells to PTP inhibition.

Indeed between subjects t-tests revealed a small number of genes whose expression was significantly different in BMOV-unresponsive, BMOV-Neuritogenic and BMOV-Apoptotic cell lines (**Figure 5.6**). An overall comparison between BMOV-unresponsive cells (SK-N-AS, SK-N-DZ, IPhNB1, SK-N-BE(2)) and BMOV-responsive cells (SH-SY5Y, SK-N-SH, LAN5, IMR32, Kelly, KCNR) revealed a statistically significant difference in the expression of 3 genes (3%). Specifically *PTPN5* and *DUSP26* were expressed at higher levels in unresponsive cells versus responsive cells (p=0.035 and 0.019 respectively), while *PTPN23* had the opposite profile (p=0.017) (**Figure 5.6A**).
A comparison between unresponsive cells and neuritogenic cells revealed differences in the overall expression of 7 genes (8%). Specifically *DUSP19* (p=0.042), *PTP4A3* (p=0.017), *MTMR10* (p=0.019) and *PTPRB* (p=0.043) were all expressed at higher levels in BMOV-unresponsive cells versus those that undergo neurite extension in response to BMOV, while *PTPN23* (p=0.008) and *PTPRO* (p<0.001) had the opposite profile (**Figure 5.6B**). The same comparison between unresponsive cells and those that undergo apoptosis in response to BMOV failed to yield any genes that were differentially expressed at a statistically significant level. Lastly BMOV-neuritogenic and BMOV-apoptotic groups showed differential expression of 3 genes (3%), namely *DUSP7* (p=0.019) and *PTPRO* (P=0.03), which were expressed at higher levels in the latter group, and *SSH1* (P=<0.001) that had the opposite profile (**Figure 5.6C**).

5.4. Discussion

Gene expression analysis is an important tool in elucidating underlying effectors of tumorigenesis and the mechanism of action of targeted therapy. So far little research has been done on the role of the phosphatome in NBL tumours, and while

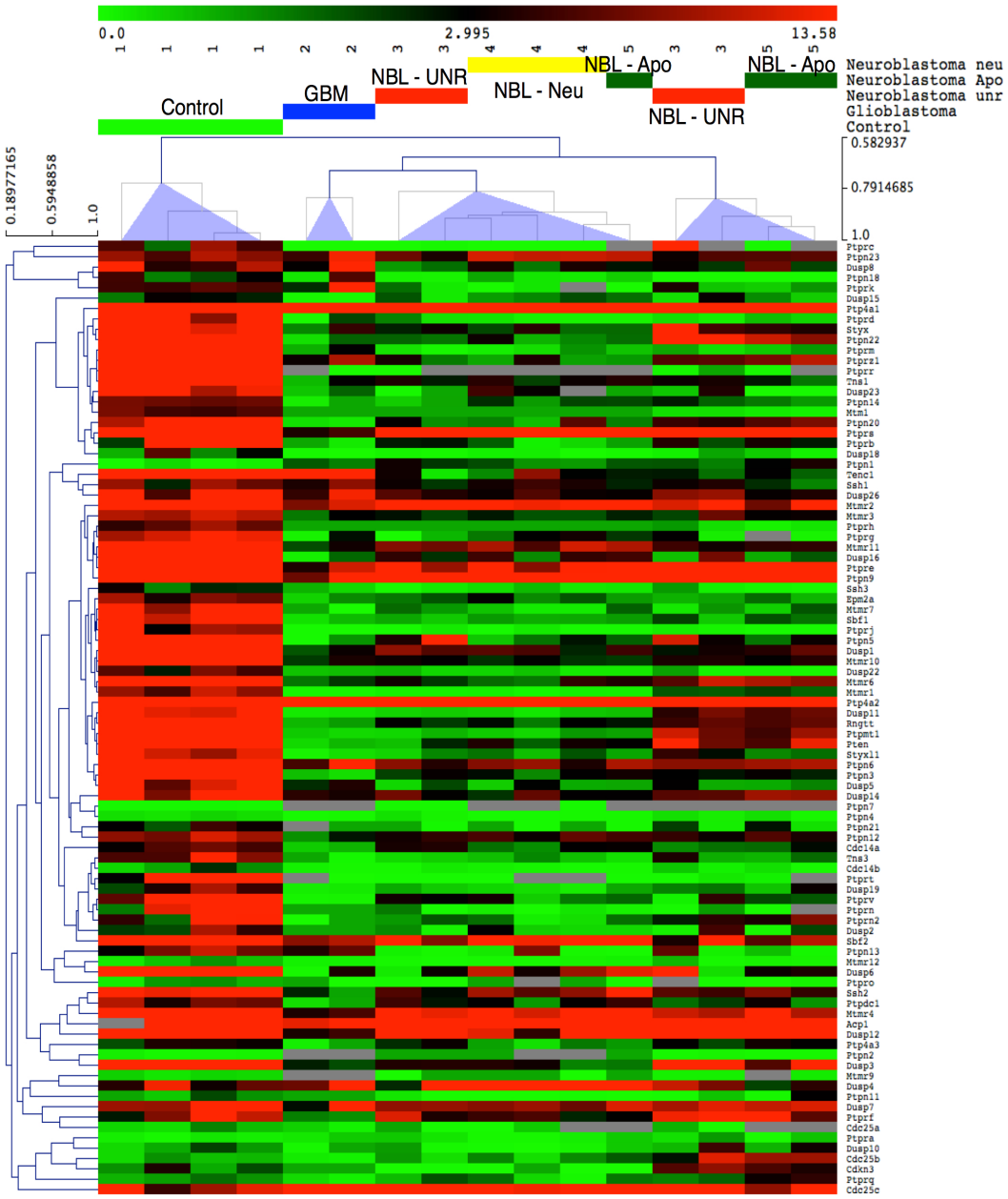

Figure 5.5. Clustering dendrogram of qPCR expression from 92 PTP genes. Strong clustering was observed for non-neoplastic neural tissue cells, however NBL cells failed to cluster on the basis of their responsiveness to BMOV. Cell lines grouped as either unresponsive to BMOV (BMOV-UNR), or those that responded to BMOV by either undergoing neuritogenesis (BMOV-Neu) or apoptosis (BMOV-apo), as well as non-neoplastic neural tissue (control) and glioblastoma cells (GBM).

the present study has broadly demonstrated a role for PTPs in suppressing differentiation and promoting cell survival via non-specific PTP inhibition, the actual drivers of these effects remain unknown. Thus we have conducted qPCR analysis of gene expression of the whole PTP gene family in multiple NBL cell lines, as well as comparison groups of an alternative neural tumour glioblastoma, and non-neoplastic neural tissue. Although the analysis of this sample set has been fairly limited, a number of interesting points can be drawn from this data set. Firstly several candidate tumour suppressors have been highlighted in both NBL and glioblastoma. This is based on stark differences between expression of certain PTPs in non-neoplastic and tumour cells. Interestingly several of these PTPs such as *PTPRT, PTPRG, PTPN3* and *PTPN13* (Wang et al., 2004) and *PTPRH* (Keane et al., 1996), function as tumour suppressors in other cancers, but have not been the subject of functional studies in NBL. Overexpression studies, which would be relatively simple to carry out, might reveal a growth inhibitory or apoptosis-promoting role for such PTPs, as well as highlighting unknown substrates whose activity would be increased by the loss of such tumour suppressors.

At the opposite end of the spectrum, several PTPs are very highly expressed in comparison to the candidate tumour-suppressive PTPs, as well as to levels seen in non-neoplastic neural cells. Follow-up studies from this gene set could potentially highlight PTP oncogenes, of which very few have been identified to date, especially in NBL. This is based on the hypothesis that genes that are very highly expressed in tumour cells are often crucial for the maintenance of cell survival or the suppression of differentiation. This is especially so for enzymes involved in signal transduction, which is likely to remain at steady-state equilibrium following neurogenesis. Given the crucial involvement and high expression of PTPs in general within the nervous system (Paul and Lombroso, 2003), it is curious that certain PTPs are expressed at even higher levels in neural tumour cells. In some cases these genes have already been demonstrated to play functional roles in cancer, such as the PRL phosphatases. Two of these, PRL1 and PRL2, were very highly expressed, albeit at lower levels than non-neoplastic neural tissue, and have been shown to contribute towards metastatic spread and survival signalling via Akt regulation (Stephens et al., 2008; Zeng et al., 2003). Another interesting target is *PTPRS*, which was very highly expressed in all

NBL cell lines, despite expression of type-IIa family members *PTPRF* and *PTPRD*, which have high homology and similar functions (Pulido et al., 1995), being low and very low, respectively. Of particular interest is the fact that PTPσ has recently been shown to interact with TrkC (Takahashi et al., 2011), itself highly expressed in favourable NBL tumours and with a putative role in differentiation (Brodeur et al., 1997; Edsjo et al., 2001).

Thus these genes provide targets for follow up studies, such as siRNA knockdown experiments, which could potentially demonstrate a driver function in NBL tumour formation/maintenance. Of note is that the dual-specificity phosphatases (DUSPs) are particularly enriched in this group, e.g. Dusp4, 7, 10, 8 and 3. DUSPs are considered promising candidates as cancer targets (Pulido and van Huijsduijnen, 2008a), and one such enzyme DUSP26 has been shown to function as a cancer promoting PTP in NBL (Shang et al., 2010). A possible oncogenic role of several DUSPs has also recently been demonstrated by genome-wide-association studies (J. Maris, personal communication).

In terms of the second question addressed, i.e. whether the response to BMOV/VA could delineate NBL cell lines, this analysis has not provided a definitive answer or hint at the underlying functional targets of inhibition. While we were able to perform clustering analysis, NBL sub groups i.e. those responding to PTP inhibition by undergoing neurite-outgrowth, apoptosis or not bearing any response did not cluster based on the any one subset of the PTP family. This is not surprising given that a host of genes beyond PTPs are likely involved in these mechanisms. However it is certainly interesting that a small number of PTPs have a statistically significantly different expression pattern between BMOV-phenotype subgroups. For instance, *DUSP26* was expressed at higher levels on average in BMOV-unresponsive cells versus responsive cells. This is certainly noteworthy given that this dual-specificity phosphatase is the only PTP that has been shown to have a functional oncogenic role in NBL, acting as a p53 phosphatase and causing chemoresistance in NBL cells (Shang et al., 2010). Although we found little evidence of p53-dependence in BMOV-induced apoptosis (See chapter 4), this gene would still be an interesting candidate for further investigation. *PTPN23* was found to be expressed at two-fold higher levels in cell lines that respond to BMOV by undergoing neurite extension compared

with unresponsive cells, possibly hinting at an involvement of this PTP in neurite extension, i.e. conferring resistance when highly expressed.

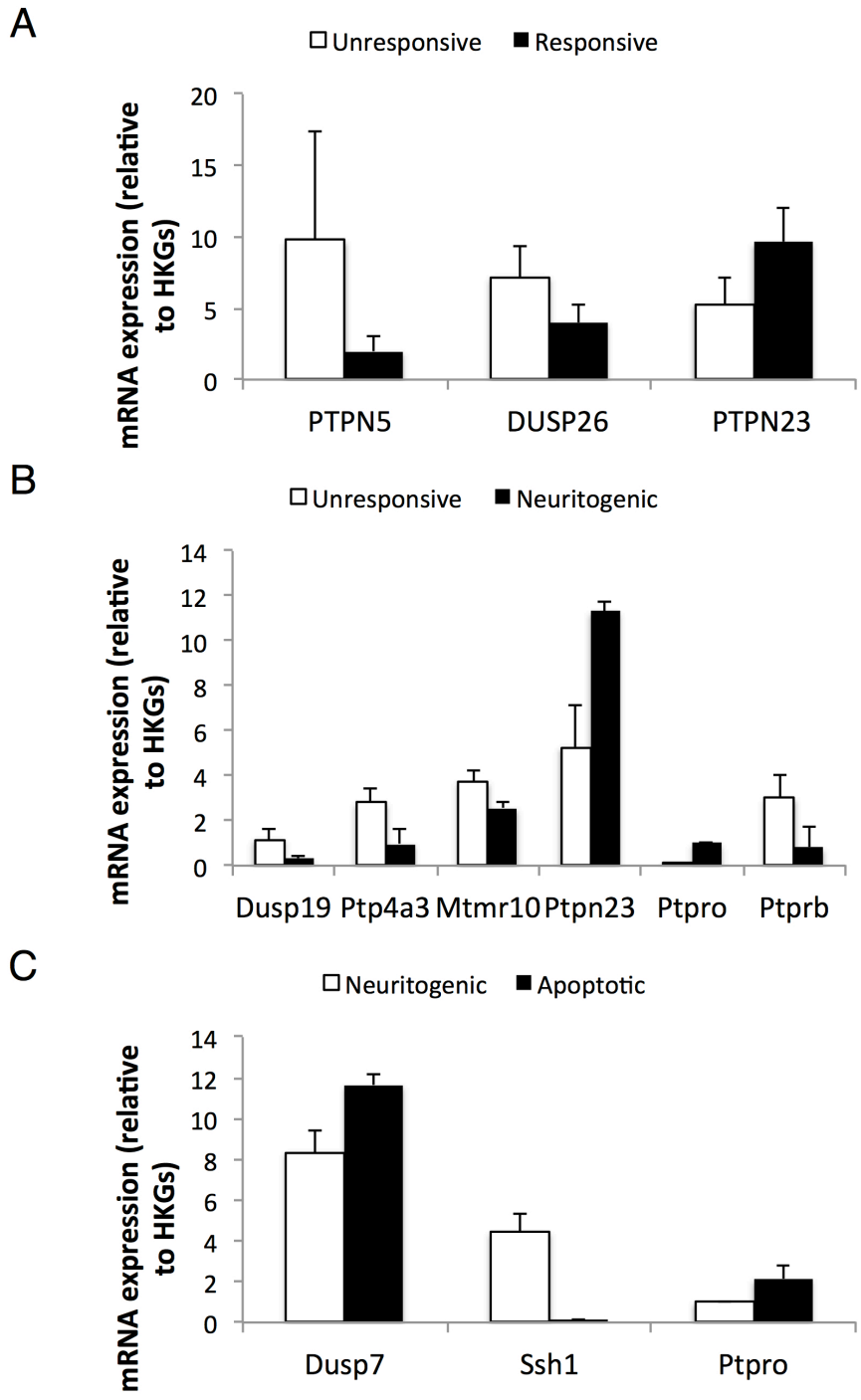

Figure 5.6. Significantly differential expression of PTPs. Graphs showing means and standard deviation of genes exhibiting statistically significant expression between BMOV-unresponsive versus BMOV-responsive cells (**A**), BMOV-unresponsive and BMOV-neuritogenic cells (**B**) and BMOV-neuritogenic and BMOV-apoptotic cells (**C**).

This gene was also expressed at high levels in NBL cells compared with non-neoplastic neural tissue, making it another candidate for further investigation. *PTP4A3* was another gene differentially expressed between these two subgroups, in the opposite manner, representing an interesting candidate in mediating BMOV-resistance given that this PTP is heavily implicated in pro-cancer functions (Kim et al., 2004; Polato et al., 2005; Zeng et al., 2003). Lastly *SSH1* exhibited a remarkably low expression in cells that respond to BMOV by undergoing apoptosis versus neuritogenesis, making it an interesting candidate in explaining this difference in phenotypic response.

This analysis is certainly not without caveats however. For instance significant differences may in some cases be artefacts of low standard deviation observed for PTPs expressed at very low levels, e.g. *PTPRO,* where differences in expression are unlikely to be of consequence given that overall expression is very low. It is also entirely subject to speculation whether differences of less that 1 fold in expression (observed for the majority of statistically significant comparisons), would have a noticeable effect on responsiveness to PTP inhibition. Furthermore differential sensitivity may not simply be a function of differential gene or protein expression, for example KCNR cells and SH-SY5Y cells both respond to PTP inhibition in a similar biochemical manner but leading to highly different phenotypic consequences, presumably reflecting differences in their underlying molecular make-up. Similarly it is not well understood how broad PTP inhibitors may differently inhibit PTP family members, for instance one PTP may be highly expressed while another expressed at lower levels, but the latter may actually be more effectively inhibited due to that lower level of expression, or even a higher sensitivity to the inhibitor. Another caveat is the lack of uniformity within subgroups of NBL lines, for example KCNR cells are more sensitive to BMOV than LAN-5 cells, though both have an apoptotic component of cells following treatment. Furthermore the latter cell line also undergoes neuritogenesis following BMOV treatment, further complicating matters. Thus it may be necessary to expand this data set by testing an even greater number of cell lines and thus increasing the sample size and power of statistical comparisons. However at the very least this analysis has provided some putative targets for

knockdown experiments and specific inhibitors, which may provide a more definitive answer as to the underlying PTPs responsible for the effects of BMOV/VA.

Chapter 6. Concluding remarks

As a diverse group of enzymes with the capacity for the regulation of cell differentiation, survival and proliferation, PTPs are an emergent source of targets for investigation into the pathogenesis, maintenance, and treatment of cancer (Julien et al., 2011; Ostman et al., 2006). Despite the fact that NBL has been classified as the most common and deadly solid tumour of infancy, initiating much research into its underlying causes and targets for intervention (Brodeur, 2003; Janoueix-Lerosey et al., 2010; Maris, 2010; Maris et al., 2007), very few *bona fide* oncogenes and tumour suppressors with a driving role in oncogenesis/tumour maintenance have been identified. Thus as an untapped source of such agents, we sought to examine the role of PTPs in this cancer focussing primarily on the capacity of PTPs to potentially suppress differentiation and apoptosis, thus providing therapeutic targets.

To précis this investigation, we have shown that PTPs in general harbour the capacity to suppress both differentiation and apoptosis, revealing that use of broad PTP inhibitors is a potentially viable therapeutic intervention. When used in combination with an established differentiation-induction agent RA, PTP inhibitors can cause irreversible senescence, while when used as single agents PTP inhibitors can cause potent but selective apoptosis in a significant number of tumour-derived cell lines. Furthermore, we have sought to examine the molecular underpinnings of these effects, finding that the capacity of PTP inhibitors to relieve suppression of RTK-driven signalling pathways actually appears beneficial in mediating the effects of senescence and apoptosis, causing strong and sustained activation of PI3K/Akt signalling when combined with RA, and lower level activation of PI3K/Akt signalling in combination with altered ROS homeostasis, respectively. Finally we have provided at least a preliminary investigation into a putative sub-set of PTPs that may be particularly involved in such processes, which when combined with recent advances in the generation of more specific PTP inhibitors (Ferreira et al., 2006; Hellmuth et al., 2008; Heneberg, 2009; Jiang and Zhang, 2008; Zhang and Zhang, 2007), could lead to more effective targeted therapy in NBL. The most salient point of these findings is the dichotomy of senescence/differentiation and apoptosis, as consequences of vanadium compounds depending on putative effects of RA (**Figure 6.1**).

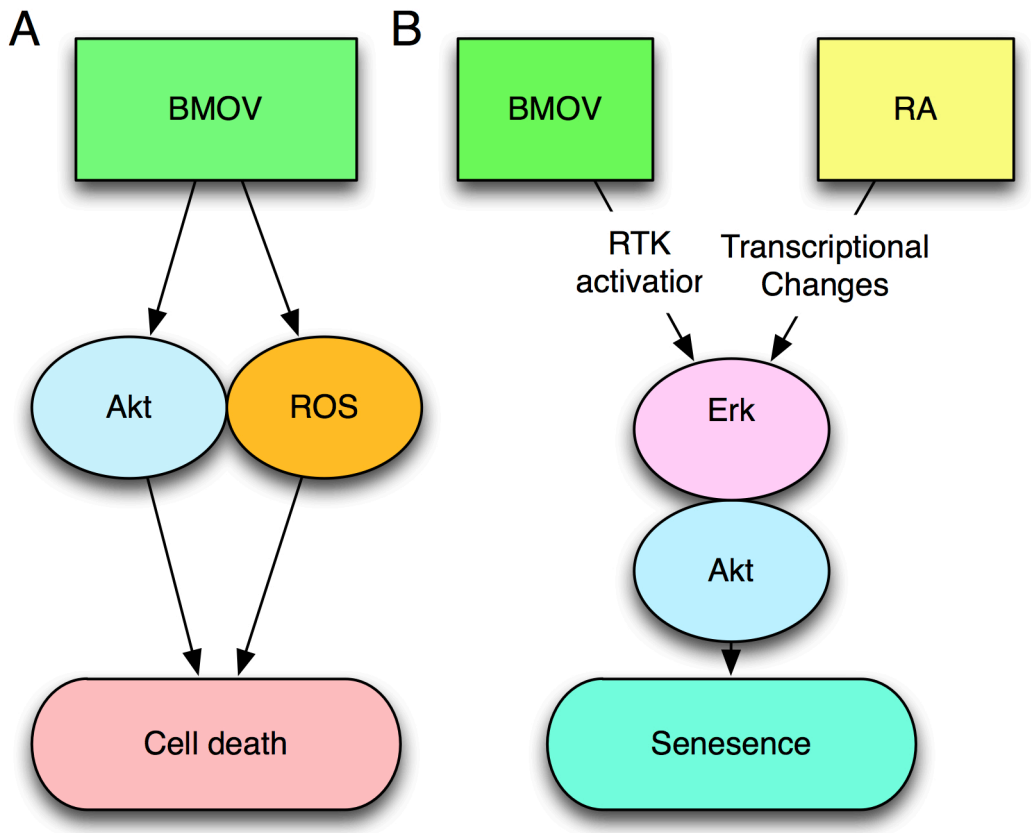

Figure 6.1. Summary of the distinct effects of BMOV in different NBL cell lines. (**A**) BMOV as a single agent causes Akt activation along with altered REDOX homeostasis characterised by ROS production and GSH downregulation, sensitising cells to oxidative apoptosis. (**B**) BMOV causes activation of Akt and Erk downstream of putative RTK signalling which when coupled with RA-induced transcriptional changes causes hyperactivation, driving cells into senescence.

Perhaps the most noteworthy point of this study is that PI3K/Akt signalling has been shown to suffer from two 'Achilles heels', namely the propensity to drive cell senescence when activated and sustained at high levels, and the propensity to selectively kill NBL cells in the presence of heightened ROS production and a lowered capacity to detoxify intracellular ROS. Both findings are paradoxical given that deregulation of PI3K/Akt signalling is a frequent and often crucial event in oncogenesis, and such signalling generally promotes proliferation and cell survival rather than mitigating such behaviour (Hennessy et al., 2005; Paez and Sellers, 2003; Vivanco and Sawyers, 2002). However such strategies are appealing given that targeting an 'Achilles heel' of cancer may not be subject to the same issues associated with targeted therapy against oncogenic drivers, i.e. direct adaptation

through pathway redundancy and/or evolution through Darwinian selection, which ultimately results in tumour relapse and intransigence to therapy (Balmanno et al., 2009; Chandarlapaty et al., 2011; Serra et al., 2011; She et al., 2010; Zhang et al., 2011). Indeed targeting events associated with, but not crucial to, oncogenic transformation, i.e. adaptive changes such as the reliance on tight regulation of an intracellular signalling cascade or stress events such as ROS production, might show greater selectivity than broadly targeting dividing cells (Raj et al., 2011).

These therapeutic strategies are of course not without their caveats. For instance although Akt has been shown to negatively regulate the lifespan of leukaemia-initiating cells (Naka et al., 2010; Tothova et al., 2007), there is still concern that efforts to augment such an anomalous feature of Akt signalling might have negative consequences such as driving proliferation of bulk tumour cells for instance. However we have provided good evidence that although vanadium compounds with any combination of second agent stimulate activation of both Akt and Erk, there is little if any effect on cell proliferation and no discernible effects on non-neoplastic cells. Furthermore there are certainly concerns over using broad inhibitors due to the potential for off-target effects. While one cannot deny that vanadium compounds could potentially have unwanted side effects due to inhibiting an entire enzyme family that carries out vital functions in cell biology, again we have found no evidence for acute non-specific toxicity in non-neoplastic cells.

Although BMOV was shown to be slightly less potent than VA (requiring a two fold dosage increase to achieve comparable effects), the introduction of vanadium compounds containing organic scaffolds was designed historically to limit toxicity-related side effects such as gastrointestinal disturbances often cited as a dosage-limiting factor in the administration of vanadium compounds to patients (Thompson et al., 2009). BMOV also has much better uptake in vivo than vanadium salts. This also highlights an advantage of the use of vanadium compounds as anticancer agents given that a number of such compounds have already been tested on human patients for treatment of type 2 diabetes (Domingo, 2002; Thompson et al., 2009). Not only this but pre-clinical studies have highlighted the efficacy of vanadium compounds on a number of solid tumours (Bishayee et al., 2010). Thus we are at a standpoint in which based on mounting *in vitro* evidence BMOV could easily

be tested on preclinical models of NBL, such as the TH-Mycn transgenic mouse model, which causes Mycn-driven tumours highly similar to primary NBL (Weiss et al., 1997).

The present study has also ruled out potential candidates for further investigation in NBL, a significant feature given the paucity of knowledge concerning NBL pathogenesis. For instance, we have provided evidence that *PTPRD* does not harbour a tumour suppressor function in NBL, despite reports of genetic associations between its expression, mutation and deletion and the development of NBL (Nair et al., 2008; Stallings et al., 2006). This perhaps highlights a general issue in the field of cancer biology that downregulation/genetic mutations often occur as 'passengers' downstream of 'driver' mutations, and may yield false positives in the search for therapeutic targets. Furthermore no evidence has been found for a role of PTEN in NBL pathogenesis, despite its widespread function as a tumour suppressor in other human cancers (Salmena et al., 2008). In fact despite gross differences in PTEN protein expression exhibited in NBL cell lines, we did not find evidence for obvious differences between endogenous Akt activity, suggesting that the PI3K/Akt pathway might be regulated by other rate-limiting factors in NBL. Similarly the finding that Mycn expression can still undergo large decreases following BMOV/RA treatment despite high levels of Akt activity also potentially reveals that targeting Mycn through inhibition of enzymes preventing its degradation (Gustafson and Weiss, 2010; Otto et al., 2009) (i.e. in this case PI3K (Chesler et al., 2006)), may not be necessary given that (a) RA, already used for the treatment of MRD potently decreases Mycn expression, (b) PI3K activity can exist independently of Mycn levels.

One further limitation of the present study is that it is as yet unclear as to why certain NBL cell lines either respond or fail to respond to vanadium compound treatment, and furthermore why some are particularly susceptible to one form of response such as pro-senescence/differentiation (e.g. SH-SY5Y), while others to another form such as apoptosis (e.g. KCNR). Obviously therapeutic resistance is almost unanimously experienced with targeted therapy, and often poorly understood, and it is very likely that BMOV treatment would not be equally effective in all NBL tumours, given their well-characterised heterogeneity and the sheer number of genetic alterations associated with high-stage NBL.

It is still unclear how BMOV exerts such different effects of differentiation and apoptosis. This is highlighted by the fact that BMOV-responsive cell lines such as KCNR seem to undergo apoptosis in response to BMOV as a single agent, yet RA exerts a seemingly neuro-protective effect, limiting cytotoxicity. One possibility is that these effects depend on the level of activity of Akt and/or Erk (which is far greater in the case of BMOV/RA versus BMOV alone), as this has been shown to affect substrate interactions (von Kriegsheim et al., 2009). However LY29/BMOV is also capable of inducing high levels of Akt activity, which result in cell death. Thus one might hypothesise that RA may limit the production of ROS and/or changes in GSH synthesis. While this is a distinct possibility, it will always be difficult to gain a complete understanding of the effects of combination BMOV/RA treatment as both agents instigate wide scale molecular changes in transcription and post-translational modification of proteins. The mechanism of action of RA is still surprisingly poorly understood despite its use in the clinic for over ten years.

One minor irritation during this investigation was the fact that the effectiveness of VA/BMOV treatments on distinct cell lines varied slightly throughout the 3-year study. For instance cell lines such as IMR32, which responded acutely to BMOV treatment by undergoing apoptosis, failed to undergo a phenotypic response at some points. Furthermore BMOV/RA-induced Akt/Erk stimulation also exhibited variability where both the endogenous and RA-mediated activation of both pathways gradually went up from barely detectable levels to significant levels as the study progressed, while the senescence responses varied in that SH-SY5Y cells became more responsive to RA and less responsive to BMOV/RA, initiating the noted later change in dosage of BMOV treatment. Unfortunately these vagaries elicit few obvious explanations. One might of course accept that the number of factors involved in mammalian cell culture (e.g. substratum, serum content, serial passaging) might introduce a certain level of inevitable variability into these experiments. Such variability might also stem however from actual instances of acquired resistance, for instance where cells might gradually increase their tolerance to oxidative stress. However, we feel it unlikely that this is occurring because passage numbers for the cells were monitored and new cell batches were used regularly throughout the study. Finally, it is possible that batch variations in the

chemicals themselves may have had a part to play, although no clear evidence of this was apparent.

Another noted caveat concerning the use of vanadium compounds is that they have been described to achieve a number of effects distinct from PTP inhibition such as oxidative stress, inhibition of ATPases and transcriptional changes (See figure 1.5.3). Thus it is possible that the effects described in the present study occur independently of PTPs. However there are a number of counter points to this argument. First, we detected no evidence of p53/p38 MAPK induction/activation, suggesting that oxidative stress and/or DNA damage is not occurring. Second, the activation of Akt and Erk would be predicted to occur following PTP inhibition, due to relief of negative feedback regulation of RTKs. Lastly the effects described in the present study were often modest, such as the production of ROS or the accumulation of pTyr, suggesting that at the given dosage vanadium compounds are capable of showing selectivity towards specific targets. However the mechanism of action of such compounds is clearly of interest, and will undoubtedly be the subject of on going investigations.

One important task is to better understand the specific PTPs crucial to the response to BMOV and/or BMOV/RA therapy. While we have undertook some analysis to this end, i.e. conducting a qPCR screen and computing clustering analysis, again it is difficult to go beyond speculation at this stage as to which PTPs are required for these responses. Not only this but the general difficulty in designing specific PTP inhibitors based on the highly conserved active site structure present in PTPs would still present a significant barrier to specific targeted therapy. Setting this aside, the functional relevance of individual PTPs to differentiation/apoptosis might be deciphered based on whole PTPome siRNA screening, whereby siRNA libraries targeted towards PTPs would reveal the effects of specific loss of function for each gene on either differentiation, which might be achieved through a high-throughput platform analysing morphological changes, or apoptosis, which could be assessed based on cell survival assays. It is also important to understand the interactions of BMOV and RA. Given that RA exerts large-scale transcriptional changes, these could be correlated with potential BMOV targets for instance PTPs that function as negative regulators of RA-target suppressors. The actual targets of BMOV could at

the same time be better understood through use of 2D-gel electrophoresis or quantitative-phosphoproteomics through stable isotope amino acid labelling in culture and mass spectrometry, revealing widespread protein expression and activation changes influenced by BMOV treatment. The hypothesis that BMOV treatment causes activation of RTKs could easily be tested using an RTK array. Once targets are better understood resistance to BMOV may be potentially revealed through mechanisms such as mutations in targets or differential expression of negative regulators. Resistance could actually be potentially modelled by analysis of changes in protein expression/activation following continual exposure to BMOV and sub-cloning of resistant cells (Engelman et al., 2007; Janne et al., 2009).

Furthermore a number of PTPs were expressed at very low levels in this study, potentially ruling them out for involvement in these effects. Lastly another conceptually interesting exercise would be to compare the expression of PTPs based on our qPCR data with their prognostic value based on the oncogenomics databases (http://home.ccr.cancer.gov/oncology/oncogenomics), whereby statistically significant differences in 5 year EFS rates based on PTP gene expression might reveal further candidates for functional analysis, Although it is difficult to infer causality in survival based simply on the fact that inhibition of PTPs causes a potentially therapeutic benefit, such prognostic analyses would still be a valid starting point.

A perhaps crucial benefit when discussing the viability of vanadium compounds as targeted therapies in NBL is that their use would essentially be drug redeployment. Such redeployment is at an advantage when compared with entirely novel agents due to the wealth of knowledge concerning clinical factors. For example, a number of vanadium compounds have been tested clinically for the use of type 2 diabetes, some under late stage clinical trials. This provides invaluable information as to toxicity issues and dosage requirements/limitations, which have already been instrumental in generating compounds such as BMOV and BEOV that are generally well tolerated clinically. Furthermore due to the ongoing efforts of the diabetes field new compounds are frequently being generated, which may have similar efficacy. Lastly as previously discussed a number of preclinical studies have been carried out describing vanadium compounds as cytotoxic agents (Bishayee et al., 2010), many of which actually predate the discovery of PTPs. Thus as with many

agents that have both been redeployed from the treatment of other diseases and entered the clinic prior to an understanding of their mechanism of action (including RA itself), basic research will undoubtedly go hand in hand with translational studies.

Thus in sum, the present study has provided evidence of a crucial role for the PTP family in both the differentiation and survival of NBL cells. We have devised at least three novel therapeutic combinations (BMOV/RA, BMOV/BSO, BMOV/LY294002) worthy of pre-clinical testing for instance in the aforementioned TH-Mycn transgenic mouse or in NBL xenografts, and provided molecular evidence for the basis of their effects on differentiation/senescence and apoptosis. Not only this but we have shown that by increasing the levels of Akt activation with BMOV one can paradoxically limit cell growth and survival, concomitant with RA-induced transcriptional changes and/or Akt activation or and BMOV-induced ROS production, respectively. This is despite the evidence that the PI3K/Akt pathway can contributes negatively toward NBL patient survival (Opel et al., 2007) and increases cell survival/proliferation in other contexts (Bender et al., 2011), raising a point that is at least conceptually worthy of interest. Lastly we have initiated expression profiling of the entire PTPome in a panel of both Mycn amplified and non-amplified NBL cells, providing useful information both in the delineation of the effects of PTP inhibition, and the search for novel oncogenes, tumour suppressors, and above all therapeutic targets.

References

(1999). Cancer Among Infants - SEER Pediatric Monograph. 1-8.

Abemayor, E., and Sidell, N. (1989). Human neuroblastoma cell lines as models for the in vitro study of neoplastic and neuronal cell differentiation. Environmental Health Perspectives *80*, 3-15.

Acosta, S., Lavarino, C., Paris, R., Garcia, I., de Torres, C., Rodriguez, E., Beleta, H., and Mora, J. (2009). Comprehensive characterization of neuroblastoma cell line subtypes reveals bilineage potential similar to neural crest stem cells. BMC Dev Biol *9*, 12.

Adhikary, S., and Eilers, M. (2005). Transcriptional regulation and transformation by Myc proteins. Nat Rev Mol Cell Biol *6*, 635-645.

Akhavan-Tafti, H., Schaap, A.P., Arghavani, Z., DeSilva, R., Eickholt, R.A., Handley, R.S., Schoenfelner, B.A., Sugioka, K., and Sugioka, Y. (1994). CCD camera imaging for the chemiluminescent detection of enzymes using new ultrasensitive reagents. J Biolumin Chemilumin *9*, 155-164.

Akram, S., Teong, H.F.C., Fliegel, L., Pervaiz, S., and Clément, M.-V. (2005). Reactive oxygen species-mediated regulation of the Na+–H+ exchanger 1 gene expression connects intracellular redox status with cells' sensitivity to death triggers. Cell Death and Differentiation *13*, 628-641.

Alimonti, A., Carracedo, A., Clohessy, J.G., Trotman, L.C., Nardella, C., Egia, A., Salmena, L., Sampieri, K., Haveman, W.J., Brogi, E*., et al.* (2010a). Subtle variations in Pten dose determine cancer susceptibility. Nat Genet *42*, 454-458.

Alimonti, A., Nardella, C., Chen, Z., Clohessy, J.G., Carracedo, A., Trotman, L.C., Cheng, K., Varmeh, S., Kozma, S.C., Thomas, G*., et al.* (2010b). A novel type of cellular senescence that can be enhanced in mouse models and human tumor xenografts to suppress prostate tumorigenesis. J Clin Invest *120*, 681-693.

Alonso, A., Sasin, J., Bottini, N., Friedberg, I., Friedberg, I., Osterman, A., Godzik, A., Hunter, T., Dixon, J., and Mustelin, T. (2004). Protein tyrosine phosphatases in the human genome. Cell *117*, 699-711.

Anderson, C.P., Tsai, J.M., Meek, W.E., Liu, R.-M., Tang, Y., Forman, H.J., and Reynolds, C.P. (1999). Depletion of Glutathione by Buthionine Sulfoximine Is Cytotoxic for Human Neuroblastoma Cell Lines via Apoptosis. Experimental Cell Research *246*, 183-192.

Anderson, D.J., and Axel, R. (1986). A bipotential neuroendocrine precursor whose choice of cell fate is determined by NGF and glucocorticoids. Cell *47*, 1079-1090.

Ara, T., Song, L., Shimada, H., Keshelava, N., Russell, H.V., Metelitsa, L.S., Groshen, S.G., Seeger, R.C., and Declerck, Y.A. (2009). Interleukin-6 in the Bone Marrow Microenvironment Promotes the Growth and Survival of Neuroblastoma Cells. Cancer Research *69*, 329-337.

Araki, T., Nawa, H., and Neel, B.G. (2003). Tyrosyl phosphorylation of Shp2 is required for normal ERK activation in response to some, but not all, growth factors. J Biol Chem *278*, 41677-41684.

Arboleda, M.J., Lyons, J.F., Kabbinavar, F.F., Bray, M.R., Snow, B.E., Ayala, R., Danino, M., Karlan, B.Y., and Slamon, D.J. (2003). Overexpression of AKT2/protein kinase Bbeta leads to up-regulation of beta1 integrins, increased invasion, and metastasis of human breast and ovarian cancer cells. Cancer Res *63*, 196-206.

Ardini, E., Agresti, R., Tagliabue, E., Greco, M., Aiello, P., Yang, L.T., Menard, S., and Sap, J. (2000). Expression of protein tyrosine phosphatase alpha (RPTPalpha) in human breast cancer correlates with low tumor grade, and inhibits tumor cell growth in vitro and in vivo. Oncogene *19*, 4979-4987.

Arias-Romero, L.E., Saha, S., Villamar-Cruz, O., Yip, S.-C., Ethier, S.P., Zhang, Z.-Y., and Chernoff, J. (2009). Activation of Src by protein tyrosine phosphatase 1B Is required for ErbB2 transformation of human breast epithelial cells. Cancer Research *69*, 4582-4588.

Arnold, H.K., Zhang, X., Daniel, C.J., Tibbitts, D., Escamilla-Powers, J., Farrell, A., Tokarz, S., Morgan, C., and Sears, R.C. (2009). The Axin1 scaffold protein promotes formation of a degradation complex for c-Myc. EMBO J *28*, 500-512.

Balmanno, K., Chell, S.D., Gillings, A.S., Hayat, S., and Cook, S.J. (2009). Intrinsic resistance to the MEK1/2 inhibitor AZD6244 (ARRY-142886) is associated with weak ERK1/2 signalling and/or strong PI3K signalling in colorectal cancer cell lines. Int J Cancer *125*, 2332-2341.

Barbero, S., Mielgo, A., Torres, V., Teitz, T., Shields, D.J., Mikolon, D., Bogyo, M., Barilà, D., Lahti, J.M., Schlaepfer, D.*, et al.* (2009). Caspase-8 association with the

focal adhesion complex promotes tumor cell migration and metastasis. Cancer Research *69*, 3755-3763.

Bard-Chapeau, Emilie A., Li, S., Ding, J., Zhang, Sharon S., Zhu, Helen H., Princen, F., Fang, Diane D., Han, T., Bailly-Maitre, B., Poli, V.*, et al.* (2011). Ptpn11/Shp2 Acts as a Tumor Suppressor in Hepatocellular Carcinogenesis. Cancer Cell *19*, 629-639.

Barr, A.J., Ugochukwu, E., Lee, W.H., King, O.N.F., Filippakopoulos, P., Alfano, I., Savitsky, P., Burgess-Brown, N.A., Müller, S., and Knapp, S. (2009). Large-scale structural analysis of the classical human protein tyrosine phosphatome. Cell *136*, 352-363.

Beauséjour, C.M., Krtolica, A., Galimi, F., Narita, M., Lowe, S.W., Yaswen, P., and Campisi, J. (2003). Reversal of human cellular senescence: roles of the p53 and p16 pathways. EMBO J *22*, 4212-4222.

Beierle, E.A., Ma, X., Trujillo, A., Kurenova, E.V., Cance, W.G., and Golubovskaya, V.M. (2010). Inhibition of focal adhesion kinase and src increases detachment and apoptosis in human neuroblastoma cell lines. Mol Carcinog *49*, 224-234.

Beierle, E.A., Trujillo, A., Nagaram, A., Kurenova, E.V., Finch, R., Ma, X., Vella, J., Cance, W.G., and Golubovskaya, V.M. (2007). N-MYC regulates focal adhesion kinase expression in human neuroblastoma. J Biol Chem *282*, 12503-12516.

Bell, E., Chen, L., Liu, T., Marshall, G.M., Lunec, J., and Tweddle, D.A. (2010). MYCN oncoprotein targets and their therapeutic potential. Cancer Lett *293*, 144-157.

Bell, E., Premkumar, R., Carr, J., Lu, X., Lovat, P.E., Kees, U.R., Lunec, J., and Tweddle, D.A. (2006). The role of MYCN in the failure of MYCN amplified neuroblastoma cell lines to G1 arrest after DNA damage. Cell Cycle *5*, 2639-2647.

Beltinger, C.P., White, P.S., Sulman, E.P., Maris, J.M., and Brodeur, G.M. (1995). No CDKN2 mutations in neuroblastomas. Cancer Research *55*, 2053-2055.

Beltran, P.J., and Bixby, J.L. (2003). Receptor protein tyrosine phosphatases as mediators of cellular adhesion. Front Biosci *8*, d87-99.

Bender, A., Opel, D., Naumann, I., Kappler, R., Friedman, L., von Schweinitz, D., Debatin, K.-M., and Fulda, S. (2011). PI3K inhibitors prime neuroblastoma cells for chemotherapy by shifting the balance towards pro-apoptotic Bcl-2 proteins and enhanced mitochondrial apoptosis. Oncogene *30*, 494-503.

Benitogutierrez, E., Garciafernandez, J., and Comella, J. (2006). Origin and evolution of the Trk family of neurotrophic receptors. Molecular and Cellular Neuroscience *31*, 179-192.

Bensaad, K., and Vousden, K.H. (2005). Savior and slayer: the two faces of p53. Nat Med *11*, 1278-1279.

Bentires-Alj, M., and Neel, B.G. (2007). Protein-Tyrosine Phosphatase 1B Is Required for HER2/Neu-Induced Breast Cancer. Cancer Res *15;67*, 2420-2424.

Bentires-Alj, M., Paez, J.G., David, F.S., Keilhack, H., Halmos, B., Naoki, K., Maris, J.M., Richardson, A., Bardelli, A., Sugarbaker, D.J.*, et al.* (2004). Activating mutations of the noonan syndrome-associated SHP2/PTPN11 gene in human solid tumors and adult acute myelogenous leukemia. Cancer Research *64*, 8816-8820.

Berger, A.H., and Pandolfi, P.P. (2010). Haplo-insufficiency: a driving force in cancer. J Pathol *223*, 138-147.

Bialy, L., and Waldmann, H. (2005). Inhibitors of protein tyrosine phosphatases: next-generation drugs? Angew Chem Int Ed Engl *44*, 3814-3839.

Biedler, J.L., Roffler-Tarlov, S., Schachner, M., and Freedman, L.S. (1978). Multiple neurotransmitter synthesis by human neuroblastoma cell lines and clones. Cancer Res *38*, 3751-3757.

Bilwes, A.M., Den Hertog, J., Hunter, T., and Noel, J.P. (1996). Structural basis for inhibition of receptor protein-tyrosine phosphatase-alpha by dimerization. Nature *382*, 555-559.

Birnboim, H.C., and Doly, J. (1979). A rapid alkaline extraction procedure for screening recombinant plasmid DNA. Nucleic Acids Res *7*, 1513-1523.

Bishayee, A., Karmakar, R., Mandal, A., Kundu, S.N., and Chatterjee, M. (1997). Vanadium-mediated chemoprotection against chemical hepatocarcinogenesis in rats: haematological and histological characteristics. Eur J Cancer Prev *6*, 58-70.

Bishayee, A., Waghray, A., Patel, M.A., and Chatterjee, M. (2010). Vanadium in the detection, prevention and treatment of cancer: the in vivo evidence. Cancer Letters *294*, 1-12.

Bjelfman, C., Meyerson, G., Cartwright, C.A., Mellstrom, K., Hammerling, U., and Pahlman, S. (1990). Early activation of endogenous pp60^{src} kinase activity during

neuronal differentiation of cultured human neuroblastoma cells. Mol Cell Biol *10*, 361-370.

Bjorge, J.D., Pang, A., and Fujita, D.J. (2000). Identification of protein-tyrosine phosphatase 1B as the major tyrosine phosphatase activity capable of dephosphorylating and activating c-Src in several human breast cancer cell lines. J Biol Chem *275*, 41439-41446.

Blasco-Gutierrez, M. (2007). TrkC: A New Predictive Marker in Breast Cancer? LCNV.

Blume-Jensen, P., and Hunter, T. (2001). Oncogenic kinase signalling. Nature *411*, 355-365.

Boussif, O., Lezoualc'h, F., Zanta, M.A., Mergny, M.D., Scherman, D., Demeneix, B., and Behr, J.P. (1995). A versatile vector for gene and oligonucleotide transfer into cells in culture and in vivo: polyethylenimine. Proc Natl Acad Sci USA *92*, 7297-7301.

Bown, N., Cotterill, S., Lastowska, M., O'Neill, S., Pearson, A.D., Plantaz, D., Meddeb, M., Danglot, G., Brinkschmidt, C., Christiansen, H*., et al.* (1999). Gain of chromosome arm 17q and adverse outcome in patients with neuroblastoma. N Engl J Med *340*, 1954-1961.

Braig, M., and Schmitt, C.A. (2006). Oncogene-induced senescence: putting the brakes on tumor development. Cancer Research *66*, 2881-2884.

Brodeur, G., Seeger, R., Schwab, M., Varmus, H., and Bishop, J. (1984). Amplification of N-myc in untreated human neuroblastomas correlates with advanced disease stage. Science *224*, 1121-1124.

Brodeur, G.M. (2003). Neuroblastoma: biological insights into a clinical enigma. Nat Rev Cancer *3*, 203-216.

Brodeur, G.M. (2010). Getting into the AKT. JNCI Journal of the National Cancer Institute *102*, 747-749.

Brodeur, G.M., Minturn, J.E., Ho, R., Simpson, A.M., Iyer, R., Varela, C.R., Light, J.E., Kolla, V., and Evans, A.E. (2009). Trk receptor expression and inhibition in neuroblastomas. Clin Cancer Res *15*, 3244-3250.

Brodeur, G.M., Nakagawara, A., Yamashiro, D.J., Ikegaki, N., Liu, X.G., Azar, C.G., Lee, C.P., and Evans, A.E. (1997). Expression of TrkA, TrkB and TrkC in human neuroblastomas. J Neurooncol *31*, 49-55.

Brodeur, G.M., Pritchard, J., Berthold, F., Carlsen, N.L., Castel, V., Castelberry, R.P., De Bernardi, B., Evans, A.E., Favrot, M., and Hedborg, F. (1993). Revisions of the international criteria for neuroblastoma diagnosis, staging, and response to treatment. J Clin Oncol *11*, 1466-1477.

Brodeur, G.M., and Seeger, R.C. (1986). Gene amplification in human neuroblastomas: basic mechanisms and clinical implications. Cancer Genet Cytogenet *19*, 101-111.

Brodeur, G.M., Seeger, R.C., Barrett, A., Berthold, F., Castleberry, R.P., D'Angio, G., De Bernardi, B., Evans, A.E., Favrot, M., and Freeman, A.I. (1988). International criteria for diagnosis, staging, and response to treatment in patients with neuroblastoma. J Clin Oncol *6*, 1874-1881.

Bröker, L.E., Kruyt, F.A.E., and Giaccone, G. (2005). Cell death independent of caspases: a review. Clin Cancer Res *11*, 3155-3162.

Bronner Fraser, M. (1994). Neural crest cell formation and migration in the developing embryo. Faseb J *8*, 699-706.

Brunet, A., Bonni, A., Zigmond, M.J., Lin, M.Z., Juo, P., Hu, L.S., Anderson, M.J., Arden, K.C., Blenis, J., and Greenberg, M.E. (1999). Akt promotes cell survival by phosphorylating and inhibiting a Forkhead transcription factor. Cell *96*, 857-868.

Brunton, V.G., and Frame, M.C. (2008). Src and focal adhesion kinase as therapeutic targets in cancer. Curr Opin Pharmacol *8*, 427-432.

Brunton, V.G., Ozanne, B.W., Paraskeva, C., and Frame, M.C. (1997). A role for epidermal growth factor receptor, c-Src and focal adhesion kinase in an in vitro model for the progression of colon cancer. Oncogene *14*, 283-293.

Buist, A., Zhang, Y.L., Keng, Y.F., Wu, L., Zhang, Z.Y., and den Hertog, J. (1999). Restoration of potent protein-tyrosine phosphatase activity into the membrane-distal domain of receptor protein-tyrosine phosphatase alpha. Biochemistry *38*, 914-922.

Burgoyne, A.M., Palomo, J.M., Phillips-Mason, P.J., Burden-Gulley, S.M., Major, D.L., Zaremba, A., Robinson, S., Sloan, A.E., Vogelbaum, M.A., Miller, R.H.*, et al.* (2009). PTPmu suppresses glioma cell migration and dispersal. Neuro-Oncology *11*, 767-778.

Burnette, W.N. (1981). "Western blotting": electrophoretic transfer of proteins from sodium dodecyl sulfate--polyacrylamide gels to unmodified nitrocellulose and radiographic detection with antibody and radioiodinated protein A. Anal Biochem *112*, 195-203.

Cane, K.N., and Anderson, C.R. (2009). Generating diversity: Mechanisms regulating the differentiation of autonomic neuron phenotypes. Auton Neurosci *151*, 17-29.

Carr-Wilkinson, J., O'Toole, K., Wood, K.M., Challen, C.C., Baker, A.G., Board, J.R., Evans, L., Cole, M., Cheung, N.-K.V., Boos, J.*, et al.* (2010). High Frequency of p53/MDM2/p14ARF Pathway Abnormalities in Relapsed Neuroblastoma. Clin Cancer Res *16*, 1108-1118.

Carracedo, A., Alimonti, A., and Pandolfi, P.P. (2011). PTEN Level in Tumor Suppression: How Much Is Too Little? Cancer Res *71*, 629-633.

Castaño, Z., Gordon-Weeks, P.R., and Kypta, R.M. (2010). The neuron-specific isoform of glycogen synthase kinase-3beta is required for axon growth. J Neurochem *113*, 117-130.

Chan, G., Kalaitzidis, D., and Neel, B.G. (2008). The tyrosine phosphatase Shp2 (PTPN11) in cancer. Cancer Metastasis Rev *27*, 179-192.

Chandarlapaty, S., Sawai, A., Scaltriti, M., Rodrik-Outmezguine, V., Grbovic-Huezo, O., Serra, V., Majumder, P.K., Baselga, J., and Rosen, N. (2011). AKT Inhibition Relieves Feedback Suppression of Receptor Tyrosine Kinase Expression and Activity. Cancer Cell *19*, 58-71.

Chen, I., and Dubnau, D. (2004). DNA uptake during bacterial transformation. Nat Rev Micro *2*, 241-249.

Chen, L., Iraci, N., Gherardi, S., Gamble, L.D., Wood, K.M., Perini, G., Lunec, J., and Tweddle, D.A. (2010a). p53 is a direct transcriptional target of MYCN in neuroblastoma. Cancer Research *70*, 1377-1388.

Chen, L., Liu, L., Yin, J., Luo, Y., and Huang, S. (2009). Hydrogen peroxide-induced neuronal apoptosis is associated with inhibition of protein phosphatase 2A and 5, leading to activation of MAPK pathway. Int J Biochem Cell Biol *41*, 1284-1295.

Chen, L., Malcolm, A.J., Wood, K.M., Cole, M., Variend, S., Cullinane, C., Pearson, A.D.J., Lunec, J., and Tweddle, D.A. (2007). p53 is nuclear and functional in both undifferentiated and differentiated neuroblastoma. Cell Cycle *6*, 2685-2696.

Chen, L., Xu, B., Liu, L., Luo, Y., Yin, J., Zhou, H., Chen, W., Shen, T., Han, X., and Huang, S. (2010b). Hydrogen peroxide inhibits mTOR signaling by activation of AMPKα leading to apoptosis of neuronal cells. Laboratory Investigation *90*, 762-773.

Chen, X., Zhong, Z., Xu, Z., Chen, L., and Wang, Y. (2010c). 2',7'-Dichlorodihydrofluorescein as a fluorescent probe for reactive oxygen species measurement: Forty years of application and controversy. Free Radic Res *44*, 587-604.

Chen, Y., Takita, J., Choi, Y.L., Kato, M., Ohira, M., Sanada, M., Wang, L., Soda, M., Kikuchi, A., Igarashi, T.*, et al.* (2008). Oncogenic mutations of ALK kinase in neuroblastoma. Nature *455*, 971-974.

Chen, Z., Trotman, L.C., Shaffer, D., Lin, H.-K., Dotan, Z.A., Niki, M., Koutcher, J.A., Scher, H.I., Ludwig, T., Gerald, W.*, et al.* (2005). Crucial role of p53-dependent cellular senescence in suppression of Pten-deficient tumorigenesis. Nature *436*, 725-730.

Chesler, L., Goldenberg, D.D., Collins, R., Grimmer, M., Kim, G.E., Tihan, T., Nguyen, K., Yakovenko, S., Matthay, K.K., and Weiss, W.A. (2008). Chemotherapy-induced apoptosis in a transgenic model of neuroblastoma proceeds through p53 induction. Neoplasia (New York, NY) *10*, 1268-1274.

Chesler, L., Schlieve, C., Goldenberg, D.D., Kenney, A., Kim, G., McMillan, A., Matthay, K.K., Rowitch, D., and Weiss, W.A. (2006). Inhibition of phosphatidylinositol 3-kinase destabilizes Mycn protein and blocks malignant progression in neuroblastoma. Cancer Research *66*, 8139-8146.

Chesler, L., and Weiss, W.A. (2011). Genetically engineered murine models - Contribution to our understanding of the genetics, molecular pathology and therapeutic targeting of neuroblastoma. Seminars in Cancer Biology *21*, 245-255.

Cheung, A.K.L., Lung, H.L., Hung, S.C., Law, E.W.L., Cheng, Y., Yau, W.L., Bangarusamy, D.K., Miller, L.D., Liu, E.T.-B., Shao, J.-Y.*, et al.* (2008). Functional analysis of a cell cycle-associated, tumor-suppressive gene, protein tyrosine

phosphatase receptor type G, in nasopharyngeal carcinoma. Cancer Res *68*, 8137-8145.

Chevrier, L., Meunier, A.-C., Cochaud, S., Muller, J.-M., and Chadéneau, C. (2008). Vasoactive intestinal peptide decreases MYCN expression and synergizes with retinoic acid in a human MYCN-amplified neuroblastoma cell line. Int J Oncol *33*, 1081-1089.

Chiarugi, P., Pani, G., Giannoni, E., Taddei, L., Colavitti, R., Raugei, G., Symons, M., Borrello, S., Galeotti, T., and Ramponi, G. (2003). Reactive oxygen species as essential mediators of cell adhesion: the oxidative inhibition of a FAK tyrosine phosphatase is required for cell adhesion. J Cell Biol *161*, 933-944.

Chin, L.S., Murray, S.F., Harter, D.H., Doherty, P.F., and Singh, S.K. (1999). Sodium Vanadate Inhibits Apoptosis in Malignant Glioma Cells: A Role for Akt/PKB. Journal of Biomedical Science *6*, 213-218.

Chintala, S.K., Kyritsis, A.P., Mohan, P.M., Mohanam, S., Sawaya, R., Gokslan, Z., Yung, W.K., Steck, P., Uhm, J.H., Aggarwal, B.B*., et al.* (1999). Altered actin cytoskeleton and inhibition of matrix metalloproteinase expression by vanadate and phenylarsine oxide, inhibitors of phosphotyrosine phosphatases: Modulation of migration and invasion of human malignant glioma cells. Mol Carcinog *26*, 274-285.

Christie, K.J., Webber, C.A., Martinez, J.A., Singh, B., and Zochodne, D.W. (2010). PTEN inhibition to facilitate intrinsic regenerative outgrowth of adult peripheral axons. J Neurosci *30*, 9306-9315.

Clagett-Dame, M., Mcneill, E.M., and Muley, P.D. (2006). Role of all-trans retinoic acid in neurite outgrowth and axonal elongation. J Neurobiol *66*, 739-756.

Cohn, S.L., and Tweddle, D.A. (2004). MYCN amplification remains prognostically strong 20 years after its "clinical debut". Eur J Cancer *40*, 2639-2642.

Collado, M., Blasco, M.A., and Serrano, M. (2007). Cellular senescence in cancer and aging. Cell *130*, 223-233.

Collado, M., and Serrano, M. (2010). Senescence in tumours: evidence from mice and humans. Nat Rev Cancer *10*, 51-57.

Courtois-Cox, S., Genther Williams, S.M., Reczek, E.E., Johnson, B.W., McGillicuddy, L.T., Johannessen, C.M., Hollstein, P.E., MacCollin, M., and Cichowski,

K. (2006). A negative feedback signaling network underlies oncogene-induced senescence. Cancer Cell *10*, 459-472.

Cross, F.R., Garber, E.A., Pellman, D., and Hanafusa, H. (1984). A short sequence in the p60src N terminus is required for p60src myristylation and membrane association and for cell transformation. Mol Cell Biol *4*, 1834-1842.

Crossthwaite, A.J., Hasan, S., and Williams, R.J. (2002). Hydrogen peroxide-mediated phosphorylation of ERK1/2, Akt/PKB and JNK in cortical neurones: dependence on Ca(2+) and PI3-kinase. J Neurochem *80*, 24-35.

Cushing, H., and Wolbach, S.B. (1927). The transformation of a malignant paravertebral sympathicoblastom into a benign ganglioneuroma. AM J Pathol *3*, 203-2016.2017.

Daouti, S., Li, W.-h., Qian, H., Huang, K.-S., Holmgren, J., Levin, W., Reik, L., McGady, D.L., Gillespie, P., Perrotta, A.*, et al.* (2008). A selective phosphatase of regenerating liver phosphatase inhibitor suppresses tumor cell anchorage-independent growth by a novel mechanism involving p130Cas cleavage. Cancer Res *68*, 1162-1169.

Davies, K.J. (1995). Oxidative stress: the paradox of aerobic life. Biochem Soc Symp *61*, 1-31.

De Brouwer, S., De Preter, K., Kumps, C., Zabrocki, P., Porcu, M., Westerhout, E.M., Lakeman, A., Vandesompele, J., Hoebeeck, J., Van Maerken, T.*, et al.* (2010). Meta-analysis of neuroblastomas reveals a skewed ALK mutation spectrum in tumors with MYCN amplification. In Clin Cancer Res, pp. 4353-4362.

De Preter, K., Vandesompele, J., Heimann, P., and Yigit, N. (2006). Human fetal neuroblast and neuroblastoma transcriptome analysis confirms neuroblast origin and highlights neuroblastoma candidate

genes. Genome Biol *7*, R84.

de Tudela, M.V.-P., Delgado-Esteban, M., Cuende, J., Bolaños, J.P., and Almeida, A. (2010). Human neuroblastoma cells with MYCN amplification are selectively resistant to oxidative stress by transcriptionally up-regulating glutamate cysteine ligase. J Neurochem *113*, 819-825.

den Hertog, J., Groen, A., and van der Wijk, T. (2005). Redox regulation of protein-tyrosine phosphatases. Arch Biochem Biophys *434*, 11-15.

den Hertog, J., Pals, C.E., Peppelenbosch, M.P., Tertoolen, L.G., de Laat, S.W., and Kruijer, W. (1993). Receptor protein tyrosine phosphatase alpha activates pp60c-src and is involved in neuronal differentiation. Embo J *12*, 3789-3798.

den Hertog, J., Tracy, S., and Hunter, T. (1994). Phosphorylation of receptor protein-tyrosine phosphatase alpha on Tyr789, a binding site for the SH3-SH2-SH3 adaptor protein GRB-2 in vivo. EMBO Journal *13*, 3020-3032.

Denicola, G.M., Karreth, F.A., Humpton, T.J., Gopinathan, A., Wei, C., Frese, K., Mangal, D., Yu, K.H., Yeo, C.J., Calhoun, E.S.*, et al.* (2011). Oncogene-induced Nrf2 transcription promotes ROS detoxification and tumorigenesis. Nature *475*, 106-109.

Denu, J.M., Lohse, D.L., Vijayalakshmi, J., Saper, M.A., and Dixon, J.E. (1996). Visualization of intermediate and transition-state structures in protein-tyrosine phosphatase catalysis. Proceedings of the National Academy of Sciences of the United States of America *93*, 2493-2498.

Dewang, P.M., Hsu, N.M., Peng, S.Z., and Li, W.R. (2005). Protein tyrosine phosphatases and their inhibitors. Curr Med Chem *12*, 1-22.

Di Cristofano, A., Pesce, B., Cordon-Cardo, C., and Pandolfi, P.P. (1998). Pten is essential for embryonic development and tumour suppression. Nat Genet *19*, 348-355.

Diehn, M., Cho, R.W., Lobo, N.A., Kalisky, T., Dorie, M.J., Kulp, A.N., Qian, D., Lam, J.S., Ailles, L.E., Wong, M.*, et al.* (2009). Association of reactive oxygen species levels and radioresistance in cancer stem cells. Nature *458*, 780-783.

Dimri, G.P., Lee, X., Basile, G., Acosta, M., Scott, G., Roskelley, C., Medrano, E.E., Linskens, M., Rubelj, I., and Pereira-Smith, O. (1995). A biomarker that identifies senescent human cells in culture and in aging skin in vivo. Proc Natl Acad Sci USA *92*, 9363-9367.

Ding, L., Ellis, M.J., Li, S., Larson, D.E., Chen, K., Wallis, J.W., Harris, C.C., McLellan, M.D., Fulton, R.S., Fulton, L.L.*, et al.* (2010). Genome remodelling in a basal-like breast cancer metastasis and xenograft. Nature *464*, 999-1005.

Domenicotti, C., Marengo, B., Nitti, M., Verzola, D., Garibotto, G., Cottalasso, D., Poli, G., Melloni, E., Pronzato, M.A., and Marinari, U.M. (2003a). A novel role of protein kinase C-delta in cell signaling triggered by glutathione depletion. Biochem Pharmacol *66*, 1521-1526.

Domenicotti, C., Marengo, B., Verzola, D., Garibotto, G., Traverso, N., Patriarca, S., Maloberti, G., Cottalasso, D., Poli, G., Passalacqua, M.*, et al.* (2003b). Role of PKC-delta activity in glutathione-depleted neuroblastoma cells. Free Radic Biol Med *35*, 504-516.

Domenicotti, C., Paola, D., Vitali, A., Nitti, M., d'Abramo, C., Cottalasso, D., Maloberti, G., Biasi, F., Poli, G., Chiarpotto, E.*, et al.* (2000). Glutathione depletion induces apoptosis of rat hepatocytes through activation of protein kinase C novel isoforms and dependent increase in AP-1 nuclear binding. Free Radic Biol Med *29*, 1280-1290.

Domingo, J.L. (2002). Vanadium and tungsten derivatives as antidiabetic agents: a review of their toxic effects. Biol Trace Elem Res *88*, 97-112.

Domingo, J.L., Gomez, M., Sanchez, D.J., Llobet, J.M., and Keen, C.L. (1995). Toxicology of vanadium compounds in diabetic rats: the action of chelating agents on vanadium accumulation. Mol Cell Biochem *153*, 233-240.

Downward, J. (2003). Targeting RAS signalling pathways in cancer therapy. Nature Reviews Cancer *3*, 11-22.

Duester, G. (2008). Retinoic acid synthesis and signaling during early organogenesis. Cell *134*, 921-931.

Easton, J.B., Royer, A.R., and Middlemas, D.S. (2006). The protein tyrosine phosphatase, Shp2, is required for the complete activation of the RAS/MAPK pathway by brain-derived neurotrophic factor. J Neurochem *97*, 834-845.

Easty, D., Gallagher, W., and Bennett, D.C. (2006). Protein tyrosine phosphatases, new targets for cancer therapy. Curr Cancer Drug Targets *6*, 519-532.

Edsjo, A., Hallberg, B., Fagerstrom, S., Larsson, C., Axelson, H., and Pahlman, S. (2001). Differences in early and late responses between neurotrophin-stimulated trkA- and trkC-transfected SH-SY5Y neuroblastoma cells. Cell Growth Differ *12*, 39-50.

Edwards, J.G., Campbell, G., Grierson, A.W., and Kinn, S.R. (1991). Vanadate inhibits both intercellular adhesion and spreading on fibronectin of BHK21 cells and transformed derivatives. J Cell Sci *98*, 363-368.

Eggert, A., Grotzer, M.A., Ikegaki, N., Liu, X.G., Evans, A.E., and Brodeur, G.M. (2002). Expression of the neurotrophin receptor TrkA down-regulates expression and

function of angiogenic stimulators in SH-SY5Y neuroblastoma cells. Cancer Res *62*, 1802-1808.

Eggert, A., Ikegaki, N., Liu, X.G., and Brodeur, G.M. (2000). Prognostic and biological role of neurotrophin-receptor TrkA and TrkB in neuroblastoma. Klin Padiatr *212*, 200-205.

Elberg, G., Li, J., and Shechter, Y. (1994). Vanadium activates or inhibits receptor and non-receptor protein tyrosine kinases in cell-free experiments, depending on its oxidation state. Possible role of endogenous vanadium in controlling cellular protein tyrosine kinase activity. J Biol Chem *269*, 9521-9527.

Elchebly, M., Payette, P., Michaliszyn, E., Cromlish, W., Collins, S., Loy, A.L., Normandin, D., Cheng, A., Himms-Hagen, J., Chan, C.C.*, et al.* (1999). Increased insulin sensitivity and obesity resistance in mice lacking the protein tyrosine phosphatase-1B gene. Science *283*, 1544-1548.

Elgendy, M., Sheridan, C., Brumatti, G., and Martin, S.J. (2011). Oncogenic Ras-Induced Expression of Noxa and Beclin-1 Promotes Autophagic Cell Death and Limits Clonogenic Survival. Molecular Cell *8;42*, 23-35.

Emmendörffer, A., Hecht, M., Lohmann-Matthes, M.-L., and Roesler, J. (1990). A fast and easy method to determine the production of reactive oxygen intermediates by human and murine phagocytes using dihydrorhodamine 123. Journal of Immunological Methods *131*, 269-275.

Encinas, M., Iglesias, M., Liu, Y., Wang, H., Muhaisen, A., Cena, V., Gallego, C., and Comella, J. (2000a). Sequential treatment of SH-SY5Y cells with retinoic acid and brain-derived neurotrophic factor gives rise to fully differentiated, neurotrophic factor-dependent, human neuron-like cells. J Neurochem *75*, 991.

Encinas, M., Iglesias, M., Liu, Y., Wang, H., Muhaisen, A., Ceña, V., Gallego, C., and Comella, J.X. (2000b). Sequential treatment of SH-SY5Y cells with retinoic acid and brain-derived neurotrophic factor gives rise to fully differentiated, neurotrophic factor-dependent, human neuron-like cells. J Neurochem *75*, 991-1003.

Endl, E., and Gerdes, J. (2000). The Ki-67 protein: fascinating forms and an unknown function. In Exp Cell Res, pp. 231-237.

Engel, R.H., and Evens, A.M. (2006). Oxidative stress and apoptosis: a new treatment paradigm in cancer. Front Biosci *11*, 300-312.

Engelman, J.A., Zejnullahu, K., Mitsudomi, T., Song, Y., Hyland, C., Park, J.O., Lindeman, N., Gale, C.-M., Zhao, X., Christensen, J.*, et al.* (2007). MET amplification leads to gefitinib resistance in lung cancer by activating ERBB3 signaling. Science (New York, NY) *316*, 1039-1043.

Ensslen-Craig, S.E., and Brady-Kalnay, S.M. (2004). Receptor protein tyrosine phosphatases regulate neural development and axon guidance. Dev Biol *275*, 12-22.

Eruslanov, E., and Kusmartsev, S. (2010). Identification of ROS using oxidized DCFDA and flow-cytometry. Methods Mol Biol *594*, 57-72.

Evangelou, A.M. (2002). Vanadium in cancer treatment. Crit Rev Oncol Hematol *42*, 249-265.

Evans, A.E., D'Angio, G.J., and Randolph, J. (1971). A proposed staging for children with neuroblastoma. Children's cancer study group A. Cancer *27*, 374-378.

Evans, A.E., Kisselbach, K.D., Liu, X., Eggert, A., Ikegaki, N., Camoratto, A.M., Dionne, C., and Brodeur, G.M. (2001). Effect of CEP-751 (KT-6587) on neuroblastoma xenografts expressing TrkB. Med Pediatr Oncol *36*, 181-184.

Evans, A.E., Kisselbach, K.D., Yamashiro, D.J., Ikegaki, N., Camoratto, A.M., Dionne, C.A., and Brodeur, G.M. (1999). Antitumor activity of CEP-751 (KT-6587) on human neuroblastoma and medulloblastoma xenografts. Clin Cancer Res *5*, 3594-3602.

Fan, Q.-W., Cheng, C., Hackett, C., Feldman, M., Houseman, B.T., Nicolaides, T., Haas-Kogan, D., James, C.D., Oakes, S.A., Debnath, J.*, et al.* (2010). Akt and autophagy cooperate to promote survival of drug-resistant glioma. Science Signaling *9;3*, ra81.

Fan, Q.-W., Knight, Z.A., Goldenberg, D.D., Yu, W., Mostov, K.E., Stokoe, D., Shokat, K.M., and Weiss, W.A. (2006). A dual PI3 kinase/mTOR inhibitor reveals emergent efficacy in glioma. Cancer Cell *9*, 341-349.

Faure, R., Vincent, M., Dufour, M., Shaver, A., and Posner, B.I. (1995). Arrest at the G2/M transition of the cell cycle by protein-tyrosine phosphatase inhibition: studies on a neuronal and a glial cell line. J Cell Biochem *59*, 389-401.

Faux, C., Hawadle, M., Nixon, J., Wallace, A., Lee, S., Murray, S., and Stoker, A. (2007). PTPsigma binds and dephosphorylates neurotrophin receptors and can

suppress NGF-dependent neurite outgrowth from sensory neurons. Biochim Biophys Acta *1773*, 1689-1700.

Fawal, M., Espinos, E., Jean-Jean, O., and Morello, D. (2011). Looking for the functions of RNA granules in ALK-transformed cells. BioArchitecture *1*, 91-95.

Felgner, P.L., Gadek, T.R., Holm, M., Roman, R., Chan, H.W., Wenz, M., Northrop, J.P., Ringold, G.M., and Danielsen, M. (1987). Lipofection: a highly efficient, lipid-mediated DNA-transfection procedure. Proceedings of the National Academy of Sciences of the United States of America *84*, 7413-7417.

Ferrari-Toninelli, G., Bonini, S.A., Uberti, D., Buizza, L., Bettinsoli, P., Poliani, P.L., Facchetti, F., and Memo, M. (2010). Targeting Notch pathway induces growth inhibition and differentiation of neuroblastoma cells. Neuro-oncology *12*, 1231-1243.

Ferreira, C.V., Justo, G.Z., Souza, A.C., Queiroz, K.C., Zambuzzi, W.F., Aoyama, H., and Peppelenbosch, M.P. (2006). Natural compounds as a source of protein tyrosine phosphatase inhibitors: Application to the rational design of small-molecule derivatives. Biochimie *88*, 159-173.

Filomeni, G., Rotilio, G., and Ciriolo, M.R. (2002). Cell signalling and the glutathione redox system. Biochem Pharmacol *64*, 1057-1064.

Finkel, T. (2000). Redox-dependent signal transduction. FEBS Lett *476*, 52-54.

Finlay, D., and Vuori, K. (2007). Novel noncatalytic role for caspase-8 in promoting SRC-mediated adhesion and Erk signaling in neuroblastoma cells. Cancer Res *67*, 11704-11711.

Fiordalisi, J.J., Keller, P.J., and Cox, A.D. (2006). PRL tyrosine phosphatases regulate rho family GTPases to promote invasion and motility. Cancer Res *66*, 3153-3161.

Foehr, E.D., Lorente, G., Kuo, J., Ram, R., Nikolich, K., and Urfer, R. (2006). Targeting of the Receptor Protein Tyrosine Phosphatase {beta} with a Monoclonal Antibody Delays Tumor Growth in a Glioblastoma Model. Cancer Res *66*, 2271-2278.

Fotsis, T., Breit, S., Lutz, W., Rössler, J., Hatzi, E., Schwab, M., and Schweigerer, L. (1999). Down-regulation of endothelial cell growth inhibitors by enhanced MYCN oncogene expression in human neuroblastoma cells. Eur J Biochem *263*, 757-764.

Foukas, L.C., Berenjeno, I.M., Gray, A., Khwaja, A., and Vanhaesebroeck, B. (2010). Activity of any class IA PI3K isoform can sustain cell proliferation and survival. Proceedings of the National Academy of Sciences *107*, 11381-11386.

Frank, C., Burkhardt, C., Imhof, D., Ringel, J., Zschornig, O., Wieligmann, K., Zacharias, M., and Bohmer, F.D. (2004). Effective dephosphorylation of Src substrates by SHP-1. J Biol Chem *279*, 11375-11383.

Franke, T.F., Yang, S.I., Chan, T.O., Datta, K., Kazlauskas, A., Morrison, D.K., Kaplan, D.R., and Tsichlis, P.N. (1995). The protein kinase encoded by the Akt proto-oncogene is a target of the PDGF-activated phosphatidylinositol 3-kinase. Cell *81*, 727-736.

Frisch, S.M., Vuori, K., Ruoslahti, E., and Chan-Hui, P.Y. (1996). Control of adhesion-dependent cell survival by focal adhesion kinase. J Cell Biol *134*, 793-799.

Fulda, S., Lutz, W., Schwab, M., and Debatin, K.-M. (2000). MycN sensitizes neuroblastoma cells for drug-triggered apoptosis. Medical and pediatric oncology *35*, 582-584.

Fulda, S., Lutz, W., Schwab, M., and Debatin, K.M. (1999). MycN sensitizes neuroblastoma cells for drug-induced apoptosis. Oncogene *18*, 1479-1486.

Futami, H., and Sakai, R. (2010). All-trans retinoic acid downregulates ALK in neuroblastoma cell lines and induces apoptosis in neuroblastoma cell lines with activated ALK. Cancer Lett *28;297*, 220-225.

Gamble, L.D., Kees, U.R., Tweddle, D.A., and Lunec, J. (2011). MYCN sensitizes neuroblastoma to the MDM2-p53 antagonists Nutlin-3 and MI-63. Oncogene.

Gamero, A.M., and Larner, A.C. (2001). Vanadate facilitates interferon alpha-mediated apoptosis that is dependent on the Jak/Stat pathway. J Biol Chem *276*, 13547-13553.

Gartenhaus, R.B., Prachand, S.N., Paniaqua, M., Li, Y., and Gordon, L.I. (2002). Arsenic trioxide cytotoxicity in steroid and chemotherapy-resistant myeloma cell lines: enhancement of apoptosis by manipulation of cellular redox state. Clin Cancer Res *8*, 566-572.

Gebbink, M.F., Zondag, G.C., Wubbolts, R.W., Beijersbergen, R.L., van Etten, I., and Moolenaar, W.H. (1993). Cell-cell adhesion mediated by a receptor-like protein tyrosine phosphatase. J Biol Chem *268*, 16101-16104.

George, R.E., Sanda, T., Hanna, M., Fröhling, S., Luther, W., Zhang, J., Ahn, Y., Zhou, W., London, W.B., McGrady, P.*, et al.* (2008). Activating mutations in ALK provide a therapeutic target in neuroblastoma. Nature *455*, 975-978.

Gerling, N., Culmsee, C., Klumpp, S., and Krieglstein, J. (2004). The tyrosine phosphatase inhibitor orthovanadate mimics NGF-induced neuroprotective signaling in rat hippocampal neurons. Neurochem Int *44*, 505-520.

Ghosh, P., D'Cruz, O.J., Narla, R.K., and Uckun, F.M. (2000). Apoptosis-inducing vanadocene compounds against human testicular cancer. Clin Cancer Res *6*, 1536-1545.

Gillory, L., and Beierle, E.A. (2010). Focal Adhesion Kinase Targeting in Neuroblastoma. Anticancer Agents Med Chem *10*, 714-721.

Gluzman, Y. (1981). SV40-transformed simian cells support the replication of early SV40 mutants. Cell *23*, 175-182.

Goh, A.M., Coffill, C.R., and Lane, D.P. (2010). The role of mutant p53 in human cancer. J Pathol *223*, 116-126.

Goldfine, A.B., Patti, M.E., Zuberi, L., Goldstein, B.J., LeBlanc, R., Landaker, E.J., Jiang, Z.Y., Willsky, G.R., and Kahn, C.R. (2000). Metabolic effects of vanadyl sulfate in humans with non-insulin-dependent diabetes mellitus: in vivo and in vitro studies. Metab Clin Exp *49*, 400-410.

Goldmann, T., Otto, F., and Vollmer, E. (2000). A receptor-type protein tyrosine phosphatase PTP zeta is expressed in human cutaneous melanomas. Folia Histochem Cytobiol *38*, 19-20.

Goodman, L.A., Liu, B.C.S., Thiele, C.J., Schmidt, M.L., Cohn, S.L., Yamashiro, J.M., Pai, D.S.M., Ikegaki, N., and Wada, R.K. (1997). Modulation of N-myc expression alters the invasiveness of neuroblastoma. Clinical and Experimental Metastasis *15*, 130-139.

Goodman, M., Gurney, J., Smith, M., and Olshan, A. (1999). Sympathetic Nervous System - SEER Pediatric Monograph. 1-8.

Goodwin, C.J., Holt, S.J., Downes, S., and Marshall, N.J. (1995). Microculture tetrazolium assays: a comparison between two new tetrazolium salts, XTT and MTS. Journal of Immunological Methods *179*, 95-103.

Gossen, M., and Bujard, H. (1992). Tight control of gene expression in mammalian cells by tetracycline-responsive promoters. Proc Natl Acad Sci USA *89*, 5547-5551.

Graham, F.L., Smiley, J., Russell, W.C., and Nairn, R. (1977). Characteristics of a human cell line transformed by DNA from human adenovirus type 5. J Gen Virol *36*, 59-74.

Greaves, M. (2010). Cancer stem cells: back to Darwin? Seminars in Cancer Biology *20*, 65-70.

Groen, A. (2005). Differential Oxidation of Protein-tyrosine Phosphatases. J Biol Chem *280*, 10298-10304.

Groen, A., Lemeer, S., van der Wijk, T., Overvoorde, J., Heck, A.J., Ostman, A., Barford, D., Slijper, M., and den Hertog, J. (2005). Differential oxidation of protein-tyrosine phosphatases. J Biol Chem *280*, 10298-10304.

Gschwind, A., Fischer, O.M., and Ullrich, A. (2004). The discovery of receptor tyrosine kinases: targets for cancer therapy. Nat Rev Cancer *4*, 361-370.

Gu, J., Tamura, M., and Yamada, K.M. (1998). Tumor suppressor PTEN inhibits integrin- and growth factor-mediated mitogen-activated protein (MAP) kinase signaling pathways. J Cell Biol *143*, 1375-1383.

Gualdrini, F., Corvetta, D., Cantilena, S., Chayka, O., Tanno, B., Raschellà, G., and Sala, A. (2010). Addiction of MYCN amplified tumours to B-MYB underscores a reciprocal regulatory loop. Oncotarget *1*, 278-288.

Guimarães, G.S., Latini, F.R.M., Camacho, C.P., Maciel, R.M.B., Dias-Neto, E., and Cerutti, J.M. (2006). Identification of candidates for tumor-specific alternative splicing in the thyroid. Genes Chromosomes Cancer *45*, 540-553.

Gulati, P., Klohn, P.C., Krug, H., Gottlicher, M., Markova, B., Bohmer, F.D., and Herrlich, P. (2001). Redox regulation in mammalian signal transduction. IUBMB Life *52*, 25-28.

Guo, J.Y., Chen, H.-Y., Mathew, R., Fan, J., Strohecker, A.M., Karsli-Uzunbas, G., Kamphorst, J.J., Chen, G., Lemons, J.M.S., Karantza, V.*, et al.* (2011). Activated Ras requires autophagy to maintain oxidative metabolism and tumorigenesis. Genes & Development *25*, 460-470.

Guo, K., Tang, J.P., Tan, C.P.B., Wang, H., and Zeng, Q. (2008). Monoclonal antibodies target intracellular PRL phosphatases to inhibit cancer metastases in mice. Cancer Biol Ther *7*, 750-757.

Gupta, A., Williams, B.R.G., Hanash, S.M., and Rawwas, J. (2006). Cellular retinoic acid-binding protein II is a direct transcriptional target of MycN in neuroblastoma. Cancer Research *66*, 8100-8108.

Gupta, P.B., Chaffer, C.L., and Weinberg, R.A. (2009). Cancer stem cells: mirage or reality? In Nat Med, pp. 1010-1012.

Gustafson, W.C., and Weiss, W.A. (2010). Myc proteins as therapeutic targets. Oncogene *29*, 1249-1259.

Haj, F.G., Markova, B., Klaman, L.D., Bohmer, F.D., and Neel, B.G. (2002). Regulation of receptor tyrosine kinase signaling by protein tyrosine phosphatase-1B (PTP1B). J Biol Chem *10;278*, 739-744.

Halliwell, B. (2007). Oxidative stress and cancer: have we moved forward? Biochem J *401*, 1-11.

Hampton, M.B., and Orrenius, S. (1997). Dual regulation of caspase activity by hydrogen peroxide: implications for apoptosis. FEBS Lett *414*, 552-556.

Hanahan, D., and Weinberg, R.A. (2000). The hallmarks of cancer. Cell *100*, 57-70.

Hansford, L.M., McKee, A.E., Zhang, L., George, R.E., Gerstle, J.T., Thorner, P.S., Smith, K.M., Look, A.T., Yeger, H., Miller, F.D*., et al.* (2007). Neuroblastoma cells isolated from bone marrow metastases contain a naturally enriched tumor-initiating cell. Cancer Res *67*, 11234-11243.

Hansford, L.M., Thomas, W.D., Keating, J.M., Burkhart, C.A., Peaston, A.E., Norris, M.D., Haber, M., Armati, P.J., Weiss, W.A., and Marshall, G.M. (2004). Mechanisms of embryonal tumor initiation: distinct roles for MycN expression and MYCN amplification. Proc Natl Acad Sci USA *101*, 12664-12669.

Harder, K.W., Moller, N.P., Peacock, J.W., and Jirik, F.R. (1998). Protein-tyrosine phosphatase alpha regulates Src family kinases and alters cell-substratum adhesion. J Biol Chem *273*, 31890-31900.

Hart, S.L., Arancibia-Cárcamo, C.V., Wolfert, M.A., Mailhos, C., O'Reilly, N.J., Ali, R.R., Coutelle, C., George, A.J., Harbottle, R.P., Knight, A.M*., et al.* (1998). Lipid-

mediated enhancement of transfection by a nonviral integrin-targeting vector. Hum Gene Ther *9*, 575-585.

Hayflick, L., and Moorhead, P.S. (1961). The serial cultivation of human diploid cell strains. Exp Cell Res *25*, 585-621.

Hecht, M., Schulte, J.H., Eggert, A., Wilting, J., and Schweigerer, L. (2005). The neurotrophin receptor TrkB cooperates with c-Met in enhancing neuroblastoma invasiveness. Carcinogenesis *26*, 2105-2115.

Hellberg, C.B., Burden-Gulley, S.M., Pietz, G.E., and Brady-Kalnay, S.M. (2002). Expression of the receptor protein tyrosine phosphatase, PTPmu, restores E-cadherin-dependent adhesion in human prostate carcinoma cells. J Biol Chem *277*, 11165-11773.

Hellmuth, K., Grosskopf, S., Lum, C.T., Würtele, M., Röder, N., von Kries, J.P., Rosario, M., Rademann, J., and Birchmeier, W. (2008). Specific inhibitors of the protein tyrosine phosphatase Shp2 identified by high-throughput docking. Proceedings of the National Academy of Sciences of the United States of America *105*, 7275-7280.

Hendriks, W., Elson, A., Harroch, S., and Stoker, A. (2008). Protein tyrosine phosphatases: functional inferences from mouse models and human diseases. FEBS Journal *275*, 816-830.

Hendriks, W., and Stoker, A. (2008). Protein tyrosine phosphatases: sequences and beyond. FEBS Journal *275*, 815.

Heneberg, P. (2009). Use of protein tyrosine phosphatase inhibitors as promising targeted therapeutic drugs. Curr Med Chem *16*, 706-733.

Henkens, R., Delvenne, P., Arafa, M., Moutschen, M., Zeddou, M., Tautz, L., Boniver, J., Mustelin, T., and Rahmouni, S. (2008). Cervix carcinoma is associated with an up-regulation and nuclear localization of the dual-specificity protein phosphatase VHR. BMC Cancer *8*, 147.

Hennessy, B.T., Smith, D.L., Ram, P.T., Lu, Y., and Mills, G.B. (2005). Exploiting the PI3K/AKT pathway for cancer drug discovery. Nat Rev Drug Discov *4*, 988-1004.

Herrlich, P., and Bohmer, F.D. (2000). Redox regulation of signal transduction in mammalian cells. Biochem Pharmacol *59*, 35-41.

Hertog, J., Ostman, A., and Bohmer, F. (2008). Protein tyrosine phosphatases: regulatory mechanisms. FEBS Journal *275*, 831-847.

Ho, R., Eggert, A., Hishiki, T., Minturn, J.E., Ikegaki, N., Foster, P., Camoratto, A.M., Evans, A.E., and Brodeur, G.M. (2002). Resistance to chemotherapy mediated by TrkB in neuroblastomas. Cancer Res *62*, 6462-6466.

Hogarty, M.D. (2003). The requirement for evasion of programmed cell death in neuroblastomas with MYCN amplification. CANCER LETTERS *197*, 173-179.

Hölzel, M., Huang, S., Koster, J., Ora, I., Lakeman, A., Caron, H., Nijkamp, W., Xie, J., Callens, T., Asgharzadeh, S.*, et al.* (2010). NF1 is a tumor suppressor in neuroblastoma that determines retinoic acid response and disease outcome. Cell *142*, 218-229.

Howard, M.J. (2005). Mechanisms and perspectives on differentiation of autonomic neurons. Dev Biol *277*, 271-286.

Huang, C., Zhang, Z., Ding, M., Li, J., Ye, J., Leonard, S.S., Shen, H.M., Butterworth, L., Lu, Y., Costa, M.*, et al.* (2000a). Vanadate induces p53 transactivation through hydrogen peroxide and causes apoptosis. J Biol Chem *275*, 32516-32522.

Huang, M.E., Ye, Y.C., Chen, S.R., Chai, J.R., Lu, J.X., Zhoa, L., Gu, L.J., and Wang, Z.Y. (1988). Use of all-trans retinoic acid in the treatment of acute promyelocytic leukemia. Blood *72*, 567-572.

Huang, P., Feng, L., Oldham, E.A., Keating, M.J., and Plunkett, W. (2000b). Superoxide dismutase as a target for the selective killing of cancer cells. Nature *407*, 390-395.

Huang, S., Laoukili, J., Epping, M.T., Koster, J., Hölzel, M., Westerman, B.A., Nijkamp, W., Hata, A., Asgharzadeh, S., Seeger, R.C.*, et al.* (2009). ZNF423 is critically required for retinoic acid-induced differentiation and is a marker of neuroblastoma outcome. In Cancer Cell, pp. 328-340.

Huber, K., Kalcheim, C., and Unsicker, K. (2009). The development of the chromaffin cell lineage from the neural crest. Auton Neurosci *151*, 10-16.

Huyer, G., Liu, S., Kelly, J., Moffat, J., and Payette, P. (1997). Mechanism of Inhibition of Protein-tyrosine Phosphatases by Vanadate and Pervanadate. J Biol Chem.

Irby, R.B., and Yeatman, T.J. (2000). Role of Src expression and activation in human cancer. Oncogene *19*, 5636-5642.

Irvine, S.A., Meng, Q.-H., Afzal, F., Ho, J., Wong, J.B., Hailes, H.C., Tabor, A.B., McEwan, J.R., and Hart, S.L. (2008). Receptor-targeted nanocomplexes optimized for gene transfer to primary vascular cells and explant cultures of rabbit aorta. Mol Ther *16*, 508-515.

Ish-Horowicz, D., and Burke, J.F. (1981). Rapid and efficient cosmid cloning. Nucleic Acids Res *9*, 2989-2998.

Iuliano, R., Le Pera, I., Cristofaro, C., Baudi, F., Arturi, F., Pallante, P., Martelli, M.L., Trapasso, F., Chiariotti, L., and Fusco, A. (2004). The tyrosine phosphatase PTPRJ/DEP-1 genotype affects thyroid carcinogenesis. Oncogene *23*, 8432-8438.

Jallal, B., Schlessinger, J., and Ullrich, A. (1992). Tyrosine phosphatase inhibition permits analysis of signal transduction complexes in p185HER2/neu-overexpressing human tumor cells. J Biol Chem *267*, 4357-4363.

Janne, P.A., Gray, N., and Settleman, J. (2009). Factors underlying sensitivity of cancers to small-molecule kinase inhibitors. Nature Reviews Drug Discovery *8*, 709-723.

Janoueix-Lerosey, I., Lequin, D., Brugières, L., Ribeiro, A., de Pontual, L., Combaret, V., Raynal, V., Puisieux, A., Schleiermacher, G., Pierron, G.*, et al.* (2008). Somatic and germline activating mutations of the ALK kinase receptor in neuroblastoma. Nature *455*, 967-970.

Janoueix-Lerosey, I., Schleiermacher, G., and Delattre, O. (2010). Molecular pathogenesis of peripheral neuroblastic tumors. Oncogene *18;29*, 1-14.

Janoueix-Lerosey, I., Schleiermacher, G., Michels, E., Mosseri, V., Ribeiro, A., Lequin, D., Vermeulen, J., Couturier, J., Peuchmaur, M., Valent, A.*, et al.* (2009). Overall genomic pattern is a predictor of outcome in neuroblastoma. J Clin Oncol *27*, 1026-1033.

Jiang, Z.-X., and Zhang, Z.-Y. (2008). Targeting PTPs with small molecule inhibitors in cancer treatment. Cancer Metastasis Rev *27*, 263-272.

Johnsen, J.I., Kogner, P., Albihn, A., and Henriksson, M.A. (2009). Embryonal neural tumours and cell death. Apoptosis *14*, 424-438.

Johnsen, J.I., Segerström, L., Orrego, A., Elfman, L., Henriksson, M., Kågedal, B., Eksborg, S., Sveinbjörnsson, B., and Kogner, P. (2008). Inhibitors of mammalian target of rapamycin downregulate MYCN protein expression and inhibit neuroblastoma growth in vitro and in vivo. Oncogene *27*, 2910-2922.

Johnson, K.G., and Van Vactor, D. (2003). Receptor protein tyrosine phosphatases in nervous system development. Physiol Rev *83*, 1-24.

Jones, C.J., Kipling, D., Morris, M., Hepburn, P., Skinner, J., Bounacer, A., Wyllie, F.S., Ivan, M., Bartek, J., Wynford-Thomas, D*., et al.* (2000). Evidence for a telomere-independent "clock" limiting RAS oncogene-driven proliferation of human thyroid epithelial cells. Mol Cell Biol *20*, 5690-5699.

Jones, R.J., Avizienyte, E., Wyke, A.W., Owens, D.W., Brunton, V.G., and Frame, M.C. (2002). Elevated c-Src is linked to altered cell-matrix adhesion rather than proliferation in KM12C human colorectal cancer cells. Br J Cancer *87*, 1128-1135.

Joshi, S., Guleria, R., Pan, J., DiPette, D., and Singh, U.S. (2006). Retinoic acid receptors and tissue-transglutaminase mediate short-term effect of retinoic acid on migration and invasion of neuroblastoma SH-SY5Y cells. Oncogene *25*, 240-247.

Julien, S.G., Dubé, N., Hardy, S., and Tremblay, M.L. (2011). Inside the human cancer tyrosine phosphatome. Nat Rev Cancer *11*, 35-49.

Julien, S.G., Dubé, N., Read, M., Penney, J., Paquet, M., Han, Y., Kennedy, B.P., Muller, W.J., and Tremblay, M.L. (2007). Protein tyrosine phosphatase 1B deficiency or inhibition delays ErbB2-induced mammary tumorigenesis and protects from lung metastasis. Nat Genet *39*, 338-346.

Junttila, M.R., and Evan, G.I. (2009). p53--a Jack of all trades but master of none. Nat Rev Cancer *9*, 821-829.

Kamencic, H., Lyon, A., Paterson, P.G., and Juurlink, B.H.J. (2000). Monochlorobimane Fluorometric Method to Measure Tissue Glutathione. Analytical Biochemistry *286*, 35-37.

Kaneko, Y., and Knudson, A.G. (2000). Mechanism and relevance of ploidy in neuroblastoma. Genes Chromosomes Cancer *29*, 89-95.

Kaneko, Y., Kobayashi, H., Maseki, N., Nakagawara, A., and Sakurai, M. (1999). Disomy 1 with terminal 1p deletion is frequent in mass-screening-negative/late-

presenting neuroblastomas in young children, but not in mass-screening-positive neuroblastomas in infants. Int J Cancer *80*, 54-59.

Kaplan, D.R., Matsumoto, K., Lucarelli, E., and Thiele, C.J. (1993). Induction of TrkB by retinoic acid mediates biologic responsiveness to BDNF and differentiation of human neuroblastoma cells. Eukaryotic Signal Transduction Group. Neuron *11*, 321-331.

Keane, M.M., Lowrey, G.A., Ettenberg, S.A., Dayton, M.A., and Lipkowitz, S. (1996). The protein tyrosine phosphatase DEP-1 is induced during differentiation and inhibits growth of breast cancer cells. Cancer Res *56*, 4236-4243.

Kennedy, A.L., Morton, J.P., Manoharan, I., Nelson, D.M., Jamieson, N.B., Pawlikowski, J.S., Mcbryan, T., Doyle, B., Mckay, C., Oien, K.A.*, et al.* (2011). Activation of the PIK3CA/AKT Pathway Suppresses Senescence Induced by an Activated RAS Oncogene to Promote Tumorigenesis. Molecular Cell *42*, 36-49.

Keshelava, N., Zuo, J.J., Waidyaratne, N.S., Triche, T.J., and Reynolds, C.P. (2000). p53 mutations and loss of p53 function confer multidrug resistance in neuroblastoma. Med Pediatr Oncol *35*, 563-568.

Kim, G.S., Choi, Y.K., Song, S.S., Kim, W.-K., and Han, B.H. (2005). MKP-1 contributes to oxidative stress-induced apoptosis via inactivation of ERK1/2 in SH-SY5Y cells. Biochem Biophys Res Commun *338*, 1732-1738.

Kim, K.A., Song, J.S., Jee, J., Sheen, M.R., Lee, C., Lee, T.G., Ro, S., Cho, J.M., Lee, W., Yamazaki, T.*, et al.* (2004). Structure of human PRL-3, the phosphatase associated with cancer metastasis. FEBS Lett *565*, 181-187.

Kim, Y., Song, Y.B., Kim, T.-Y., Kim, I., Han, S.-J., Ahn, Y., Cho, S.-H., Choi, C.Y., Chay, K.-O., Yang, S.Y.*, et al.* (2010). Redox regulation of the tumor suppressor PTEN by glutathione. FEBS Letters *584*, 3550-3556.

Kitamura, K., Minami, Y., Yamamoto, K., Akao, Y., Kiyoi, H., Saito, H., and Naoe, T. (2000). Involvement of CD95-independent caspase 8 activation in arsenic trioxide-induced apoptosis. Leukemia *14*, 1743-1750.

Kitanaka, C., Kato, K., Ijiri, R., Sakurada, K., Tomiyama, A., Noguchi, K., Nagashima, Y., Nakagawara, A., Momoi, T., Toyoda, Y.*, et al.* (2002). Increased Ras expression and caspase-independent neuroblastoma cell death: possible mechanism of spontaneous neuroblastoma regression. J Natl Cancer Inst *94*, 358-368.

Klarlund, J.K. (1985). Transformation of cells by an inhibitor of phosphatases acting on phosphotyrosine in proteins. Cell *41*, 707-717.

Kleppe, M., Lahortiga, I., El Chaar, T., De Keersmaecker, K., Mentens, N., Graux, C., Van Roosbroeck, K., Ferrando, A.A., Langerak, A.W., Meijerink, J.P.P.*, et al.* (2010). Deletion of the protein tyrosine phosphatase gene PTPN2 in T-cell acute lymphoblastic leukemia. Nat Genet *42*, 530-535.

Klinghoffer, R.A., and Kazlauskas, A. (1995). Identification of a putative Syp substrate, the PDGF beta receptor. J Biol Chem *270*, 22208-22217.

Knudson, A.G. (1971). Mutation and cancer: statistical study of retinoblastoma. Proc Natl Acad Sci USA *68*, 820-823.

Kohn, A.D., Takeuchi, F., and Roth, R.A. (1996). Akt, a pleckstrin homology domain containing kinase, is activated primarily by phosphorylation. J Biol Chem *271*, 21920-21926.

Kohno, T., Otsuka, A., Girard, L., Sato, M., Iwakawa, R., Ogiwara, H., Sanchez-Cespedes, M., Minna, J.D., and Yokota, J. (2010). A catalog of genes homozygously deleted in human lung cancer and the candidacy of PTPRD as a tumor suppressor gene. Genes Chromosomes Cancer *49*, 342-352.

Komarov, P.G., Komarova, E.A., Kondratov, R.V., Christov-Tselkov, K., Coon, J.S., Chernov, M.V., and Gudkov, A.V. (1999). A chemical inhibitor of p53 that protects mice from the side effects of cancer therapy. Science *285*, 1733-1737.

Koppen, A., Ait-Aissa, R., Hopman, S., Koster, J., Haneveld, F., Versteeg, R., and Valentijn, L.J. (2007). Dickkopf-1 is down-regulated by MYCN and inhibits neuroblastoma cell proliferation. Cancer Letters *256*, 218-228.

Korff, S., Woerner, S.M., Yuan, Y.P., Bork, P., Von Knebel Doeberitz, M., and Gebert, J. (2008). Frameshift mutations in coding repeats of protein tyrosine phosphatase genes in colorectal tumors with microsatellite instability. BMC Cancer *10;8*, 329.

Kovalenko, M., Denner, K., Sandström, J., Persson, C., Gross, S., Jandt, E., Vilella, R., Böhmer, F., and Ostman, A. (2000). Site-selective dephosphorylation of the platelet-derived growth factor beta-receptor by the receptor-like protein-tyrosine phosphatase DEP-1. J Biol Chem *275*, 16219-16226.

Krejsa, C.M., Nadler, S.G., Esselstyn, J.M., Kavanagh, T.J., Ledbetter, J.A., and Schieven, G.L. (1997). Role of oxidative stress in the action of vanadium phosphotyrosine phosphatase inhibitors. Redox independent activation of NF-kappaB. J Biol Chem *272*, 11541-11549.

Krejsa, C.M., and Schieven, G.L. (1998). Impact of oxidative stress on signal transduction control by phosphotyrosine phosphatases. Environmental Health Perspectives *106 Suppl 5*, 1179-1184.

Kroemer, G., and Levine, B. (2008). Autophagic cell death: the story of a misnomer. Nat Rev Mol Cell Biol *9*, 1004-1010.

Kroemer, G., and Martin, S.J. (2005). Caspase-independent cell death. Nat Med *11*, 725-730.

Kulas, D.T., Zhang, W.R., Goldstein, B.J., Furlanetto, R.W., and Mooney, R.A. (1995). Insulin receptor signaling is augmented by antisense inhibition of the protein tyrosine phosphatase LAR. J Biol Chem *270*, 2435-2438.

Kurosu, T., Fukuda, T., Miki, T., and Miura, O. (2003). BCL6 overexpression prevents increase in reactive oxygen species and inhibits apoptosis induced by chemotherapeutic reagents in B-cell lymphoma cells. Oncogene *22*, 4459-4468.

Laemmli, U.K. (1970). Cleavage of structural proteins during the assembly of the head of bacteriophage T4. Nature *227*, 680-685.

Laverdiere, C., Liu, Q., Yasui, Y., Nathan, P.C., Gurney, J.G., Stovall, M., Diller, L.R., Cheung, N.-K., Wolden, S., Robison, L.L*., et al.* (2009). Long-term Outcomes in Survivors of Neuroblastoma: A Report From the Childhood Cancer Survivor Study. JNCI Journal of the National Cancer Institute *101*, 1131-1140.

Lázcoz, P., Muñoz, J., Nistal, M., Pestaña, Á., Encío, I.J., and Castresana, J.S. (2007). Loss of heterozygosity and microsatellite instability on chromosome arm 10q in neuroblastoma. Cancer genetics and cytogenetics *174*, 1-8.

Lazo, J.S., Nemoto, K., Pestell, K.E., Cooley, K., Southwick, E.C., Mitchell, D.A., Furey, W., Gussio, R., Zaharevitz, D.W., Joo, B*., et al.* (2002). Identification of a potent and selective pharmacophore for Cdc25 dual specificity phosphatase inhibitors. Mol Pharmacol *61*, 720-728.

Lee, F.S., and Chao, M.V. (2001). Activation of Trk neurotrophin receptors in the absence of neurotrophins. Proc Natl Acad Sci USA *98*, 3555-3560.

Lee, J.-J., Kim, B.C., Park, M.-J., Lee, Y.-S., Kim, Y.-N., Lee, B.L., and Lee, J.-S. (2011). PTEN status switches cell fate between premature senescence and apoptosis in glioma exposed to ionizing radiation. Cell Death and Differentiation *18*, 666-677.

Lee, S., Faux, C., Nixon, J., Alete, D., Chilton, J., Hawadle, M., and Stoker, A.W. (2007). Dimerization of protein tyrosine phosphatase sigma governs both ligand binding and isoform specificity. Mol Cell Biol *27*, 1795-1808.

Lee, S.-R. (2002). Reversible Inactivation of the Tumor Suppressor PTEN by H2O2. J Biol Chem *277*, 20336-20342.

Lee, S.W., Reimer, C.L., Fang, L., Iruela-Arispe, M.L., and Aaronson, S.A. (2000). Overexpression of kinase-associated phosphatase (KAP) in breast and prostate cancer and inhibition of the transformed phenotype by antisense KAP expression. Mol Cell Biol *20*, 1723-1732.

Levy-Nissenbaum, O., Sagi-Assif, O., Kapon, D., Hantisteanu, S., Burg, T., Raanani, P., Avigdor, A., Ben-Bassat, I., and Witz, I.P. (2003a). Dual-specificity phosphatase Pyst2-L is constitutively highly expressed in myeloid leukemia and other malignant cells. Oncogene *22*, 7649-7660.

Levy-Nissenbaum, O., Sagi-Assif, O., Raanani, P., Avigdor, A., Ben-Bassat, I., and Witz, I.P. (2003b). Overexpression of the dual-specificity MAPK phosphatase PYST2 in acute leukemia. Cancer Letters *199*, 185-192.

Lewis-Wambi, J.S., Kim, H.R., Wambi, C., Patel, R., Pyle, J.R., Klein-Szanto, A.J., and Jordan, V.C. (2008). Buthionine sulfoximine sensitizes antihormone-resistant human breast cancer cells to estrogen-induced apoptosis. Breast Cancer Res *10*, R104.

Li, J., Yen, C., Liaw, D., Podsypanina, K., Bose, S., Wang, S.I., Puc, J., Miliaresis, C., Rodgers, L., McCombie, R.*, et al.* (1997). PTEN, a putative protein tyrosine phosphatase gene mutated in human brain, breast, and prostate cancer. Science *275*, 1943-1947.

Li, Z., Tan, F., Liewehr, D.J., Steinberg, S.M., and Thiele, C.J. (2010). In vitro and in vivo inhibition of neuroblastoma tumor cell growth by AKT inhibitor perifosine. JNCI Journal of the National Cancer Institute *102*, 758-770.

Li, Z., and Thiele, C.J. (2007). Targeting Akt to increase the sensitivity of neuroblastoma to chemotherapy: lessons learned from the brain-derived

neurotrophic factor/TrkB signal transduction pathway. In Expert Opin Ther Targets, pp. 1611-1621.

Lin, A.W., Barradas, M., Stone, J.C., Van Aelst, L., Serrano, M., and Lowe, S.W. (1998). Premature senescence involving p53 and p16 is activated in response to constitutive MEK/MAPK mitogenic signaling. Genes & Development *12*, 3008-3019.

Liu, S., Kulp, S.K., Sugimoto, Y., Jiang, J., Chang, H.-l., and Lin, Y.C. (2002). Involvement of breast epithelial-stromal interactions in the regulation of protein tyrosine phosphatase-γ (PTPγ) mRNA expression by estrogenically active agents. Breast Cancer Research and Treatment *71*, 21-35.

Lockshin, R.A., and Zakeri, Z. (2004). Caspase-independent cell death? Oncogene *23*, 2766-2773.

London, W.B., Castleberry, R.P., Matthay, K.K., Look, A.T., Seeger, R.C., Shimada, H., Thorner, P., Brodeur, G., Maris, J.M., Reynolds, C.P.*, et al.* (2005). Evidence for an age cutoff greater than 365 days for neuroblastoma risk group stratification in the Children's Oncology Group. J Clin Oncol *23*, 6459-6465.

Look, A.T., Hayes, F.A., Shuster, J.J., Douglass, E.C., Castleberry, R.P., Bowman, L.C., Smith, E.I., and Brodeur, G.M. (1991). Clinical relevance of tumor cell ploidy and N-myc gene amplification in childhood neuroblastoma: a Pediatric Oncology Group study. J Clin Oncol *9*, 581-591.

López-Carballo, G., Moreno, L., Masiá, S., Pérez, P., and Barettino, D. (2002). Activation of the phosphatidylinositol 3-kinase/Akt signaling pathway by retinoic acid is required for neural differentiation of SH-SY5Y human neuroblastoma cells. In J Biol Chem, pp. 25297-25304.

Loring, J.F., and Erickson, C.A. (1987). Neural crest cell migratory pathways in the trunk of the chick embryo. Developmental Biology *121*, 220-236.

Lovén, J., Zinin, N., Wahlström, T., Müller, I., Brodin, P., Fredlund, E., Ribacke, U., Pivarcsi, A., Påhlman, S., and Henriksson, M. (2010). MYCN-regulated microRNAs repress estrogen receptor-{alpha} (ESR1) expression and neuronal differentiation in human neuroblastoma. Proceedings of the National Academy of Sciences of the United States of America *107*, 1553-1558.

Lu, B., Ennis, D., Lai, R., Bogdanovic, E., Nikolov, R., Salamon, L., Fantus, C., Le-Tien, H., and Fantus, I.G. (2001). Enhanced sensitivity of insulin-resistant adipocytes

to vanadate is associated with oxidative stress and decreased reduction of vanadate (+5) to vanadyl (+4). J Biol Chem *276*, 35589-35598.

Lucarelli, E., Kaplan, D., and Thiele, C.J. (1997). Activation of trk-A but not trk-B signal transduction pathway inhibits growth of neuroblastoma cells. Eur J Cancer *33*, 2068-2070.

Lucarelli, E., Kaplan, D.R., and Thiele, C.J. (1995). Selective regulation of TrkA and TrkB receptors by retinoic acid and interferon-gamma in human neuroblastoma cell lines. J Biol Chem *270*, 24725-24731.

Lucci, M.A., Orlandi, R., Triulzi, T., Tagliabue, E., Balsari, A., and Villa-Moruzzi, E. (2010). Expression profile of tyrosine phosphatases in HER2 breast cancer cells and tumors. Cell Oncol *32*, 361-372.

Lutz, W., Fulda, S., Jeremias, I., Debatin, K.M., and Schwab, M. (1998). MycN and IFNgamma cooperate in apoptosis of human neuroblastoma cells. In Oncogene, pp. 339-346.

MacKeigan, J.P., Murphy, L.O., and Blenis, J. (2005). Sensitized RNAi screen of human kinases and phosphatases identifies new regulators of apoptosis and chemoresistance. Nat Cell Biol *7*, 591-600.

Madonna, M.B. (2010). Unraveling the relationship between n-myc and Focal Adhesion Kinase (FAK) in neuroblastoma? Cell Cycle *9*, 1679-1680.

Mains, R.E., and May, V. (1988). The role of a low pH intracellular compartment in the processing, storage, and secretion of ACTH and endorphin. J Biol Chem *263*, 7887-7894.

Majeti, R., Bilwes, A., Noel, J., Hunter, T., and Weiss, A. (1998). Dimerization-Induced Inhibition of Receptor Protein Tyrosine Phosphatase Function Through an inhibitory wedge. Science *2;297*, 88-91.

Majeti, R., and Weiss, A. (2001). Regulatory mechanisms for receptor protein tyrosine phosphatases. Chem Rev *101*, 2441-2448.

Majumder, P.K., Grisanzio, C., O'Connell, F., Barry, M., Brito, J.M., Xu, Q., Guney, I., Berger, R., Herman, P., Bikoff, R.*, et al.* (2008). A prostatic intraepithelial neoplasia-dependent p27 Kip1 checkpoint induces senescence and inhibits cell proliferation and cancer progression. Cancer Cell *14*, 146-155.

Mak, L.H., Vilar, R., and Woscholski, R. (2010). Characterisation of the PTEN inhibitor VO-OHpic. J Chem Biol *3*, 157-163.

Marengo, B., De Ciucis, C., Ricciarelli, R., Passalacqua, M., Nitti, M., Zingg, J.-M., Marinari, U.M., Pronzato, M.A., and Domenicotti, C. (2011). PKCδ Sensitizes Neuroblastoma Cells to L-Buthionine-Sulfoximine and Etoposide Inducing Reactive Oxygen Species Overproduction and DNA Damage. PLoS ONE *6*, e14661.

Marengo, B., De Ciucis, C., Verzola, D., Pistoia, V., Raffaghello, L., Patriarca, S., Balbis, E., Traverso, N., Cottalasso, D., Pronzato, M.A*., et al.* (2008). Mechanisms of BSO (L-buthionine-S,R-sulfoximine)-induced cytotoxic effects in neuroblastoma. Free Radic Biol Med *44*, 474-482.

Marengo, B., Raffaghello, L., Pistoia, V., Cottalasso, D., Pronzato, M.A., Marinari, U.M., and Domenicotti, C. (2005). Reactive oxygen species: biological stimuli of neuroblastoma cell response. Cancer Letters *228*, 111-116.

Maris, J.M. (2009). Unholy matrimony: Aurora A and N-Myc as malignant partners in neuroblastoma. Cancer Cell *15*, 5-6.

Maris, J.M. (2010). Recent advances in neuroblastoma. N Engl J Med *362*, 2202-2211.

Maris, J.M., Hogarty, M.D., Bagatell, R., and Cohn, S.L. (2007). Neuroblastoma. Lancet *369*, 2106-2120.

Marshall, C.J. (1995). Specificity of receptor tyrosine kinase signaling: transient versus sustained extracellular signal-regulated kinase activation. Cell *80*, 179-185.

Martinelli, S., Carta, C., Flex, E., Binni, F., Cordisco, E.L., Moretti, S., Puxeddu, E., Tonacchera, M., Pinchera, A., McDowell, H.P*., et al.* (2006). Activating PTPN11 mutations play a minor role in pediatric and adult solid tumors. Cancer Genet Cytogenet *166*, 124-129.

Mathew, S., George, S.P., Wang, Y., Siddiqui, M.R., Srinivasan, K., Tan, L., and Khurana, S. (2008). Potential molecular mechanism for c-Src kinase-mediated regulation of intestinal cell migration. J Biol Chem *283*, 22709-22722.

Matozaki, T., Murata, Y., Saito, Y., Okazawa, H., and Ohnishi, H. (2009). Protein tyrosine phosphatase SHP-2: a proto-oncogene product that promotes Ras activation. Cancer Science *100*, 1786-1793.

Matsuo, T., and Thiele, C.J. (1998). p27Kip1: a key mediator of retinoic acid induced growth arrest in the SMS-KCNR human neuroblastoma cell line. Oncogene *16*, 3337-3343.

Matthay, K.K., Reynolds, C.P., Seeger, R.C., Shimada, H., Adkins, E.S., Haas-Kogan, D., Gerbing, R.B., London, W.B., and Villablanca, J.G. (2009). Long-term results for children with high-risk neuroblastoma treated on a randomized trial of myeloablative therapy followed by 13-cis-retinoic acid: a children's oncology group study. J Clin Oncol *27*, 1007-1013.

Matthay, K.K., Villablanca, J.G., Seeger, R.C., Stram, D.O., Harris, R.E., Ramsay, N.K., Swift, P., Shimada, H., Black, C.T., Brodeur, G.M.*, et al.* (1999). Treatment of high-risk neuroblastoma with intensive chemotherapy, radiotherapy, autologous bone marrow transplantation, and 13-cis-retinoic acid. Children's Cancer Group. N Engl J Med *341*, 1165-1173.

Mazot, P., Cazes, A., Boutterin, M.C., Figueiredo, A., Raynal, V., Combaret, V., Hallberg, B., Palmer, R.H., Delattre, O., Janoueix-Lerosey, I.*, et al.* (2011). The constitutive activity of the ALK mutated at positions F1174 or R1275 impairs receptor trafficking. Oncogene *28;30*, 2017-2025.

McArdle, L., Rafferty, M., Maelandsmo, G.M., Bergin, O., Farr, C.J., Dervan, P.A., O'Loughlin, S., Herlyn, M., and Easty, D.J. (2001). Protein tyrosine phosphatase genes downregulated in melanoma. J Invest Dermatol *117*, 1255-1260.

McCubrey, J.A., Steelman, L.S., Chappell, W.H., Abrams, S.L., Wong, E.W.T., Chang, F., Lehmann, B., Terrian, D.M., Milella, M., Tafuri, A.*, et al.* (2007). Roles of the Raf/MEK/ERK pathway in cell growth, malignant transformation and drug resistance. Biochim Biophys Acta *1773*, 1263-1284.

Mclean, G.W., Carragher, N.O., Avizienyte, E., Evans, J., Brunton, V.G., and Frame, M.C. (2005). The role of focal-adhesion kinase in cancer - a new therapeutic opportunity. Nat Rev Cancer *5*, 505-515.

Mehdi, M.Z., and Srivastava, A.K. (2005). Organo-vanadium compounds are potent activators of the protein kinase B signaling pathway and protein tyrosine phosphorylation: mechanism of insulinomimesis. Arch Biochem Biophys *440*, 158-164.

Mehdi, M.Z., Vardatsikos, G., Pandey, S.K., and Srivastava, A.K. (2006). Involvement of insulin-like growth factor type 1 receptor and protein kinase Cdelta in bis(maltolato)oxovanadium(IV)-induced phosphorylation of protein kinase B in HepG2 cells. Biochemistry *45*, 11605-11615.

Melino, G., Thiele, C.J., Knight, R.A., and Piacentini, M. (1997). Retinoids and the control of growth/death decisions in human neuroblastoma cell lines. Journal of Neuro-Oncology *31*, 65-83.

Mellon, P., Parker, V., Gluzman, Y., and Maniatis, T. (1981). Identification of DNA sequences required for transcription of the human alpha 1-globin gene in a new SV40 host-vector system. Cell *27*, 279-288.

Mendoza, M.C., Er, E.E., and Blenis, J. (2011). The Ras-ERK and PI3K-mTOR pathways: cross-talk and compensation. Trends in biochemical sciences *36*, 320-328.

Michaloglou, C., Vredeveld, L.C.W., Soengas, M.S., Denoyelle, C., Kuilman, T., Van Der Horst, C.M.A.M., Majoor, D.M., Shay, J.W., Mooi, W.J., and Peeper, D.S. (2005). BRAFE600-associated senescence-like cell cycle arrest of human naevi. Nature *436*, 720-724.

Miloso, M., Villa, D., Crimi, M., Galbiati, S., Donzelli, E., Nicolini, G., and Tredici, G. (2004). Retinoic acid-induced neuritogenesis of human neuroblastoma SH-SY5Y cells is ERK independent and PKC dependent. J Neurosci Res *75*, 241-252.

Mitra, S.K., and Schlaepfer, D.D. (2006). Integrin-regulated FAK-Src signaling in normal and cancer cells. Curr Opin Cell Biol *18*, 516-523.

Mizushima, N., Yoshimori, T., and Levine, B. (2010). Methods in mammalian autophagy research. Cell *140*, 313-326.

Montagut, C., and Settleman, J. (2009). Targeting the RAF-MEK-ERK pathway in cancer therapy. CANCER LETTERS *283*, 125-134.

Montalibet, J., Skorey, K., McKay, D., Scapin, G., Asante-Appiah, E., and Kennedy, B.P. (2006). Residues distant from the active site influence protein-tyrosine phosphatase 1B inhibitor binding. J Biol Chem *281*, 5258-5266.

Moore, P.S., and Chang, Y. (2010). Why do viruses cause cancer? Highlights of the first century of human tumour virology. Nat Rev Cancer *10*, 878-889.

Morita, A., Yamamoto, S., Wang, B., Tanaka, K., Suzuki, N., Aoki, S., Ito, A., Nanao, T., Ohya, S., Yoshino, M.*, et al.* (2010). Sodium orthovanadate inhibits p53-mediated apoptosis. Cancer Research *70*, 257-265.

Mossé, Y.P., Laudenslager, M., Longo, L., Cole, K.A., Wood, A., Attiyeh, E.F., Laquaglia, M.J., Sennett, R., Lynch, J.E., Perri, P.*, et al.* (2008). Identification of ALK as a major familial neuroblastoma predisposition gene. Nature *455*, 930-935.

Motiwala, T., Kutay, H., Ghoshal, K., Bai, S., Seimiya, H., Tsuruo, T., Suster, S., Morrison, C., and Jacob, S. (2004). Protein tyrosine phosphatase receptor-type O (PTPRO) exhibits characteristics of a candidate tumor suppressor in human lung cancer. Proceedings of the National Academy of Sciences *101*, 13844.

Mukherjee, B., Patra, B., Mahapatra, S., Banerjee, P., Tiwari, A., and Chatterjee, M. (2004). Vanadium--an element of atypical biological significance. Toxicol Lett *150*, 135-143.

Muller, S., Lamszus, K., Nikolich, K., and Westphal, M. (2004). Receptor protein tyrosine phosphatase zeta as a therapeutic target for glioblastoma therapy. Expert Opin Ther Targets *8*, 211-220.

Muñoz, J., Lázcoz, P., Inda, M.M., Nistal, M., Pestaña, A., Encío, I.J., and Castresana, J.S. (2004). Homozygous deletion and expression of PTEN and DMBT1 in human primary neuroblastoma and cell lines. Int J Cancer *109*, 673-679.

Murphy, D.J., Junttila, M.R., Pouyet, L., Karnezis, A., Shchors, K., Bui, D.A., Brown-Swigart, L., Johnson, L., and Evan, G.I. (2008). Distinct Thresholds Govern Myc's Biological Output In Vivo. Cancer Cell *14*, 447-457.

Nagai, J.-i., Yazawa, T., Okudela, K., Kigasawa, H., Kitamura, H., and Osaka, H. (2004). Retinoic acid induces neuroblastoma cell death by inhibiting proteasomal degradation of retinoic acid receptor alpha. Cancer Research *64*, 7910-7917.

Nagano, H., Noguchi, T., Inagaki, K., Yoon, S., Matozaki, T., Itoh, H., Kasuga, M., and Hayashi, Y. (2003). Downregulation of stomach cancer-associated protein tyrosine phosphatase-1 (SAP-1) in advanced human hepatocellular carcinoma. Oncogene *22*, 4656-4663.

Nair, P., DePreter, K., Vandesompele, J., Speleman, F., and Stallings, R.L. (2008). Aberrant splicing of the PTPRD gene mimics microdeletions identified at this locus in neuroblastomas. Genes Chromosomes Cancer *47*, 197-202.

Naka, K., Hoshii, T., Muraguchi, T., Tadokoro, Y., Ooshio, T., Kondo, Y., Nakao, S., Motoyama, N., and Hirao, A. (2010). TGF-beta-FOXO signalling maintains leukaemia-initiating cells in chronic myeloid leukaemia. Nature *463*, 676-680.

Nakagawara, A. (1998). Molecular basis of spontaneous regression of neuroblastoma: role of neurotrophic signals and genetic abnormalities. Hum Cell *11*, 115-124.

Nakagawara, A., Arima, M., Azar, C.G., Scavarda, N.J., and Brodeur, G.M. (1992). Inverse relationship between trk expression and N-myc amplification in human neuroblastomas. Cancer Res *52*, 1364-1368.

Nakagawara, A., Arima-Nakagawara, M., Scavarda, N.J., Azar, C.G., Cantor, A.B., and Brodeur, G.M. (1993). Association between high levels of expression of the TRK gene and favorable outcome in human neuroblastoma. N Engl J Med *328*, 847-854.

Nakagawara, A., Azar, C.G., Scavarda, N.J., and Brodeur, G.M. (1994). Expression and function of TRK-B and BDNF in human neuroblastomas. Mol Cell Biol *14*, 759-767.

Nakagawara, A., and Brodeur, G.M. (1997). Role of neurotrophins and their receptors in human neuroblastomas: a primary culture study. Eur J Cancer *33*, 2050-2053.

Nakamura, M., Kishi, M., Sakaki, T., Hashimoto, H., Nakase, H., Shimada, K., Ishida, E., and Konishi, N. (2003). Novel tumor suppressor loci on 6q22-23 in primary central nervous system lymphomas. Cancer Res *63*, 737-741.

Nardella, C., Clohessy, J.G., Alimonti, A., and Pandolfi, P.P. (2011). Pro-senescence therapy for cancer treatment. Nature Reviews Cancer *11*, 503-511.

Narla, R.K., Chen, C.L., Dong, Y., and Uckun, F.M. (2001). In vivo antitumor activity of bis(4,7-dimethyl-1,10-phenanthroline) sulfatooxovanadium(IV) (METVAN [VO(SO4)(Me2-Phen)2]). Clin Cancer Res *7*, 2124-2133.

Nathan, C.F., Arrick, B.A., Murray, H.W., DeSantis, N.M., and Cohn, Z.A. (1981). Tumor cell anti-oxidant defenses. Inhibition of the glutathione redox cycle enhances macrophage-mediated cytolysis. J Exp Med *153*, 766-782.

Navis, A.C., van den Eijnden, M., Schepens, J.T.G., Hooft Van Huijsduijnen, R., Wesseling, P., and Hendriks, W.J.A.J. (2010). Protein tyrosine phosphatases in glioma biology. Acta Neuropathol *119*, 157-175.

Neumann, C.A., Krause, D.S., Carman, C.V., Das, S., Dubey, D.P., Abraham, J.L., Bronson, R.T., Fujiwara, Y., Orkin, S.H., and Van Etten, R.A. (2003). Essential role for the peroxiredoxin Prdx1 in erythrocyte antioxidant defence and tumour suppression. Nature *424*, 561-565.

Niederreither, K., and Dollé, P. (2008). Retinoic acid in development: towards an integrated view. Nature Reviews Genetics *9*, 541-553.

Niles, R.M. (2004). Signaling pathways in retinoid chemoprevention and treatment of cancer. Mutat Res *555*, 81-96.

Niwa, H., Yamamura, K., and Miyazaki, J. (1991). Efficient selection for high-expression transfectants with a novel eukaryotic vector. Gene *108*, 193-199.

Nogueira, V., Park, Y., Chen, C.-C., Xu, P.-Z., Chen, M.-L., Tonic, I., Unterman, T., and Hay, N. (2008). Akt determines replicative senescence and oxidative or oncogenic premature senescence and sensitizes cells to oxidative apoptosis. Cancer Cell *14*, 458-470.

Novellino, L., De Filippo, A., Deho, P., Perrone, F., Pilotti, S., Parmiani, G., and Castelli, C. (2008). PTPRK negatively regulates transcriptional activity of wild type and mutated oncogenic beta-catenin and affects membrane distribution of beta-catenin/E-cadherin complexes in cancer cells. Cellular Signalling *20*, 872-883.

O'Reilly, K.E., Rojo, F., She, Q.-B., Solit, D., Mills, G.B., Smith, D., Lane, H., Hofmann, F., Hicklin, D.J., Ludwig, D.L*., et al.* (2006). mTOR inhibition induces upstream receptor tyrosine kinase signaling and activates Akt. Cancer Research *66*, 1500-1508.

Obermeier, A., Bradshaw, R.A., Seedorf, K., Choidas, A., Schlessinger, J., and Ullrich, A. (1994). Neuronal differentiation signals are controlled by nerve growth factor receptor/Trk binding sites for SHC and PLG(gamma). EMBO Journal *13*, 1585-1590.

Oe, T., Sasayama, T., Nagashima, T., Muramoto, M., Yamazaki, T., Morikawa, N., Okitsu, O., Nishimura, S., Aoki, T., Katayama, Y*., et al.* (2005). Differences in gene expression profile among SH-SY5Y neuroblastoma subclones with different neurite outgrowth responses to nerve growth factor. J Neurochem *94*, 1264-1276.

Oikonomou, E., Makrodouli, E., Evagelidou, M., Joyce, T., Probert, L., and Pintzas, A. (2009). BRAF(V600E) efficient transformation and induction of

microsatellite instability versus KRAS(G12V) induction of senescence markers in human colon cancer cells. Neoplasia *11*, 1116-1131.

Omerovic, J., Clague, M.J., and Prior, I.A. (2010). Phosphatome profiling reveals PTPN2, PTPRJ and PTEN as potent negative regulators of PKB/Akt activation in Ras-mutated cancer cells. Biochem J *426*, 65-72.

Opel, D., Poremba, C., Simon, T., Debatin, K.-M., and Fulda, S. (2007). Activation of Akt Predicts Poor Outcome in Neuroblastoma. Cancer Research *67*, 735-745.

Oppenheimer, O., Cheung, N.-K., and Gerald, W.L. (2007). The RET oncogene is a critical component of transcriptional programs associated with retinoic acid-induced differentiation in neuroblastoma. Mol Cancer Ther *6*, 1300-1309.

Ormerod, M.G. (2002). Investigating the relationship between the cell cycle and apoptosis using flow cytometry. J Immunol Methods *265*, 73-80.

Ostman, A., and Böhmer, F.D. (2001). Regulation of receptor tyrosine kinase signaling by protein tyrosine phosphatases. Trends in Cell Biology *11*, 258-266.

Ostman, A., Hellberg, C., and Böhmer, F.D. (2006). Protein-tyrosine phosphatases and cancer. Nat Rev Cancer *6*, 307-320.

Otto, T., Horn, S., Brockmann, M., Eilers, U., Schüttrumpf, L., Popov, N., Kenney, A.M., Schulte, J.H., Beijersbergen, R., Christiansen, H.*, et al.* (2009). Stabilization of N-Myc is a critical function of Aurora A in human neuroblastoma. Cancer Cell *15*, 67-78.

Paez, J., and Sellers, W.R. (2003). PI3K/PTEN/AKT pathway. A critical mediator of oncogenic signaling. Cancer Treat Res *115*, 145-167.

Pannifer, A.D., Flint, A.J., Tonks, N.K., and Barford, D. (1998). Visualization of the cysteinyl-phosphate intermediate of a protein-tyrosine phosphatase by x-ray crystallography. J Biol Chem *273*, 10454-10462.

Park, J.R., Villablanca, J.G., London, W.B., Gerbing, R.B., Haas-Kogan, D., Adkins, E.S., Attiyeh, E.F., Maris, J.M., Seeger, R.C., Reynolds, C.P.*, et al.* (2009). Outcome of high-risk stage 3 neuroblastoma with myeloablative therapy and 13-cis-retinoic acid: a report from the Children's Oncology Group. Pediatr Blood Cancer *52*, 44-50.

Passoni, L., Longo, L., Collini, P., Coluccia, A.M.L., Bozzi, F., Podda, M., Gregorio, A., Gambini, C., Garaventa, A., Pistoia, V.*, et al.* (2009). Mutation-independent

anaplastic lymphoma kinase overexpression in poor prognosis neuroblastoma patients. Cancer Research *69*, 7338-7346.

Pathak, M.K., Dhawan, D., Lindner, D.J., Borden, E.C., Farver, C., and Yi, T. (2002). Pentamidine is an inhibitor of PRL phosphatases with anticancer activity. Mol Cancer Ther *1*, 1255-1264.

Patterson, K.I., Brummer, T., O'Brien, P.M., and Daly, R.J. (2009). Dual-specificity phosphatases: critical regulators with diverse cellular targets. Biochem J *418*, 475-489.

Paul, S., and Lombroso, P.J. (2003). Receptor and nonreceptor protein tyrosine phosphatases in the nervous system. Cell Mol Life Sci *60*, 2465-2482.

Peirce (2009). High level MycN expression in non-MYCN amplified neuroblastoma is induced by the combination treatment nutlin-3 and doxorubicin and enhances chemosensitivity. Oncol Rep *22*, 1-7.

Peng, L., Ning, J., Meng, L., and Shou, C. (2004). The association of the expression level of protein tyrosine phosphatase PRL-3 protein with liver metastasis and prognosis of patients with colorectal cancer. J Cancer Res Clin Oncol *130*, 521-526.

Perri, P., Bachetti, T., Longo, L., Matera, I., Seri, M., Tonini, G.P., and Ceccherini, I. (2005). PHOX2B mutations and genetic predisposition to neuroblastoma. Oncogene *24*, 3050-3053.

Peters, K.G., Davis, M.G., Howard, B.W., Pokross, M., Rastogi, V., Diven, C., Greis, K.D., Eby-Wilkens, E., Maier, M., Evdokimov, A.*, et al.* (2003). Mechanism of insulin sensitization by BMOV (bis maltolato oxo vanadium); unliganded vanadium (VO4) as the active component. Journal of Inorganic Biochemistry *96*, 321-330.

Petroni, M., Veschi, V., Prodosmo, A., Rinaldo, C., Massimi, I., Carbonari, M., Dominici, C., McDowell, H.P., Rinaldi, C., Screpanti, I.*, et al.* (2011). MYCN Sensitizes Human Neuroblastoma to Apoptosis by HIPK2 Activation through a DNA Damage Response. Molecular Cancer Research *9*, 67-77.

Polato, F., Codegoni, A., Fruscio, R., Perego, P., Mangioni, C., Saha, S., Bardelli, A., and Broggini, M. (2005). PRL-3 phosphatase is implicated in ovarian cancer growth. Clin Cancer Res *11*, 6835-6839.

Pulido, R., Serra-Pagès, C., Tang, M., and Streuli, M. (1995). The LAR/PTP delta/PTP sigma subfamily of transmembrane protein-tyrosine-phosphatases: multiple human LAR, PTP delta, and PTP sigma isoforms are expressed in a tissue-specific manner and associate with the LAR-interacting protein LIP.1. Proceedings of the National Academy of Sciences of the United States of America *92*, 11686-11690.

Pulido, R., and van Huijsduijnen, R. (2008a). Protein tyrosine phosphatases: dual-specificity phosphatases in health and disease. FEBS Journal *275*, 848-866.

Pulido, R., and van Huijsduijnen, R.H. (2008b). Protein tyrosine phosphatases: dual-specificity phosphatases in health and disease. Febs J *275*, 848-866.

Raabe, E.H., Laudenslager, M., Winter, C., Wasserman, N., Cole, K., LaQuaglia, M., Maris, D.J., Mosse, Y.P., and Maris, J.M. (2008). Prevalence and functional consequence of PHOX2B mutations in neuroblastoma. Oncogene *27*, 469-476.

Raj, L., Ide, T., Gurkar, A.U., Foley, M., Schenone, M., Li, X., Tolliday, N.J., Golub, T.R., Carr, S.A., Shamji, A.F*., et al.* (2011). Selective killing of cancer cells by a small molecule targeting the stress response to ROS. Nature *475*, 231-234.

Rane, S.G., Cosenza, S.C., Mettus, R.V., and Reddy, E.P. (2002). Germ line transmission of the Cdk4(R24C) mutation facilitates tumorigenesis and escape from cellular senescence. Mol Cell Biol *22*, 644-656.

Reiff, T., Tsarovina, K., Majdazari, A., Schmidt, M., del Pino, I., and Rohrer, H. (2010). Neuroblastoma phox2b variants stimulate proliferation and dedifferentiation of immature sympathetic neurons. J Neurosci *30*, 905-915.

Reul, B.A., Amin, S.S., Buchet, J.P., Ongemba, L.N., Crans, D.C., and Brichard, S.M. (1999). Effects of vanadium complexes with organic ligands on glucose metabolism: a comparison study in diabetic rats. Br J Pharmacol *126*, 467-477.

Reuter, S., Gupta, S.C., Chaturvedi, M.M., and Aggarwal, B.B. (2010). Oxidative stress, inflammation, and cancer: How are they linked? Free radical biology & medicine *1;49*, 1603-1616.

Reynolds, C.P., Matthay, K.K., Villablanca, J.G., and Maurer, B.J. (2003). Retinoid therapy of high-risk neuroblastoma. In CANCER LETTERS, pp. 185-192.

Reynolds, T. (1991). Differentiation therapy forces cancer cells to mature. J Natl Cancer Inst *83*, 1209-1211.

Rhee, J., Lilien, J., and Balsamo, J. (2001). Essential tyrosine residues for interaction of the non-receptor protein-tyrosine phosphatase PTP1B with N-cadherin. J Biol Chem *276*, 6640-6644.

Roberts, P.J., and Der, C.J. (2007). Targeting the Raf-MEK-ERK mitogen-activated protein kinase cascade for the treatment of cancer. Oncogene *26*, 3291-3310.

Rogers, M.V., Buensuceso, C., Montague, F., and Mahadevan, L. (1994). Vanadate stimulates differentiation and neurite outgrowth in rat pheochromocytoma PC12 cells and neurite extension in human neuroblastoma SH-SY5Y cells. Neuroscience *60*, 479-494.

Rosivatz, E., Matthews, J.G., McDonald, N.Q., Mulet, X., Ho, K.K., Lossi, N., Schmid, A.C., Mirabelli, M., Pomeranz, K.M., Erneux, C.*, et al.* (2006). A small molecule inhibitor for phosphatase and tensin homologue deleted on chromosome 10 (PTEN). ACS Chem Biol *1*, 780-790.

Ross, R., Biedler, J., and Spengler, B. (2003). A role for distinct cell types in determining malignancy in human neuroblastoma cell lines and tumors. Cancer Lett *197*, 35-39.

Ross, R., and Spengler, B. (2007). Human neuroblastoma stem cells. Seminars in Cancer Biology *17*, 241-247.

Rothenberg, A.B., Berdon, W.E., D'Angio, G.J., Yamashiro, D.J., and Cowles, R.A. (2009). Neuroblastoma-remembering the three physicians who described it a century ago: James Homer Wright, William Pepper, and Robert Hutchison. Pediatr Radiol *39*, 155-160.

Ruffels, J., Griffin, M., and Dickenson, J.M. (2004). Activation of ERK1/2, JNK and PKB by hydrogen peroxide in human SH-SY5Y neuroblastoma cells: role of ERK1/2 in H2O2-induced cell death. Eur J Pharmacol *483*, 163-173.

Ruivenkamp, C., Hermsen, M., Postma, C., Klous, A., Baak, J., Meijer, G., and Demant, P. (2003). LOH of PTPRJ occurs early in colorectal cancer and is associated with chromosomal loss of 18q12-21. Oncogene *22*, 3472-3474.

Ruivenkamp, C.A.L., van Wezel, T., Zanon, C., Stassen, A.P.M., Vlcek, C., Csikós, T., Klous, A.M., Tripodis, N., Perrakis, A., Boerrigter, L.*, et al.* (2002). Ptprj is a candidate for the mouse colon-cancer susceptibility locus Scc1 and is frequently deleted in human cancers. Nature Genetics *31*, 295-300.

Sablina, A.A., Budanov, A.V., Ilyinskaya, G.V., Agapova, L.S., Kravchenko, J.E., and Chumakov, P.M. (2005). The antioxidant function of the p53 tumor suppressor. Nat Med *11*, 1306-1313.

Sacco, F., Tinti, M., Palma, A., Ferrari, E., Nardozza, A.P., Hooft Van Huijsduijnen, R., Takahashi, T., Castagnoli, L., and Cesareni, G. (2009). Tumor suppressor density-enhanced phosphatase-1 (DEP-1) inhibits the RAS pathway by direct dephosphorylation of ERK1/2 kinases. J Biol Chem *284*, 22048-22058.

Sadakata, H., Okazawa, H., Sato, T., Supriatna, Y., Ohnishi, H., Kusakari, S., Murata, Y., Ito, T., Nishiyama, U., Minegishi, T.*, et al.* (2009). SAP-1 is a microvillus-specific protein tyrosine phosphatase that modulates intestinal tumorigenesis. Genes Cells *14*, 295-308.

Saha, S., Bardelli, A., Buckhaults, P., Velculescu, V.E., Rago, C., St Croix, B., Romans, K.E., Choti, M.A., Lengauer, C., Kinzler, K.W.*, et al.* (2001). A phosphatase associated with metastasis of colorectal cancer. Science *294*, 1343-1346.

Saiki, R.K., Gelfand, D.H., Stoffel, S., Scharf, S.J., Higuchi, R., Horn, G.T., Mullis, K.B., and Erlich, H.A. (1988). Primer-directed enzymatic amplification of DNA with a thermostable DNA polymerase. Science *239*, 487-491.

Sallee, J.L., Wittchen, E.S., and Burridge, K. (2006). Regulation of cell adhesion by protein tyrosine phosphatases 2. Cell-cell adhesion. J Biol Chem *9;281*, 15593-15596.

Salmena, L., Carracedo, A., and Pandolfi, P.P. (2008). Tenets of PTEN tumor suppression. Cell *133*, 403-414.

Sardar, S., Ghosh, R., Mondal, A., and Chatterjee, M. (1993). Protective role of vanadium in the survival of hosts during the growth of a transplantable murine lymphoma and its profound effects on the rates and patterns of biotransformation. Neoplasma *40*, 27-30.

Sarkisian, C.J., Keister, B.A., Stairs, D.B., Boxer, R.B., Moody, S.E., and Chodosh, L.A. (2007). Dose-dependent oncogene-induced senescence in vivo and its evasion during mammary tumorigenesis. Nat Cell Biol *9*, 493-505.

Schaller, M.D., Hildebrand, J.D., Shannon, J.D., Fox, J.W., Vines, R.R., and Parsons, J.T. (1994). Autophosphorylation of the focal adhesion kinase, pp125(FAK), directs SH2- dependent binding of pp60(src). Mol Cell Biol *14*, 1680-1688.

Schlaepfer, D.D., and Hunter, T. (1996). Evidence for in vivo phosphorylation of the Grb2 SH2-domain binding site on focal adhesion kinase by Src-family protein-tyrosine kinases. Mol Cell Biol *16*, 5623-5633.

Schleiermacher, G., Peter, M., Michon, J., Hugot, J.P., Vielh, P., Zucker, J.M., Magdelénat, H., Thomas, G., and Delattre, O. (1994). Two distinct deleted regions on the short arm of chromosome 1 in neuroblastoma. Genes Chromosomes Cancer *10*, 275-281.

Schmelzle, T., and Hall, M.N. (2000). TOR, a central controller of cell growth. Cell *103*, 253-262.

Schmitt, C.A., Fridman, J.S., Yang, M., Lee, S., Baranov, E., Hoffman, R.M., and Lowe, S.W. (2002). A senescence program controlled by p53 and p16INK4a contributes to the outcome of cancer therapy. Cell *109*, 335-346.

Schramm, A., Schulte, J.H., Astrahantseff, K., Apostolov, O., Limpt, V., Sieverts, H., Kuhfittig-Kulle, S., Pfeiffer, P., Versteeg, R., and Eggert, A. (2005). Biological effects of TrkA and TrkB receptor signaling in neuroblastoma. Cancer Lett *228*, 143-153.

Schulte, J.H., Schramm, A., Klein-Hitpass, L., Klenk, M., Wessels, H., Hauffa, B.P., Eils, J., Eils, R., Brodeur, G.M., Schweigerer, L.*, et al.* (2005). Microarray analysis reveals differential gene expression patterns and regulation of single target genes contributing to the opposing phenotype of TrkA- and TrkB-expressing neuroblastomas. Oncogene *24*, 165-177.

Schwab, M. (2004). MYCN in neuronal tumours. Cancer Lett *204*, 179-187.

Schwab, M., Varmus, H.E., and Bishop, J.M. (1985). Human N-myc gene contributes to neoplastic transformation of mammalian cells in culture. Nature *316*, 160-162.

Schweigerer, L., Breit, S., Wenzel, A., Tsunamoto, K., Ludwig, R., and Schwab, M. (1990). Augmented MYCN expression advances the malignant phenotype of human neuroblastoma cells: evidence for induction of autocrine growth factor activity. Cancer Research *50*, 4411-4416.

Scuteri, A., Galimberti, A., Ravasi, M., Pasini, S., Donzelli, E., Cavaletti, G., and Tredici, G. (2010). NGF protects Dorsal Root Ganglion neurons from oxaliplatin by modulating JNK/Sapk and ERK1/2. Neurosci Lett *17;486*, 141-145.

Seeger, R.C., Brodeur, G.M., Sather, H., Dalton, A., Siegel, S.E., Wong, K.Y., and Hammond, D. (1985). Association of Multiple Copies of the N-myc Oncogene with Rapid Progression of Neuroblastomas. New England Journal of Medicine *313*, 1111-1116.

Seely, B.L., Staubs, P.A., Reichart, D.R., Berhanu, P., Milarski, K.L., Saltiel, A.R., Kusari, J., and Olefsky, J.M. (1996). Protein tyrosine phosphatase 1B interacts with the activated insulin receptor. Diabetes *45*, 1379-1385.

Sekar, V., Thompson, D.V., Maroney, M.J., Bookland, R.G., and Adang, M.J. (1987). Molecular cloning and characterization of the insecticidal crystal protein gene of Bacillus thuringiensis var. tenebrionis. Proc Natl Acad Sci USA *84*, 7036-7040.

Serra, V., Scaltriti, M., Prudkin, L., Eichhorn, P.J.A., Ibrahim, Y.H., Chandarlapaty, S., Markman, B., Rodriguez, O., Guzman, M., Rodriguez, S*., et al.* (2011). PI3K inhibition results in enhanced HER signaling and acquired ERK dependency in HER2-overexpressing breast cancer. Oncogene *2;30*, 2547-2557.

Serrano, M., Lin, A.W., McCurrach, M.E., Beach, D., and Lowe, S.W. (1997). Oncogenic ras provokes premature cell senescence associated with accumulation of p53 and p16INK4a. Cell *88*, 593-602.

Shang, X., Vasudevan, S.A., Yu, Y., Ge, N., Ludwig, A.D., Wesson, C.L., Wang, K., Burlingame, S.M., Zhao, Y.-j., Rao, P.H*., et al.* (2010). Dual-specificity phosphatase 26 is a novel p53 phosphatase and inhibits p53 tumor suppressor functions in human neuroblastoma. Oncogene *2;29*, 4938-4946.

Shaw, G., Morse, S., Ararat, M., and Graham, F.L. (2002). Preferential transformation of human neuronal cells by human adenoviruses and the origin of HEK 293 cells. FASEB J *16*, 869-871.

She, Q.-B., Halilovic, E., Ye, Q., Zhen, W., Shirasawa, S., Sasazuki, T., Solit, D.B., and Rosen, N. (2010). 4E-BP1 is a key effector of the oncogenic activation of the AKT and ERK signaling pathways that integrates their function in tumors. Cancer Cell *18*, 39-51.

Shea, T.B., Fischer, I., and Sapirstein, V.S. (1985). Effect of retinoic acid on growth and morphological differentiation of mouse NB2a neuroblastoma cells in culture. Dev Brain Res *21*, 307-314.

Shenoy, K., Wu, Y., and Pervaiz, S. (2009). LY303511 enhances TRAIL sensitivity of SHEP-1 neuroblastoma cells via hydrogen peroxide-mediated mitogen-activated protein kinase activation and up-regulation of death receptors. Cancer Research *69*, 1941-1950.

Shioda, N., Han, F., Morioka, M., and Fukunaga, K. (2008). Bis(1-oxy-2-pyridinethiolato)oxovanadium(IV) enhances neurogenesis via phosphatidylinositol 3-kinase/Akt and extracellular signal regulated kinase activation in the hippocampal subgranular zone after mouse focal cerebral ischemia. Neuroscience *155*, 876-887.

Shioda, N., Ishigami, T., Han, F., Moriguchi, S., Shibuya, M., Iwabuchi, Y., and Fukunaga, K. (2007). Activation of phosphatidylinositol 3-kinase/protein kinase B pathway by a vanadyl compound mediates its neuroprotective effect in mouse brain ischemia. Neuroscience *148*, 221-229.

Sidell, N., Altman, A., Haussler, M.R., and Seeger, R.C. (1983). Effects of retinoic acid (RA) on the growth and phenotypic expression of several human neuroblastoma cell lines. Exp Cell Res *148*, 21-30.

Sidell, N., Wada, R., Han, G., Chang, B., Shack, S., Moore, T., and Samid, D. (1995). Phenylacetate synergizes with retinoic acid in inducing the differentiation of human neuroblastoma cells. Int J Cancer *60*, 507-514.

Singh, U.S., Pan, J., Kao, Y.-L., Joshi, S., Young, K.L., and Baker, K.M. (2003). Tissue transglutaminase mediates activation of RhoA and MAP kinase pathways during retinoic acid-induced neuronal differentiation of SH-SY5Y cells. J Biol Chem *278*, 391-399.

Slack, A., Chen, Z., Tonelli, R., Pule, M., Hunt, L., Pession, A., and Shohet, J.M. (2005). The p53 regulatory gene MDM2 is a direct transcriptional target of MYCN in neuroblastoma. Proc Natl Acad Sci USA *102*, 731-736.

Slee, E.A., Zhu, H., Chow, S.C., MacFarlane, M., Nicholson, D.W., and Cohen, G.M. (1996). Benzyloxycarbonyl-Val-Ala-Asp (OMe) fluoromethylketone (Z-VAD.FMK) inhibits apoptosis by blocking the processing of CPP32. Biochem J *315 (Pt 1)*, 21-24.

Smith, D.M., Pickering, R.M., and Lewith, G.T. (2008). A systematic review of vanadium oral supplements for glycaemic control in type 2 diabetes mellitus. QJM *101*, 351-358.

Smith, K.M., Datti, A., Fujitani, M., Grinshtein, N., Zhang, L., Morozova, O., Blakely, K.M., Rotenberg, S.A., Hansford, L.M., Miller, F.D.*, et al.* (2010). Selective targeting of neuroblastoma tumour-initiating cells by compounds identified in stem cell-based small molecule screens. EMBO Mol Med *2*, 371-384.

Smith, M.A., Ries, L.A.G., Gurney, J.G., and Ross, J.A. (1999). Leukemia - SEER Pediatric Monograph. 1-18.

Solomon, D.A., Kim, J.-S., Cronin, J.C., Sibenaller, Z., Ryken, T., Rosenberg, S.A., Ressom, H., Jean, W., Bigner, D., Yan, H.*, et al.* (2008). Mutational Inactivation of PTPRD in Glioblastoma Multiforme and Malignant Melanoma. Cancer Research *68*, 10300-10306.

Song, L., Ara, T., Wu, H.-W., Woo, C.-W., Reynolds, C.P., Seeger, R.C., DeClerck, Y.A., Thiele, C.J., Sposto, R., and Metelitsa, L.S. (2007). Oncogene MYCN regulates localization of NKT cells to the site of disease in neuroblastoma. J Clin Invest *117*, 2702-2712.

Song, M., Park, J.E., Park, S.G., Lee, D.H., Choi, H.-K., Park, B.C., Ryu, S.E., Kim, J.H., and Cho, S. (2009). NSC-87877, inhibitor of SHP-1/2 PTPs, inhibits dual-specificity phosphatase 26 (DUSP26). Biochem Biophys Res Commun *381*, 491-495.

Song, M.S., Carracedo, A., Salmena, L., Song, S.J., Egia, A., Malumbres, M., and Pandolfi, P.P. (2011). Nuclear PTEN Regulates the APC-CDH1 Tumor-Suppressive Complex in a Phosphatase-Independent Manner. Cell *144*, 187-199.

Sorby, M., and Ostman, A. (1996). Protein-tyrosine phosphatase-mediated decrease of epidermal growth factor and platelet-derived growth factor receptor tyrosine phosphorylation in high cell density cultures. J Biol Chem *271*, 10963-10966.

Soucek, L., and Evan, G.I. (2010). The ups and downs of Myc biology. Curr Opin Genet Dev *20*, 91-95.

Spitzenberg, V., König, C., Ulm, S., Marone, R., Röpke, L., Müller, J.P., Grün, M., Bauer, R., Rubio, I., Wymann, M.P.*, et al.* (2010). Targeting PI3K in neuroblastoma. J Cancer Res Clin Oncol *136*, 1881-1890.

Srivastava (2009). Bis(maltolato)-oxovanadium (IV)-induced phosphorylation of PKB, GSK-3 and FOXO1 contributes toits glucoregulatory responses (Review). Int J Mol Med *24*, 1-7.

Srivastava, A.K., and Mehdi, M.Z. (2005). Insulino-mimetic and anti-diabetic effects of vanadium compounds. Diabet Med *22*, 2-13.

Stallings, R.L., Nair, P., Maris, J.M., Catchpoole, D., McDermott, M., O'Meara, A., and Breatnach, F. (2006). High-resolution analysis of chromosomal breakpoints and genomic instability identifies PTPRD as a candidate tumor suppressor gene in neuroblastoma. Cancer Res *66*, 3673-3680.

Stallings, R.L., Yoon, K., Kwek, S., and Ko, D. (2007). The origin of chromosome imbalances in neuroblastoma. Cancer Genet Cytogenet *176*, 28-34.

Stephens, B., Han, H., Hostetter, G., Demeure, M.J., and Von Hoff, D.D. (2008). Small interfering RNA-mediated knockdown of PRL phosphatases results in altered Akt phosphorylation and reduced clonogenicity of pancreatic cancer cells. Molecular Cancer Therapeutics *7*, 202-210.

Stoker, A.W. (2005). Protein tyrosine phosphatases and signalling. J Endocrinol *185*, 19-33.

Suarez Pestana, E., Tenev, T., Gross, S., Stoyanov, B., Ogata, M., and Bohmer, F.D. (1999). The transmembrane protein tyrosine phosphatase RPTPsigma modulates signaling of the epidermal growth factor receptor in A431 cells. Oncogene *18*, 4069-4079.

Sugihara, E., Kanai, M., Matsui, A., Onodera, M., Schwab, M., and Miwa, M. (2004). Enhanced expression of MYCN leads to centrosome hyperamplification after DNA damage in neuroblastoma cells. In Oncogene, pp. 1005-1009.

Sun, H., and Tonks, N.K. (1994). The coordinated action of protein tyrosine phosphatases and kinases in cell signaling. Trends Biochem Sci *19*, 480-485.

Sun, T., Aceto, N., Meerbrey, K.L., Kessler, J.D., Zhou, C., Migliaccio, I., Nguyen, D.X., Pavlova, N.N., Botero, M., Huang, J.*, et al.* (2011). Activation of multiple proto-oncogenic tyrosine kinases in breast cancer via loss of the PTPN12 phosphatase. Cell *144*, 703-718.

Tabernero, L., Aricescu, A., Jones, E., and Szedlacsek, S. (2008). Protein tyrosine phosphatases: structure-function relationships. FEBS Journal *275*, 867-882.

Tabin, C.J., Bradley, S.M., Bargmann, C.I., Weinberg, R.A., Papageorge, A.G., Scolnick, E.M., Dhar, R., Lowy, D.R., and Chang, E.H. (1982). Mechanism of activation of a human oncogene. Nature *300*, 143-149.

Tacconelli, A., Farina, A.R., Cappabianca, L., Desantis, G., Tessitore, A., Vetuschi, A., Sferra, R., Rucci, N., Argenti, B., Screpanti, I.*, et al.* (2004). TrkA alternative splicing: a regulated tumor-promoting switch in human neuroblastoma. Cancer Cell *6*, 347-360.

Tait, S.W.G., and Green, D.R. (2008). Caspase-independent cell death: leaving the set without the final cut. Oncogene *27*, 6452-6461.

Takahashi, H., Arstikaitis, P., Prasad, T., Bartlett, T.E., Wang, Y.T., Murphy, T.H., and Craig, A.M. (2011). Postsynaptic TrkC and Presynaptic PTPσ Function as a Bidirectional Excitatory Synaptic Organizing Complex. Neuron *69*, 287-303.

Tanaka, H., and Yao, M.-C. (2009). Palindromic gene amplification--an evolutionarily conserved role for DNA inverted repeats in the genome. Nat Rev Cancer *9*, 216-224.

Tang, H., Hao, Q., Rutherford, S.A., Low, B., and Zhao, Z.J. (2005). Inactivation of SRC family tyrosine kinases by reactive oxygen species in vivo. J Biol Chem *280*, 23918-23925.

Tarcic, G., Boguslavsky, S., Wakim, J., Kiuchi, T., Liu, A., Reinitz, F., Nathanson, D., Takahashi, T., Mischel, P., Ng, T.*, et al.* (2009). An Unbiased Screen Identifies DEP-1 Tumor Suppressor as a Phosphatase Controlling EGFR Endocytosis. Curr Biol *17;19*, 1788-1798.

Tartaglia, M., Niemeyer, C.M., Fragale, A., Song, X., Buechner, J., Jung, A., Hahlen, K., Hasle, H., Licht, J.D., and Gelb, B.D. (2003). Somatic mutations in PTPN11 in juvenile myelomonocytic leukemia, myelodysplastic syndromes and acute myeloid leukemia. Nat Genet *34*, 148-150.

Tartaglia, M., Niemeyer, C.M., Shannon, K.M., and Loh, M.L. (2004). SHP-2 and myeloid malignancies. Curr Opin Hematol *11*, 44-50.

Taylor, S.D. (2003). Inhibitors of protein tyrosine phosphatase 1B (PTP1B). Curr Top Med Chem *3*, 759-782.

Teitz, T., Stanke, J.J., Federico, S., Bradley, C.L., Brennan, R., Zhang, J., Johnson, M.D., Sedlacik, J., Inoue, M., Zhang, Z.M.*, et al.* (2011). Preclinical models for neuroblastoma: establishing a baseline for treatment. PLoS ONE *6*, e19133.

Thiele, C. (2006). Neuroblastoma Cell Lines -- Molecular Features. 1-35.

Thiele, C.J., Reynolds, C.P., and Israel, M.A. (1985). Decreased expression of N-myc precedes retinoic acid-induced morphological differentiation of human neuroblastoma. Nature *313*, 404-406.

Thompson, H.J., Chasteen, N.D., and Meeker, L.D. (1984). Dietary vanadyl(IV) sulfate inhibits chemically-induced mammary carcinogenesis. Carcinogenesis *5*, 849-851.

Thompson, K.H., Lichter, J., Lebel, C., Scaife, M.C., Mcneill, J.H., and Orvig, C. (2009). Vanadium treatment of type 2 diabetes: a view to the future. Journal of Inorganic Biochemistry *103*, 554-558.

Tibes, R., Trent, J., and Kurzrock, R. (2005). Tyrosine kinase inhibitors and the dawn of molecular cancer therapeutics. Annu Rev Pharmacol Toxicol *45*, 357-384.

Tiganis, T., and Bennett, A.M. (2007). Protein tyrosine phosphatase function: the substrate perspective. Biochem J *402*, 1-15.

Tonks, N., and Muthuswamy, S. (2007). A Brake Becomes an Accelerator: PTP1B—A New Therapeutic Target for Breast Cancer. Cancer Cell *11*, 214-216.

Tonks, N.K. (2005). Redox redux: revisiting PTPs and the control of cell signaling. Cell *121*, 667-670.

Tonks, N.K. (2006). Protein tyrosine phosphatases: from genes, to function, to disease. Nat Rev Mol Cell Biol *7*, 833-846.

Tothova, Z., Kollipara, R., Huntly, B.J., Lee, B.H., Castrillon, D.H., Cullen, D.E., McDowell, E.P., Lazo-Kallanian, S., Williams, I.R., Sears, C.*, et al.* (2007). FoxOs are critical mediators of hematopoietic stem cell resistance to physiologic oxidative stress. Cell *128*, 325-339.

Towbin, H., Staehelin, T., and Gordon, J. (1979). Electrophoretic transfer of proteins from polyacrylamide gels to nitrocellulose sheets: procedure and some applications. Proc Natl Acad Sci USA *76*, 4350-4354.

Trachootham, D., Lu, W., Ogasawara, M.A., Nilsa, R.-D.V., and Huang, P. (2008). Redox regulation of cell survival. Antioxid Redox Signal *10*, 1343-1374.

Trapasso, F., Drusco, A., Costinean, S., Alder, H., Aqeilan, R.I., Iuliano, R., Gaudio, E., Raso, C., Zanesi, N., Croce, C.M.*, et al.* (2006). Genetic Ablation of Ptprj, a Mouse Cancer Susceptibility Gene, Results in Normal Growth and Development and Does Not Predispose to Spontaneous Tumorigenesis. DNA Cell Biol *25*, 376-382.

Traxler, P. (2003). Tyrosine kinases as targets in cancer therapy - successes and failures. Expert Opin Ther Targets *7*, 215-234.

Tremblay, M.L. (2009). The PTP family photo album. Cell *136*, 213-214.

Trotman, L.C., Niki, M., Dotan, Z.A., Koutcher, J.A., Di Cristofano, A., Xiao, A., Khoo, A.S., Roy-Burman, P., Greenberg, N.M., Van Dyke, T.*, et al.* (2003). Pten dose dictates cancer progression in the prostate. Plos Biol *1*, E59.

Tsuruda, A., Suzuki, S., Maekawa, T., and Oka, S. (2004). Constitutively active Src facilitates NGF-induced phosphorylation of TrkA and causes enhancement of the MAPK signaling in SK-N-MC cells. FEBS Letters *560*, 215-220.

Tweddle, D. (2003). The p53 pathway and its inactivation in neuroblastoma. Cancer Lett *197*, 93-98.

Tweddle, D.A., Malcolm, A.J., Bown, N., Pearson, A.D., and Lunec, J. (2001). Evidence for the development of p53 mutations after cytotoxic therapy in a neuroblastoma cell line. Cancer Res *61*, 8-13.

Uemura, K., Kitagawa, N., Kohno, R., Kuzuya, A., Kageyama, T., Shibasaki, H., and Shimohama, S. (2003). Presenilin 1 mediates retinoic acid-induced differentiation of SH-SY5Y cells through facilitation of Wnt signaling. J Neurosci Res *73*, 166-175.

Umezawa, K., Kawakami, M., and Watanabe, T. (2003). Molecular design and biological activities of protein-tyrosine phosphatase inhibitors. Pharmacol Ther *99*, 15-24.

Van Der Wijk, T., Blanchetot, C., and den Hertog, J. (2005). Regulation of receptor protein-tyrosine phosphatase dimerization. Methods *35*, 73-79.

van Doorn, R., Zoutman, W.H., Dijkman, R., de Menezes, R.X., Commandeur, S., Mulder, A.A., van der Velden, P.A., Vermeer, M.H., Willemze, R., Yan, P.S.*, et al.* (2005). Epigenetic profiling of cutaneous T-cell lymphoma: promoter hypermethylation of multiple tumor suppressor genes including BCL7a, PTPRG, and p73. J Clin Oncol *23*, 3886-3896.

Van Maerken, T., Rihani, A., Dreidax, D., De Clercq, S., Yigit, N., Marine, J.-C., Westermann, F., De Paepe, A., Vandesompele, J., and Speleman, F. (2011). Functional analysis of the p53 pathway in neuroblastoma cells using the small-molecule MDM2 antagonist nutlin-3. Molecular Cancer Therapeutics *10*, 983-993.

Van Maerken, T., Speleman, F., Vermeulen, J., Lambertz, I., De Clercq, S., De Smet, E., Yigit, N., Coppens, V., Philippé, J., De Paepe, A*., et al.* (2006). Small-molecule MDM2 antagonists as a new therapy concept for neuroblastoma. Cancer Research *66*, 9646-9655.

Van Maerken, T., Vandesompele, J., Rihani, A., De Paepe, A., and Speleman, F. (2009). Escape from p53-mediated tumor surveillance in neuroblastoma: switching off the p14(ARF)-MDM2-p53 axis. Cell Death and Differentiation *16*, 1563-1572.

van Niekerk, C.C., and Poels, L.G. (1999). Reduced expression of protein tyrosine phosphatase gamma in lung and ovarian tumors. Cancer Lett *137*, 61-73.

Veeriah, S., Brennan, C., Meng, S., Singh, B., Fagin, J.A., Solit, D.B., Paty, P.B., Rohle, D., Vivanco, I., Chmielecki, J*., et al.* (2009). The tyrosine phosphatase PTPRD is a tumor suppressor that is frequently inactivated and mutated in glioblastoma and other human cancers. Proceedings of the National Academy of Sciences of the United States of America *106*, 9435-9440.

Vezzalini, M., Mombello, A., Menestrina, F., Mafficini, A., Della Peruta, M., van Niekerk, C., Barbareschi, M., Scarpa, A., and Sorio, C. (2007). Expression of transmembrane protein tyrosine phosphatase gamma (PTPgamma) in normal and neoplastic human tissues. Histopathology *50*, 615-628.

Villablanca, J.G., Khan, A.A., Avramis, V.I., Seeger, R.C., Matthay, K.K., Ramsay, N.K., and Reynolds, C.P. (1995). Phase I trial of 13-cis-retinoic acid in children with neuroblastoma following bone marrow transplantation. J Clin Oncol *13*, 894-901.

Villablanca, J.G., Krailo, M.D., Ames, M.M., Reid, J.M., Reaman, G.H., and Reynolds, C.P. (2006). Phase I trial of oral fenretinide in children with high-risk solid tumors: a report from the Children's Oncology Group (CCG 09709). J Clin Oncol *24*, 3423-3430.

Vintonyak, V.V., Antonchick, A.P., Rauh, D., and Waldmann, H. (2009). The therapeutic potential of phosphatase inhibitors. Current Opinion in Chemical Biology *13*, 272-283.

Vivanco, I., and Sawyers, C.L. (2002). The phosphatidylinositol 3-Kinase AKT pathway in human cancer. Nat Rev Cancer *2*, 489-501.

Vlahos, C.J., Matter, W.F., Hui, K.Y., and Brown, R.F. (1994). A specific inhibitor of phosphatidylinositol 3-kinase, 2-(4-morpholinyl)-8-phenyl-4H-1-benzopyran-4-one (LY294002). J Biol Chem *269*, 5241-5248.

Voena, C., Conte, C., Ambrogio, C., Boeri Erba, E., Boccalatte, F., Mohammed, S., Jensen, O.N., Palestro, G., Inghirami, G., and Chiarle, R. (2007). The tyrosine phosphatase Shp2 interacts with NPM-ALK and regulates anaplastic lymphoma cell growth and migration. Cancer Research *67*, 4278-4286.

von Kriegsheim, A., Baiocchi, D., Birtwistle, M., Sumpton, D., Bienvenut, W., Morrice, N., Yamada, K., Lamond, A., Kalna, G., Orton, R*., et al.* (2009). Cell fate decisions are specified by the dynamic ERK interactome. Nat Cell Biol *11*, 1458-1464.

Wainwright, L.J., Lasorella, A., and Iavarone, A. (2001). Distinct mechanisms of cell cycle arrest control the decision between differentiation and senescence in human neuroblastoma cells. Proceedings of the National Academy of Sciences of the United States of America *98*, 9396-9400.

Wajapeyee, N., Serra, R.W., Zhu, X., Mahalingam, M., and Green, M.R. (2008). Oncogenic BRAF induces senescence and apoptosis through pathways mediated by the secreted protein IGFBP7. Cell *132*, 363-374.

Walton, J.D., Kattan, D.R., Thomas, S.K., Spengler, B.A., Guo, H.-F., Biedler, J.L., Cheung, N.-K.V., and Ross, R.A. (2004). Characteristics of stem cells from human neuroblastoma cell lines and in tumors. NEO *6*, 838-845.

Wang, H.-y., Cheng, Z., and Malbon, C.C. (2003). Overexpression of mitogen-activated protein kinase phosphatases MKP1, MKP2 in human breast cancer. Cancer Letters *191*, 229-237.

Wang, J.-F., and Dai, D.-Q. (2007). Metastatic suppressor genes inactivated by aberrant methylation in gastric cancer. World J Gastroenterol *13*, 5692-5698.

Wang, Q., Liu, T.-T., Fu, Y., Wang, K., and Yang, X.-G. (2010). Vanadium compounds discriminate hepatoma and normal hepatic cells by differential regulation of reactive oxygen species. J Biol Inorg Chem *15*, 1087-1097.

Wang, Y., Li, Z.-F., He, J., Li, Y.-L., Zhu, G.-B., Zhang, L.-H., and Li, Y.-L. (2007). Expression of the human phosphatases of regenerating liver (PRLs) in colonic adenocarcinoma and its correlation with lymph node metastasis. International Journal of Colorectal Disease *22*, 1179-1184.

Wang, Z., Shen, D., Parsons, D.W., Bardelli, A., Sager, J., Szabo, S., Ptak, J., Silliman, N., Peters, B.A., van der Heijden, M.S.*, et al.* (2004). Mutational analysis of the tyrosine phosphatome in colorectal cancers. Science *304*, 1164-1166.

Wardman, P. (2007). Fluorescent and luminescent probes for measurement of oxidative and nitrosative species in cells and tissues: progress, pitfalls, and prospects. Free Radic Biol Med *43*, 995-1022.

Weinberg, F., Hamanaka, R., Wheaton, W.W., Weinberg, S., Joseph, J., Lopez, M., Kalyanaraman, B., Mutlu, G.M., Budinger, G.R.S., and Chandel, N.S. (2010). Mitochondrial metabolism and ROS generation are essential for Kras-mediated tumorigenicity. Proceedings of the National Academy of Sciences of the United States of America *107*, 8788-8793.

Weiner, T.M., Liu, E.T., Craven, R.J., and Cance, W.G. (1993). Expression of focal adhesion kinase gene and invasive cancer. Lancet *342*, 1024-1025.

Weinstein, I.B. (2002). Cancer. Addiction to oncogenes--the Achilles heal of cancer. Science *297*, 63-64.

Weinstein, I.B., and Joe, A. (2008). Oncogene addiction. Cancer Research *68*, 3077-3080; discussion 3080.

Weiss, B., and Richardson, C.C. (1967). Enzymatic breakage and joining of deoxyribonucleic acid, I. Repair of single-strand breaks in DNA by an enzyme system from Escherichia coli infected with T4 bacteriophage. Proc Natl Acad Sci USA *57*, 1021-1028.

Weiss, W.A., Aldape, K., Mohapatra, G., Feuerstein, B.G., and Bishop, J.M. (1997). Targeted expression of MYCN causes neuroblastoma in transgenic mice. EMBO J *16*, 2985-2995.

Wellen, K.E., and Thompson, C.B. (2010). Cellular metabolic stress: considering how cells respond to nutrient excess. Molecular Cell *40*, 323-332.

Wellstein, A., and Toretsky, J.A. (2011). Hunting ALK to feed targeted cancer therapy. Nature Medicine *17*, 290-291.

Wendel, H.-G., De Stanchina, E., Fridman, J.S., Malina, A., Ray, S., Kogan, S., Cordon-Cardo, C., Pelletier, J., and Lowe, S.W. (2004). Survival signalling by Akt and eIF4E in oncogenesis and cancer therapy. Nature *428*, 332-337.

White, E., and Dipaola, R.S. (2009). The double-edged sword of autophagy modulation in cancer. Clin Cancer Res *15*, 5308-5316.

Wiesmann, C., Barr, K.J., Kung, J., Zhu, J., Erlanson, D.A., Shen, W., Fahr, B.J., Zhong, M., Taylor, L., Randal, M.*, et al.* (2004). Allosteric inhibition of protein tyrosine phosphatase 1B. Nat Struct Mol Biol *11*, 730-737.

Willsky, G.R., Goldfine, A.B., Kostyniak, P.J., McNeill, J.H., Yang, L.Q., Khan, H.R., and Crans, D.C. (2001). Effect of vanadium(IV) compounds in the treatment of diabetes: in vivo and in vitro studies with vanadyl sulfate and bis(maltolato)oxovandium(IV). Journal of Inorganic Biochemistry *85*, 33-42.

Woessmann, W., Chen, X., and Borkhardt, A. (2002). Ras-mediated activation of ERK by cisplatin induces cell death independently of p53 in osteosarcoma and neuroblastoma cell lines. In Cancer Chemother Pharmacol, pp. 397-404.

Woo, C.-W., Lucarelli, E., and Thiele, C.J. (2004). NGF activation of TrkA decreases N-myc expression via MAPK path leading to a decrease in neuroblastoma cell number. Oncogene *23*, 1522-1530.

Woodings, J.A., Sharp, S.J., and Machesky, L.M. (2003). MIM-B, a putative metastasis suppressor protein, binds to actin and to protein tyrosine phosphatase delta. Biochem J *371*, 463-471.

Wu, C.-H., van Riggelen, J., Yetil, A., Fan, A.C., Bachireddy, P., and Felsher, D.W. (2007). Cellular senescence is an important mechanism of tumor regression upon c-Myc inactivation. Proc Natl Acad Sci USA *104*, 13028-13033.

Wu, C.-W., Chen, J.-H., Kao, H.-L., Li, A.F.Y., Lai, C.-H., Chi, C.-W., and Lin, W.-C. (2006). PTPN3 and PTPN4 tyrosine phosphatase expression in human gastric adenocarcinoma. Anticancer Res *26*, 1643-1649.

Wu, H., Ichikawa, S., Tani, C., Zhu, B., Tada, M., Shimoishi, Y., Murata, Y., and Nakamura, Y. (2009). Docosahexaenoic acid induces ERK1/2 activation and neuritogenesis via intracellular reactive oxygen species production in human neuroblastoma SH-SY5Y cells. Biochimica et biophysica acta *1791*, 8-16.

Wu, L., Bernard-Trifilo, J.A., Lim, Y., Lim, S.-T., Mitra, S.K., Uryu, S., Chen, M., Pallen, C.J., Cheung, N.-K., Mikolon, D.*, et al.* (2008). Distinct FAK-Src activation events promote alpha5beta1 and alpha4beta1 integrin-stimulated neuroblastoma cell motility. Oncogene *27*, 1439-1448.

Xia, Z., Dickens, M., Raingeaud, J., Davis, R.J., and Greenberg, M.E. (1995). Opposing effects of ERK and JNK-p38 MAP kinases on apoptosis. Science *270*, 1326-1331.

Xu, D., Rovira, I.I., and Finkel, T. (2002). Oxidants painting the cysteine chapel: redox regulation of PTPs. Dev Cell *2*, 251-252.

Xue, W., Zender, L., Miething, C., Dickins, R.A., Hernando, E., Krizhanovsky, V., Cordon-Cardo, C., and Lowe, S.W. (2007). Senescence and tumour clearance is triggered by p53 restoration in murine liver carcinomas. Nature *445*, 656-660.

Yang, B., Keshelava, N., Anderson, C.P., and Reynolds, C.P. (2003). Antagonism of buthionine sulfoximine cytotoxicity for human neuroblastoma cell lines by hypoxia is reversed by the bioreductive agent tirapazamine. Cancer Res *63*, 1520-1526.

Yang, N.-C., and Hu, M.-L. (2005). The limitations and validities of senescence associated-beta-galactosidase activity as an aging marker for human foreskin fibroblast Hs68 cells. Exp Gerontol *40*, 813-819.

Yang, S., Wang, X., Contino, G., Liesa, M., Sahin, E., Ying, H., Bause, A., Li, Y., Stommel, J.M., Dell'antonio, G*., et al.* (2011). Pancreatic cancers require autophagy for tumor growth. Genes & Development *25*, 717-729.

Yeatman, T.J. (2004). A renaissance for SRC. Nat Rev Cancer *4*, 470-480.

Yeh, C.T., Lu, S.C., Chen, T.C., Peng, C.Y., and Liaw, Y.F. (2000). Aberrant transcripts of the cyclin-dependent kinase-associated protein phosphatase in hepatocellular carcinoma. Cancer Res *60*, 4697-4700.

Yeh, S.-H., Wu, D.-C., Tsai, C.-Y., Kuo, T.-J., Yu, W.-C., Chang, Y.-S., Chen, C.-L., Chang, C.-F., Chen, D.-S., and Chen, P.-J. (2006). Genetic characterization of fas-associated phosphatase-1 as a putative tumor suppressor gene on chromosome 4q21.3 in hepatocellular carcinoma. Clin Cancer Res *12*, 1097-1108.

Yu, J., Becka, S., Zhang, P., Zhang, X., Brady-Kalnay, S.M., and Wang, Z. (2008). Tumor-derived extracellular mutations of PTPRT /PTPrho are defective in cell adhesion. Mol Cancer Res *6*, 1106-1113.

Yu, W., Imoto, I., Inoue, J., Onda, M., Emi, M., and Inazawa, J. (2007). A novel amplification target, DUSP26, promotes anaplastic thyroid cancer cell growth by inhibiting p38 MAPK activity. Oncogene *26*, 1178-1187.

Yu, Y.-M., Han, P.-L., and Lee, J.-K. (2003). JNK pathway is required for retinoic acid-induced neurite outgrowth of human neuroblastoma, SH-SY5Y. NeuroReport *14*, 941-945.

Yuza, Y., Agawa, M., Matsuzaki, M., Yamada, H., and Urashima, M. (2003). Gene and protein expression profiling during differentiation of neuroblastoma cells triggered by 13-cis retinoic acid. J Pediatr Hematol Oncol *25*, 715-720.

Zage, P.E., Graham, T.C., Zeng, L., Fang, W., Pien, C., Thress, K., Omer, C., Brown, J.L., and Zweidler-McKay, P.A. (2010a). The selective Trk inhibitor AZ623 inhibits brain-derived neurotrophic factor-mediated neuroblastoma cell proliferation and signaling and is synergistic with topotecan. Cancer *15;117*, 1321-1391.

Zage, P.E., Zeng, L., Palla, S., Fang, W., Nilsson, M.B., Heymach, J.V., and Zweidler-Mckay, P.A. (2010b). A novel therapeutic combination for neuroblastoma: the vascular endothelial growth factor receptor/epidermal growth factor receptor/rearranged during transfection inhibitor vandetanib with 13-cis-retinoic acid. Cancer *116*, 2465-2475.

Zeng, M., and Zhou, J.-N. (2008). Roles of autophagy and mTOR signaling in neuronal differentiation of mouse neuroblastoma cells. Cell Signal *20*, 659-665.

Zeng, Q., Dong, J.M., Guo, K., Li, J., Tan, H.X., Koh, V., Pallen, C.J., Manser, E., and Hong, W. (2003). PRL-3 and PRL-1 promote cell migration, invasion, and metastasis. Cancer Res *63*, 2716-2722.

Zhang, S., Huang, W.-C., Li, P., Guo, H., Poh, S.-B., Brady, S.W., Xiong, Y., Tseng, L.-M., Li, S.-H., Ding, Z*., et al.* (2011). Combating trastuzumab resistance by targeting SRC, a common node downstream of multiple resistance pathways. Nature Medicine *17*, 461-469.

Zhang, S., and Zhang, Z.-Y. (2007). PTP1B as a drug target: recent developments in PTP1B inhibitor discovery. Drug Discov Today *12*, 373-381.

Zhang, S.Q., Yang, W., Kontaridis, M.I., Bivona, T.G., Wen, G., Araki, T., Luo, J., Thompson, J.A., Schraven, B.L., Philips, M.R*., et al.* (2004). Shp2 regulates SRC family kinase activity and Ras/Erk activation by controlling Csk recruitment. Mol Cell *13*, 341-355.

Zhang, X., Guo, A., Yu, J., Possemato, A., Chen, Y., Zheng, W., Polakiewicz, R.D., Kinzler, K.W., Vogelstein, B., Velculescu, V.E*., et al.* (2007). Identification of STAT3 as

a substrate of receptor protein tyrosine phosphatase T. Proceedings of the National Academy of Sciences of the United States of America *104*, 4060-4064.

Zhang, X., He, Y., Liu, S., Yu, Z., Jiang, Z.-X., Yang, Z., Dong, Y., Nabinger, S.C., Wu, L., Gunawan, A.M.*, et al.* (2010). Salicylic acid based small molecule inhibitor for the oncogenic Src homology-2 domain containing protein tyrosine phosphatase-2 (SHP2). J Med Chem *53*, 2482-2493.

Zhang, Y., Siebert, R., Matthiesen, P., Yang, Y., Ha, H., and Schlegelberger, B. (1998). Cytogenetical assignment and physical mapping of the human R-PTP-kappa gene (PTPRK) to the putative tumor suppressor gene region 6q22.2-q22.3. Genomics *51*, 309-311.

Zhang, Z., He, H., Chen, F., Huang, C., and Shi, X. (2002). MAPKs mediate S phase arrest induced by vanadate through a p53-dependent pathway in mouse epidermal C141 cells. Chem Res Toxicol *15*, 950-956.

Zhang, Z., Leonard, S.S., Huang, C., Vallyathan, V., Castranova, V., and Shi, X. (2003). Role of reactive oxygen species and MAPKs in vanadate-induced G(2)/M phase arrest. Free Radic Biol Med *34*, 1333-1342.

Zhang, Z.Y., and Lee, S.Y. (2003). PTP1B inhibitors as potential therapeutics in the treatment of type 2 diabetes and obesity. Expert Opin Investig Drugs *12*, 223-233.

Zhao, Y., Zhang, X., Guda, K., Lawrence, E., Sun, Q., Watanabe, T., Iwakura, Y., Asano, M., Wei, L., Yang, Z.*, et al.* (2010). Identification and functional characterization of paxillin as a target of protein tyrosine phosphatase receptor T. Proceedings of the National Academy of Sciences *107*, 2592-2597.

Zheng, X.M., Resnick, R.J., and Shalloway, D. (2000). A phosphotyrosine displacement mechanism for activation of Src by PTPalpha. Embo J *19*, 964-978.

Zheng, X.M., Wang, Y., and Pallen, C.J. (1992). Cell transformation and activation of $pp60^{c\text{-}src}$ by overexpression of a protein tyrosine phosphatase. Nature *359*, 336-339.

Zhi, H.-Y., Hou, S.-W., Li, R.-S., Basir, Z., Xiang, Q., Szabo, A., and Chen, G. (2010). PTPH1 cooperates with vitamin D receptor to stimulate breast cancer growth through their mutual stabilization. Oncogene *7*, 1706-1715.

Zhou, B.P., Hu, M.C., Miller, S.A., Yu, Z., Xia, W., Lin, S.Y., and Hung, M.C. (2000). HER-2/neu blocks tumor necrosis factor-induced apoptosis via the Akt/NF-kappaB pathway. J Biol Chem *275*, 8027-8031.

Zoncu, R., Efeyan, A., and Sabatini, D.M. (2011). mTOR: from growth signal integration to cancer, diabetes and ageing. Nat Rev Mol Cell Biol *12*, 21-35.

Zwick, E., Bange, J., and Ullrich, A. (2001). Receptor tyrosine kinase signalling as a target for cancer intervention strategies. Endocrine-Related Cancer *8*, 161-173.